

N 70 41089

CR 113796

T70-01854



**CASE FILE  
COPY**

**MASSACHUSETTS INSTITUTE OF TECHNOLOGY**

MVT-70-3

SENSORY FEEDBACK  
IN HUMAN POSTURE CONTROL

by

Lewis Michael Nashner

June, 1970

Sc.D. Thesis

**MAN-VEHICLE LABORATORY**  
CENTER FOR SPACE RESEARCH  
MASSACHUSETTS INSTITUTE OF TECHNOLOGY  
CAMBRIDGE, MASSACHUSETTS 02139

WGL-22-009-156

SENSORY FEEDBACK  
IN HUMAN POSTURE CONTROL

by

LEWIS MICHAEL NASHNER

S.B., Massachusetts Institute of Technology, 1965

S.M., Massachusetts Institute of Technology, 1967

SUBMITTED IN PARTIAL FULFILLMENT  
OF THE REQUIREMENTS FOR THE  
DEGREE OF DOCTOR OF SCIENCE

at the

MASSACHUSETTS INSTITUTE OF TECHNOLOGY

June, 1970



SENSORY FEEDBACK  
IN HUMAN POSTURE CONTROL

by

Lewis Michael Nashner

Submitted to the Department of Aeronautics and Astronautics, Massachusetts Institute of Technology, on May 4, 1970, in partial fulfillment of the requirements for the degree of Doctor of Science.

ABSTRACT

Current models for physiological components and a series of experiments on human subjects form the basis for a multiloop control model which describes how a human uses multiple feedback sensors to control his orientation. Particular emphasis is placed on defining functional interfaces between the feedback sensors and postural responses. Because of the inherent complexities within the posture control system, analysis is simplified by considering only control of forward and backward rotational motions about the ankle joints during quiet standing tasks.

The research effort is divided into three segments. First, a general posture control model is assembled given current models for motor and sensory components. This general model forms the basis for a series of experiments with human subjects using a specially designed two-degree-of-freedom simulator. Finally, experimental observations are combined with the general model, developing specific models which predict the observed postural responses.

During quiet standing on a rigid surface ankle reflex gain is about one third that necessary for postural stability. Ankle reflexes, however, are adequate to fully

stabilize very small deflections due to the presence of "stiction" forces acting between fibers in intra- and extra-fusal muscle fibers. Quiet standing is punctuated by frequent transients during which the subject "breaks out" of static reflex stability and begins to diverge. A kinesthetic threshold is reached, commanding a transient multiplicative increase in reflex gain proportional to disturbance amplitude. A static sense, either vision or utricle otolith is necessary to correct slow drift of this reflex/kinesthetic control loop.

When reflex and visual feedback are removed, the vestibular sensors are able to fully stabilize posture. The utricle otoliths and semicircular canals act as frequency selective feedback sensors. The canals detect sway divergence and initiate corrective postural responses. The utricle otoliths provide a static vertical reference to stabilize slow drift of the canal control loop. Otolith cues are shown to be ambiguous at higher frequencies because of interactions between linear motion and gravitational stimuli.

Control strategy is observed in one subject with complete loss of vestibular function but with normal motor control. When eyes are open, the subject shows reflex/kinesthetic control strategy which is very nearly normal. The subject is also able to stand with eyes closed; however, this required great effort. Tests show eyes closed control strategy to be radically different. Extensor reflex gains were increased six-fold, allocating almost complete control of function to reflex "rigidity".

Thesis Supervisor: Jacob L. Meiry

Title: Assistant Professor of  
Aeronautics and Astronautics

Thesis Supervisor: Laurence R. Young

Title: Professor of Aeronautics and  
Astronautics

Thesis Supervisor: Yao Tzu Li

Title: Professor of Aeronautics and  
Astronautics

Thesis Supervisor: James C. Houk

Title: Assistant Professor of Physi-  
ology (Harvard Medical School)

ACKNOWLEDGMENTS

The author wishes to thank his thesis advisors, Professor J. L. Meiry, Professor L. R. Young, Professor Y. T. Li, and Dr. J. C. Houk. As chairman, Professor Meiry provided both the freedom for exploration during the initial development of the thesis and valuable criticism during its unfolding in the final months. The author is grateful to Professor Young for providing a sense of excitement and accomplishment as the thesis began to crystalize. Special thanks go to Dr. Houk for his advice on the many physiological questions which arose during the research.

The author thanks Dr. A. D. Weiss, Massachusetts General Hospital, for enlisting the aid of one of his patients for a series of experiments. His advice concerning the medical implications of the research also was valuable.

Also appreciated was the assistance of fellow students, Noel Van Houtte and Chuck Oman, in programming and operating the computer facility. The author also thanks Mr. John Barley for providing valuable technical advice in the design and construction of hydraulic servomechanisms, Annette Markowitz for typing the manuscript, and the subjects for their patience during the many hours of experimentation.

To his wife, Gail, for her invaluable support and understanding during the long effort, the author dedicates this thesis.

This research was supported by a grant from NASA, ~~NSG-22-009-025~~. NGR 22-009-156.

TABLE OF CONTENTS

<u>Chapter No.</u>		<u>Page No.</u>
1	Introduction	1
2	Physiology of Posture Regulation	8
3	The Stretch Reflexes	38
4	The Vestibular Senses	75
5	Visual and Exteroceptive Senses	103
6	Posture Control Without Vestibular Senses	121
7	Conclusions	135
<u>Appendices</u>		
A	Body Dynamics	143
B	The Two-Degree of Freedom Experimental Platform	147
C	Digital Computer Programs	154
D	Analog Computer Programs	157
E	Experimental Data	162
<u>References</u>		188
<u>Biographical Sketch</u>		198

LIST OF FIGURES

<u>Figure No.</u>		<u>Page No.</u>
2.1	Anatomy of the Lower Leg	9
2.2	Anatomical Dimensions of the Lower Leg	11
2.3	Force-Velocity Characteristics of Muscle According to Hill's Equation	15
2.4	Experimentally Observed Force-Velocity Characteristics of Cat Soleus Muscle During Various Rates of Activation	16
2.5	Approximate Length-Tension Characteristics of Muscle as a Function of Activation Rate	17
2.6	Lumped Parameter Model for Muscular Contraction	20
2.7	Representation of the General Features of the Mammalian Muscle Spindle	22
2.8	A Dynamic Model for the Utricle Otoliths	27
2.9	Representation of the Features of a Spinal Motoneuron	29
2.10	The Integrating Functions of a Neuron	31
2.11	General Features of the Sensory-Motor System Controlling Posture	36
3.1	The Reflex Control System	40
3.2	A Simple Mechanism by Which the Gamma Motor System Controls Position of the Limb	43

<u>Figure No.</u>		<u>Page No.</u>
3.3	A Simple Mechanism by which the Gamma Motor System Controls the Stiffness of a Joint	44
3.4	An Agonist/Antagonist Muscle Pair	46
3.5	Typical Reflex Responses to 1/2 Degree Steps Extending and Flexing the Ankle Joint	50
3.6	Average Ankle Reflex Gain as a Function of Step Size	52
3.7	Average Ankle Reflex Responses Grouped According to Gain for 1/4 and 1/2 Degree Steps	53
3.8	Force-Velocity Data Showing "Stiction" Effects at Moderate Stimulus Rates	56
3.9	Active Reflex Tension in Cat Gastrocnemius and Soleus Muscle as a Function of Displacement	56
3.10	Typical Body Angle and Ankle Torque Response Sequences During Quiet Standing on a Rigid Surface	57
3.11	A Proposed Model for the Enhancement of the Reflex Gain as a Function of Ankle Deflection and Damping Ratio	59
3.12	Natural Frequency and Damping Ratio as a Function of Reflex Amplitude, Compensatory Response	60
3.13	An Equivalent Reflex Control System	61
3.14	Muscle Tension Generated by Stretch to Three Lengths as a Function of Vestibular Stimulus Rate	63
3.15	Single Shock Vestibular Influence on Dorsal Root - Ventral Root First Peak Amplitude Reflex Responses	64

<u>Figure No.</u>		<u>Page No.</u>
3.16	The Reflex Posture Control Model and Its Response Characteristics	67
3.17a	Distribution of Reflex Gains for 1/2 Degree Steps in Ankle Angle	71
3.17b	Distribution of Reflex Gains for 1/2 Degree Steps in Ankle Angle	72
4.1	The Body and Its Sway Dynamics	79
4.2	Postural Sway Induced by Lateral Deflection of the Platform	81
4.3	Typical Postural Responses to Induced Sway Motion	85
4.4	Vestibular Threshold Response Characteristics to Induced Sway Motion	86
4.5	The Semicircular Canal Model	88
4.6	The Utricle Otolith Model	90
4.7	Response Threshold as a Function of the Initial Angle Offset of the Body, Simulation of the Vestibular Model	92
4.8	The Amplitude of Oscillation Just Necessary to Produce a Threshold Response in Each Vestibular Organ as a Function of Sway Frequency	93
4.9	Typical Body Angle and Ankle Torque Response Sequences During Vestibular Regulation of Posture	95
4.10	Average Body Angle and Ankle Torque Responses During Vestibular Regulation of Posture	97
4.11	Model for Vestibular Regulation of Posture	99

<u>Figure No.</u>		<u>Page No.</u>
4.12	Vestibular Control Model Characteristics Compared with Experimental Data	101
5.1	RMS Error for Control of an Inverted Pendulum	106
5.2	Average Body Angle and Ankle Torque Response Sequence During Three Control Conditions	109
5.3	Amplitude Ratio Comparing Fourier Coefficients of Body Sway Motion With and Without Reflex/Exteroceptive Control	113
5.4	Amplitude Ratio Comparing Fourier Coefficients of Body Sway Motion With and Without Visual Cues	114
5.5	Revised Model for Reflex Control of Posture Including the Exteroceptive and Utricle Otolith Feedback Loops	116
5.6	Characteristics of the Reflex/Exteroceptive Control Model Compared with Experimental Data	117
5.7	A Model for Vestibular and Visual Control of Posture	119
5.8	Vestibular/Visual Control Model Characteristics Compared with Experimental Data	119
6.1	Distribution of Reflex Gains for 1/4 Degree Steps, Vestibular Defective Subject Standing with Eyes Open	124
6.2	Distribution of Reflex Gains for 1/4 Degree Steps, Vestibular Defective Subject Standing with Eyes Closed	125
6.3	Response Threshold to Induced Sway Motion of the Vestibular Defective Subject	126

<u>Figure No.</u>		<u>Page No.</u>
6.4	Typical Postural Responses of the Vestibular Defective Subject, Standing on a Rigid, Flat Surface	128
6.5	Fourier Coefficients of Body Sway Motion for the Vestibular Defective Subject Standing on a Rigid, Flat Surface with Eyes Open	130
6.6	Fourier Coefficients of Body Sway Motion for the Vestibular Defective Subject Standing on a Rigid, Flat Surface with Eyes Closed	131
7.1	The Basic Features of the Postural Control System	139
7.2	Properties of the Posture Control Sensors	140
A.1	Physical Characteristics of the Body	144
B.1	The Experimental Platform	148
B.2	Reading Torque on the Platform Base	149
B.3	Characteristics of the Torque Measurement	149
B.4	Reading Body Angle with Respect to Vertical	151
B.5	The Two Degrees of Platform Motion	151
D.1	Analog Patch for Simulation of Reflex Gain Control	158
D.2	Analog Patch for Simulation of the Vestibular Sensor Dynamic Characteristics	159
D.3	Analog Patch for Simulation of the Vestibular Posture Control Model	160
D.4	Analog Patch for Simulation of Reflex/Exteroceptive Control of Posture	161
E.1- E.12	Reflex Responses to Steps in Platform Angle	163- 174

<u>Figure No.</u>		<u>Page No.</u>
E.13	Distribution of Reflex Response Gains for Five Step Sizes	175
E.14- E.25	Fourier Coefficients for Body Sway Motion	176- 187

## CHAPTER 1

### INTRODUCTION

The sensory-motor system is the mechanism through which man interacts with his physical environment. This system is necessary for survival since it provides the means for detecting features of the environment, spatial configuration, smell, temperature, etc., and for coordinating motor activities in response to the sensory information. Thus man could gather food, build shelter, and move quickly from place to place. In the technological world of today, man has constructed machines which greatly extend his capability to perform these basic sensory-motor tasks. This technology has provided man with problems and challenges. Most of these machines still require a man as the ultimate master. Hence, man, with the same basic sensory-motor system adapted to simple bipedal locomotion is asked to control mechanical "extensions" of his physical body with far more complex dynamic characteristics, under conditions considerably more exacting. In solving the problems that arise from man-machine interactions, engineers and physiologists have sought greater understanding of the neuro-

physiological mechanisms that control orientation of the body in space.

The same technological understanding which extends man's motor capabilities can also help to restore artificially the sensory and motor functions in people in which injuries or disease have impaired these mechanisms. Here too, a thorough understanding of posture control function is necessary before artificial components can be successfully integrated with natural motor and sensory functions.

To gain a greater understanding of postural mechanisms, physiologists have studied in detail the components involved in motor and sensory functions. More recently, physiologists and engineers, using control theory techniques with physiological data, have developed models which define and predict response characteristics for many of the motor and sensory components.

The thesis research attempts to carry the control theory description of postural mechanisms one step further. A series of experiments with human subjects forms the basis for a multiloop control model which describes the way a human uses multiple feedback sensors to control his orientation during a simple quiet standing task. The current models for motor and sensory components are used in this model. Particular emphasis is placed on defining the role of each sensor and on modelling the functional interfaces between these sensors and postural responses.

## 1.1 Scope of the Research

The thesis seeks to define the basic functional properties of the posture control system during a relaxed standing task. Because of the inherent complexity of even this basic control task, analysis is simplified by considering only control of forward and backward rotational motions of the body about the ankle joint, hereafter termed body sway or body angle motion. Body sway motion represents the critical mode in control of posture because of the inherently unstable "inverted pendulum" characteristics of the body. Therefore, this simplification is justified. Relative motion between upper body segments is of considerably less consequence during quiet standing and may be neglected here. Hence, the goal of the postural control system in this simple task is to assess the current status of body sway motion and generate appropriate ankle reaction torques to maintain stability.

The research is divided into three segments. First, a general posture control model is assembled, given current models for motor and sensory components and the general properties of neural processing described in the literature. This general model then forms the basis for a series of experiments. Finally, experimental observations are combined with the general physiological model to develop specific models for the sensory-motor interface.

In both the design of the experiments and development of the final models, the highly adaptable and non-stationary characteristics of the system are recognized. Experiments use transient disturbances which probe the states of the system at specific instances in time or during very short periods in which characteristics remain relatively constant. The models also define transient rather than continuous control processes.

Sensory deprivation techniques are employed during experiments to isolate characteristics of the individual sensory feedback modes. These methods allow observation of a number of control strategies and enable a more complete determination of the range of adaptability of the various sensory feedback modes.

## 1.2 Applications of the Research

### 1.2.1 Basic Physiology

Physiology of posture control mechanisms has been the topic of considerable research effort. To date there have been descriptions of the characteristics of individual sensory, neural, and muscular components. The validity of these descriptions has been reinforced with the development of control type models for these components which predict their input-output characteristics. Descriptions of overall posture control processes, however, have been limited to general cases based primarily on "educated speculation."

This thesis attempts to expand the knowledge of sensory-motor processing by describing specific functional relationships between the feedback sensors and the initiation of postural commands. Although these descriptions of neural processing in the model are purely functional, care is taken that the defined relationships have basis in the physiology. The completed model thus suggests a general framework in which more specific physiological experiments may be interpreted.

### 1.2.2 Medical Applications

Possible medical applications fall into two general categories:

1. Diagnosis of sensory disabilities affecting posture control
2. The development of artificial limbs which are involved in the regulation of posture.

A number of experimental techniques are developed which, in conjunction with the model, enable a rapid determination of the sensory modes being employed by a subject to control posture. In addition, sensory deprivation techniques allow independent observation of several sensory feedback modes. These techniques, together with a body of data on performance of normal subjects, should enable diagnosis of some types of sensory deficiencies.

Natural "feel" in the operation of an artificial limb is a major factor in its acceptance and successful use by a

patient. In the case of artificial legs, the posture control model might help in the development of natural responsiveness in the limb by answering the following questions:

1. What active motor functions are most important to include in the artificial limb?
2. What feedback senses are most important to enable efficient regulation of the limb's active function?
3. How might the active limb best be integrated into the central nervous system?

### 1.2.3 Technology

Engineers developing control interfaces between a pilot and his vehicle have been intrigued by the simple, almost effortless way in which a human controls his own orientation. They have contemplated ways to link the man-vehicle interface to this posture control system so that the pilot's postural responses might also control the orientation of his vehicle. As is the case in developing artificial limbs, success of such a scheme requires that the sensory feedback and control effector interfaces have the feel of "natural" postural processes. Hence, the posture control model may help answer some of the same questions confronting the designers of artificial limbs. In addition, the man-vehicle engineer faces some other questions that the model may help answer:

1. What are the maximum performance capabilities of the posture control system during a given control task?
2. How might these capabilities be enhanced by pre-processing of the postural stimuli presented to the men?

## CHAPTER 2

PHYSIOLOGY OF POSTURE REGULATION

Sensors in all areas of the body are used in the control of posture. Some of these sensors measure within a body reference frame, while others indicate orientation of the body with respect to its external environment. In the central nervous system, the task of sensory processing and generation of muscle commands is multilevel, the lowest levels of coordination located at the spinal ventral roots and subsequent levels extending upward to the highest brain centers.

Although understanding of posture physiology is far from complete, many features of organization and function have been described. The current literature on posture physiology is reviewed here and a general model is assembled using the properties of the muscular, sensory, and neural components described in this literature.

2.1 Anatomy of the Lower Leg<sup>23,78</sup>

Figure 2.1 introduces the basic bone and muscle structure of the lower leg and foot. The following paragraphs consider

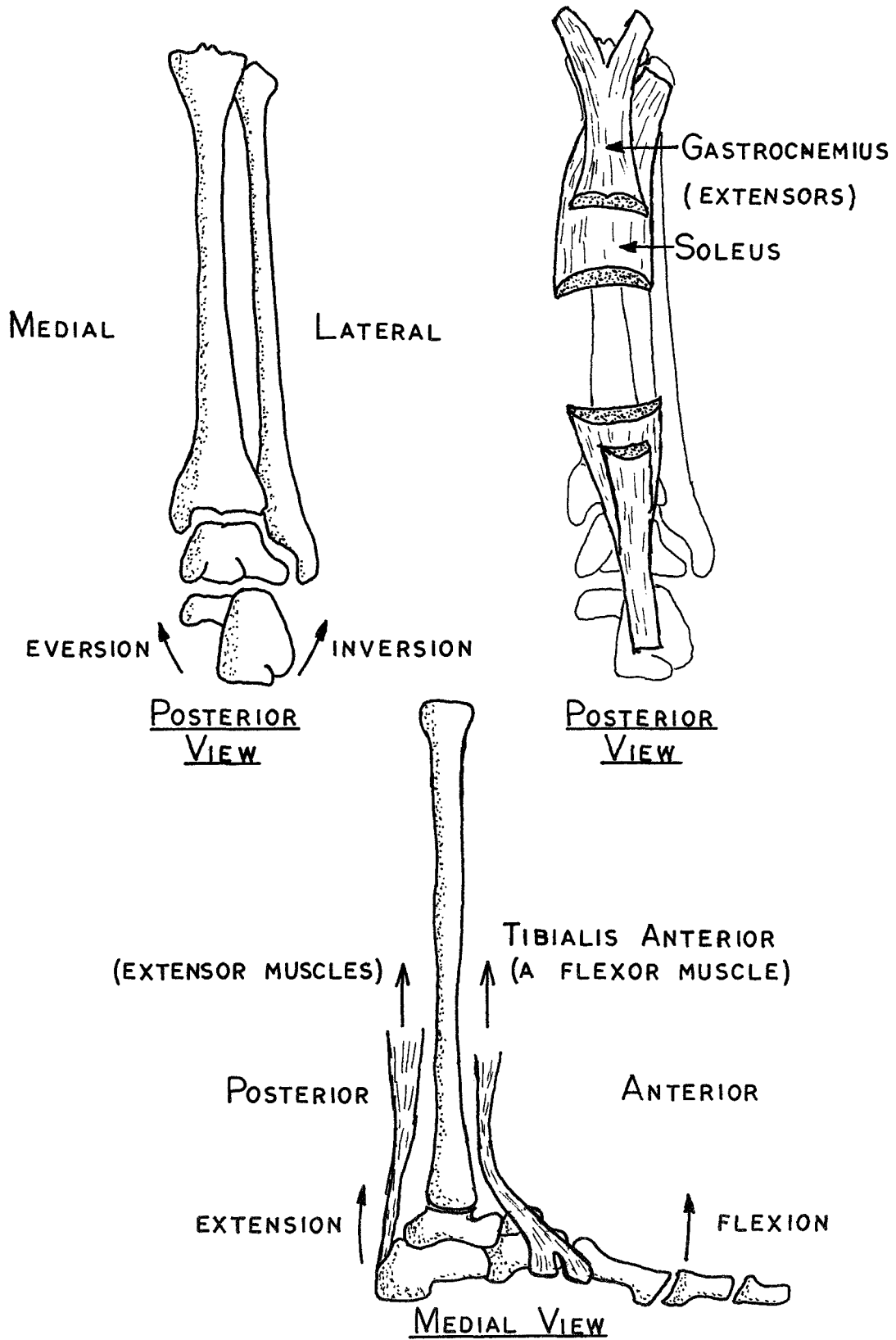


FIGURE 2.1 ANATOMY OF THE LOWER LEG (REF. 78)

the mechanical properties of joint motion and the generation of ankle torques during posture control.

Positive body angle, leaning forward, (dorsiflexion), corresponds to flexion of the ankle joint; negative body angle, to ankle joint extension (plantarflexion). The gastrocnemius and soleus muscles are the primary effectors of ankle joint extension. Their point of insertion (Achilles tendon) on the calcaneus bone of the foot is within the plane of ankle extension-flexion motion, therefore, gastrocnemius-soleus force produces pure extensor ankle joint motion.

Function of the muscles effecting ankle joint flexion is somewhat more complex. The tibialis anterior inserts at a point medial (toward center line) to the plane of extension-flexion motion. Therefore, tibialis anterior force produces a combination of ankle joint flexion and eversion. Force in the peroneus tertius produces a combination of ankle flexion and inversion. Coordinated activation of these two muscles produces pure ankle flexion motion.

An adequate model for muscular initiation of ankle torque lumps flexor and extensor muscles into a single agonist/antagonist pair.

A determination of maximum magnitude of extensor and flexor muscle motions, velocities and changes in length is necessary in developing models for muscle force characteristics. Anatomical dimensions and body angle motion characteristics are required in order to compute these values. The

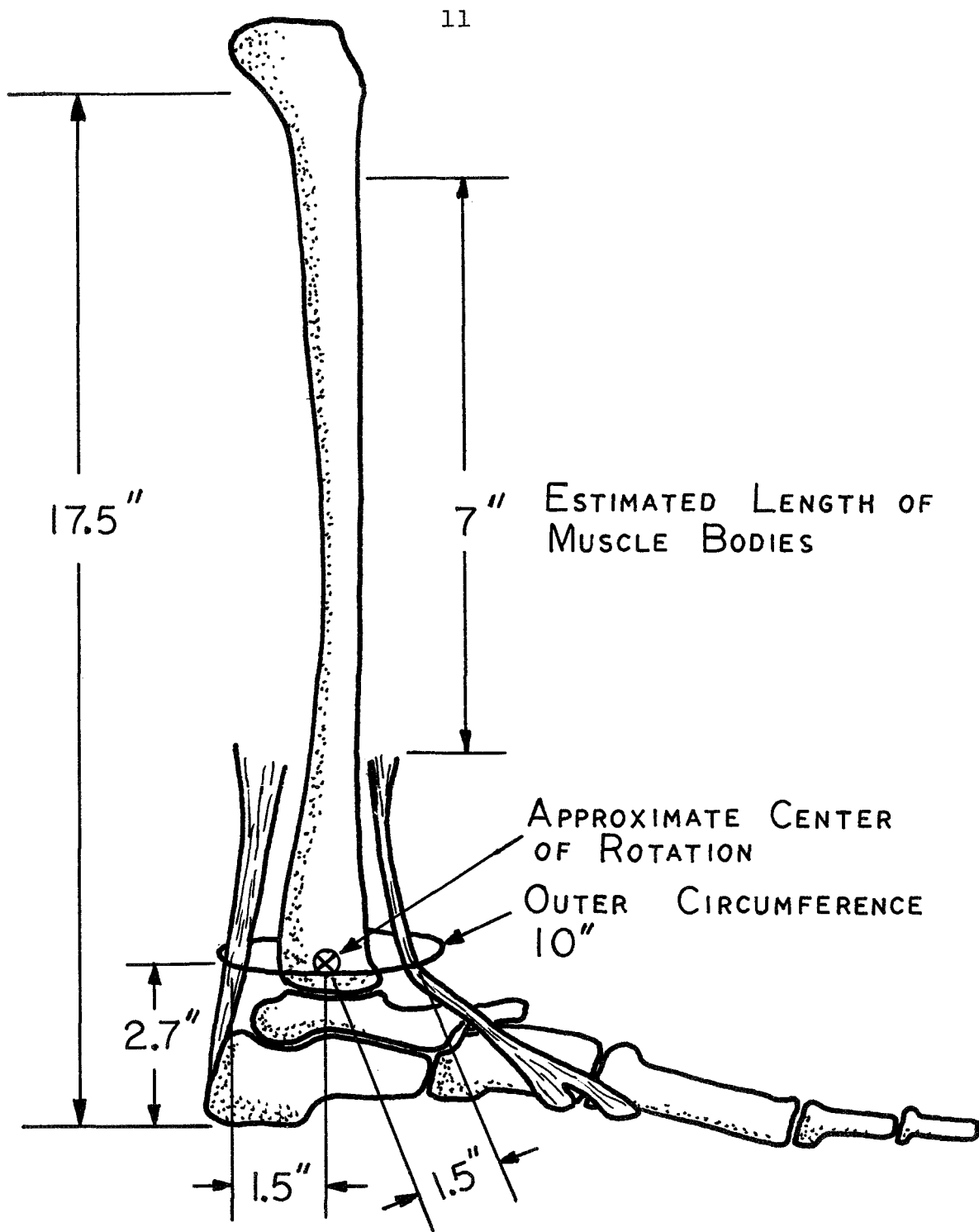


FIGURE 2.2 ANATOMICAL DIMENSIONS OF THE LOWER LEG

latter are provided by experimental studies within the thesis. Estimates of the anatomical dimensions are made using drawings (78) and Demotser's data on the average dimensions of body segments (23). These are shown in Figure 2.2.

Experiments in Chapters 4 and 5 show that angular motions of the ankle joint are restricted to a range of  $\pm 2$  degrees and that the frequency of these motions is less than 0.5 hz during posture control tasks examined in this thesis.

Using these parameters, the following maximum values for muscle stretch velocity and length change are found:

$$|\Delta L| < 0.0075L_0$$

$$|V| < 0.0225L_0/\text{SEC.}$$

where  $L_0$  is the resting length of the muscle.

## 2.2 Posture Muscles -- The Response Effectors<sup>15,19,47,53,68</sup><sub>76,89,107,108,115</sub>

This section contains a brief description of the tension generating characteristics of skeletal muscle. Effects of neural innervation, muscle length, and muscle stretch velocity on tension are considered.

Skeletal muscles are composed of numerous muscle fibers, each extending the entire length of the muscle. All fibers are roughly parallel in orientation. A single muscle fiber is in turn subdivided into several thousand parallel units called myofibrils. The mechanisms of contraction lie within these tiny myofibrils.

Skeletal muscle is innervated by axons from alpha motoneurons. Each motoneuron innervates a number of muscle fibers

which always act in unison. This group of fibers is termed a motor unit, thus forming the basic functional unit of muscular contraction.

The total muscle output is the summation of tension developed by each of the motor units within the muscle. Simplified muscle models, considering the muscle as a single force generating unit, predict input-output characteristics. A single component model is considered here.

The variables affecting muscle output (tension) are the following:

1. activation level (in the single component model this is the average activation level of all motor units in the muscle.)
2. instantaneous length of the muscle
3. shortening velocity of the muscle

Hill (53) proposed a general relationship between force output and shortening velocity of muscles:

$$(P + a)(V + b) = b(P_0 + a) \quad (2.1)$$

where  $P$  = muscle force  
 $V$  = shortening velocity  
 $P_0$  = isometric (i.e.,  $V = 0$ ) maximum tension  
 $a$  and  $b$  = constants

For maximally stimulated shortening muscle, the relationship fits experimental data fairly well. The equation also applies for less than maximum activation levels if  $P_0$  is replaced by  $P_A$ , the maximum isometric tension for a given level of muscle activation. The relation, however, breaks down for all but

very slow rates of muscle lengthening. Studies since Hill's first proposal have also shown definite errors in the relationship for predicting the fine details of muscle response characteristics. The basic relationship, however, is useful as a modelling tool. Figures 2.3 and 2.4 compare theoretical force-velocity relationship with experimental data of Joyce et al (68).

Force generating characteristics of muscle are also dependent on the length of the muscle. Strictly speaking, Hill's force-velocity relationship is valid for constant length; it is able to predict instantaneous force levels only.

Force-length characteristics of muscle are dependent on both active and passive mechanical properties of muscle. Figure 2.5 shows these relationships. The passive mechanical resistance is only present for large stretch lengths. Active properties show a "bell" shaped curve; tension for a given rate of stimulation is maximum at rest length and decreases if the muscle is either shorter or longer than this optimal length.

Most muscle-initiated movements involve muscle action within the general region of rest length. For this operating region a roughly linear relationship, dependent only on muscle activation level, can be defined. These roughly linear segments of the length-tension curve are shown as dotted lines in Figure 2.5.

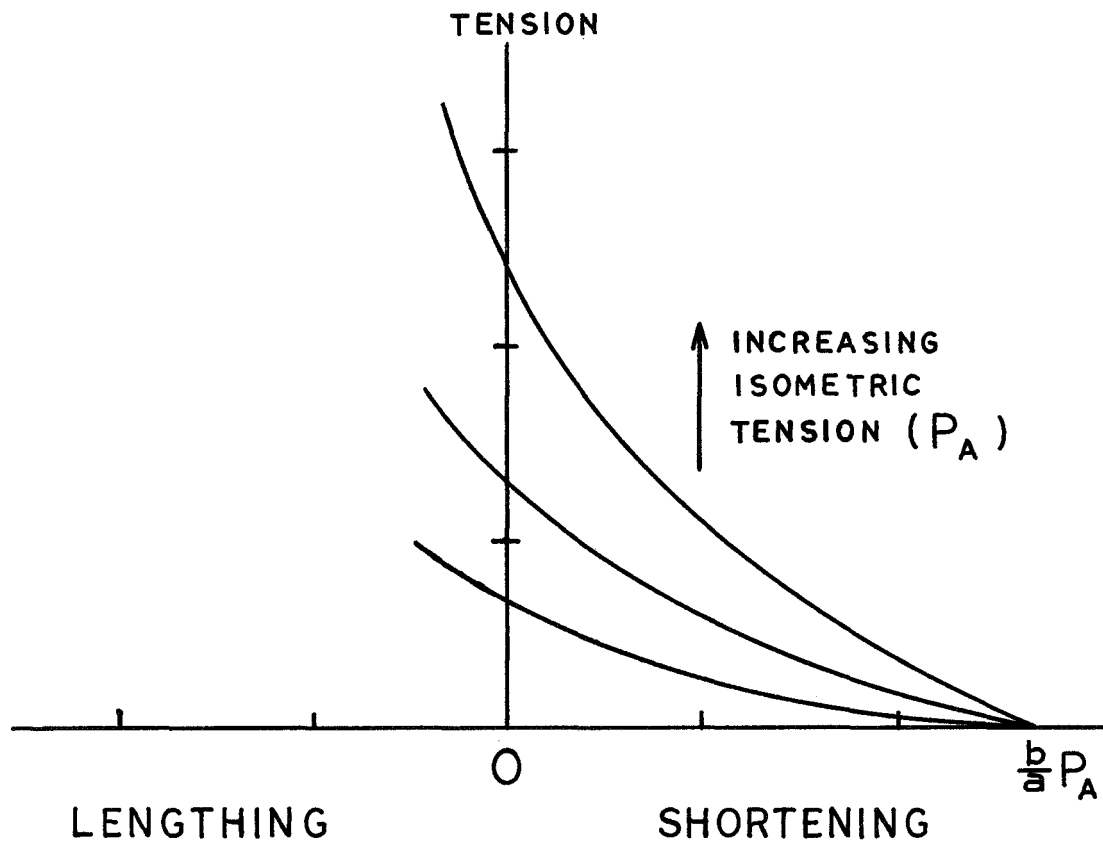


FIGURE 2.3 FORCE-VELOCITY CHARACTERISTICS OF MUSCLE ACCORDING TO HILL'S EQUATION

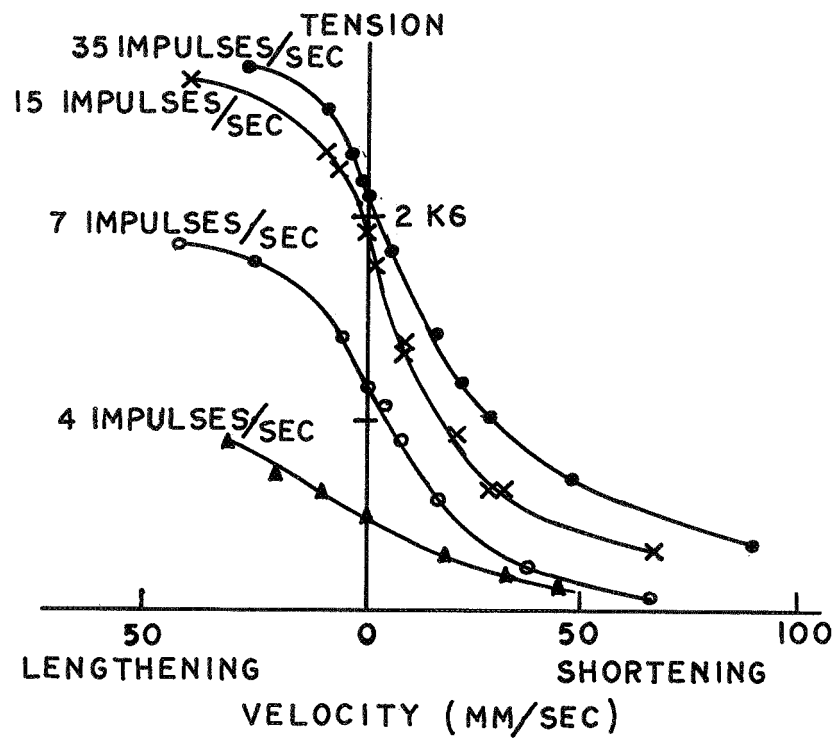


FIGURE 2.4 EXPERIMENTALLY OBSERVED FORCE-VELOCITY CHARACTERISTICS OF CAT SOLEUS MUSCLE DURING VARIOUS RATES OF ACTIVATION (REF. 68)

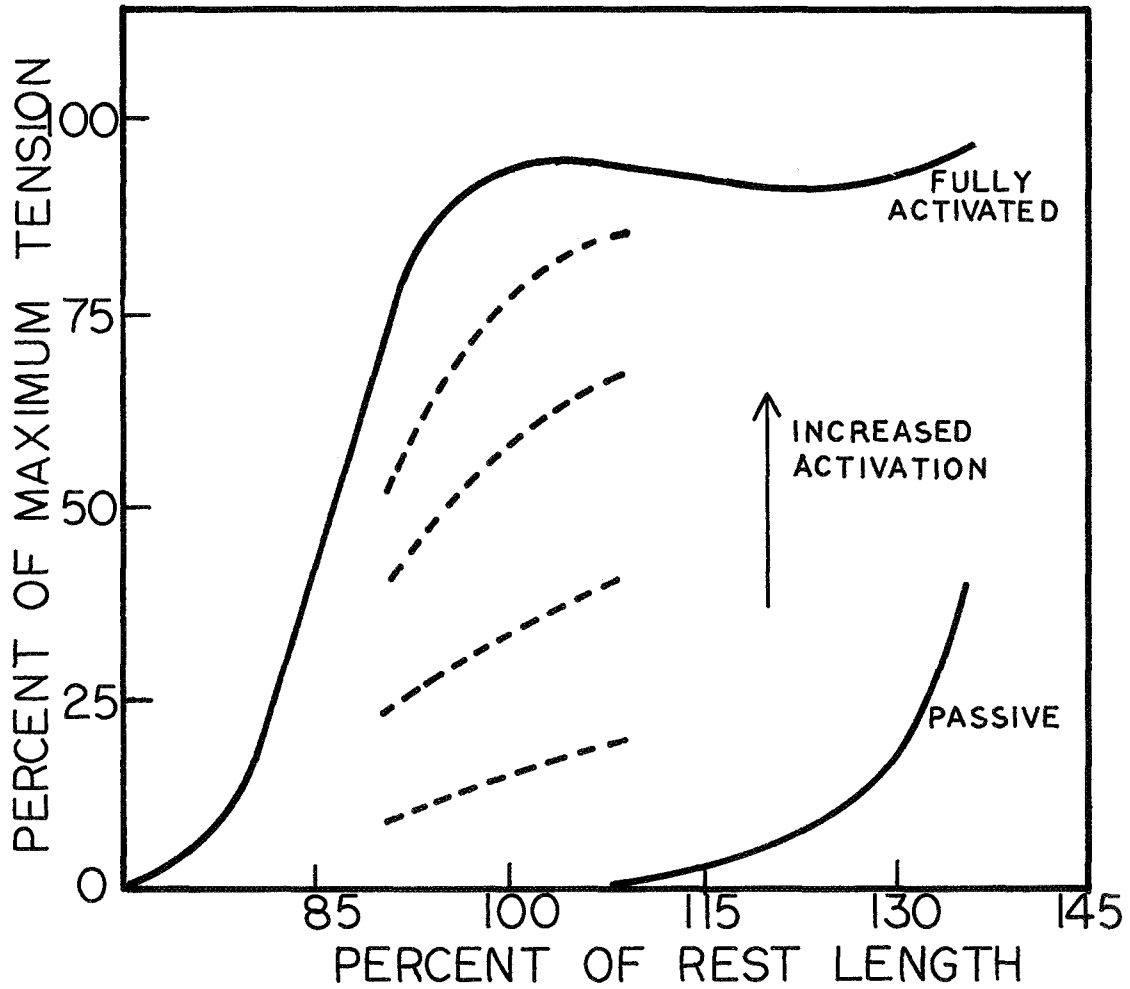


FIGURE 2.5 APPROXIMATE LENGTH-TENSION CHARACTERISTICS OF MUSCLE AS A FUNCTION OF ACTIVATION RATE (REF. 76)

The posture control tasks in this thesis involve only small changes in length and velocity. Calculations in section 2.1 show that changes in length are about  $\pm 0.75\%$  of rest length with maximum expected stretch velocities of about 2.25% per second. In this case, the preceding relationships can be combined into a linearized equation in which effects of activation, length, and stretch velocity are independent of one another:

$$P = P_0(f_0, L_0, V_0) + \left( \frac{\partial P}{\partial f} \Delta f + \frac{\partial P}{\partial L} \Delta L + \frac{\partial P}{\partial V} V \right) \left\{ \begin{array}{l} f=f_0 \\ L=L_0 \\ V=V_0=0 \end{array} \right\} \quad (2.2)$$

where

$\Delta f$  = small changes in activation level (impulses/sec)

$\Delta L$  = small changes in length (mm)

$V$  = small stretch velocities (mm/sec)

The relationship for changes in tension thus reduce to the simple form:

$$\Delta P = K_f \Delta f + K_L \Delta L + B_m V \quad (2.3)$$

where

$$K_L = K_L(f_0)$$

$$B_m = B_m(f_0)$$

Equation 2.3 adequately describes the force generating component of muscle. The addition of an elastic element in series with the force generator,  $K_s$ , attributable to tendon and connecting tissue, is necessary for the model to describe

experimental observations. The complete lumped parameter model commonly used to describe muscle dynamics is shown in Figure 2.6.

For this model, the isometric step response is approximately:

$$\frac{P}{\Delta f} (s) = \frac{K_f}{1 + \frac{B_m}{K_s} s} \quad (2.4)$$

where  $s$  is the LaPlace transform operator. Isometric step response time is highly dependent on the rate at which the muscle is stimulated. At large tetanic stimulus rates (15) the step response time constant for a slow skeletal muscle (soleus) ranges from 50 to 100 milliseconds. For slower stimulus rates, response time is considerably longer than 100 milliseconds (75).

## 2.3 The Feedback Sensors<sup>2,4,14,42,57,61,64,72,81,98,113</sup>

### 2.3.1 Muscle Spindles

Structure:

Muscle spindle receptors, several centimeters in length are interspersed throughout muscles. Each measures local muscle length. Muscles involved in fine control have more receptors per unit weight than those performing coarse movements.

The spindle is composed of several small intrafusal muscle fibers of two types, nuclear bag and nuclear chain fibers. Collaterals from a single primary group I afferent

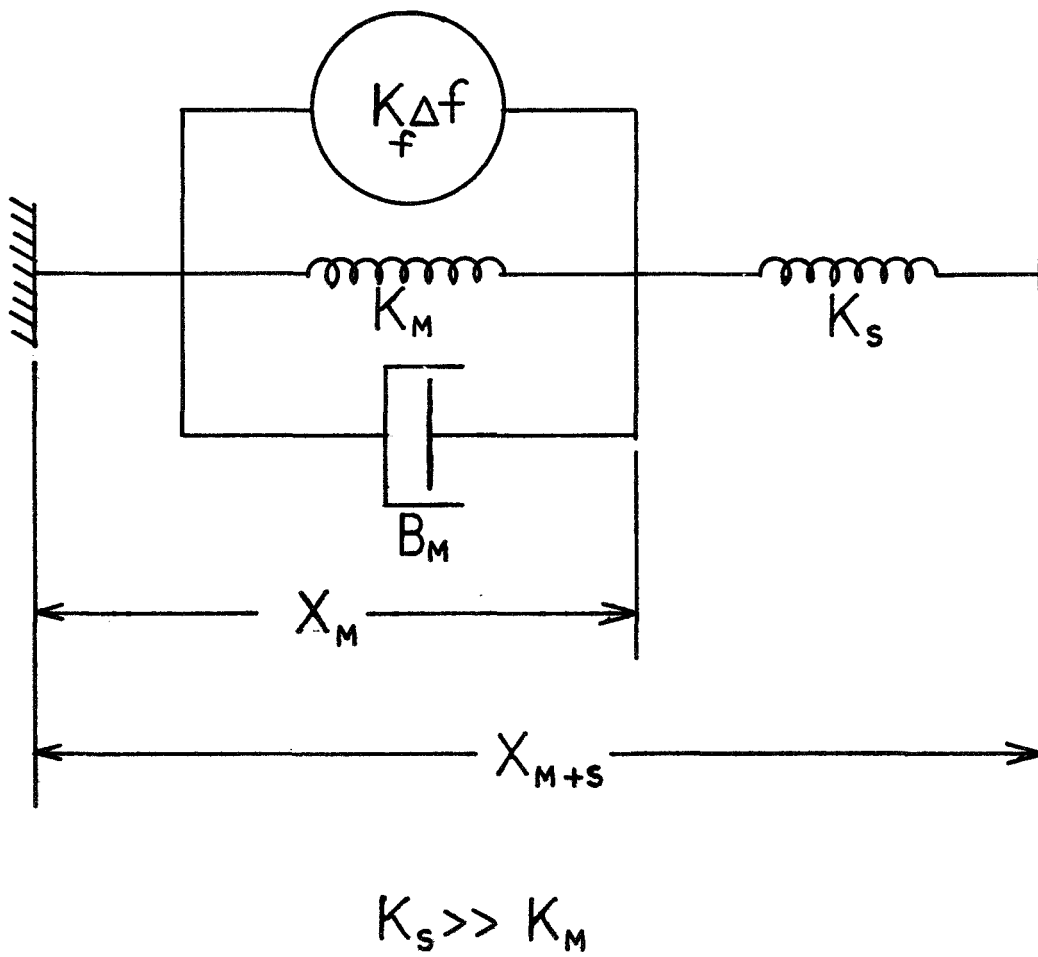


FIGURE 2.6 LUMPED PARAMETER MODEL FOR MUSCULAR CONTRACTION (REF. 98)

nerve fiber spiral around the central region of each spindle fiber (annulospiral endings). Collaterals from a small secondary group II afferent fiber form diffuse endings (flower spray endings) adjacent to the central region, generally on nuclear chain fibers, but occasionally on nuclear bag fibers as well.

Intrafusal muscle fibers are innervated by small  $\gamma$ -efferents, separated anatomically into two groups according to the type of ending:

1. plate endings; mostly on bag but also on a few chain fibers
2. trail endings on both bag and chain fibers

Figure 2.7 illustrates muscle spindle structures.

**Function:**

Evidence suggests that primary and secondary afferent response levels of the spindle are directly proportional to deformation of intrafusal fibers in the region of sensory ending. Annulospiral endings of the primary afferent fiber respond in proportion to both length and the rate of stretch of the intrafusal fibers. Secondary endings respond primarily in proportion to the length of the intrafusal fiber.

Functionally,  $\gamma$ -efferents can be separated into two groups,  $\gamma$ -dynamic and  $\gamma$ -static fibers. There is no consistent relationship between functional and anatomical definitions. Increased  $\gamma$ -dynamic activity increases the velocity sensitivity of the primary afferent response. Activity of the  $\gamma$ -static

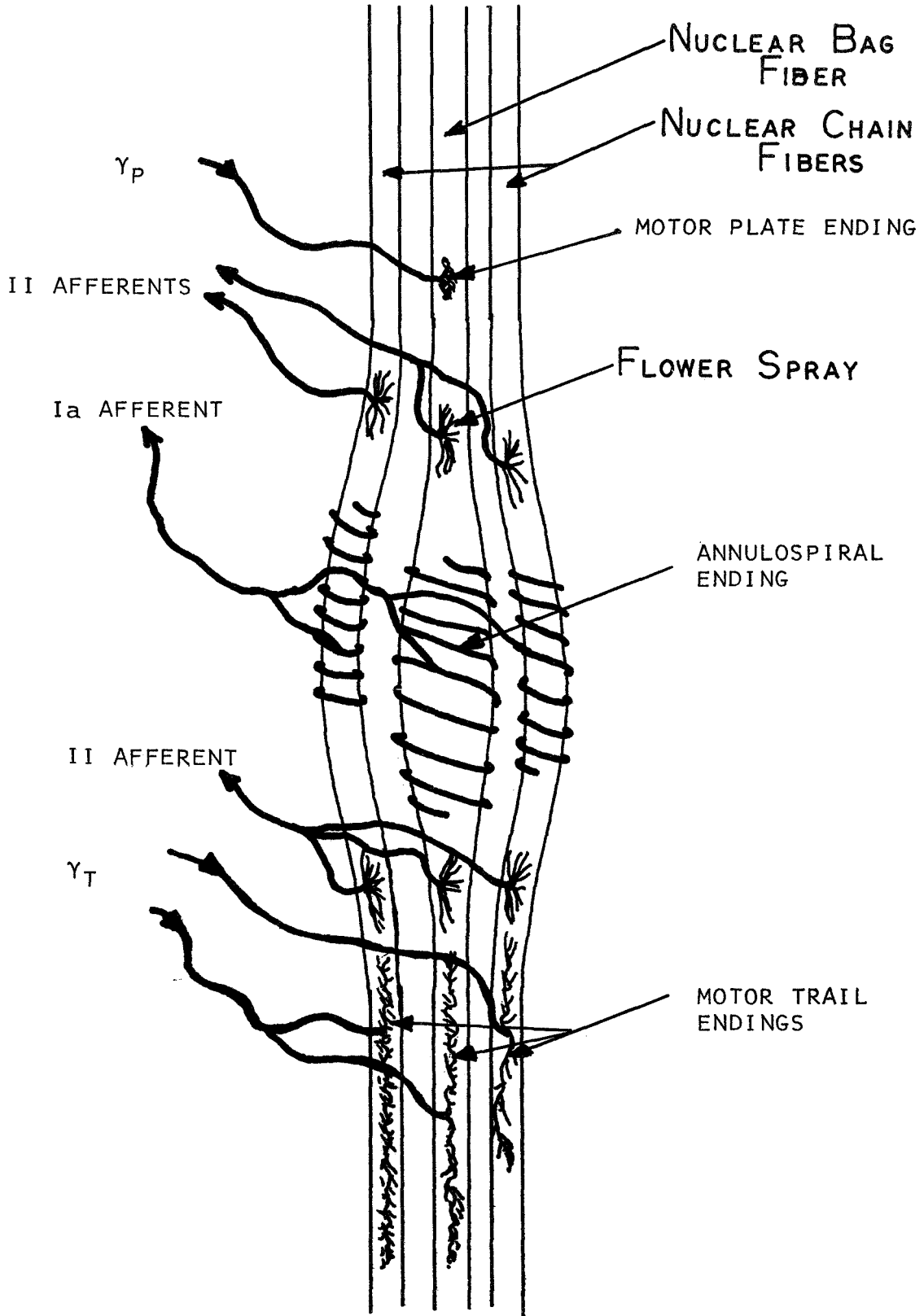


FIGURE 2.7 REPRESENTATION OF THE GENERAL FEATURE OF THE MAMMALIAN MUSCLE SPINDLE

fibers determines the bias discharge levels in the responses of both the primary and secondary afferents. Jansen et al. (64) recording from individual primary and secondary afferents, conclude that static and dynamic response characteristics may have relatively independent control.

Models:

Investigators (56,61,98,113) have developed models for the primary afferent response of the muscle spindle in the general form:

$$f(s) = \frac{K(T_1s + 1)}{(\alpha T_1s + 1)(T_2s + 1)} X_m(s) \quad (2.5)$$

$f(s)$  = output firing rate in pulses/sec

$X_m(s)$  = muscle spindle length in mm

$K$  = muscle spindle gain in pulses/sec/mm

Agarwal et al. (2), using this model to match step response data of Lippold et al. (72) found the following parameter values:

$$T_1 = 0.28 \text{ sec}$$

$$T_2 = 0.0055 \text{ sec}$$

$$\alpha = 0.21$$

They show that the "lead-lag" model is adequate to predict the basic form for the response of the mammalian muscle spindle to stretch inputs.

### 2.3.2 Golgi Tendon Organs<sup>56, 58,59,60</sup>

The Golgi tendon organ is a muscle force transducer. Each ending is located in series with a small number, 3 to 25, of extrafusal muscle fibers, and it measures the total force exerted by the group. The group of muscle

fibers comprising one organ unit are generally from different motor units; thus, each organ samples the level of activity in several motor units. The Golgi organ has no motor innervation.

Afferent fiber endings in the Golgi tendon apparatus closely resemble the flower spray endings of the spindle secondary afferent fiber.

In the past, Golgi organs were thought to function only as force limiters, inhibiting muscle response only when excessive loads threatened permanent damage. Because of this assumption, relatively little effort has been made to more accurately define Golgi organ response characteristics. Recently, Houk et al. (59) have shown that Golgi organs provide a high resolution reading of muscle tension throughout the force range of the muscle. They observe absolute threshold levels for each organ of less than 0.1 gram, concluding that the Golgi organs provide an accurate filtered sample of the active forces produced by the muscle. They define the following average response function:

$$h(t) = K(1 + B + C) U_0(t) - K[bBe^{-bt} + cCe^{-ct}] U_1(t)$$

where

$$K = 4 \text{ pulses/sec/gram}$$

$$B = 1.0, b = 2.0/\text{sec}$$

$$C = 2.0, c = 25/\text{sec}$$

$$h(t) = \text{output firing rate}$$

$$U_0(t) = \text{unit step function}$$

$$U_1(t) = \text{unit impulse function} \quad (18)$$

Functionally, Golgi organ afferents form an inhibitory disynaptic pathway with motoneurons of the same muscle.

Houk et al. (58) postulate that Golgi organ feedback acts as a continuous force regulating loop, correcting for variations in muscle response characteristics due to fatigue and to length and velocity changes.

### 2.3.3 Joint Receptors<sup>11,20,36,98,105</sup>

Three types of sensory endings within the joints of limbs are responsive to rotation:

1. free endings in both the joint capsule and ligaments surrounding the joint
2. non-encapsulated spray endings, Raffini joint receptors, primarily within the joint capsule
3. encapsulated endings in ligaments and the joint capsule.

By far the most common are the "spray type" endings located within the connective tissue of the capsule. Some receptors respond over a limited angular range, while others respond within a much broader range. At any given angle it is likely that a number of receptors are active.

Recordings from first order afferents innervating the capsule of the knee joint, by Boyd et al. (11) show that in the cat responses are proportional to both position of the joint and its rate of movement.

Viernstein (105) observed transient response characteristics of first order afferents in the knee joint of the monkey, sensitive to angular motion of the joint. He concluded that a simple "lead-lag" transfer function can be

used to characterize the relationship between angular position and impulse frequency response.

#### 2.3.4 Deep Pressure Sensors<sup>9,36,47</sup>

Very little quantitative data relevant to a control description of the deep pressure sensors are available. Bouvassa et al. (9) observing cortical evoked responses, found that only very few peripheral afferent fibers need be active for perception. Unfortunately, no data are available to indicate linearity or dynamic range of pressure discrimination. Little is known about how responses of the individual receptors are combined to enable integrated perception of body motions and forces.

#### 2.3.5 The Vestibular System<sup>83,111,112</sup>

Characteristics of the vestibular system are well documented. A complete description can be found in the references listed above; a review of the details pertinent to posture control is given here.

Angular acceleration in three dimensional space is sensed by three approximately orthogonal semicircular canals in each inner ear. The utricle otoliths, one in each inner ear, are multi-dimensional linear accelerometers. They sense specific forces (linear acceleration plus gravity) in a plane rotated 30 degrees with reference to the horizontal plane of the head. Hence, combined canal receptors sense all relevant angular motions of the body; utricle otoliths

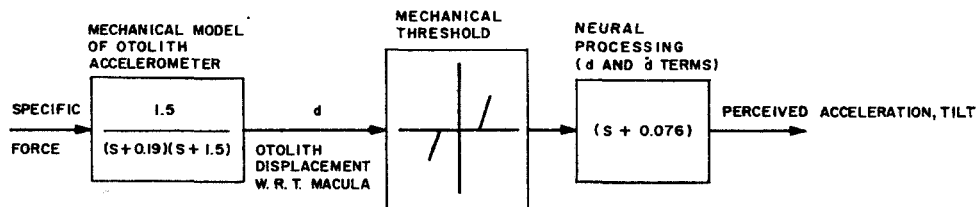
sense the summation of all linear and gravitational forces.

The canals are heavily damped accelerometers, with perceived output corresponding to angular velocity. Dynamic characteristics of the pitch axis canals are:

$$\frac{\text{Subjective angular velocity (s)}}{\text{Input angular acceleration (s)}} = \frac{7}{(7s+1)(0.1s+1)}$$

The threshold of perception of angular velocity is heavily dependent on the sensory mode in which it is measured. A thorough discussion of this point is included in Chapter 4.

The utricle otoliths are also heavily damped accelerometers, sensing both tilt angle and linear velocity. The revised non-linear otolith model of Young and Meiry (112), based on input-output data only, is given in Figure 2.8.



A DYNAMIC MODEL FOR THE UTRICLE OTOLITHS (REF. 112)

Figure 2.8

## 2.4 Organization of the Sensory-Motor Nervous System

### 2.4.1 Properties of the Single Neuron<sup>22,70</sup>

Integration in the nervous system is the result of summation of the integrating characteristics of individual neurons. A brief summary of neuron function follows.

Figure 2.9 shows the general form of a neuron. Three basic components of each cell include the dendrites, the soma or cell body, and a single axon. The nerve impulse, initiated by electrochemical activity in the cell membrane of the dendrites and soma is transmitted along the axon.

The synapse is the junction between neurons, or between nerve and muscle cells; transmission of a nerve impulse from one cell to the next occurs here. Reception and integration of these synaptic inputs take place along the dendrites and cell body of the neuron. This is a local, graded process in which incoming messages raise or lower the local membrane potential. Spatial and temporal summation of the many inputs determines the membrane potential at the point of emergence of the axon from the soma, the axon hillock. When the membrane potential at the axon hillock reaches a threshold value, a single response, in the form of an action potential or "spike" is generated and transmitted down the axon to other neurons or muscle fibers.

Since an impulse must cross the synaptic junction in order to effect a change in the membrane potential of the subsequent cell, the synapse is a locus for control of neural

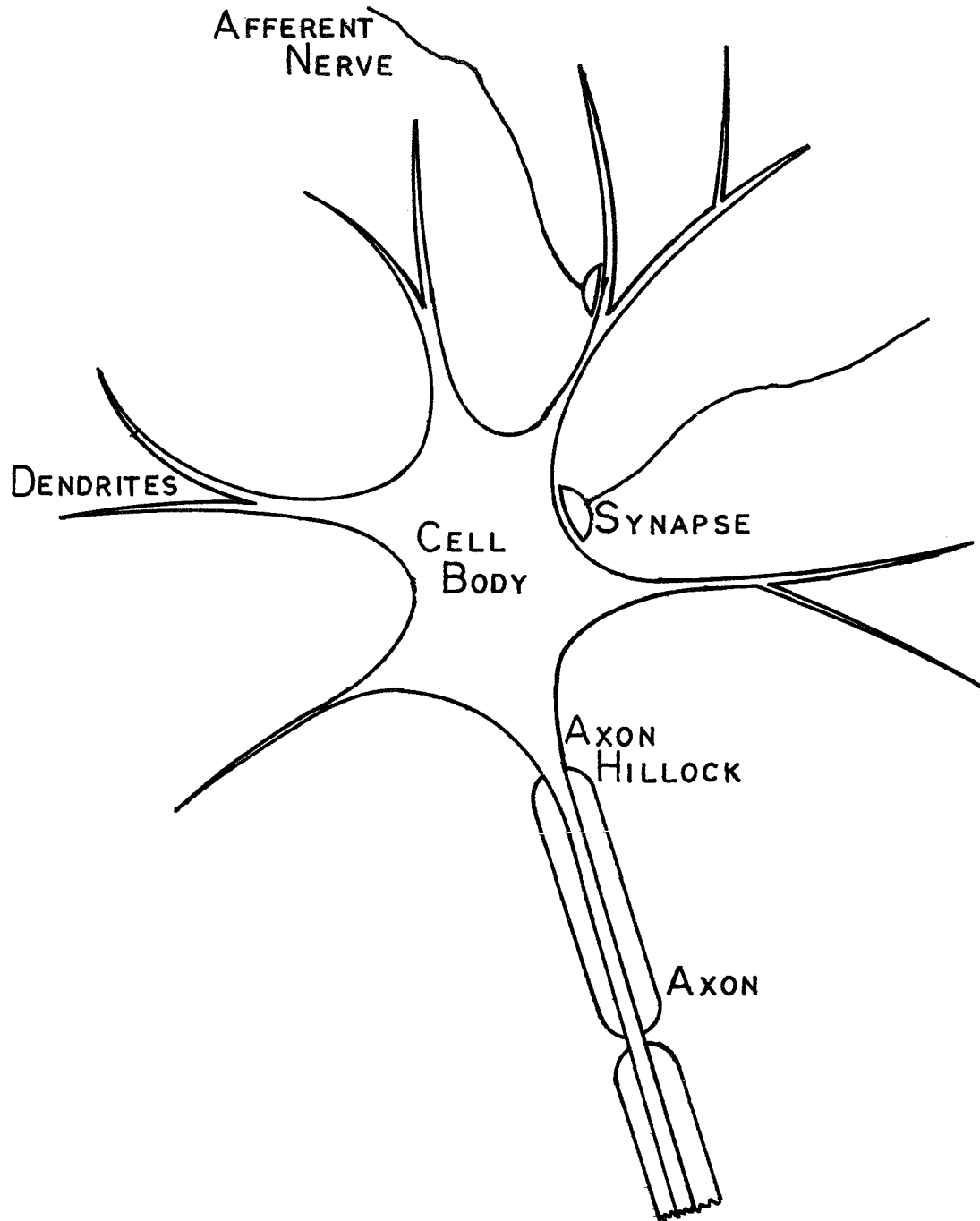


FIGURE 2.9 REPRESENTATION OF THE FEATURES OF A SPINAL MOTONEURON

activity. This control can be effected either pre- or postsynaptically.

Postsynaptic effects are either excitatory or inhibitory. Excitatory impulses drive the membrane potential toward the action potential threshold; inhibitory impulses stabilize the membrane potential or drive it away from the threshold.

Presynaptic effects do not directly change membrane potential levels; rather they interfere with the ability of other synapses to function, either as excitatory or inhibitory effects on the membrane potential. They inhibit transmission across the synapse.

Spatial location of a given synapse is also an important characteristic. Synapses near or on the soma are able to affect strong, rapid changes in membrane potential at the axon hillock. Synaptic activity more distant along the dendrites have weaker and slower acting effects.

Figure 2.10 briefly summarizes the integrative functions of a single neuron.

#### 2.4.2 The Spinal Cord Structure and Function <sup>8,10,12;29,31,32,33,38,44,62,74,95</sup>

A cross section through the spinal cord reveals a butterfly-shaped gray region surrounded by a white region. The white periphery contains ascending and descending tracts going to or originating from the higher brain centers. The central grey region is composed of cell bodies of interneurons, motoneurons, and ascending nerve fibers.

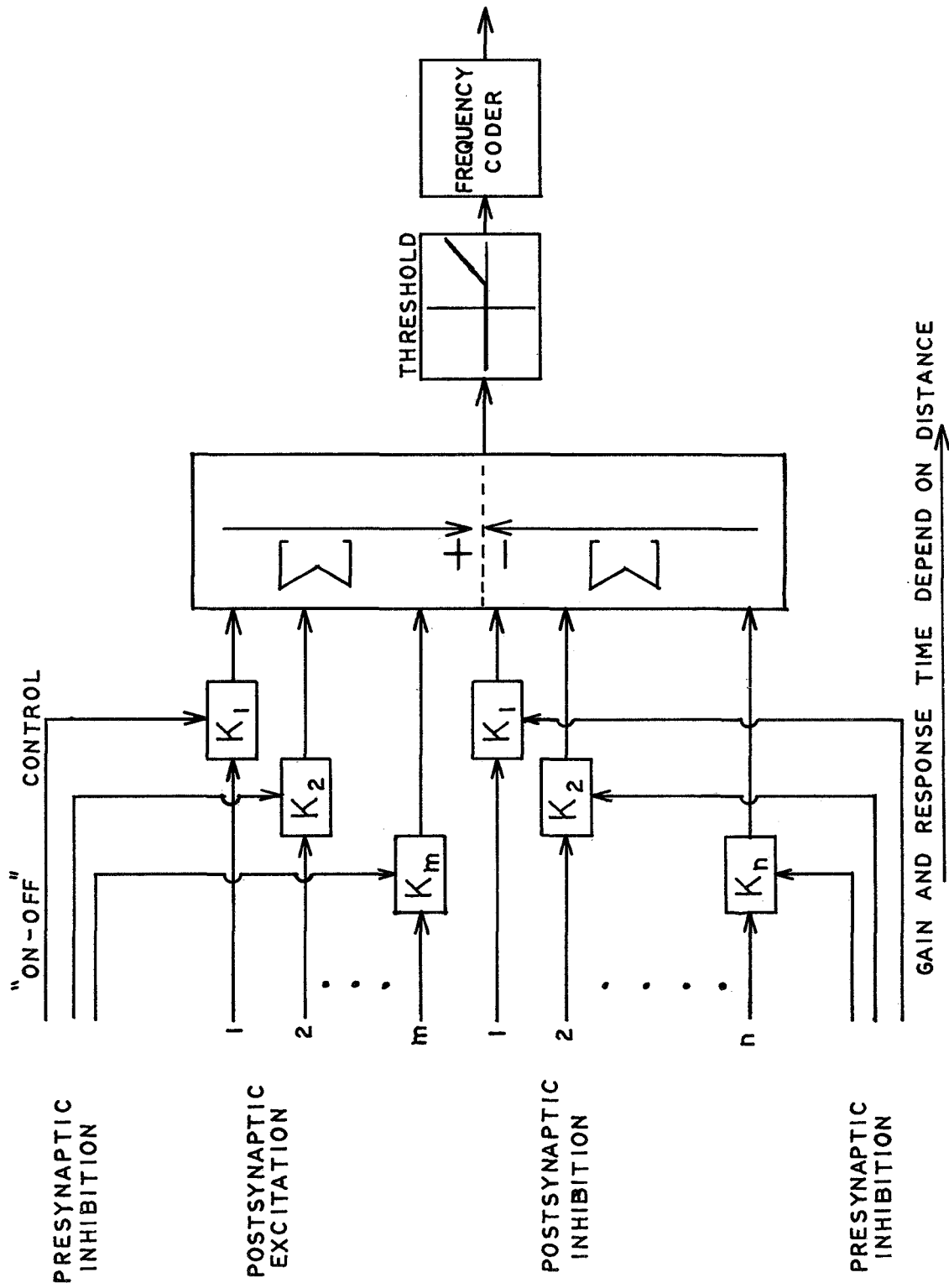


FIGURE 2.10 THE INTEGRATING FUNCTIONS OF A NEURON

Cell bodies of motoneurons are located in the ventral region of the gray matter. Axons of the motoneurons leave the spinal cord to innervate either skeletal or intrafusal muscle fibers. Alpha-motoneurons innervate skeletal muscle; smaller gamma-motoneurons innervate intrafusal fibers in muscle spindles. It appears that the effect of each gamma-motoneuron is exclusively "dynamic" or "static," so that independent control of phasic and static length feedback is preserved at the spinal level.

The primary group Ia afferent fiber of each muscle spindle enters the dorsal region of the gray matter and impinges monosynaptically on an alpha-motoneuron, activating the homonomous skeletal muscle. Collaterals from each afferent also innervate interneurons and neurons ascending the spinal tracts to the higher brain centers.

Muscle spindle secondary group II afferents impinge only on interneurons and on neurons ascending the spinal tracts to the higher brain centers. The effects of spindle secondary feedback is not understood.

Afferent fibers from Golgi tendon organs impinge on interneurons and neurons ascending the spinal tracts. Via simple disynaptic feedback pathways (an interneuron to an alpha-motoneuron) afferent fibers from Golgi organs act to inhibit activity in homonomous muscle fibers. Through this simple inhibitory mechanism, Golgi organs are believed to act as muscle force regulators. Pressure, touch and joint

receptors are associated with the more complex flexor, placing, and scratching reflexes. They also initiate actively in ascending spinal tracts.

A great deal of input integration takes place within the complex net of interneurons in the spinal cord gray matter. Although much of this integrative activity is not understood, investigators have found definite patterns of organization among sensory inputs and higher center commands. The following paragraphs include a few simple organizational patterns which have been observed. Several general models of sensory-motor organization at the spinal level are then proposed.

#### 2.4.3 Interaction Between Spinal Reflex Pathways

Simple mechanisms enable reciprocal action between stretch reflexes in extensor and flexor muscle pairs. When a stretch reflex is excited in one muscle of the pair, the stretch reflex in the opposing muscle is inhibited. The converse is also true; a decrease in afferent activity in muscle proprioceptors removes inhibition from the proprioceptor feedback paths to the opposing muscle, effectively facilitating the reflex path in the opposing muscle. These reciprocal pathways insure that total reflex activity in opposing muscles acts in concert, providing smooth, efficient regulation of motion.

The flexor reflex, activated by high threshold cutaneous afferents, strongly activates the flexor muscles of the limb,

withdrawing it from the source of painful stimulus. Flexor reflex afferents also act to inhibit transmission of Ia afferents (muscle spindle position feedback) in the extensor and flexor muscles. The effect of this inhibition is to open both position feedback loops to enable a maximum rate of withdrawal, i.e., "open loop " control.

#### 2.4.4 Function of the Higher Brain Centers

Remarks on the functions of the higher brain centers must be limited to a few generalizations.

Voluntary commands are generated in the "highest" brain area, the cerebral cortex, where information about the states of the body and the external environment reaches conscious experience.

Physiology of the cerebellum suggests that it is a coordinating center for motor control. Investigators have found that its microstructure is well suited to process complex sensory patterns.

Higher center commands act via descending tracts in the white matter of the spinal cord. These descending axons form synaptic junctions with interneurons and motoneurons, interacting with the spinal reflex pathways to determine the outflow from the motoneurons.

Descending fibers originate in the cerebral cortex and in the nuclei (large nerve masses) of the brain stem. Both the cerebral cortex and cerebellum exert an influence on activity in the brain stem nuclei.

The direct cerebral cortex efferents are believed to exercise strong, independent control over both the alpha and gamma motor systems. The less direct effect of the cerebellar influence suggests that its function is primarily that of a coordinating center.

Experiments have shown very general functional properties of the descending spinal tracts. Weak stimulation within the brain stem nuclei may either enhance or inhibit the stretch, force, and flexor reflexes. While these studies have shown only general inhibitory and facilitory functions, it is not unreasonable to assume that higher center mechanisms exhibit a high degree of selectivity in control of spinal level reflex mechanisms. The studies suggest that higher centers may determine the mode of reflex control; either force feedback, position feedback, open loop, or a combination of these.

## 2.5 Conclusions - A General Model for Regulation of Posture

Figure 2.11 depicts a general configuration for the feedback of sensory information and the initiation of motor commands in the postural control system.

Major features of the model include:

1. Position and force feedback loops at the spinal level
2. Higher center control of position and force feedback gains

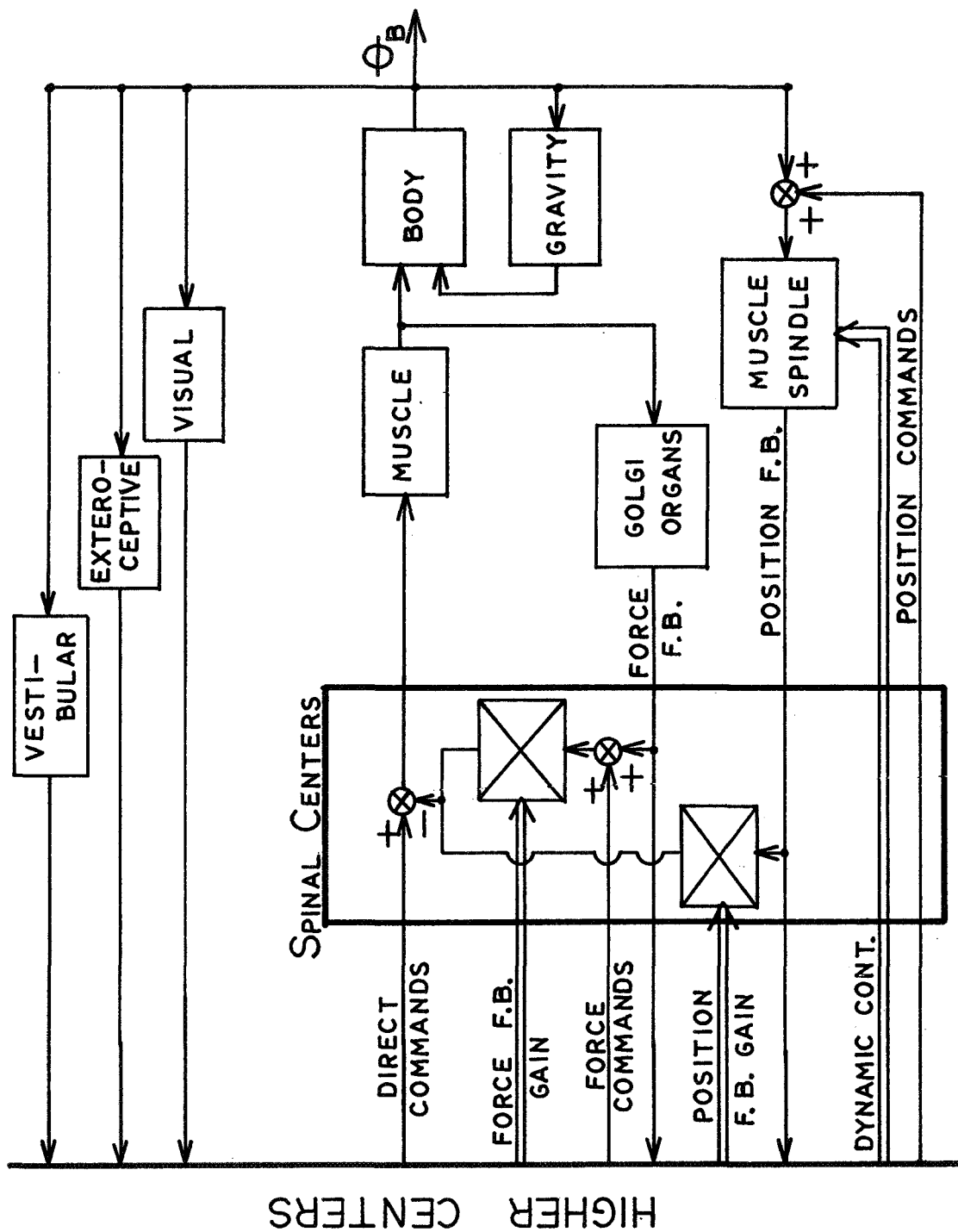


FIGURE 2.11 GENERAL FEATURES OF THE SENSORY-MOTOR SYSTEM CONTROLLING POSTURE

3. Higher center position and force commands
4. Direct higher center activation of postural muscle
5. Feedback of sensory information from the vestibular system, the visual system, and the kinesthetic senses to the higher, conscious centers.

In subsequent chapters, specific properties and functions of this multiloop system are explored using both experimental observations and automatic control modelling techniques. Characteristics of each feedback loop are defined to the extent possible. Strategies for the coordination of the many feedback control loops are demonstrated for a number of posture control tasks.

## CHAPTER 3

THE STRETCH REFLEXES

The stretch reflex is one of the simplest examples of feedback compensation in the human body. Reflex control in extensor and flexor muscles about a given joint may be compared to a position servomechanism, resisting changes in muscle length through both mechanical and spinal level active processes. Sensitivities of the reflex responses are regulated by the higher centers.

The ankle joint stretch reflex acts to inhibit body sway. Experiments presented in this chapter attempt to quantify the contribution of the ankle joint reflex responses to overall postural stability under a variety of conditions. To this end, an experimental platform has been developed to measure ankle reflex responses of human subjects during a number of posture control tasks.

A model is developed which describes the reflex control loop and the modes by which higher centers modulate reflex response gains. Control of small transient disturbances through multiplicative increase in reflex gain is shown.

The strategy of setting reflex gain is shown to be dependent only on the nature of the supporting surface. Rigid supporting surfaces afford maximum reflex control, while compliant surfaces render reflex control useless.

### 3.1 The Stretch Reflex as a Feedback Controller

#### 3.1.1 Physiological Background

Recently, models for neuromuscular mechanisms have been developed using control theory applied to current physiological data (55, 67, 76). These component models form the basis for the description of integrated posture regulatory processes in this thesis.

The reflex control mechanism, including proprioceptive feedback pathways and higher center inputs, is illustrated in Figure 3.1. Characteristics of individual components have been presented in Chapter 2. Components include postural muscles responsive to both active neural stimulation and to mechanical stretch and position feedback via the muscle spindles which respond in proportion to length and rate of stretch. The following paragraphs describe reflex-feedback regulation and the effects of higher center commands on the reflex control loop.

Two direct mechanical mechanisms resist length changes in flexor and extensor muscles. During constant stimulation, muscle tensions vary in proportion to small length changes about a median length, Figure 2.5. Rate of stretch also

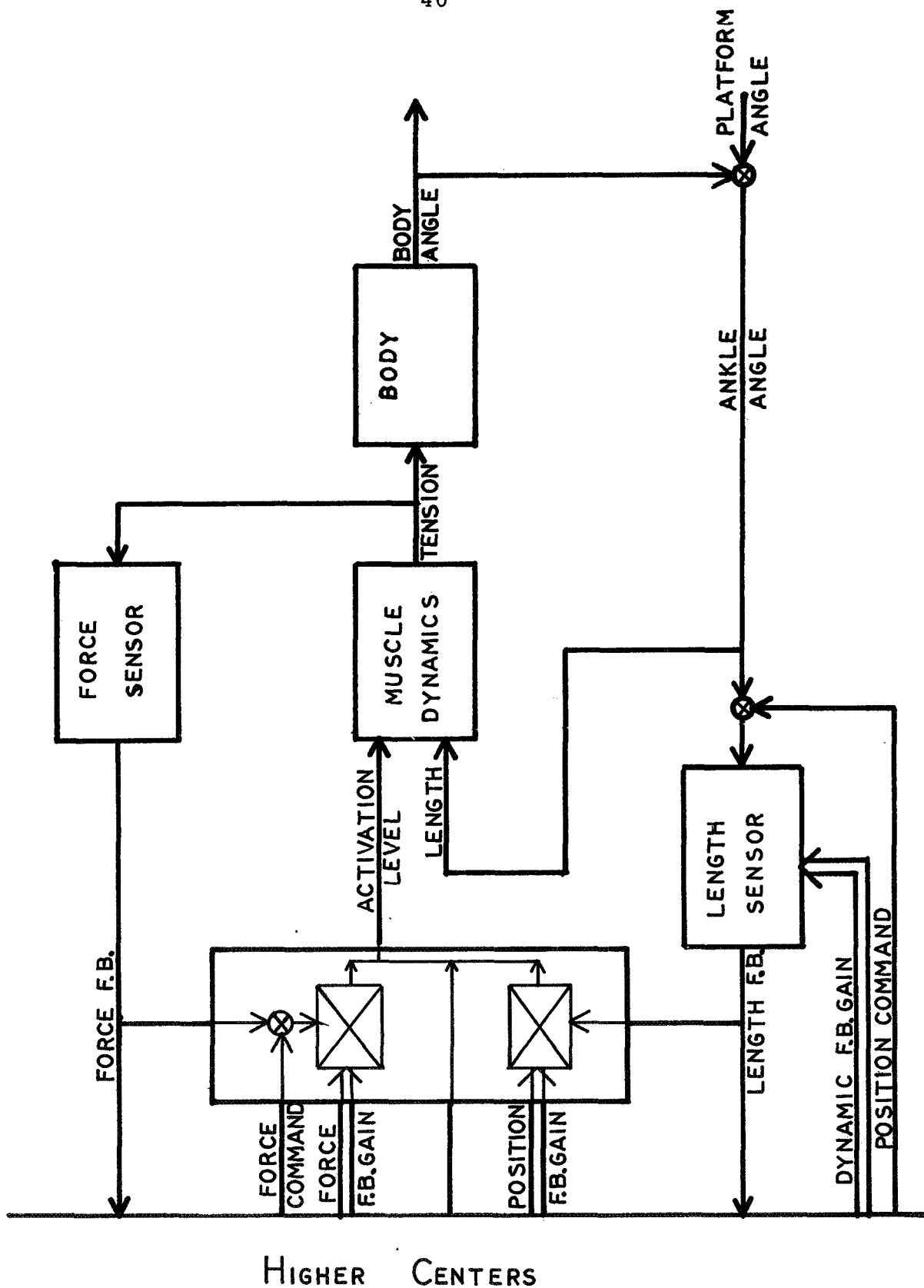


FIGURE 3.1 THE REFLEX CONTROL SYSTEM

affects tension of the muscle under constant stimulation, Figure 2.3. Both the length-change and velocity induced tensions act to resist overall change in muscle length. It should be noted that the sensitivity of both of these mechanisms varies in response to the activation level of the muscle itself.

In addition to the "mechanical" mechanisms varying tension to resist muscle length change, there is active resistance initiated by muscle spindle reflexes.

Stretching skeletal muscle produces a corresponding stretch of the muscle spindle receptors interspersed throughout the muscle. Stretching a muscle spindle increases its afferent discharge, which then acts through the alpha motoneuron pool to contract skeletal muscle fibers in the region of the stretched spindle. Increase of muscle tension is achieved by a combination of the recruitment of additional motor units and increased activation of units already firing.

Higher center activity influences the reflex feedback functions in the following ways:

1. Muscle "mechanical" properties are dependent on the level of muscle activation.
2. Muscle spindle feedback "gains" are controlled by higher center commands.
3. Higher centers may act on the alpha-motoneuron pool, exercising direct control over the activation level of the muscle.

The intensity of the muscle spindle response to stretch

may be altered by activating intrafusal muscle fibers by way of the  $\gamma$ -motoneuron pool.  $\gamma$ -fibers can be separated functionally into two groups: those affecting static and those affecting dynamic components of the spindle response (64).

Activation of  $\gamma$ -static fibers may produce either limb movement or change in the mechanical reflex gain, or muscle tone. Consider increased  $\gamma$ -static activity in one muscle of an antagonistic muscle pair. Figure 3.2 shows how the length-tension relationship for this muscle shifts, moving the limb from equilibrium position R to position R'. Equal changes in  $\gamma$ -static activity of both muscles of the pair change the equilibrium activation levels of both the agonist and antagonist muscles. Figure 3.3 shows how this affects an increase in stiffness of the joint.

Increasing the intensity of the phasic spindle response to a given rate of stretch  $\gamma$ -dynamic fibers, increases the intensity of the active reflex response. A change in phasic response gain has no effect on the equilibrium position of the limb.

In describing control mechanisms of the reflex arc, physiologists have recognized its likeness to a position servo-mechanism. Only recently, however, have investigators integrated functional descriptions of the individual physiological components into models of the reflex control system.

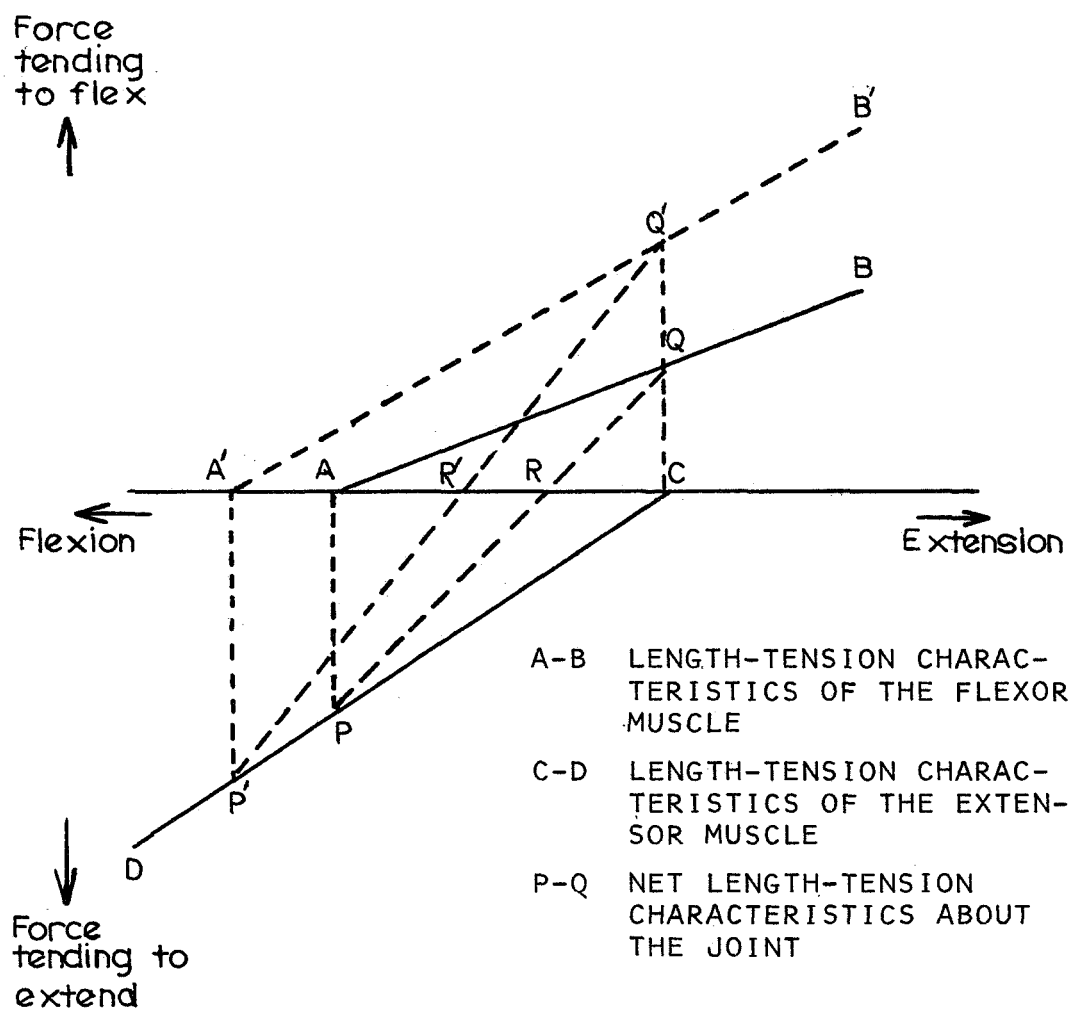


FIGURE 3.2 A SIMPLE MECHANISM BY WHICH THE GAMMA MOTOR SYSTEM CONTROLS POSITION OF THE LIMB (REF. 90)

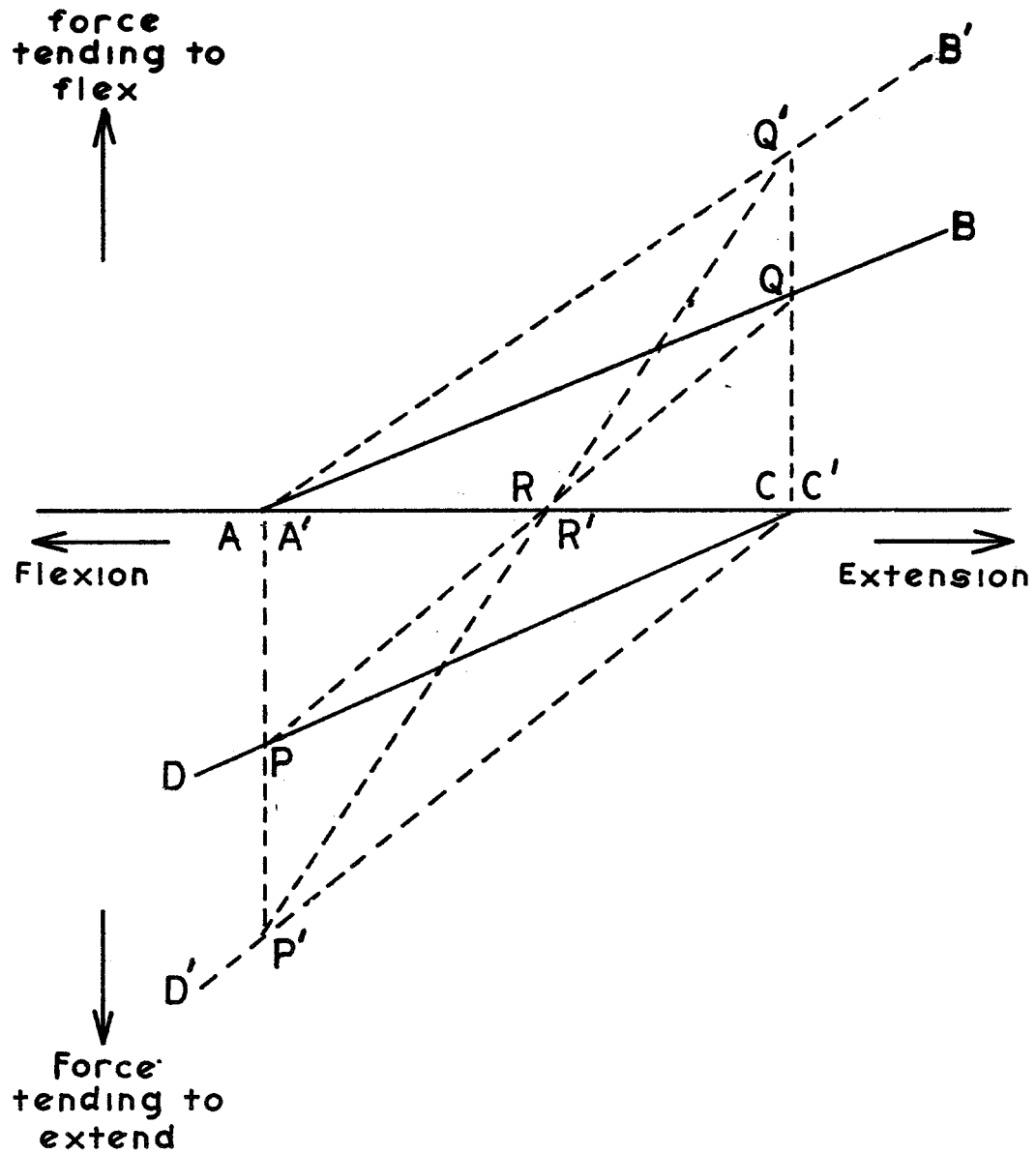


FIGURE 3.3 A SIMPLE MECHANISM BY WHICH THE GAMMA MOTOR SYSTEM CONTROLS THE STIFFNESS OF A JOINT

Johnson (67) developed a linear component model for postural reflex control. He measured the mechanical impedance of the human wrist postural reflex and was able to show that his linear model could predict the experimental results. By incorporating into the model the functional changes brought about by several diseases affecting reflex control, his model predicted the mechanical impedance of several afflicted subjects.

Houk (55) studied wrist rotation, integrating mathematical models for each physiological component into a complete reflex control model. He compared a linearized reflex model to the responses of human subjects determining specific parameter values for each of the components in his model.

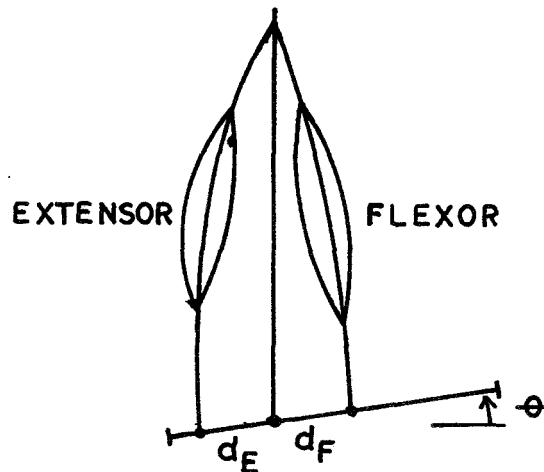
McRuer et al (76) developed a neuromuscular activation model using both recent physiological data and describing-function data from human operators. Linear models were used. Muscle models were lumped into a single agonist/antagonist model describing both mechanical muscle and active reflex response characteristics. Model dynamics were comparable to the describing-function data.

These studies show that linearized component models and equivalent bilateral muscle models can with fair accuracy predict postural responses. Further investigations of posture control mechanisms described in this thesis begin with these premises.

Before proceeding further, a brief description of the lumped agonist/antagonist muscle model is in order. The relationship of muscle tension,  $P$ , to small changes in length ( $\Delta L$ ), small stretch velocities,  $V$ , and small changes in stimulation frequency ( $\Delta f$ ) derived in Section 2.2 is as follows:

$$P = P_0(f_0, L_0, V_0) + \left[ \frac{\partial P}{\partial f} \Delta f + \frac{\partial P}{\partial L} \Delta L + \frac{\partial P}{\partial V} V \right] \left| \begin{array}{l} f = f_0 \\ L = L_0 \\ V = V_0 = 0 \end{array} \right. \quad (3.1)$$

Using this relationship, net torque produced by the agonist/antagonist pair shown in Figure 3.4 may be given as follows:



AN AGONIST/ANTAGONIST MUSCLE PAIR

Figure 3.4

$$T = d_E \left[ P_{O_E} + \frac{\partial P_E}{\partial f} \Delta f_E + \frac{\partial P_E}{\partial L} \frac{\partial L_E}{\partial \theta} \Delta \theta + \frac{\partial P_E}{\partial V} \frac{\partial V_E}{\partial \dot{\theta}} \dot{\theta} \right] - d_F \left[ P_{O_F} + \frac{\partial P_F}{\partial f} \Delta f_F + \frac{\partial P_F}{\partial L} \frac{\partial L_F}{\partial \theta} \Delta \theta + \frac{\partial P_F}{\partial V} \frac{\partial V_F}{\partial \dot{\theta}} \dot{\theta} \right] \quad (3.2)$$

Assuming the joint is initially at equilibrium:

$$\begin{aligned} d_E P_{O_E} &= d_F P_{O_F} \\ V_E &= V_F = 0 \\ V_E &= d_E \dot{\theta} \end{aligned} \quad (3.3)$$

Assuming reciprocal innervation:

$$\Delta f_E = -\Delta f_F = \Delta f \quad (3.4)$$

Combining 3.2, 3.3, and 3.4:

$$\begin{aligned} \Delta T = \left( \frac{\partial P_E}{\partial f} d_E + \frac{\partial P_F}{\partial f} d_F \right) \Delta f + \left( \frac{\partial P_E}{\partial \theta} d_E + \frac{\partial P_F}{\partial \theta} d_F \right) \Delta \theta + \\ \left( \frac{\partial P_E}{\partial \dot{\theta}} d_E + \frac{\partial P_F}{\partial \dot{\theta}} d_F \right) \dot{\theta} \end{aligned} \quad (3.5)$$

Equation 3.4 shows that the combined agonist/antagonist muscle model is of the same form as the single muscle model. Lumped model parameter values are a weighed sum of the parameter values of each muscle. Active and passive response characteristics remain independent of one another within the scope of the original approximations.

A perturbation model for small motions about the equilibrium position is developed in the form:

$$T(s) = K_R(s) f(s) + K_M(s) \theta(s) \quad (3.6)$$

$K_R(s)$  are the reflex response characteristics;  $K_M(s)$ , the muscle response characteristics.

Active response may be modeled as a simple first order lag (15, 19, 75):

$$K_R(s) \approx \frac{K_f}{1 + \tau_M s} \quad (3.7)$$

The muscle response is modeled as a spring constant with series damping:

$$K_m(s) = B_m(f_o) s + K_m(f_o) \quad (3.8)$$

Spring constant,  $K_m$ , and viscous damping,  $B_m$ , vary with the background stimulation level, or muscle tone, as shown in Figures 2.5 and 2.3.

### 3.1.2 Reflex Responses During Quiet Standing

The following is a description of the experiment conducted to determine specific values of the parameters for the ankle stretch reflex control loop. The reflex response parameters obtained are then formulated into a model which quantifies the contribution of the ankle reflex control loop to overall postural stability, providing the basis for further experiments exploring the strategy of reflex parameter adaptation to changing control conditions.

The subject stands relaxed on the experimental platform (described in Appendix B), arms folded above the waist and feet ten to twelve inches apart. The subject's knees are locked. He is asked to avoid shifting his stance during the three minute duration of each test run. The platform detects the subject's reaction torques and his sway angle about the ankle joint. A hydraulic position servo allows rotations of the platform about an axis colinear with that of the subject's ankle joints. The ankle stretch reflex is excited by small steps of the platform.

The experiment is controlled by a hybrid program, "Test", which initiates each step disturbance, initializes the torque and body angle readings, and stores the responses on digital tape. ("Test" is described in Appendix C.) The direction of each step is random about zero platform angle. The time between steps is random within an interval of 5 to 15 seconds.

During each test run the subject is asked to stand relaxed with his eyes open. To prevent fatigue, each test run is limited to 16 step samples, or approximately 3 minutes. Seven test runs are conducted for each of five step sizes:  $1/10$ ,  $1/4$ ,  $1/2$ ,  $1$ , and  $1\ 1/2$  degrees. A test run consists of one step size only. The ordering of step size test runs is random.

Typical extensor and flexor muscle responses are shown in Figure 3.5. Responses are characterized by a peak within 80-125 milliseconds, a compensatory response peak at 400-800 milliseconds, then gradual return to equilibrium. Within the first 50 milliseconds, a large difference is evident between the muscle extensor and flexor responses. The extensor response shows an acceleration peak at ten milliseconds and strong viscosity component at 10-50 milliseconds, while the flexor response shows neither of these effects strongly. A possible explanation for the differences in these muscle responses is:

The foot is a nonlinear elastic component which transmits the platform step to the ankle joint. Normally

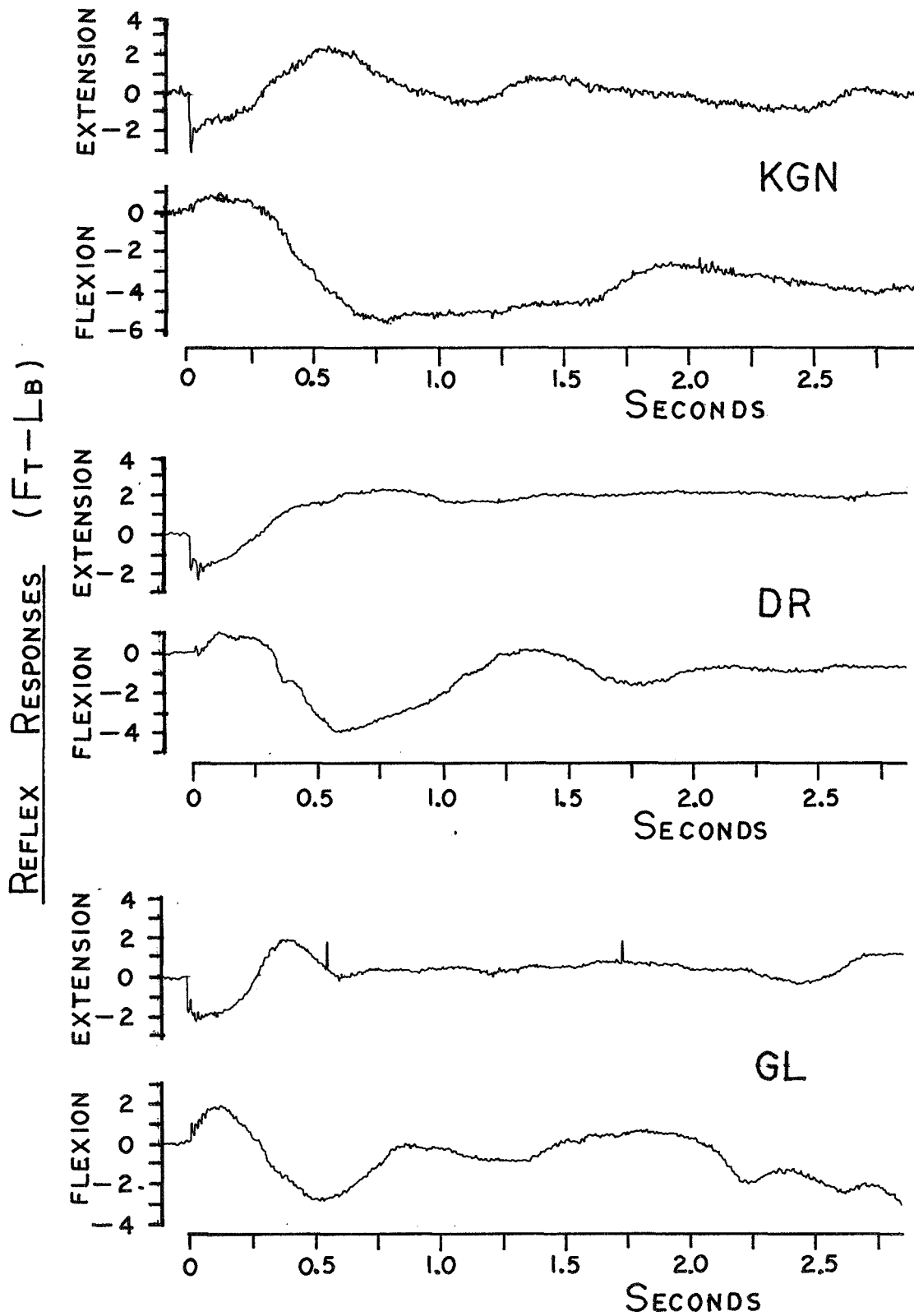


FIGURE 3.5 TYPICAL REFLEX RESPONSES TO 1/2 DEGREE STEPS EXTENDING AND FLEXING THE ANKLE JOINT

the subject stands with his center of gravity forward of the ankle joint, compressing the foot. The foot is forced upward during excitation of the extensor reflex response. Because it is already compressed, the foot is nearly rigid to further compression. The foot drops downward, and is decompressed during excitation of the flexor reflex response. The foot is elastic to decompression.

The reflex response amplitude, defined as the maximum ankle torque occurring within 80 to 125 milliseconds after initiation of the step disturbance, is determined for each step response. Reflex gain is defined as response torque amplitude divided by the ankle step size. The composite average gain as a function of step size is shown in Figure 3.6. Variation among subjects is statistically insignificant,  $p > 0.1$ . (Histograms showing the distribution of gains are included in Appendix E.)

To examine the later compensatory phase, average responses of each subject to the 1/4 and the 1/2 degree steps are computed. These response groups are further subdivided according to initial gain into three levels, those in the lowest third, those in the middle third, and those in the highest third for each sample group. (Complete response averages for each of the six cases are shown in Appendix E.) Combined response averages for each case are shown in Figure 3.7.

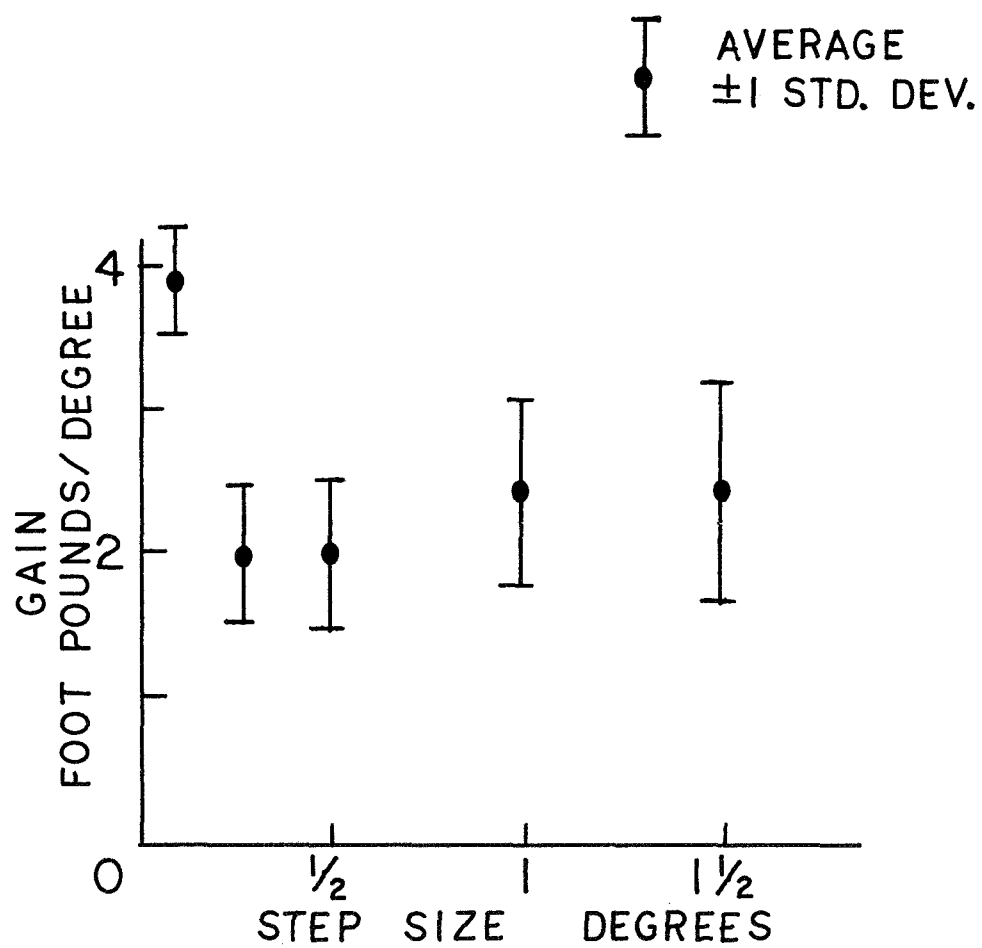


FIGURE 3.6 AVERAGE ANKLE REFLEX GAIN AS A FUNCTION OF STEP SIZE

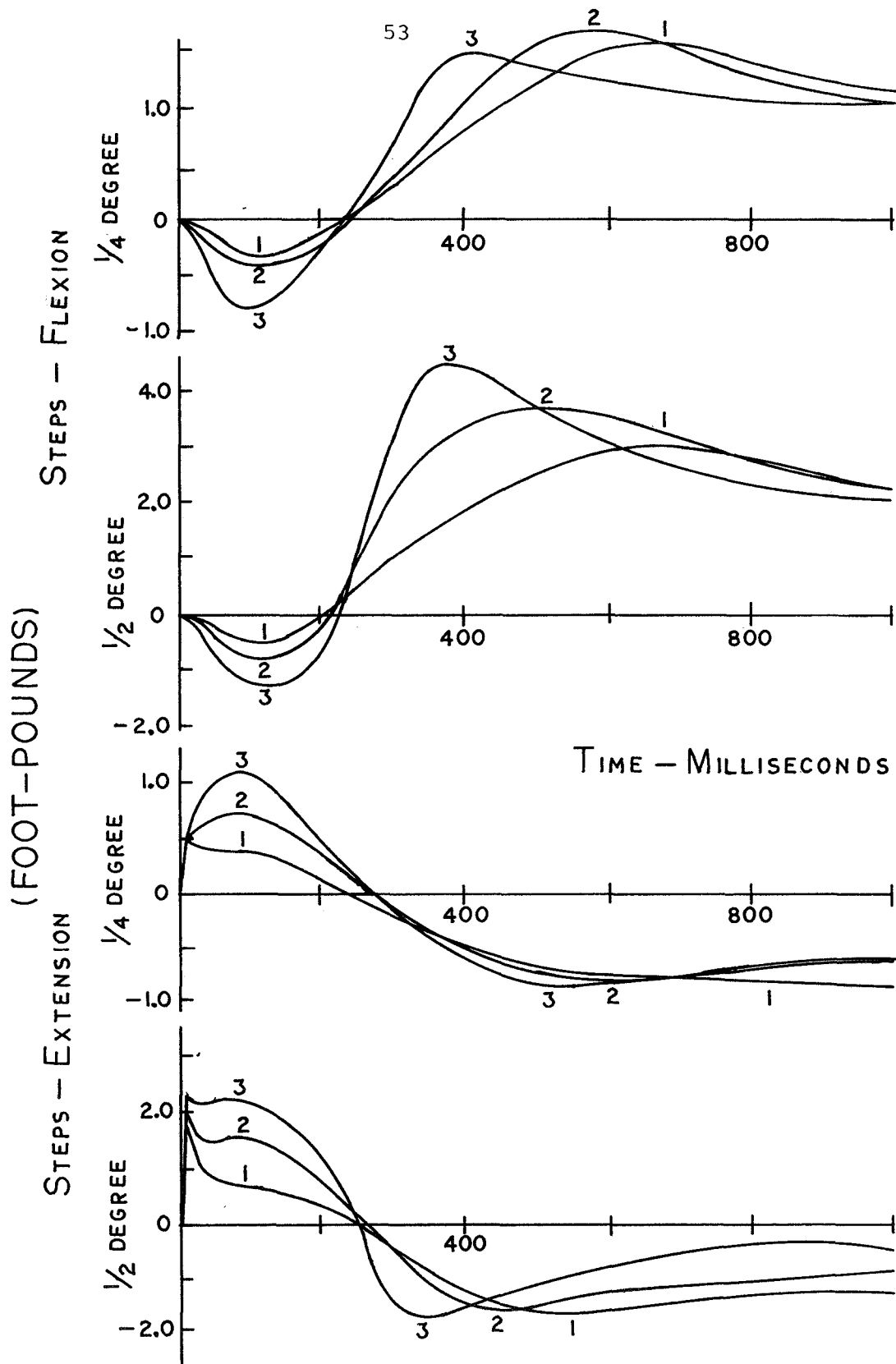


FIGURE 3.7 AVERAGE ANKLE REFLEX RESPONSES GROUPED ACCORDING TO GAIN FOR 1/4 AND 1/2 DEGREE STEPS

### 3.1.3 Conclusions

The reflex response characteristics determined in the experiments described above are in good agreement with the physiological data of reflex time delay and slow skeletal muscle response times presented in Chapter 2.

A significant feature of the reflex control loop is the large increase in gain for disturbances of very small amplitude. While gains for steps of  $1/4$  to  $1/2$  degrees are considerably below that necessary for postural stability (2 ft-lb/degree versus about 5 ft-lb/degree), the two-fold increase in gain for  $1/10^\circ$  steps (4 ft-lb/degree) suggests that reflex control alone may fully stabilize the body for disturbances below  $1/10^\circ$ . This is substantiated by current physiological evidence.

Evidence of large gain increases in muscle responses to small length changes is found in the work of Hill (54) and Joyce et al. (69). Brown et al. (14) observe a large gain increase in muscle spindle response at the onset of stretch. Similar gain increases in the reflex response is shown by Matthews (80). Hill observed an elastic effect in frog sartorius muscle for small length changes, up to 0.2% of muscle length. Beyond this point, further changes in length at constant velocity produce no further increase in tension. Joyce et al., observed tension changes during length changes at various velocities in cat soleus muscle.

At a moderate rate of stimulation isometric tension exceeded the tension during either lengthening or shortening. See Figure 3.8.

Matthew determined the relationship between the change in active reflex tension and the extent of displacement in cat soleus muscle. He found the gain of the reflex response to be two to four times greater for changes of length less than 0.3 millimeters than that for larger stretches, Figure 3.9. Brown et al. found a large burst of spindle afferent activity at the beginning of stretch. They suggest that these effects are due to the persistence of stable bonds between actin and myosin filaments of the intrafusal fibers, i.e. fibers tend to remain "stuck" at their initial setting.

Recordings of ankle torque and body angle responses during quiet standing, Figure 3.10, indicate that the reflex loop fully stabilizes very small amplitude body sway motions. All subjects exhibit frequent periods of five or more seconds duration in which no motion within measurement resolution ( $T = \pm 0.10$  ft-lb  $\theta_B \pm 0.02$  degrees) can be observed. All higher center feedback controls are limited by thresholds considerably larger than the measurement resolutions. (Results, Chapters 4 and 5) Therefore, reflex feedback control must be responsible for these stable periods.

On the basis of forementioned physiological and experimental evidence, a reflex gain function is defined in Figure 3.11. Both muscular and reflex responses show gain

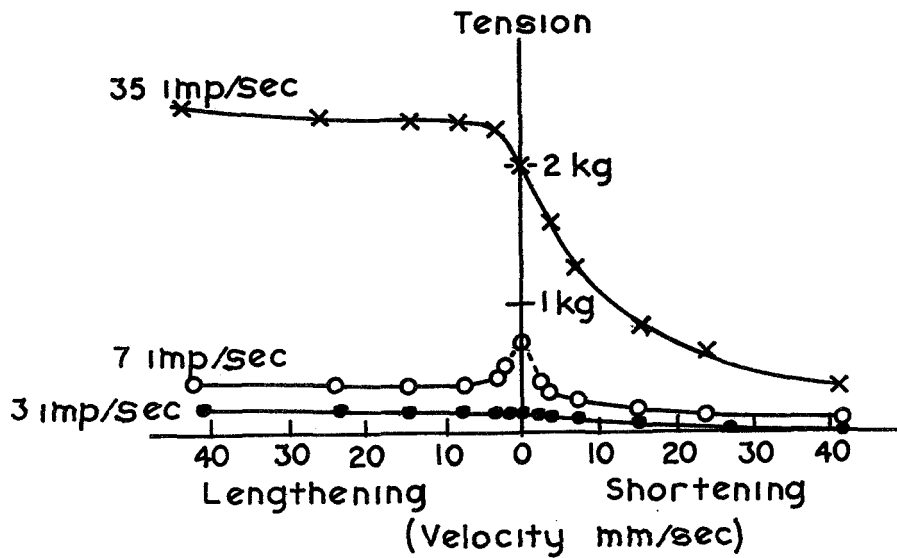


FIGURE 3.8 FORCE-VELOCITY DATA SHOWING "STICTION" EFFECTS AT MODERATE STIMULUS RATES (REF. 69)

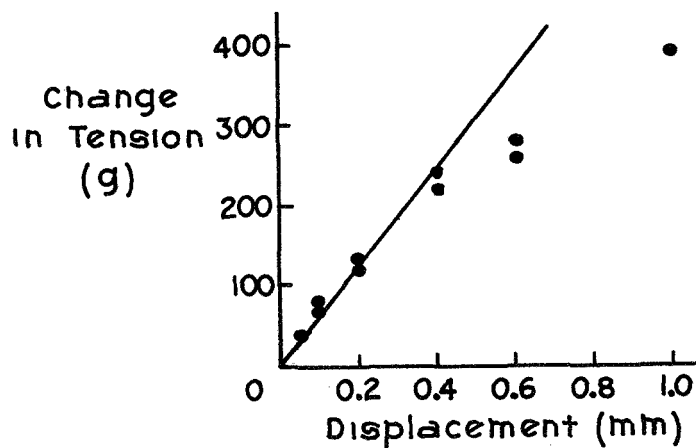


FIGURE 3.9 ACTIVE REFLEX TENSION IN CAT GASTROCNEMIUS AND SOLEUS MUSCLE AS A FUNCTION OF DISPLACEMENT (REF. 80)

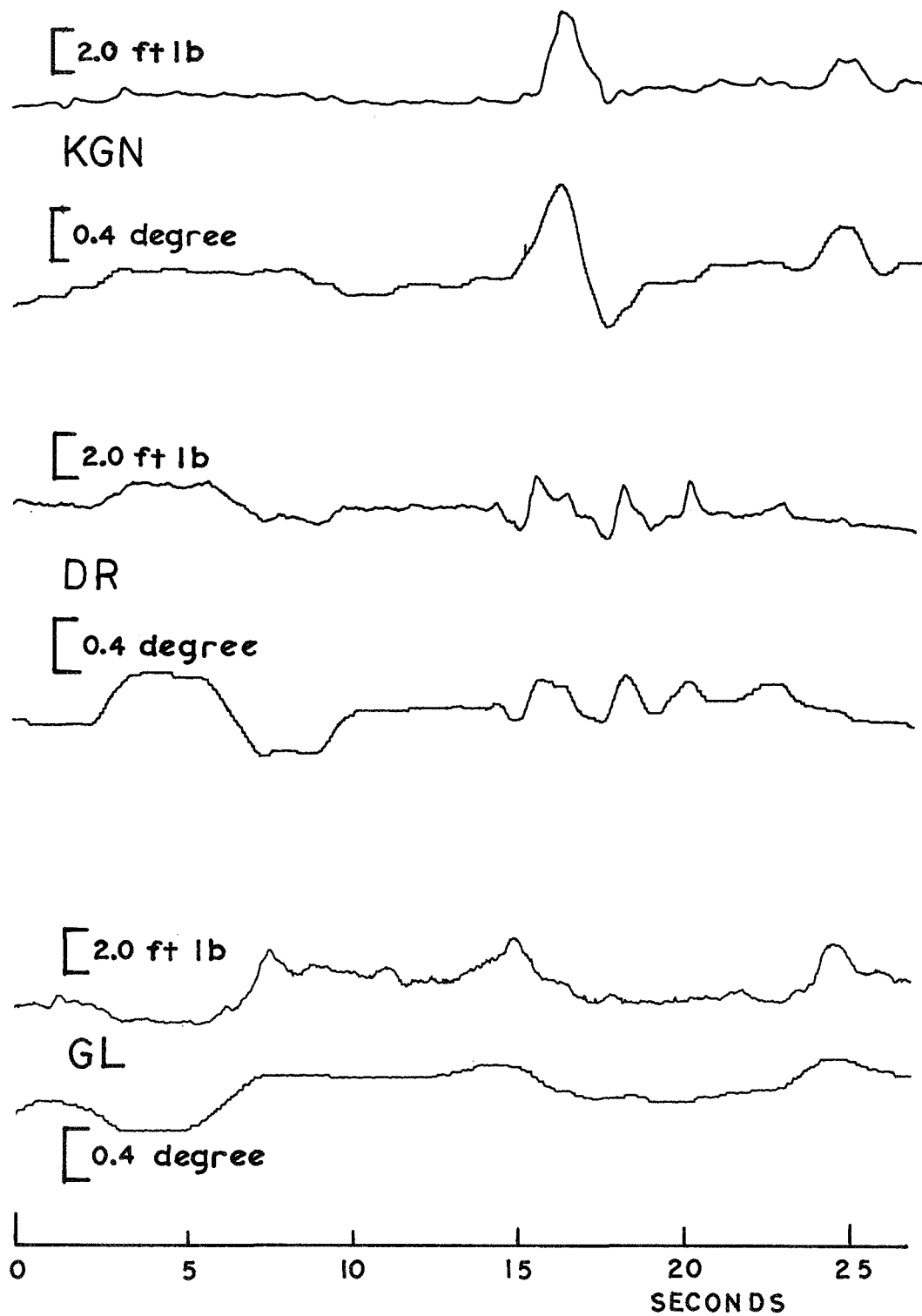


FIGURE 3.10 TYPICAL BODY ANGLE AND ANKLE TORQUE RESPONSE SEQUENCES DURING QUIET STANDING ON A RIGID SURFACE

increases due to stiction for deflections less than  $0.15^\circ$ . Reflex feedback gain is sufficient for complete postural stability for deflections less than  $0.05^\circ$ .

The compensatory response is initiated by higher center commands. Observed delay time, about 200 milliseconds, agrees with physiological evidence for higher center response delay; it also agrees with vestibular response delays measured by the author and reported in Chapter 4.

Figure 3.12 shows the compensatory response natural frequency and damping ratio as a function of the initial reflex disturbance amplitude. Included in each figure for comparison are the response characteristics as a function of gain for the following roughly equivalent system: an inverted pendulum stabilized with a rate compensated feedback, with system dynamics roughly equivalent to those of the body reflex control system. (Figure 3.13) Results suggest that higher centers enhance the total reflex gain during a transient disturbance in proportion to the perceived disturbance amplitude. Reports of several investigators also indicate reflex gain control as a likely higher center control mechanism.

Kim and Partridge (71) show that total reflex gain ( $\Delta$  tension/ $\Delta$  length) in cat soleus muscle is enhanced by factors of two to three times when the vestibular nerve is stimulated continuously. They note that neck rotations also enhance reflex gain. For a given amount of stretch, the reflex tension generated is proportional to the

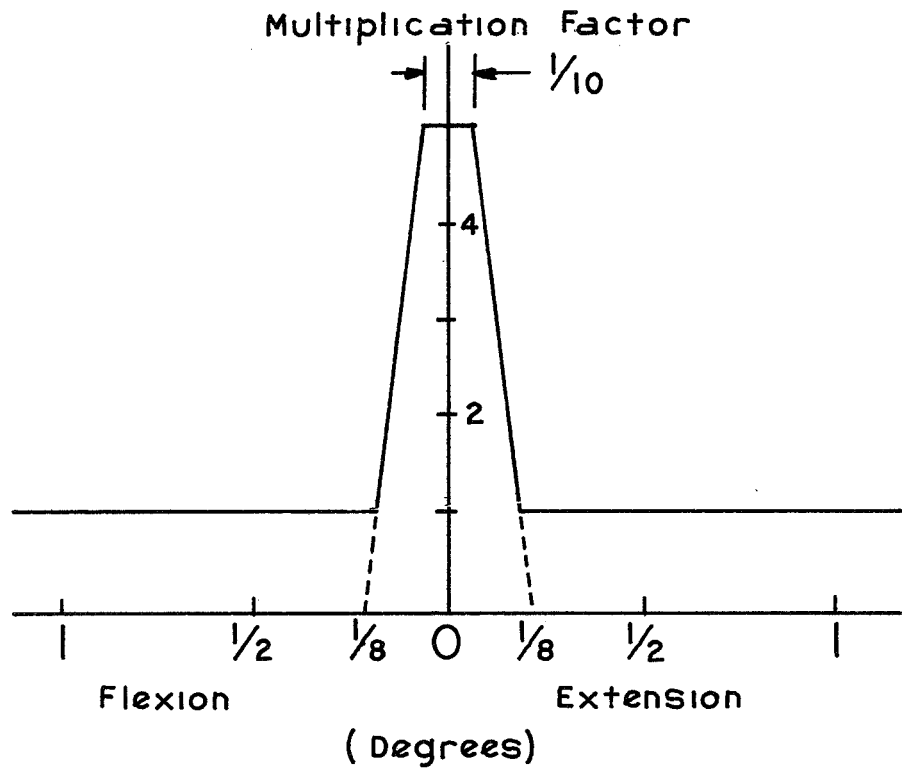


FIGURE 3.11 A PROPOSED MODEL FOR THE ENHANCEMENT OF THE REFLEX GAIN AS A FUNCTION OF ANKLE DEFLECTION

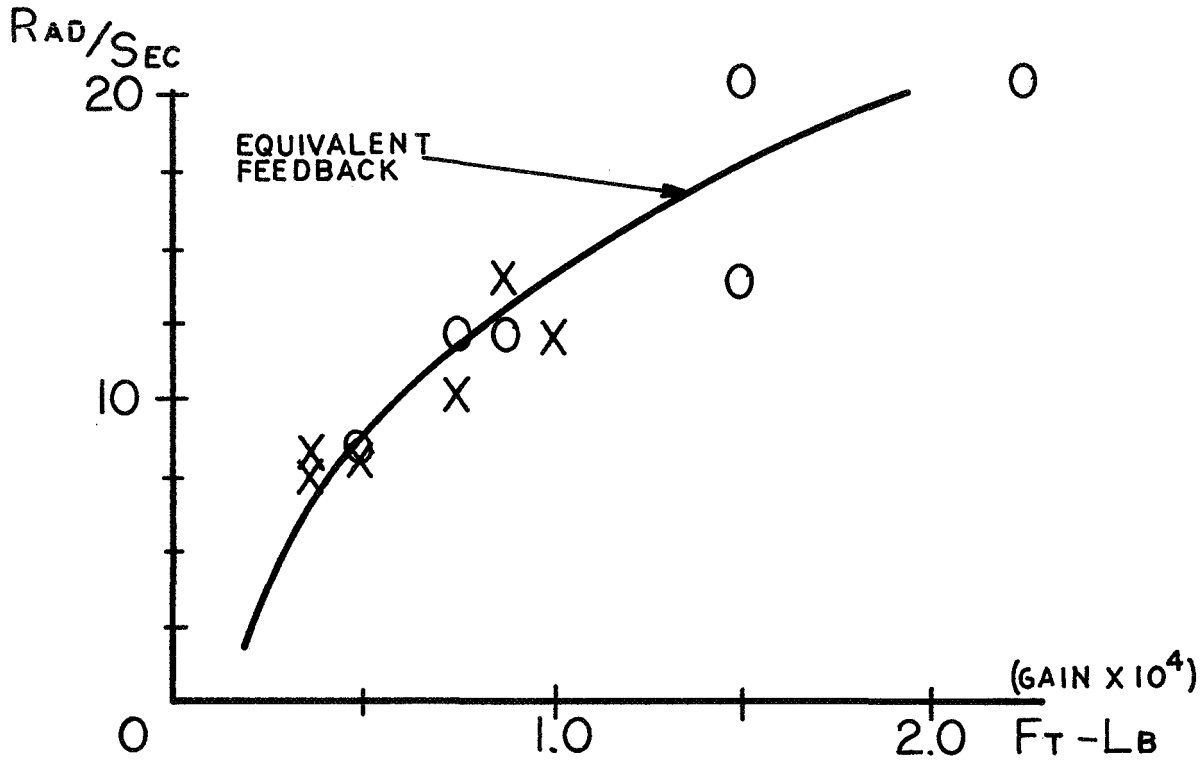


FIGURE 3.12a NATURAL FREQUENCY AS A FUNCTION OF REFLEX AMPLITUDE, COMPENSATORY RESPONSE

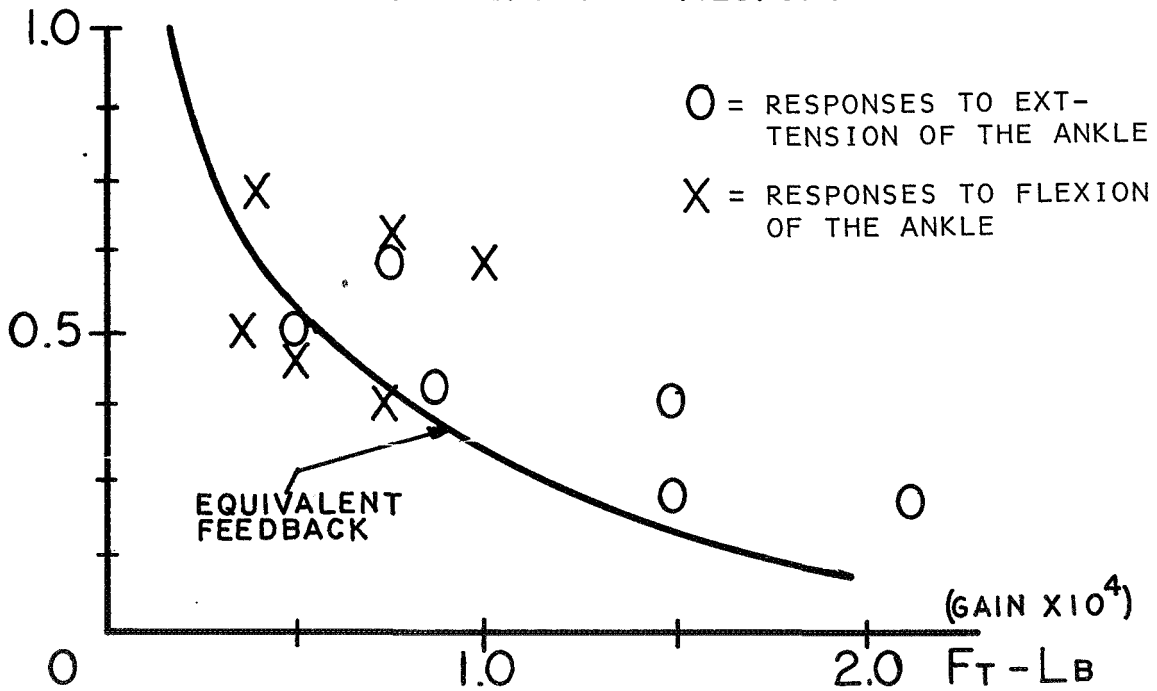


FIGURE 3.12b DAMPING RATIO AS A FUNCTION OF REFLEX AMPLITUDE, COMPENSATORY RESPONSE

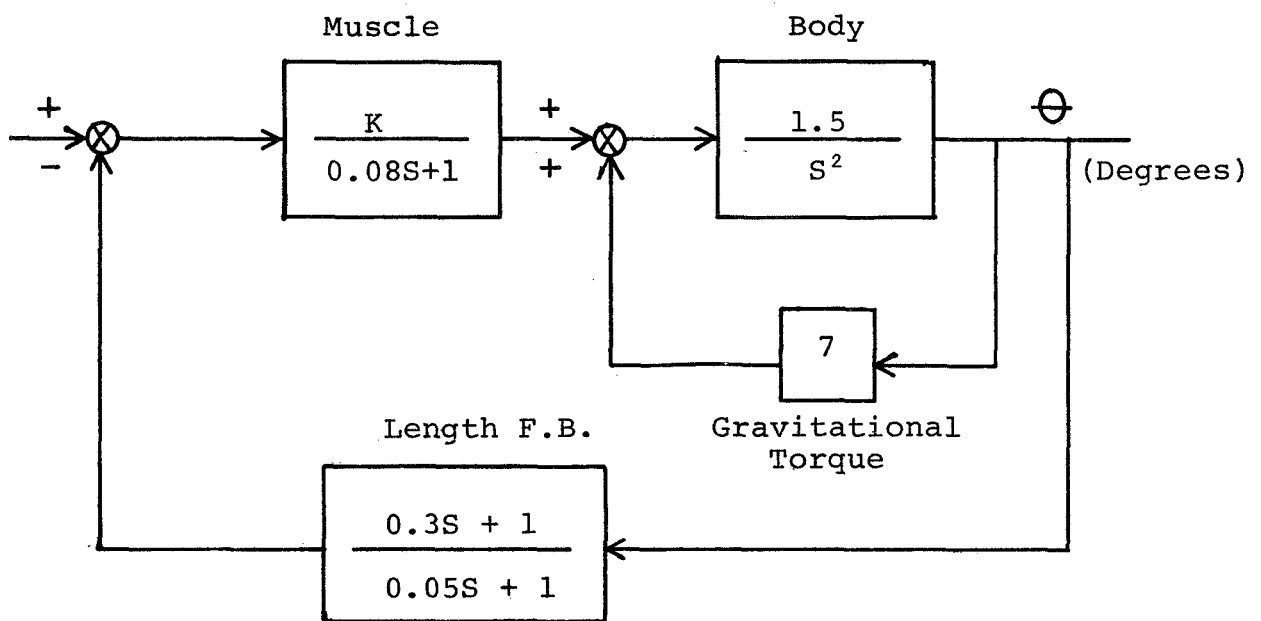


FIGURE 3.13 AN EQUIVALENT REFLEX CONTROL SYSTEM

vestibular stimulus rate. (Figure 3.14) In a further study, Partridge and Kim (87) find that isometric tension varies less than 1% of maximum muscle tension during sinusoidally modulated vestibular stimulation.

Gernandt et al. (39) have shown that vestibular stimulation in anesthetized cats strongly affects the dorsal to ventral root response amplitude at the cervical and lumbrosacral levels of the spine. They observe a sequence of strong enhancement, interference, then re-enhancement with single shocks to the vestibular nerve, Figure 3.15. Since the period of enhancement is considerably greater than that for interference, one would expect that a train of shocks would produce continuous enhancement of the dorsal to ventral gain.

A question arises in regard to vestibular regulation of reflex gain. Experiments in Chapter 4 show conclusively that vestibular responses are able to mediate the operating torque of ankle joint muscles in the absence of ankle joint movement. This finding appears to be in direct conflict with the vestibular reflex gain control mechanism proposed by Partridge, Kim, and Gernandt.

Recent experiments by Houk, Singer, and Goldman (unpublished) have shown that reflex gain is dependent on the operating level of the muscle. At higher operating levels they observe larger reflex gains. This nonlinear characteristic allows higher centers to effect reflex loop gain changes through increases in the muscle operating

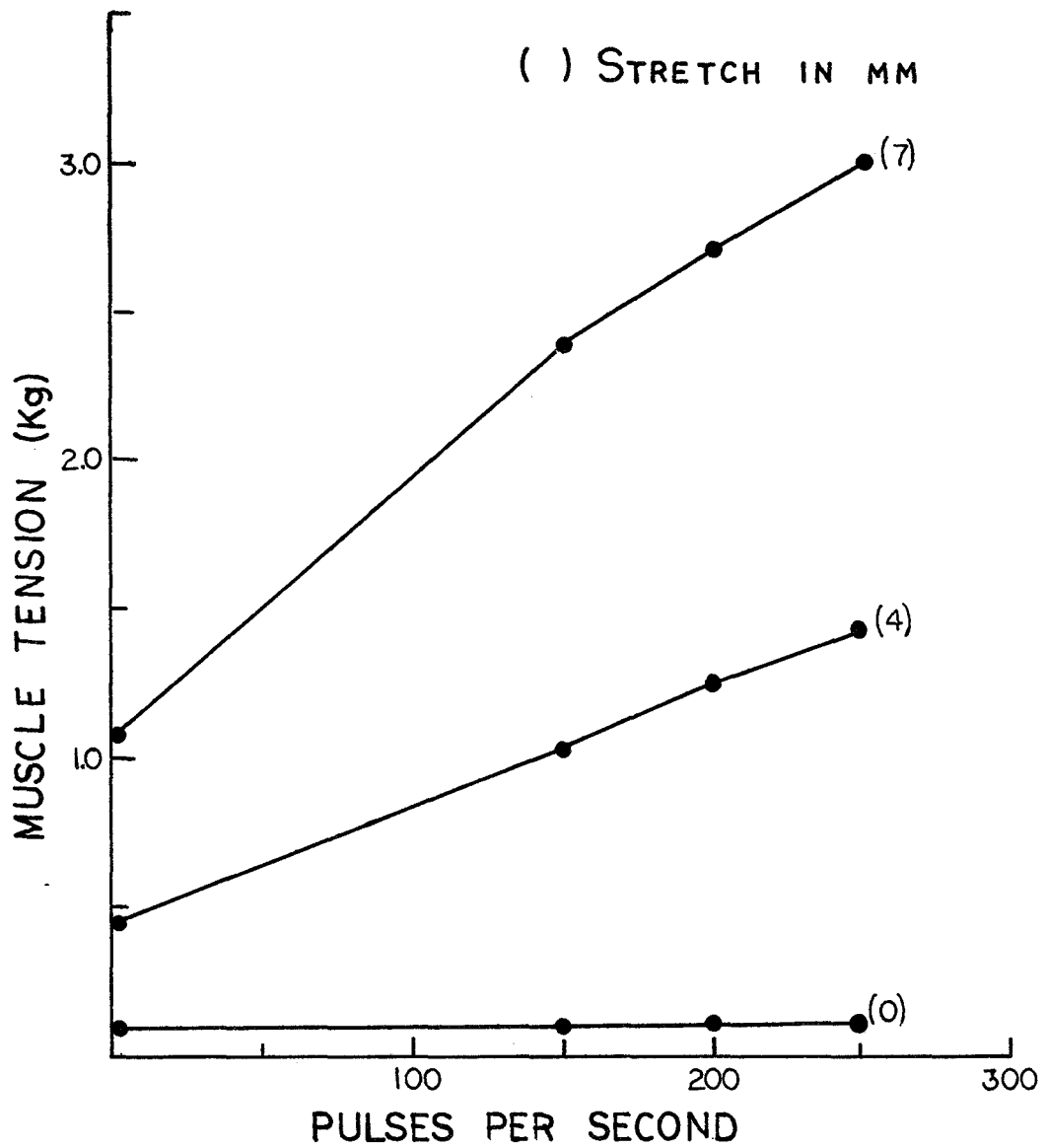


FIGURE 3.14 MUSCLE TENSION GENERATED BY STRETCH TO THREE LENGTHS AS A FUNCTION OF VESTIBULAR STIMULUS RATE (REF. 71)

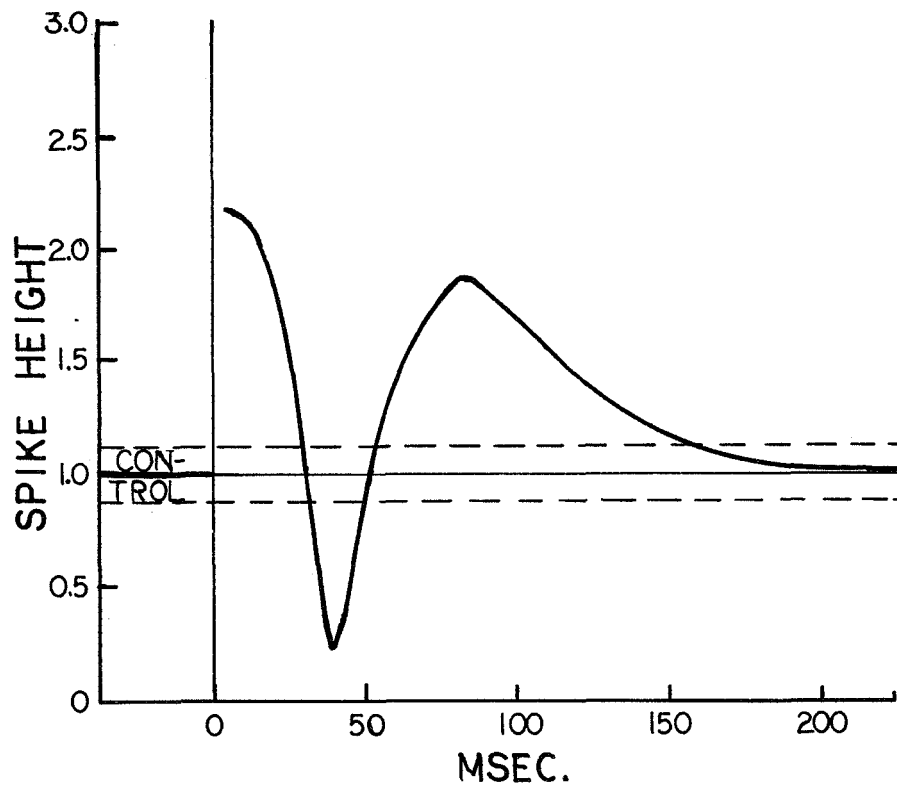


FIGURE 3.15 SINGLE SHOCK VESTIBULAR INFLUENCE ON DORSAL ROOT-VENTRAL ROOT FIRST PEAK AMPLITUDE REFLEX RESPONSES (REF. 39)

levels, or muscle "tone". Perhaps this mechanism for reflex gain control is more consistent with observations in this chapter and in Chapter 4. In summary, two physiological mechanisms for reflex gain enhancement are proposed; multiplicative increase in the dorsal to ventral reflex gain, and control of the operating tension levels of muscle. Functionally the mechanisms are equivalent.

The strategy of gain enhancement shows an excellent combination of higher and lower levels of sensory information. The higher center gain command involves no complex processing and can be effected with a minimum of delay. Additional corrective computation takes place at the spinal level through enhanced resistance of body displacements. This mechanism is a crude one, but in most situations a good "first guess". More complex higher level mechanisms requiring longer processing time may intervene somewhat later to fine-tune the initial crude corrections.

#### 3.1.4 A Proposed Mechanism for Reflex Postural Control

A simplified model is assembled from the experimental results and conclusions described above. This model attempts to demonstrate the validity of the reflex gain control mechanism. Basic operational features of the model include:

1. separation of muscle and reflex responses
2. large increase in muscle and reflex gain for very small deflections

3. modulation of reflex gain by higher center commands during transient disturbances.

A linearized perturbation model for muscle in the form described in Equation 3.6 is assumed. A lead-lag model for the muscle spindle length feedback is used.

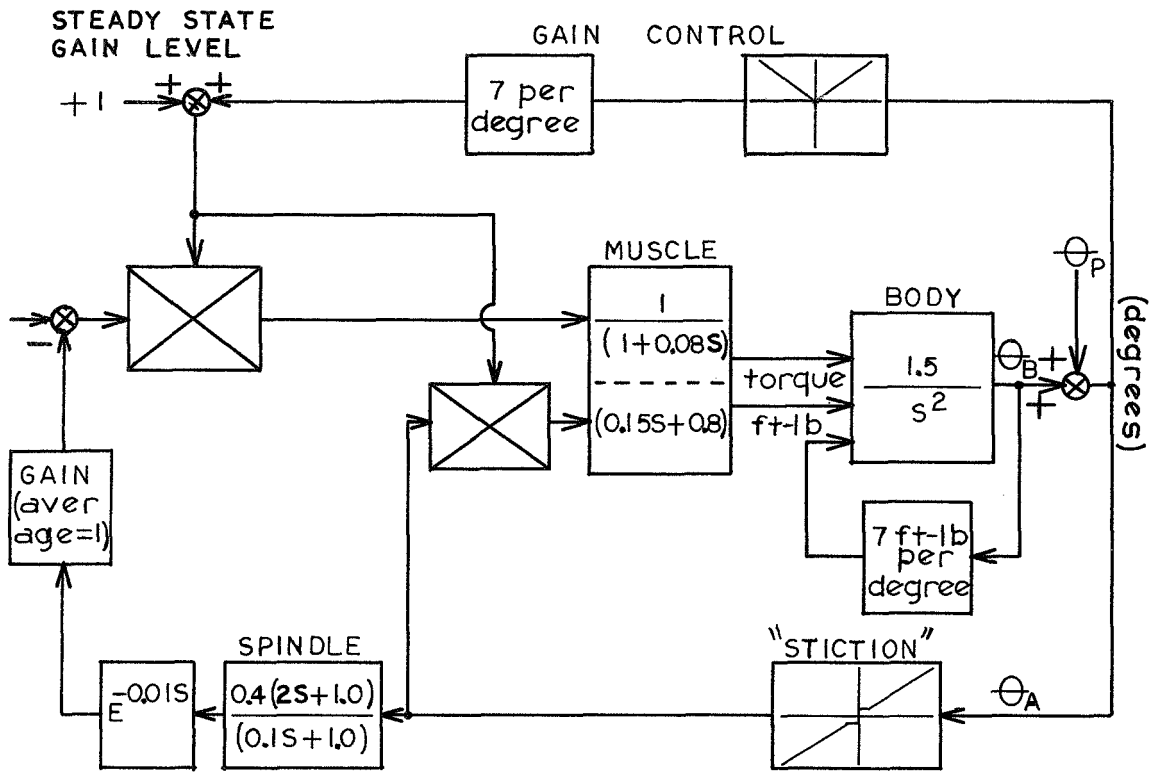
Parameters for the muscle and muscle spindle models are determined by matching the initial reflex response characteristics of the model with average experimental observations shown in Figure 3.7. Reflex gain control parameters are determined which match model compensatory responses with the experimental results. Figure 3.16 shows the model and computed responses.

### 3.1.5 Conclusions

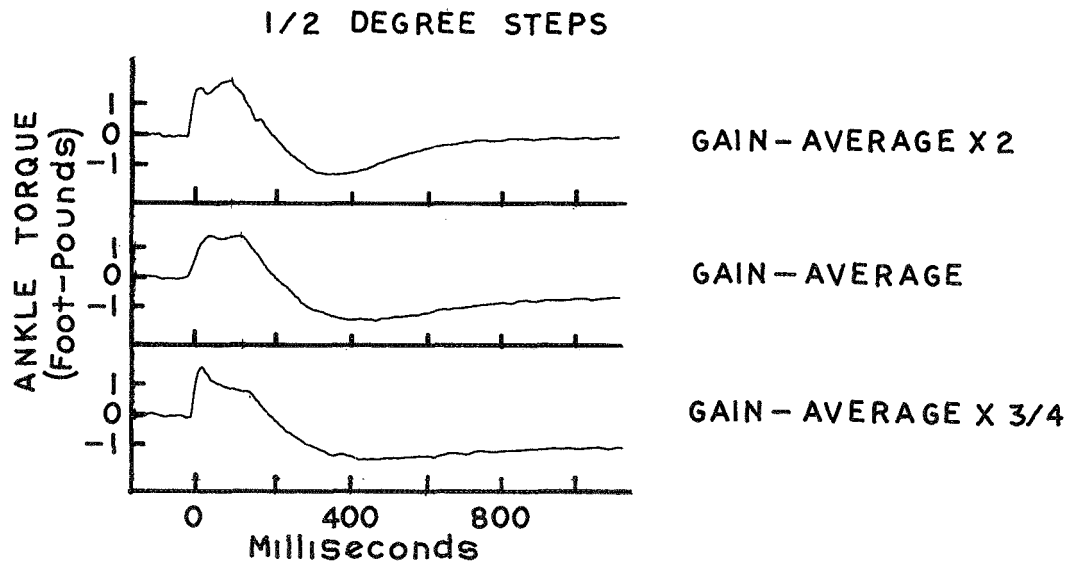
The reflex gain control model demonstrates the relative roles of reflex and higher center control during quiet standing. Reflex responses insure only static stability, while higher center gain control provides stability during small transient disturbances.

The gain control strategy makes good sense if we assume the human wishes to achieve postural stability within the following constraints:

1. a minimum of the amount of physical effort necessary to remain stable
2. a minimization of the frequency at which the higher centers must intervene to maintain stability.



MODEL—SMALL STEPS IN PLATFORM ANGLE



CHARACTERISTICS OF THE MODEL

FIGURE 3.16 THE REFLEX GAIN CONTROL MODEL AND ITS RESPONSE CHARACTERISTICS

Increasing reflex loop gain decreases the number of times the higher centers must act to prevent the body from diverging. However, increasing reflex rigidity calls for an increased expenditure of muscular energy and more rapid fatigue. Normal posture control can be seen as the "optimal" combination of continuous reflex and intermittent higher center feedback control.

The preceding model establishes gain control as a likely mechanism for achieving postural stability when the ankle joint reflexes are active (i.e. standing on a rigid surface). A more complete development of this model is given in Chapter 5 after a definition of higher center sensory modes, vestibular, visual, and exteroceptive, in Chapters 4 and 5.

## 3.2 The Role of Ankle Reflex Control in Posture Stability

### 3.2.1 Implications of Ankle Reflex Control

Stretch reflexes are the simplest of the posture feedback control loops. Simplicity gives reflex control the advantage of rapid response to posture disturbances. Reflex control has the limitation of operating within the body reference frame, that of relative motion between body parts.

The ankle stretch reflex feedback helps stabilize body sway motion. The reflex model has shown that reflex control, in combination with a simple gain control from higher centers, is able to fully stabilize small body disturbances. In many circumstances, however, independent reflex control cannot

stabilize the body. When the supporting surface is rigid, ankle angle motion can provide both body and inertial reference information necessary for stability. On non-rigid surfaces inertial information is lost and the higher center sensory loops (eyes and vestibular organs) must mediate or override the reflex responses to provide postural stability.

### 3.2.2 Reflex Adaptation (Experiments by the Author)

The following experiments explore more fully the relationship of reflex and higher center control strategy, illustrating reflex gain during a variety of circumstances which alter the effectiveness of the reflex control loop. Test conditions are designed to determine the effects of the following on feedback parameters:

1. visual feedback: enhancement and elimination
2. conscious posture set
3. random ankle angle disturbances
4. elimination of ankle position feedback

#### Method:

The reflex response parameters are measured using the technique developed in the previous experiments. In cases where platform motions other than the steps are present, the steps are added to the motion. In all cases, the step velocity is several orders of magnitude greater than the other ankle motions so that direct effects of the other motions to the step transient are negligible. One-half

degree steps are used. Subjects stand quietly under the following test conditions:

1. relaxed on rigid platform; eyes closed
2. rigid platform; visual display of  $\theta_B$ ,  $1^\circ = 6$  centimeters
3. rigid platform; eyes open; try to minimize sway
4. small random low frequency platform rotations; eyes open
5. small random low frequency platform rotations; eyes closed
6. platform is servoed to maintain zero ankle angle; eyes open
7. platform is servoed to maintain zero ankle angle; eyes closed

The random appearing platform disturbances are composed of six sinusoids:

<u>Radians per Second</u>	<u>AMP</u>
0.1	$1^\circ$
0.15	$1^\circ$
0.21	$1^\circ$
0.29	$0.5^\circ$
0.33	$0.5^\circ$
0.61	$0.5^\circ$

Maximum amplitude of the composite signal never exceeds  $\pm 2^\circ$ . The frequencies were chosen to be well within the range of normally occurring postural responses. (See section 5.2 for frequency response data.)

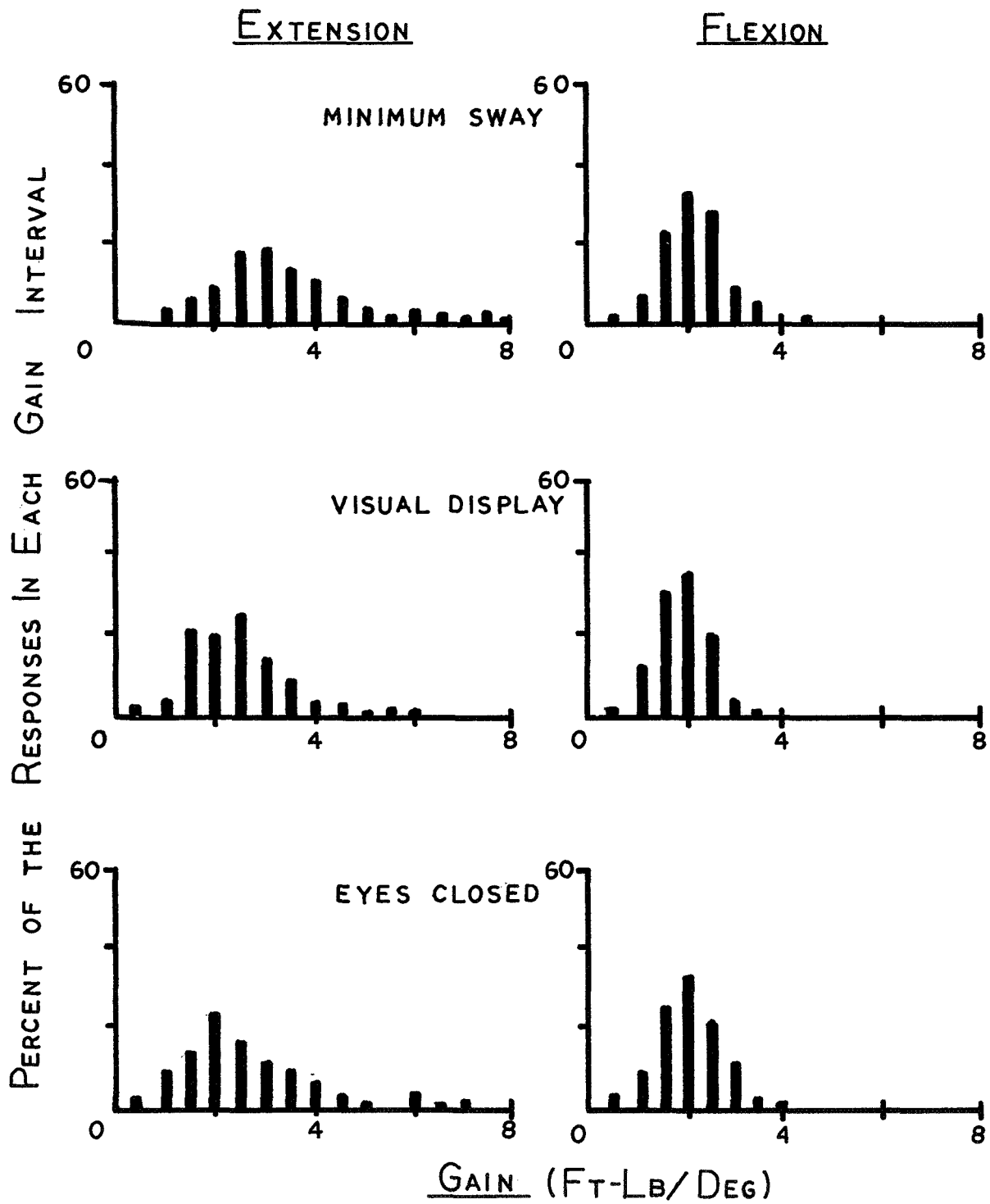


FIGURE 3.17a DISTRIBUTION OF REFLEX GAINS FOR 1/2 DEGREE STEPS IN ANKLE ANGLE

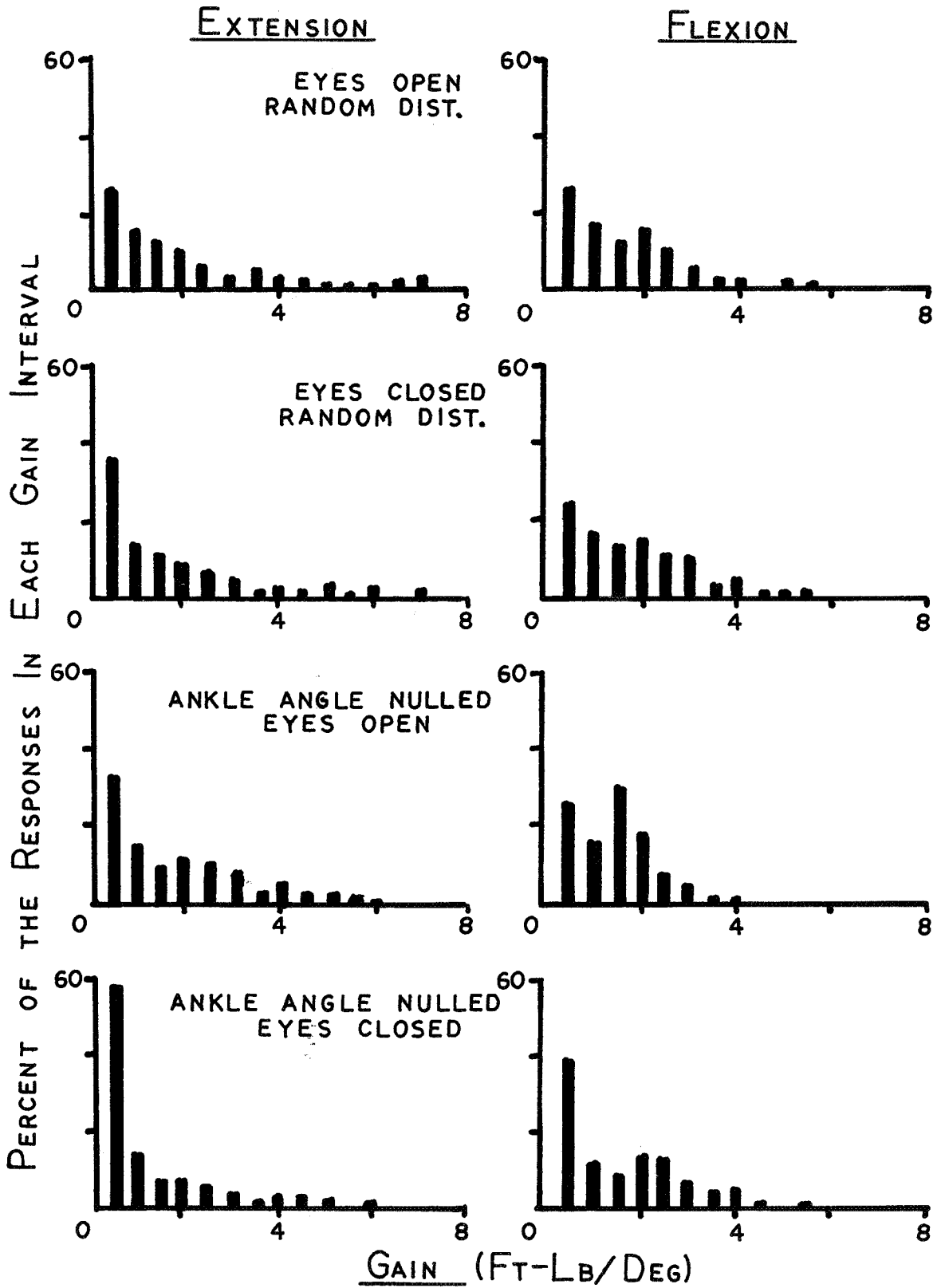


FIGURE 3.17b DISTRIBUTION OF REFLEX GAINS FOR 1/2 DEGREE STEPS IN ANKLE ANGLE

### 3.2.3 Results and Conclusions

All subjects clearly demonstrate adaptation of the reflex gain in response to changes in posture control conditions. Composite gain histograms for each of the eight experimental conditions are shown in Figure 3.17.

Subjects are able to increase reflex gain when asked to exert special effort to minimize sway. They all reported, however, that this condition was quite uncomfortable if maintained for more than a few minutes.

When given a high sensitivity visual display of body orientation with respect to vertical, their reflex gain decrease only slightly compared to normal gain, while their ability to reduce body sway increased significantly. Subjects reported that this condition too was tiring after several minutes.

When small random disturbances are introduced, average reflex gain decreases to nearly one-half the "normal" (eyes open or eyes closed, standing on a rigid surface) gain. In this case the distribution of reflex gains, rather than being "bell" shaped is more broadly distributed. These results suggest that the random disturbances cause suppression of reflex control a significant part of the time, since about 30 per cent of the reflex responses are at or near zero gain.

When the reflex position feedback loop is fully suppressed by maintaining zero ankle angle with platform rota-

tions, suppression of reflex control is nearly complete. About 65 per cent of the reflex responses are at or near zero gain.

Elimination of visual feedback has little effect on reflex control strategy under any of the tested conditions. All runs identical for eyes open or eyes closed showed no significant changes in the distribution of reflex gains.

According to subjects' reports, increased utilization of either reflex (when trying to minimize sway) or higher center (when controlling with highly sensitive visual feedback display) control results in rapid subject fatigue. An "optimal" combination of these two types of feedback during normal postural control is thus indicated.

The availability of the supporting surface for body and inertial reference information determines the reflex gain setting. Reflex gain is reduced as the reflex control loop becomes a less effective mode of stabilization. Changes in the state of higher center feedback sensors (i.e. eyes open or eyes closed) seem to have a much smaller effect on the strategy for reflex gain setting.

Reflex strategy is integrated into the complete posture control mode after development of the higher center control models in Chapters 4 and 5.

## CHAPTER 4

THE VESTIBULAR SENSES

The vestibular organs, the utricles, the saccules, and the semicircular canals are the prime motion sensors in the human. Vestibular cues contribute important sensory information for the regulation of posture.

In a series of experiments observing posture control in human subjects, all sensory information relative to postural orientation but that from the vestibular system is eliminated. Results demonstrate specific regulating functions for the linear motion sensors, the utricle otoliths, and the angular motion sensors, the semicircular canals.

As the body begins to fall, the semicircular canals detect this motion and initiate corrective postural responses. The semicircular canal feedback loop is unable, however, to detect or stabilize very low frequency drift.

The linear motion sensors provide excellent steady state and very low frequency body angle information, correcting the low frequency drift of the canal feedback loop. Analysis of linear motion stimulation during body sway shows an

ambiguity in the sign of the input at higher frequencies due to the interaction of gravitational and linear acceleration stimuli.

A model is developed which accurately describes these vestibular regulatory processes.

#### 4.1 The Vestibular System, Response Characteristics

The physiology of the vestibular sensors, the utricles, the saccules, and the semicircular canals is presented in Chapter 2. A review of recent data on the input-output characteristics of these sensors follows.

Meiry (83) analyzes the vestibular organs in detail by using sinusoidally varying linear and angular stimuli on human subjects whose subjective responses are then measured. He shows that the semicircular canals function as angular accelerometers with input axes fixed to the head. Response characteristics are second order and heavily damped; hence, output is proportional to angular velocity over the range of input frequencies between 0.15 and about 10 radians per second. Meiry reports that a subjective threshold to perception of angular accelerations about the roll and pitch axes is about  $0.5^\circ/\text{sec}^2$ , with a rather sharp separation between sensation and a lack of it. Subjective threshold in yaw is significantly less, averaging  $0.14^\circ/\text{sec}^2$ .

Young et al. (112) show that the linear motion sensors in the horizontal plane, generally believed to be the utricle otoliths, are accelerometers with overdamped, second

order characteristics. Output sensation indicates both linear velocity and orientation with respect to gravity. Meiry (83) estimates a linear acceleration threshold of 0.005g, equivalent to a 0.30 degree threshold for subjective orientation.

Angular acceleration threshold values for the semi-circular canals reported in the literature vary over a wide range. Clark and Stewart (17) find detection of steady state angular accelerations with the oculogyral illusion at values ranging from 0.04 to 0.28/sec<sup>2</sup>. The illusion does not involve a direct sensation of movement, rather the subject, seated in a dark enclosure during angular acceleration, perceives movement of a light spot which is actually fixed with respect to him. The illusion of movement is believed to be caused by the action of canal output responses on the visual system. Their results show that canal responses influence visual sensation at levels of angular acceleration significantly below the levels which can be detected subjectively.

Clark and Stewart also test subjective threshold for perception of pitch axis accelerations in normal human subjects. Average threshold is 0.67°/sec<sup>2</sup>; intersubject variability, however, is very high, ranging from 0.06 to 2.24°/sec<sup>2</sup>. Other investigators cited by them report subjective thresholds which vary over a wide range: Hilding (52), 0.25 to 3.0°/sec<sup>2</sup>, Groen et al. (46), 0.28 to 2.0°/sec<sup>2</sup>.

While descriptions of semicircular canal and utricle otolith dynamics are reasonably accurate, there is a large uncertainty in the observed values of the angular acceleration threshold of the semicircular canals. Present data indicate that canal angular acceleration threshold varies with input axis and is heavily dependent on the response modality, subjective, ocular, etc. Posture control represents one of the primary functions of the pitch and roll axis motion sensors; therefore, posture responses to vestibular stimulation should presumably be sensitive indicators of the vestibular response thresholds.

#### 4.2 Vestibular Stimulation by Body Angle Motion

Angular acceleration of a rigid human body about the ankle joints is directly equivalent to the accelerating input to the pitch axis semicircular canals. Since the posture control model to be developed here considers only quiet standing during which the upper body remains relatively rigid, equivalence of body angle acceleration and pitch axis angular accelerations may be assumed.

Stimulation of the utricle otolith organs by body sway motions is considerably more complex since both gravitational and linear acceleration reaction forces act as inputs. During uncontrolled sway divergence of the body, gravitational ( $f_g$ ) and tangential acceleration reaction force ( $f_t$ ) act in opposite directions.

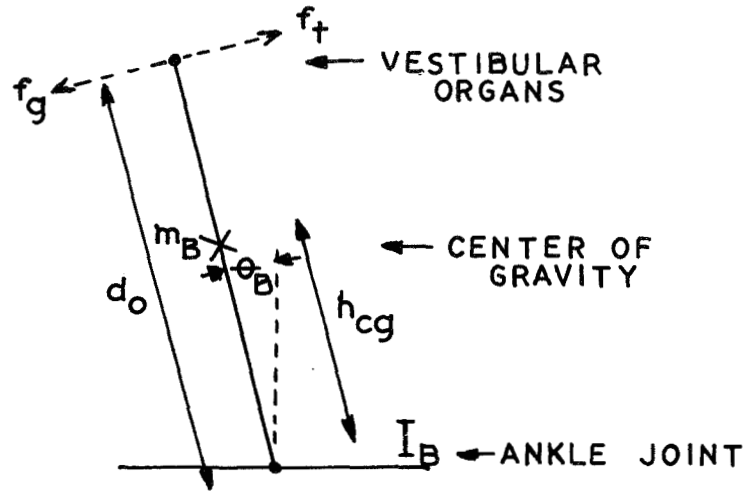


Figure 4.1 The Body and its Sway Dynamics

$$I_B \ddot{\theta}_B = m_B g h_{cg} \theta_B + T_A \quad (4.1)$$

where

$T_A$  = reaction torque about the ankle joint

$\theta_B \approx \sin \theta_B$ , small angle approximation

The net reaction force on the otolith during free fall

( $T_A = 0$ ) is:

$$f_0 = \theta_B \left( g - \frac{m_B g h_{cg} d}{I_B} \right) \quad (4.2)$$

Because the utricle otolith organs are located well above the center of mass of the body, the net reaction force on the otolith is negative during free-fall sway divergence of the body, (i.e., it is opposite to the force on the otolith due to gravity alone). If the body diverges with partial resistance from postural responses, the net force acting on the otolith may be negative, zero, or positive depending on the intensity of postural resistance. Recalling that reflex responses oppose body sway with a torque roughly proportional to angular deflection of the

ankle joint, the following relations demonstrate the ambiguity of the sign of the linear motion sensor:

$$T_A = -K \theta_B \quad (4.3)$$

$$f_0 = \theta_B \left( g - \frac{m_B g h_{cg} d_0}{I_B} + \frac{K d_0}{I_B} \right) \quad (4.4)$$

Using body parameter values derived in Appendix A, we find that:

$$f_0 > 0 \text{ if } K > 4 \text{ ft-lb/degree}$$

$$f_0 < 0 \text{ if } K < 4 \text{ ft-lb/degree}$$

During stabilizing postural responses, body angle is accelerating towards zero angle, tangential and gravitational forces on the otolith are always of the same sign.

Experiments described in the following section induce postural sway by displacing the experimental platform in either a forward or backwards direction at constant velocity. The subsequent analysis establishes the effect of these lateral displacements on the body sway motions and vestibular sensor stimulation.

Figure 4.2 illustrates the mode in which body angle motion is induced by the platform and defines the variables to be used in the analysis. Equations relating linear motion of the center of mass to linear and angular motion at the ankle joints are as follows:

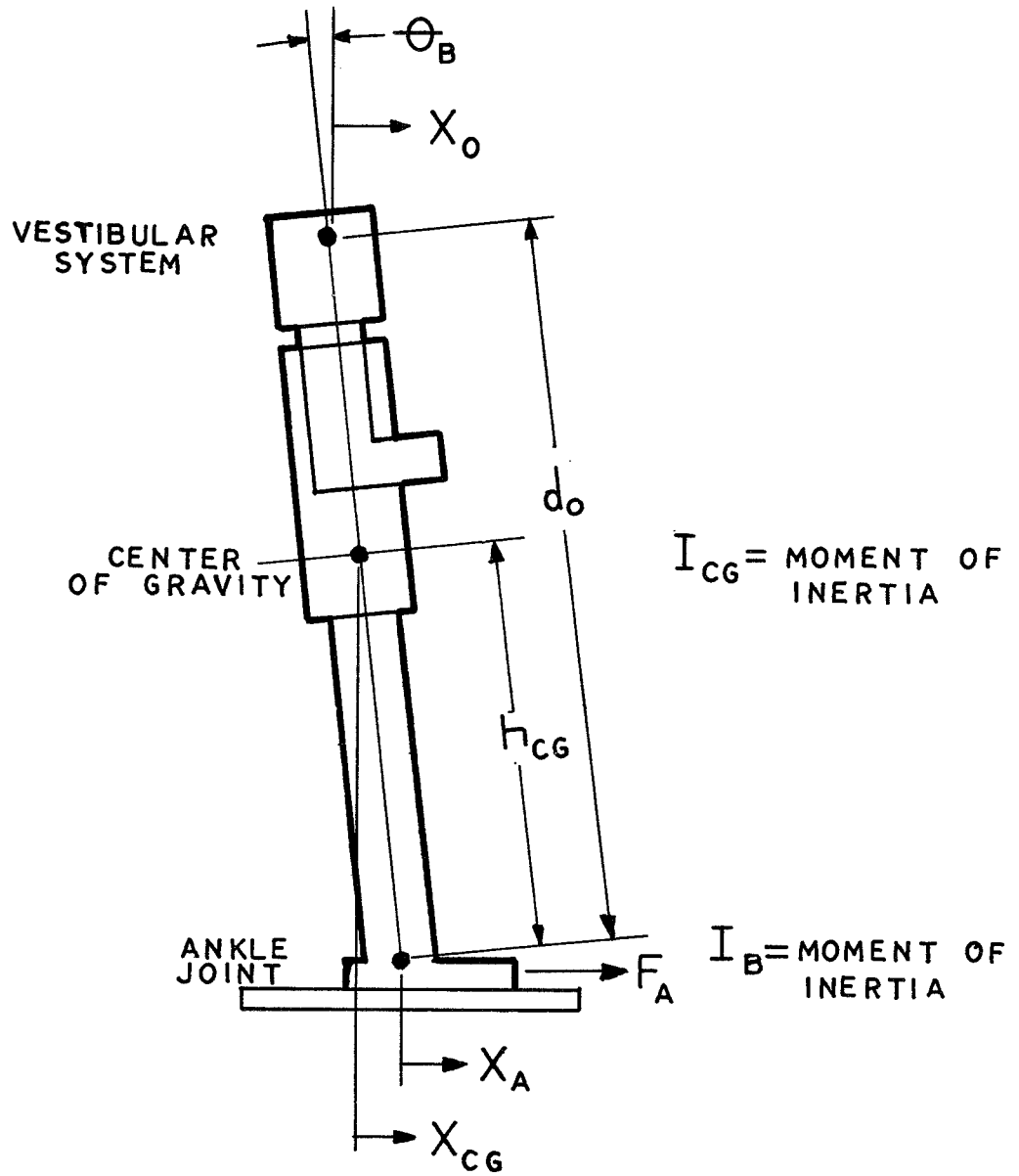


FIGURE 4.2 POSTURAL SWAY INDUCED BY LATERAL DEFLECTION OF THE PLATFORM

$$\dot{x}_A = \dot{x}_{cg} + h_{cg} \dot{\theta}_B \quad (4.5)$$

$$\ddot{x}_A = \ddot{x}_{cg} + h_{cg} \ddot{\theta}_B \quad (4.6)$$

A horizontal force acting at the ankle joint has the effects:

$$\ddot{x}_{cg} = \frac{F_A}{m_B} \quad (4.7)$$

$$\ddot{\theta}_A = \frac{F_A h_{cg}}{I_{cg}} \quad (4.8)$$

Combining results of (4.6), (4.7) and (4.8):

$$\ddot{x}_A = \frac{F_A}{M_{EQ}}, \quad M_{EQ} = \left( m_B + \frac{I_{cg}}{h_{cg}^2} \right) \quad (4.9)$$

Given an acceleration impulse,  $v_a u_1(t)$ , such that  $x_a(0^+) = v_a$ , the momentum delivered to the body at the ankle joints becomes:

$$P_A = M_{EQ} v_A \quad (4.10)$$

The acceleration impulse at the center of mass is:

$$\ddot{x}_{cg} u_1(t) = \frac{P_A}{m_B} = \frac{v_A M_{EQ}}{m_B} \quad (4.11)$$

Effects of the acceleration impulse on semicircular canal and utricle otolith stimulation are:

$$\ddot{\theta}_B u_1(t) = \frac{v_A}{h_{cg}} \left( 1 - \frac{M_{EQ}}{m_B} \right) \quad (4.12)$$

$$\ddot{x}_O u_1(t) = v_A \left( 1 - \frac{d_o}{h_{cg}} \left( 1 - \frac{M_{EQ}}{m_B} \right) \right) \quad (4.13)$$

So long as the platform continues at constant velocity after the initial acceleration impulse, no further lateral

forces act between the body and the platform. Only gravitational torque acts to induce further angular accelerations.

### 4.3 Postural Responses to Vestibular Stimulation

#### 4.3.1 Methods

The subject stands relaxed on the experimental platform. Sway is induced using small forward or backward platform displacements at constant velocity, introduced by the experimenter when the subject shows no movement. The platform disturbance induces a step change in body angular velocity.

Elimination of all other modes of sensory feedback is necessary to insure that postural responses to the induced sway are vestibular in origin. To remove reflex responses and kinesthetic cues, the platform is rotated to track the motions of the body; thus, maintaining an ankle angle of zero. Nulling ankle angle during body angle motion effectively opens the reflex position feedback loop but does not interfere with the subject's ability to generate isometric ankle control torques. Removal of reflex feedback also eliminates any advanced exteroceptive cues. (This point is more clearly explained in section 5.1.) Subjects are tested with eyes open and eyes closed to determine effects of visual cues on vestibular detection of body sway.

The hybrid computer program, Test, records ankle reaction torque and body angle on digital tape during each

response sample (the program is presented in Appendix C). Each run consists of 16 samplings of the induced sway response threshold. Induced sway rates range from 0.15 to 3.0°/sec.

#### 4.3.2 Results

Figure 4.3 shows typical postural responses to rapid and to slow induced body motion stimuli. Responses are characterized by an initial period during which the body angle begins to increase while the ankle torque remains unchanged. When the motion is detected by the vestibular sensors, ankle reaction torque increases rapidly, returning the body to a stable position. Threshold of the vestibular feedback sensors is defined in terms of the time after initiation of motion at which the ankle torque level has increased 0.25 foot pounds above its initial level.

Because subjects tend to oscillate almost continuously when their eyes are closed and reflex and kinesthetic feedback is removed, an accurate vestibular threshold function could not be determined for this condition. Instead, subjects are tested with eyes closed when the platform is rotated to track only the induced component of body angle motion. To show that this method does not introduce significant reflex and kinesthetic cues, a similar test is made with eyes open and the results compared to those in which all ankle angle motion is removed.

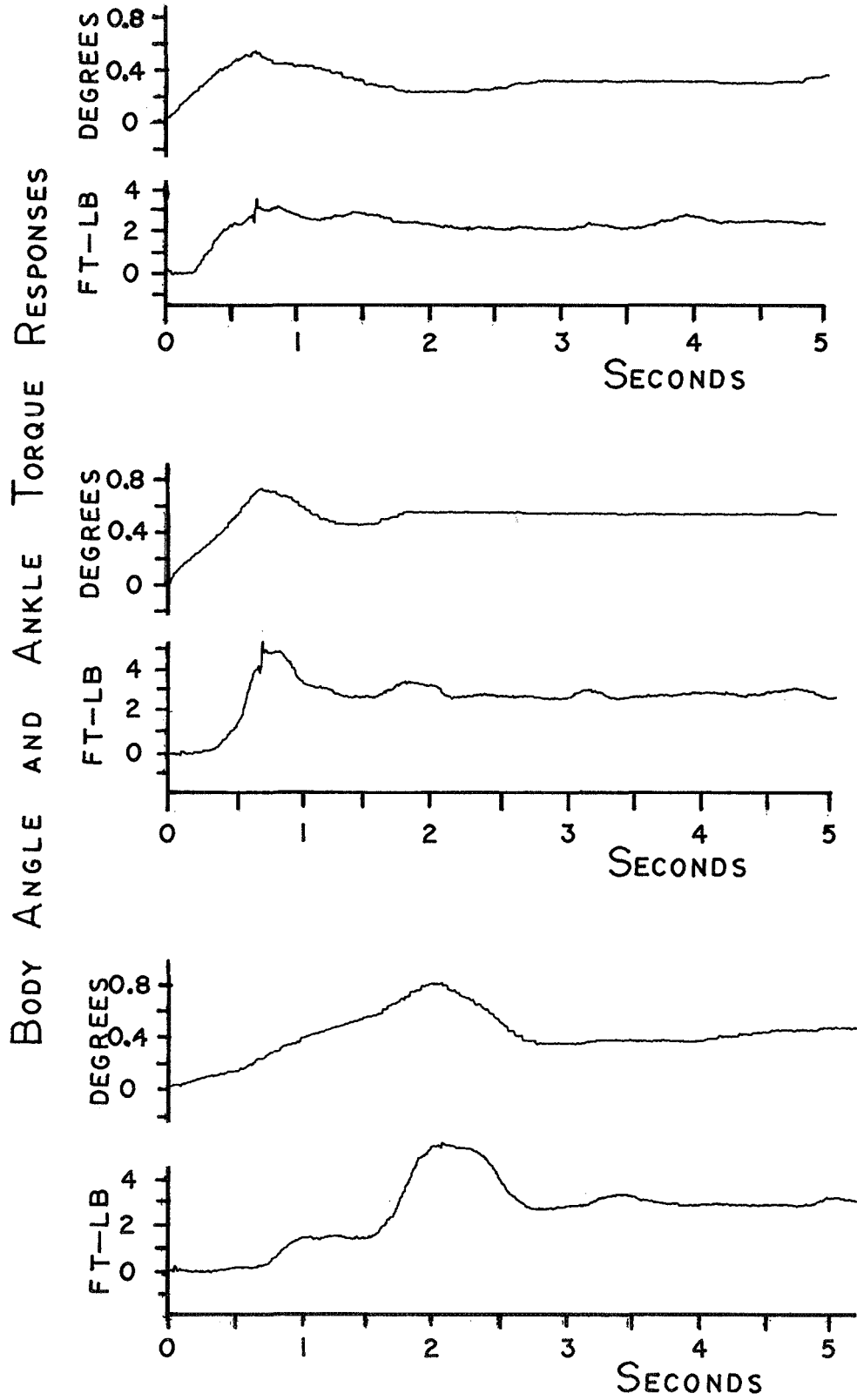


FIGURE 4.3 TYPICAL POSTURAL RESPONSES TO INDUCED SWAY MOTION

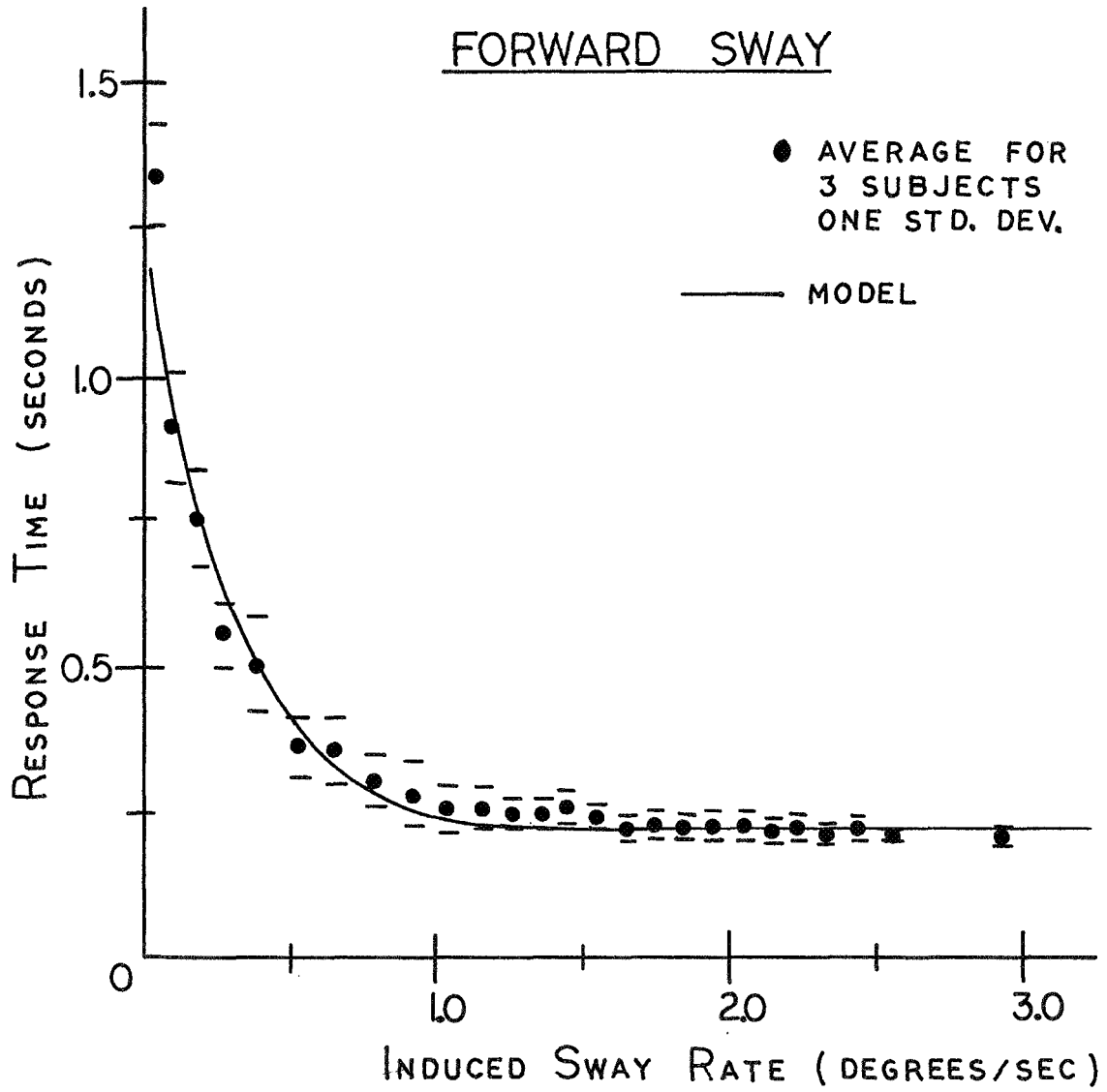


FIGURE 4.4a VESTIBULAR THRESHOLD RESPONSE CHARACTERISTICS TO INDUCED SWAY MOTION

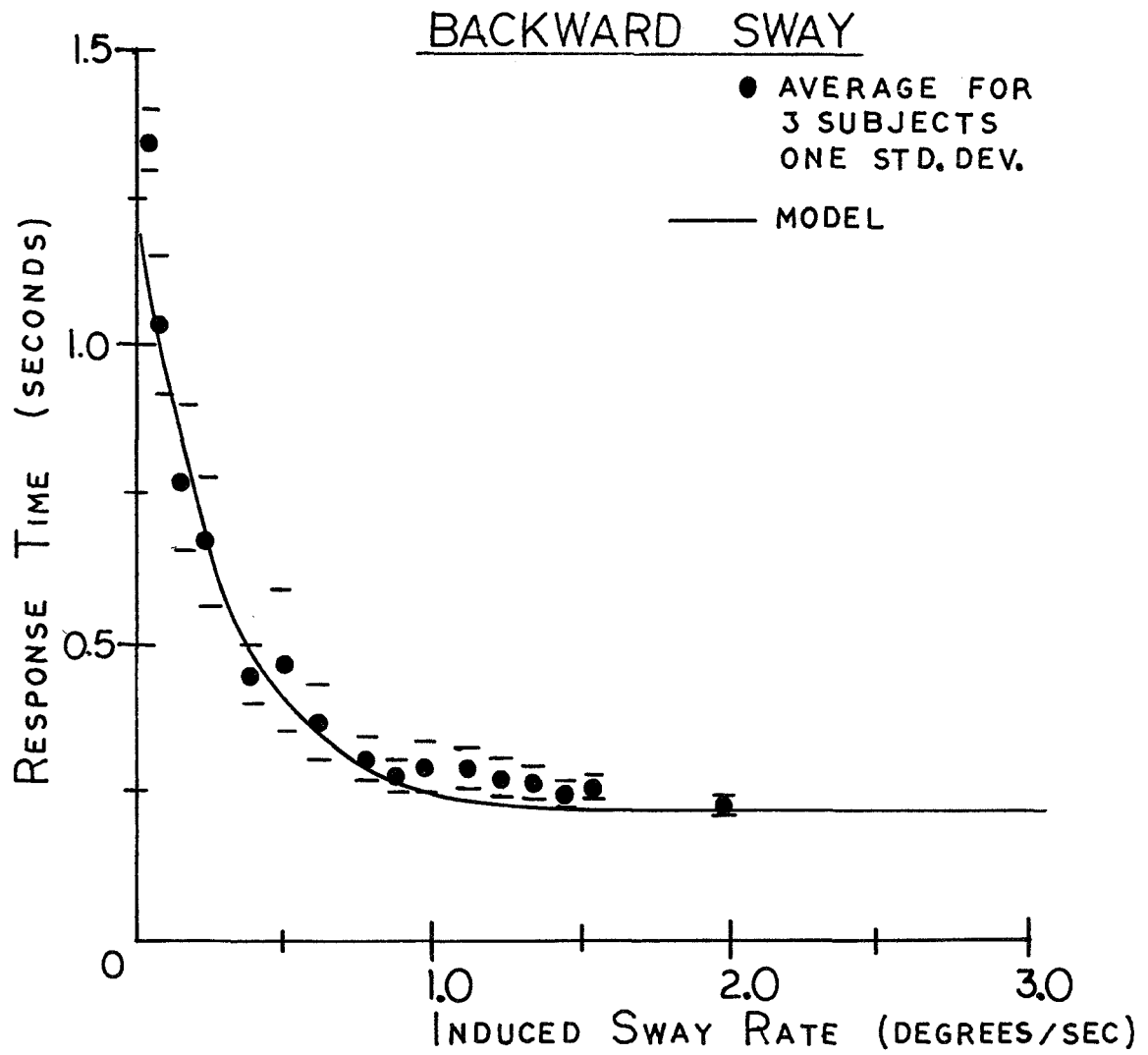


FIGURE 4.4 b VESTIBULAR THRESHOLD RESPONSE CHARACTERISTICS TO INDUCED SWAY MOTION

### 4.3.3 Conclusions - the Vestibular Model

Threshold characteristics for forward and for backward sway are identical. Variations among the subjects and among the three test conditions are statistically insignificant,  $p > 0.1$  for all samples. Composite threshold functions for the three test conditions are compared to the semicircular canal model threshold characteristics in Figure 4.4. The following semicircular canal model predicts the observed threshold characteristics over the complete range of induced sway rates:

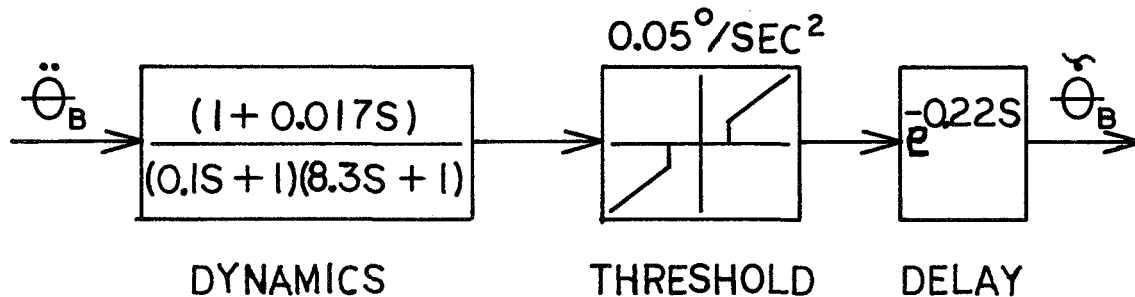


FIGURE 4.5 THE SEMICIRCULAR CANAL MODEL

Linear dynamic characteristics of the semicircular canal model compare closely with Meiry's canal model. The addition of a very small lead term is necessary to predict the minimum response time characteristics for large impulsive inputs. This term has no effect on threshold response properties within the dynamic range of normal body angle motions.

New values are derived for the pitch semicircular canal acceleration threshold and response transmission time delay. The  $0.05^\circ/\text{sec}^2$  acceleration threshold is considerably less than those observed with subjective reports. The following arguments are posed to account for the wide disparity between subjective and posture response thresholds.

All methods of measuring canal responses short of direct eighth nerve measurements necessarily introduce characteristics of additional neural elements between the original sensation and the observed response. Characteristics of these additional elements vary with the modality of measured response, and may also be affected by other states within the system. A case in point is the large difference in Stewart and Clark's data reporting yaw axis subjective and oculogyral illusion thresholds.

Yemelyanov et al. (110) report "...that while balancing himself a man's vestibular sensitivity thresholds decrease two- or three-fold..." Their observations show how the task at hand largely determines the characteristics of the intermediate elements between vestibular output and measured response.

Postural responses appear to result from relatively direct coupling with vestibular output. Threshold values measured by the author are among the lowest observed and are consistent from trial to trial and subject to subject.

Responses are measured during active control of posture which, according to Yemelyanov et al., affords a minimum of interference from intermediate elements. The short response delay time, 225 milliseconds, further substantiates that postural responses are initiated with little intermediate interference.

Lowest canal threshold values have been found by other investigators for angular acceleration about the yaw axis. Considering their measurement techniques, subjective and oculogyral illusion, this conclusion might be expected. Voluntary head and eye movements are predominantly within the horizontal plane; hence, the close functional link between the yaw sensitive canals and subjective and ocular responses. On the other hand, roll and pitch are the critical axes in the control of posture. Posture responses, therefore, should show close coupling with pitch and roll motion sensations.

The induced sway experiments add no detail to the characteristics of the linear acceleration sensors, the utricle otoliths, given by Young and Meiry. This model, Figure 4.6, will be used in future analyses.

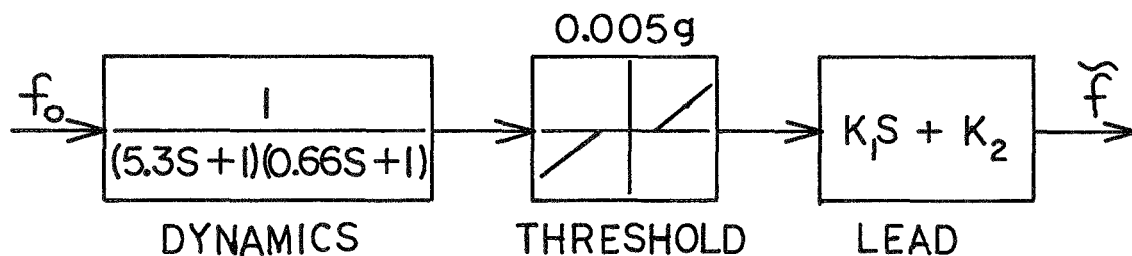


Figure 4.6 The Utricle Otolith Model

A hybrid computer model for the semicircular canal and utricle otolith dynamics is developed in Appendix D. Threshold response characteristics for detection of body angle during free-fall divergence are determined for each sensor. Figure 4.7 shows the body angle at which sway is first detected as a function of the initial body offset angle,  $\theta_b(0)$ , where  $\dot{\theta}_b(0) \neq 0$  and  $\theta_b(0) = 0$ . Data points shown in the figure are results of body angle threshold detection experiments described in sections 4.4 and 5.2.

Linear motion sensors probably play no role in the detection of postural responses during free-fall divergence. Simulation of the otolith dynamic model indicates that the linear acceleration threshold must be an order of magnitude less than the lowest values reported in the literature, even in the limit, as the initial body angle offset amplitude approaches zero. The utricle otolith organ threshold is sufficient to account for observed response threshold levels only in the static or nearly static range, since the body free-fall divergence rate ( $\omega_B = 3$  r/sec) is fast compared to the very slow dynamics of the otolith organs.

The role of linear and angular acceleration cues in posture regulation are made clear by observing the frequency ranges at which each component of the vestibular apparatus is most effective in responding to sinusoidal postural sway. Figure 4.8 shows the sinusoidal body angle amplitude necessary just to achieve detection of motion as a function

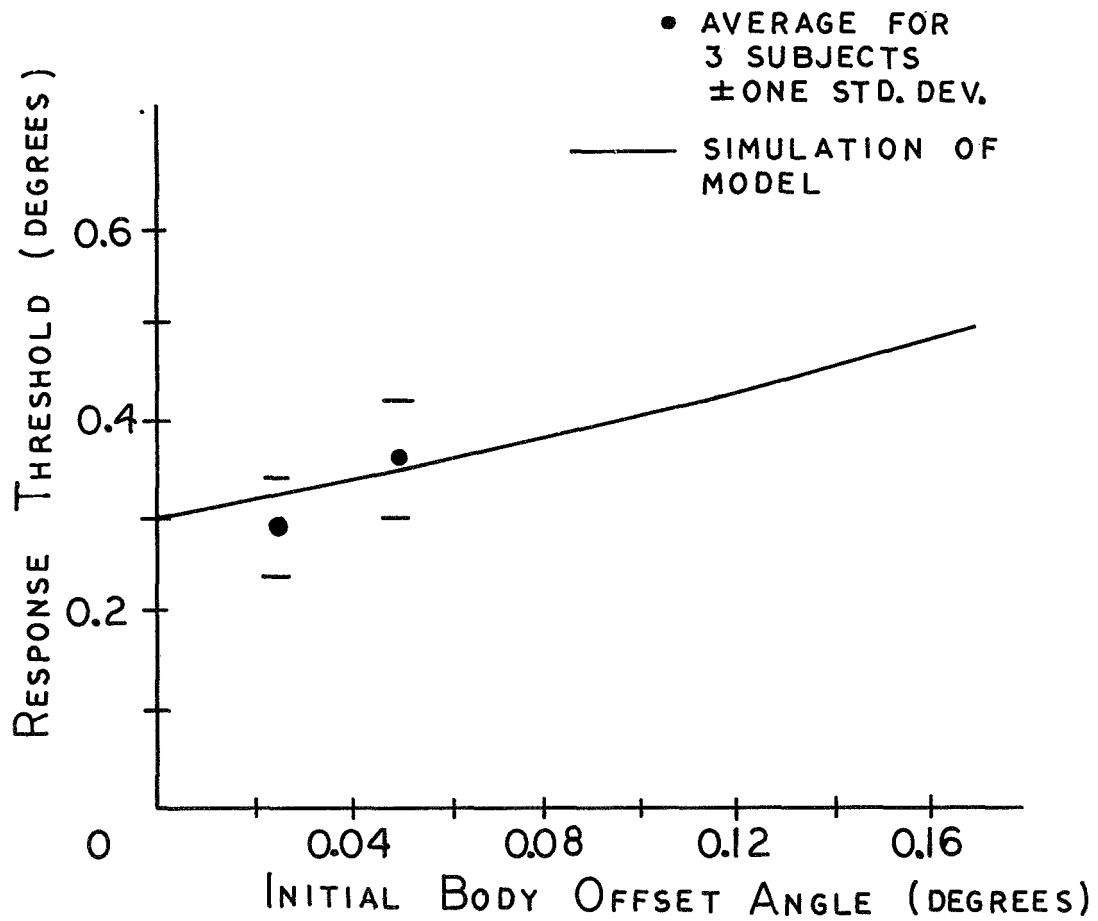


FIGURE 4.7 RESPONSE THRESHOLD AS A FUNCTION OF THE INITIAL ANGLE OFFSET OF THE BODY, SIMULATION OF THE VESTIBULAR MODEL

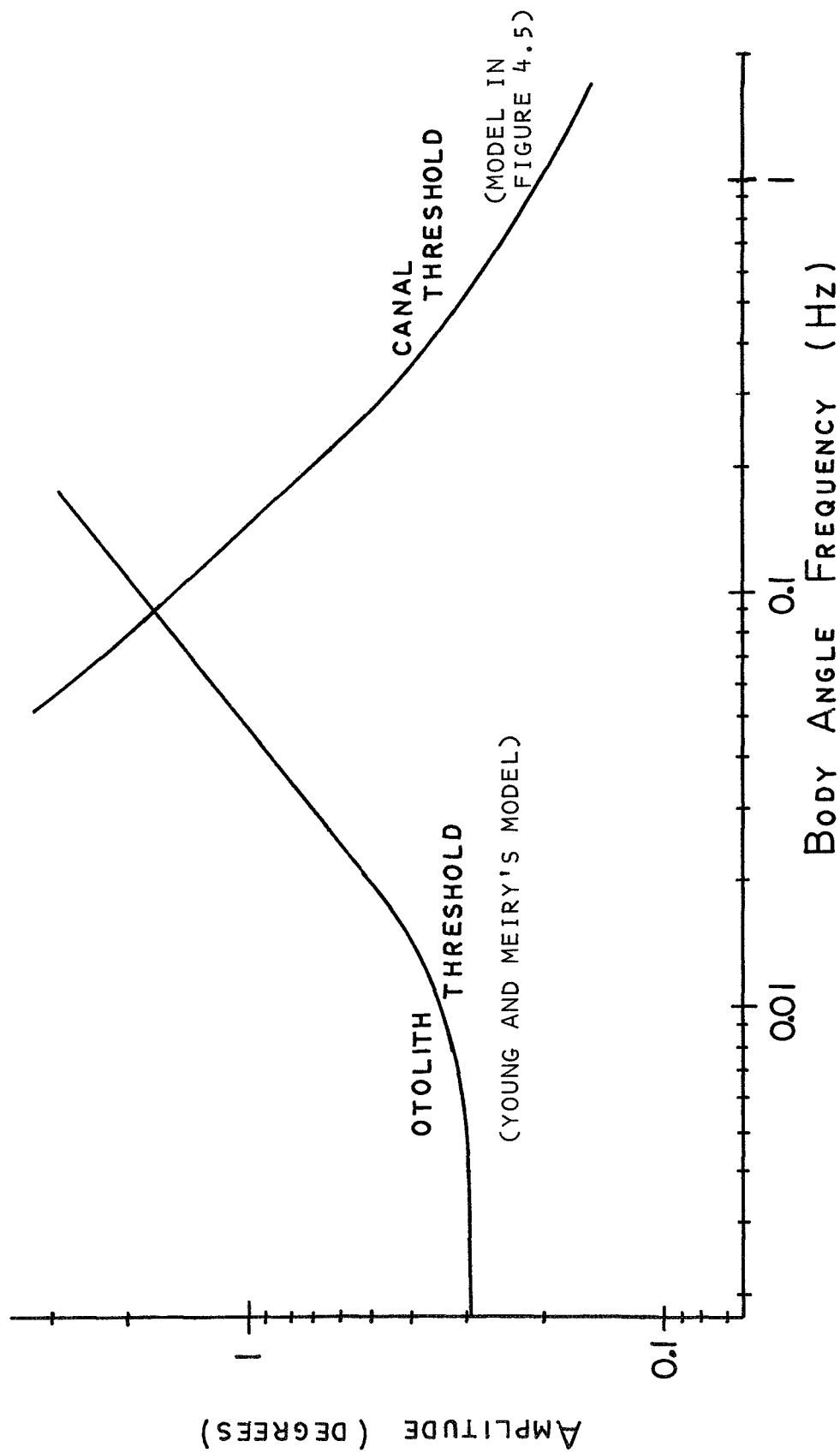


FIGURE 4.8 THE AMPLITUDE OF OSCILLATION JUST NECESSARY TO PRODUCE A THRESHOLD RESPONSE IN EACH VESTIBULAR ORGAN AS A FUNCTION OF SWAY FREQUENCY

of sway frequency. Note the clear separation of the functional frequency range for each sensor. The thresholds for each sensor within its frequency range of maximum sensitivity are approximately the same.

The poor response characteristics of the utricle otolith organs, which exclude from participating in the detection of postural responses is not surprising. Functional arguments support these results. Since linear motion stimulus is ambiguous during body angle divergence, the extra processing necessary to resolve the sensory ambiguity makes the utricle otolith an unlikely candidate for initiating short delay postural responses. Low pass filtering of utricle otolith response resolves this ambiguity quite effectively since the sign reversal occurs only at higher frequencies. The low frequency otolith output is an excellent estimate of average orientation with respect to gravity.

#### 4.4 Postural Regulation with Vestibular Feedback

Posture control with vestibular feedback alone is observed. Subjects stand with eyes closed on the experimental platform. Ankle angle is maintained at zero by rotating the platform to track body angle motion. Ankle reaction torque and body angle are recorded continuously. A typical response sequence, shown in Figure 4.9, is composed of the following stages:

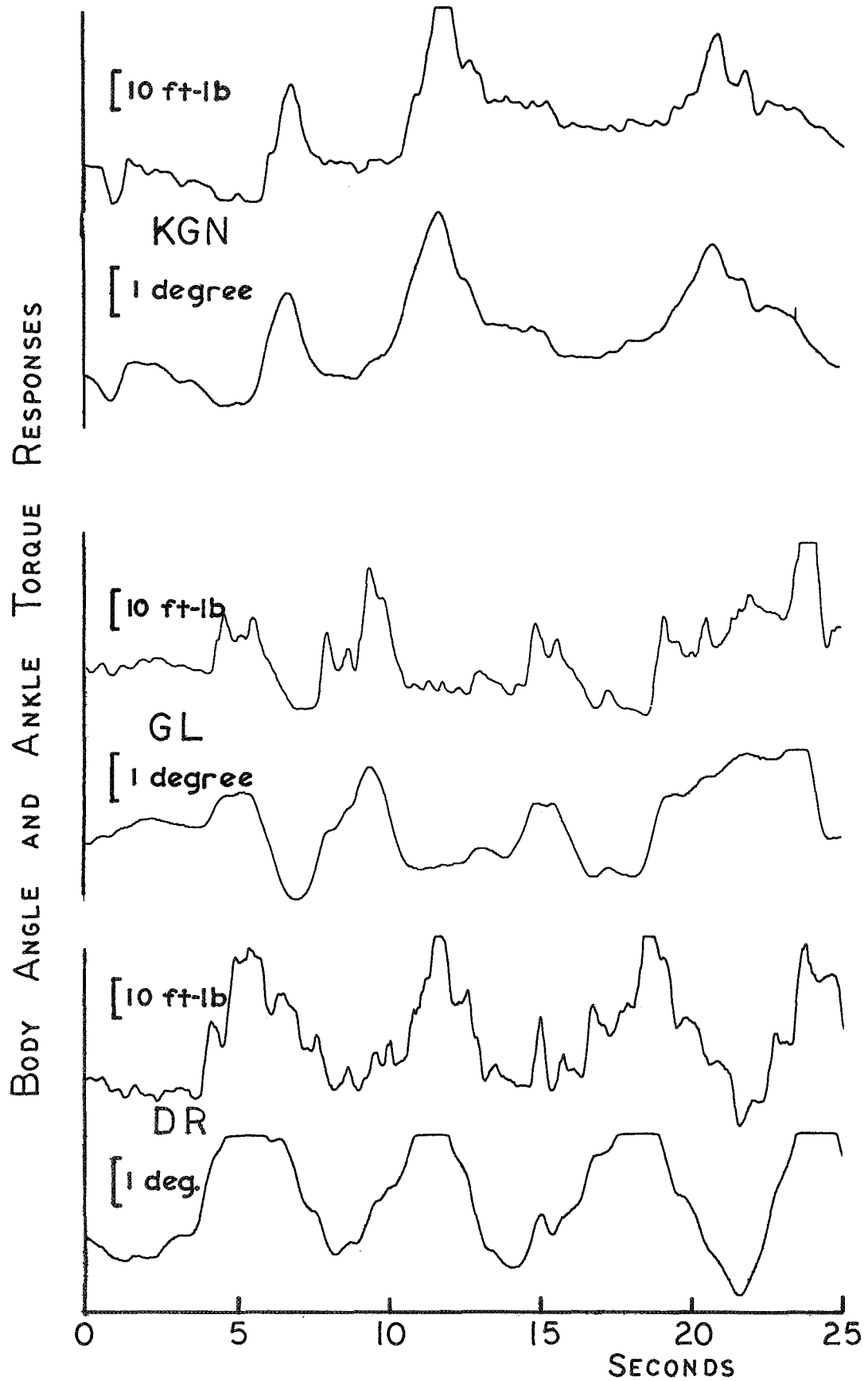


FIGURE 4.9 TYPICAL BODY ANGLE AND ANKLE TORQUE RESPONSE SEQUENCES DURING VESTIBULAR REGULATION OF POSTURE

1. stable period with no movement lasting several seconds
2. sway divergence begins
3. threshold is reached; ankle torque increases to restabilize body
4. one or several oscillations occur before quiet standing is re-established.

Ten of these response sequences are averaged for each subject, Figure 4.10, to determine transient response properties of the vestibular posture control loop.

Transients to be averaged are lined up with one another by defining time zero as one second before initiation of the torque response. Only changes in angle and torque are considered, both  $\theta_B(0)$  and  $T_A(0)$  are defined as zero. Transients are averaged only for a five second interval because beyond this time other factors begin to cause wide differences among the responses.

The transient response patterns are consistent among subjects. Average canal threshold is  $0.36^\circ$ . Variations among subjects are insignificant,  $p > 0.1$ . On the average subjects diverge about  $0.5^\circ$  in the first second, equivalent to an average of  $0.05^\circ$  initial body angle error. Referring to Figure 4.7, actual divergence canal responses show close correlation with those of the simulated canal mode.

#### 4.5 Postural Regulation with Vestibular Feedback -- A Model

The inverted pendulum configuration of the human body is stabilized with a combination of body angle and body

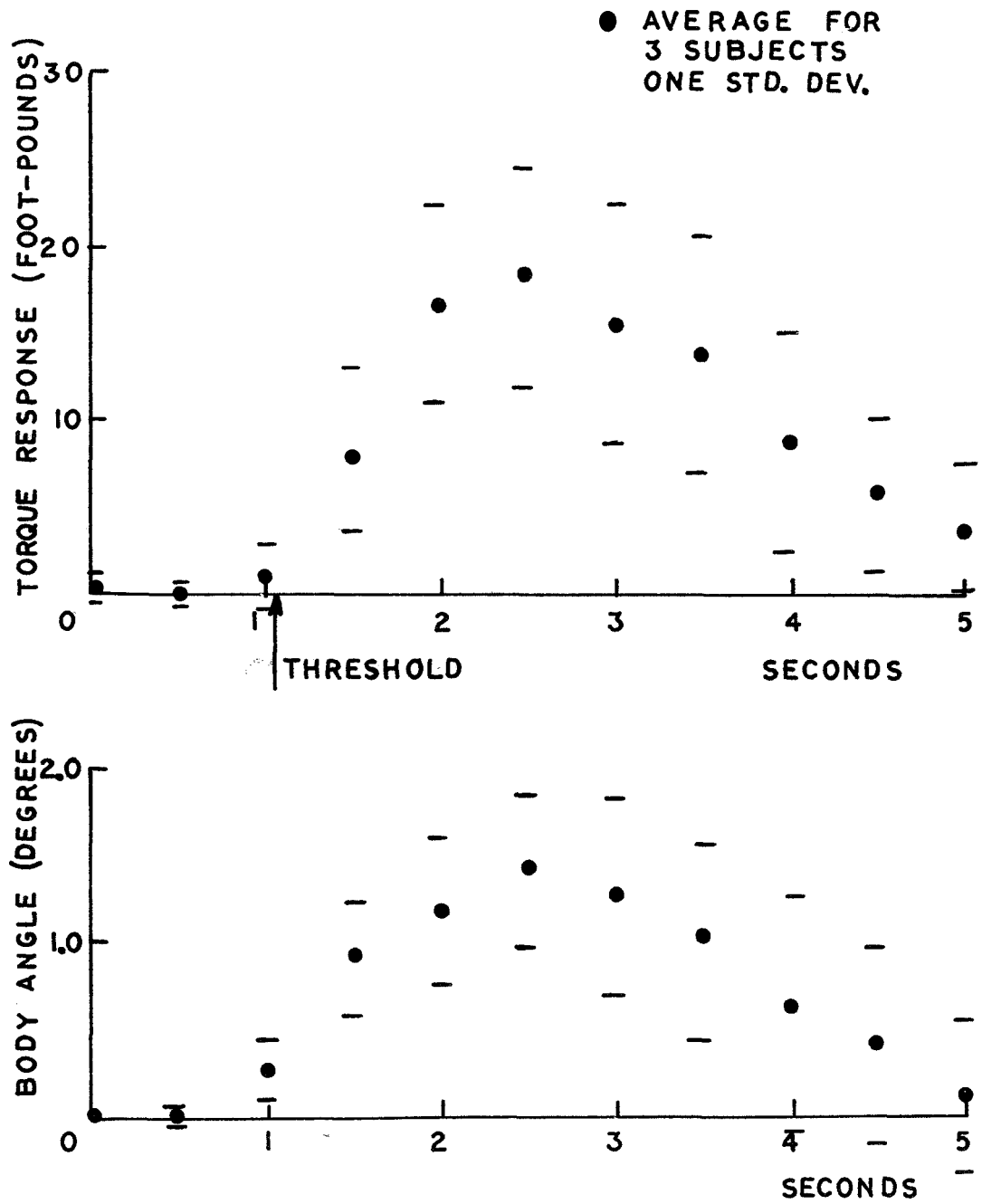


FIGURE 4.10 AVERAGE BODY ANGLE AND ANKLE TORQUE RESPONSES DURING VESTIBULAR REGULATION OF POSTURE

angle rate feedback. Two modes of vestibular sensation provide dynamic feedback information of body angle. The semicircular canals provide a good estimate of sway rate for frequencies above 0.1 Hz, while the otoliths indicate sway angle below 0.1 Hz. Because of frequency response limitations of each sensor, the canal feedback control loop is unable to respond to rapid sway divergence. Thus, stability can only be attained through the combination of two frequency selective feedback loops, each of which in isolation is unable to provide stability.

In the proposed vestibular control model, the canal output, body angle rate, is used for an initial estimate of both body angle rate and, through neural integration, body angle. The low frequency utricle otolith estimate of body angle updates the initial canal estimate. The model configuration is shown in Figure 4.11.

Several comments about the configuration of the model relevant to physiology are in order. The threshold characteristics of the semicircular canal model which best predicts postural responses to detection of sway features a step in output at the time of detection. This small step might be interpreted as an initially high sensitivity in the loop which habituates rapidly after the onset of the postural response. Predicted response characteristics of the model are insensitive to the type of otolith threshold.

Neural compensation of semicircular canal feedback includes a pure integration. Most likely, the physiological

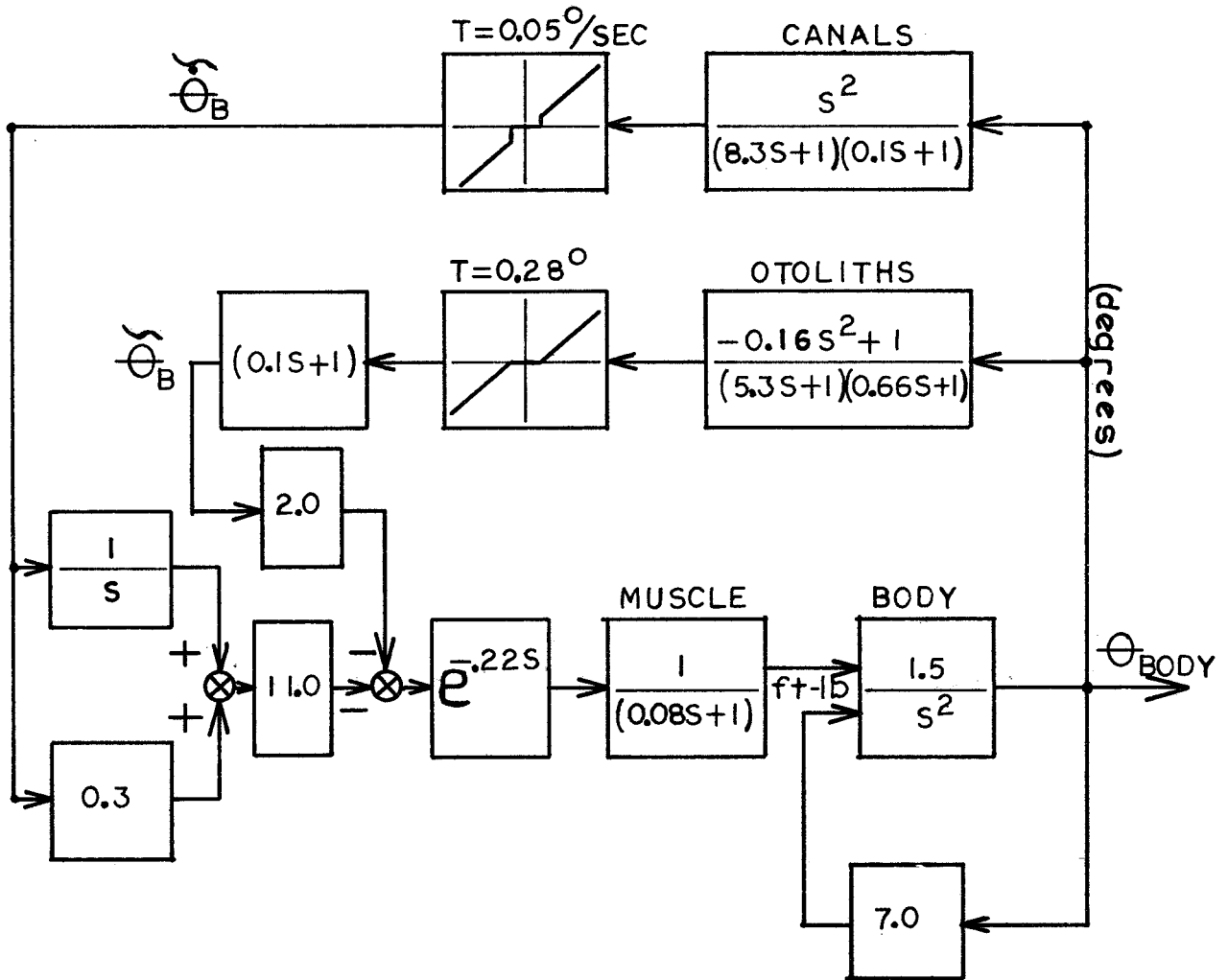


FIGURE 4.11 MODEL FOR VESTIBULAR REGULATION OF POSTURE

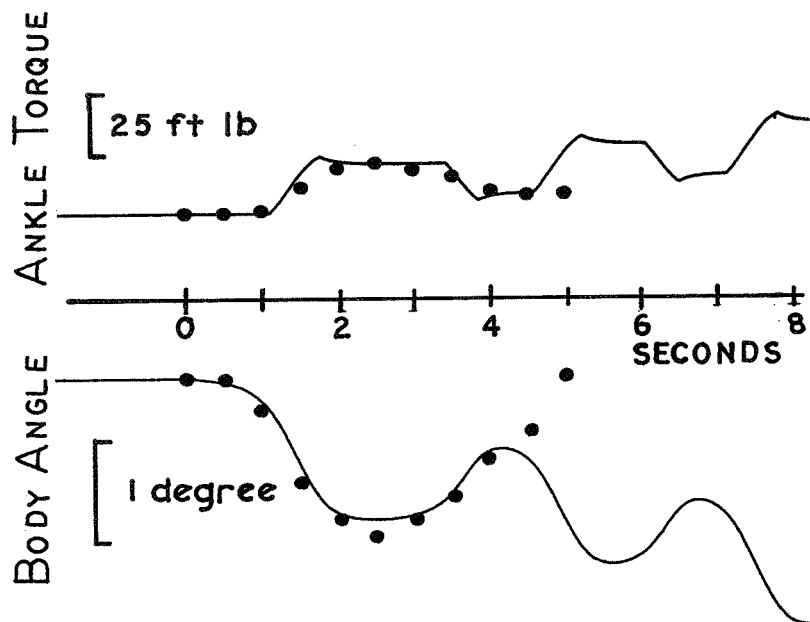
mechanism is a lag of the form  $\frac{K}{KS + 1}$ , rather than a pure integration. In this case otolith feedback would not only effect static stability but also would serve to "re-set" the neural "integration" in canal feedback loop.

The goal of the vestibular control model is to predict the response characteristics of a single cycle in the regulation process. Discrete response characteristics of the complete body-motor sensory model are shown in Figure 4.12. The presence of canal feedback alone shows the expected low frequency divergence. Stability is achieved when utricle otolith feedback is included to correct this. Note that the simulation results can be compared to actual responses only during the first cycle, since no provision is made in the model to "reset" the vestibular thresholds.

#### 4.6 Conclusions

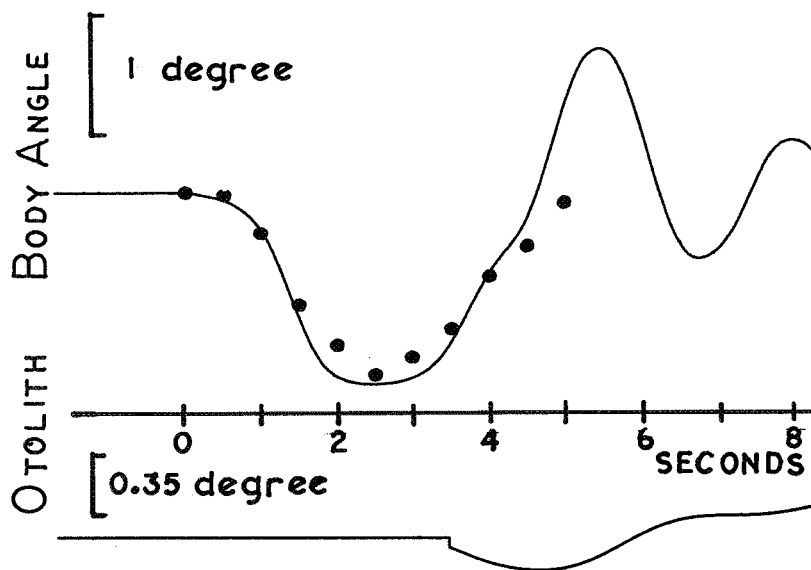
If indeed the vestibular system has evolved primarily as a posture regulatory device, the preceding analysis has shown it to be well adapted to perform that function. A high sensitivity to sway is achieved over the entire range of postural motion frequencies using two frequency selective sensors, Figure 4.8.

Orientation with respect to the gravitational field (vertical) is best measured with a linear accelerometer. Hence, the evolution of utricle otolith type organs in all including the most primitive forms of animal life which



MODEL RESPONSE - CANAL  
FEEDBACK ONLY

• AVERAGE FOR THREE  
SUBJECTS (FIG. 4.10)



MODEL RESPONSE - COMPLETE  
VESTIBULAR FEEDBACK

FIGURE 4.12 VESTIBULAR CONTROL MODEL CHARACTERISTICS  
COMPARED WITH EXPERIMENTAL DATA

have a preferred orientation with respect to vertical.

In higher forms of animal life, complex locomotion has necessitated more sophisticated modes of orientation. Rapid maneuverability requires bodies that are inherently less stable. The resulting rapid angular motions cause conflicts between linear acceleration and gravitational stimuli (section 4.2).

To eliminate sensory ambiguities, higher animal forms have evolved angular motion sensors, restricting the linear motion sense to very low frequencies. The angular motion sensors provide unambiguous motion sensation, but their static sensitivity is poor. In combination, utricle otolith and semicircular canals provide the complete spectrum of unambiguous motion information.

## CHAPTER 5

VISUAL AND EXTEROCEPTIVE SENSES

General models for visual and exteroceptive feedback are developed which indicate the ways that these senses modify vestibular responses. Analysis is limited to more general models for the following reasons:

1. In normal subjects visual and exteroceptive responses cannot be observed in isolation.
2. Present physiology does not permit construction of detailed models of the visual and exteroceptive senses.

Visual and exteroceptive senses are shown to be functionally separable in the same manner as the separation found between the otolith and semicircular canal sensors. Exteroceptive cues exhibit a very low body angle threshold ( $0.12^\circ$ ) but have little effect on slow phase correction. The high angular resolution of vision is limited to the low frequencies ( $< 0.1$  cps) during slow phase correction.

5.1 Function of Exteroceptive and Visual Senses

Exteroceptive cues are provided by ankle joint rotation and by changes in the distribution of pressures within the

foot and lower leg. Vision detects relative orientation of the body with respect to surrounding objects.

Exteroceptive cues are strongly dependent on the quality of the supporting surface and on reflex loop and higher center responses. A rigid supporting surface is required for the ankle angle receptors unambiguously to sense body motion. Deep pressure sensation is considerably more complex, since changes in muscle tension are the primary mode of stimulating these receptors. Free-falling body motions, causing changes in tension due to muscle and reflex responses, activate deep pressure sensors. After the initiation of higher center responses, deep pressure feedback information is primarily redundant efferent feedback.

Physiological descriptions of exteroceptive and visual senses are too complex to allow input-output modelling of these processes. Models of these feedback sensors must therefore be limited to more general functional descriptions.

Raffini's end organs are the primary receptors of joint angulation. Each joint contains a large number of receptors, each responding in proportion to joint angle and angular rate. Angular information is transmitted both as frequency and spatial distributions.

No quantitative data are available to indicate the resolution or dynamic characteristics of deep pressure sensation. Recordings from single pressure receptors show

that excitation is primarily sensitive to changes in pressure. Habituation rapidly degrades static pressure sensitivity.

Vision, the most complex of all human senses, is also the most difficult to describe quantitatively. Two point visual acuity at the fovea is excellent, resolving separations of about  $1/2$  minute of arc. Because of the multiple levels of visual processing, however, visual-motor response delays are longer than those for vestibular or kinesthetic responses. Okabe (86) observed eye-wrist response delays of 0.32 seconds. This experimenter found eye-ankle delays of 0.40 seconds.

Meiry (83) observed the performance of subjects stabilizing a vehicle with inverted pendulum dynamics over a range of divergence frequencies, Figure 5.1. He found that performance with visual cues, while superior to vestibular cues at low frequencies, degraded rapidly for frequencies above 1 rad/sec. With vestibular and tactile cues, subjects could stabilize a vehicle with divergence frequencies up to 2.6 rps but showed poorer low frequency performance. The combination of visual, vestibular, and tactile cues resulted in the best overall performance. Several, more extensive investigations into the use of visual and motion cues in manual control tasks parallel Meiry's results (26, 96).

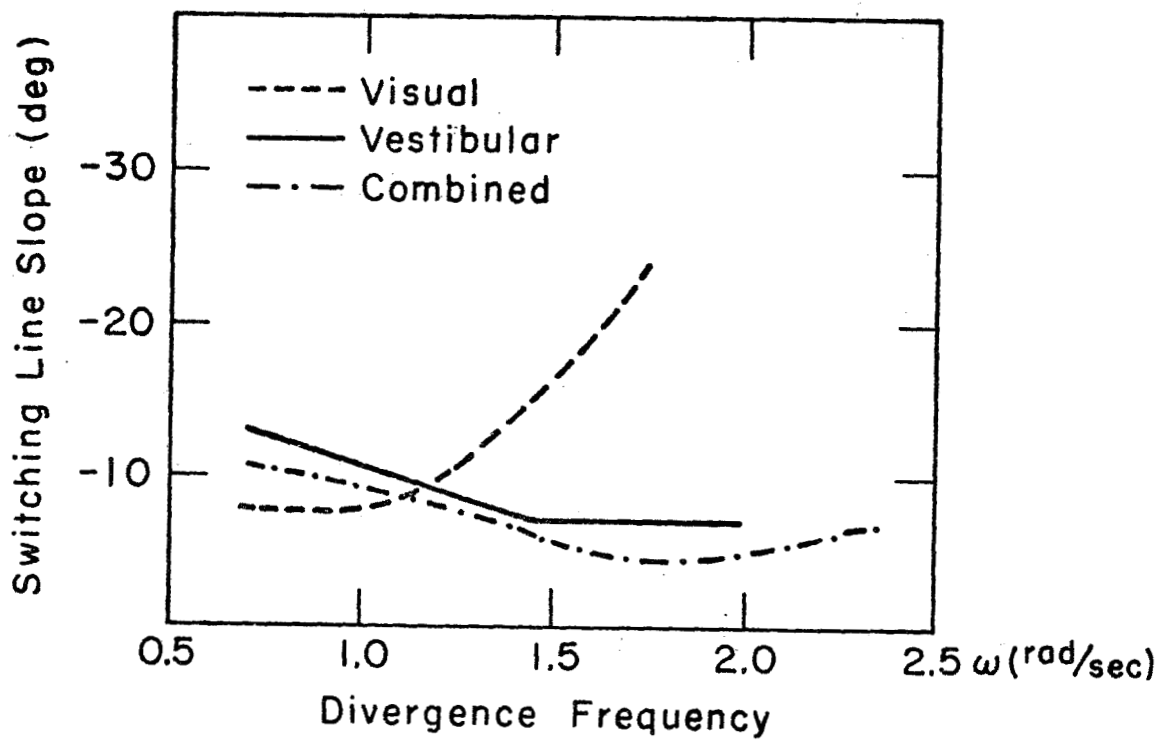


FIGURE 5.1 RMS ERROR FOR CONTROL OF AN INVERTED PENDULUM

Since removal of vestibular responses in normal subjects is not possible, the roles of the visual and kinesthetic senses may be studied only by observing how each sense modifies the vestibular postural responses.

## 5.2 Posture Regulation with Vestibular, Visual, and Exteroceptive Senses

### 5.2.1 The Experiments

Effects of including visual and/or exteroceptive cues during vestibular control of posture are considered. Subjects stand on the experimental platform under the following conditions:

1. eyes open; platform rotates to remove ankle angle feedback
2. eyes closed; platform rigid
3. eyes open; platform rigid.

Measurement techniques employed are similar to those used in Section 4.4; reaction torques and body angle are measured continuously.

In each of the above conditions, posture control follows the same basic pattern seen during vestibular feedback control: quiet period, body divergence, transient responses, and re-establishment of quiet stability.

For each subject ten transient responses of each test condition are averaged. In cases 2 and 3, special caution was exercised to include only responses in which the onset

of body motion clearly precedes initiation of the postural response. Figure 5.2 shows composite average responses for each test condition. At all sample times, variations among subject means were less than those within each subject's sample.

The basic strategy of control in case 1, vestibular and visual cues only, is similar to control strategy with vestibular cues only, defined in Figure 4.11. Control strategies in cases 2 and 3, however, are different, since the rigid platform enables full activation of the reflex control loop. Here control resembles that in the reflex model in Figure 3.16. Subsequent analysis develops each of these control models to include effects of visual and exteroceptive cues.

### 5.2.2 Vestibular and Visual Control

Comparing vestibular initiated responses with and without visual cues, Figures 4.10 and 5.2, three effects of the visual cues are evident:

1. The slow phase transient response is more highly damped when visual cues are added, (eyes open  $\rho \approx 0.5$ , eyes closed:  $\rho \approx 0.1$ ).
2. Peak amplitude of the slow phase transient response is reduced to less than one-half size when visual cues are included (eyes open: peak  $\theta_B = 0.6^\circ$ , eyes closed: peak  $\theta_B = 1.4^\circ$ ).
3. Offset error at the termination of the slow phase correction, as indicated by the rate at which the

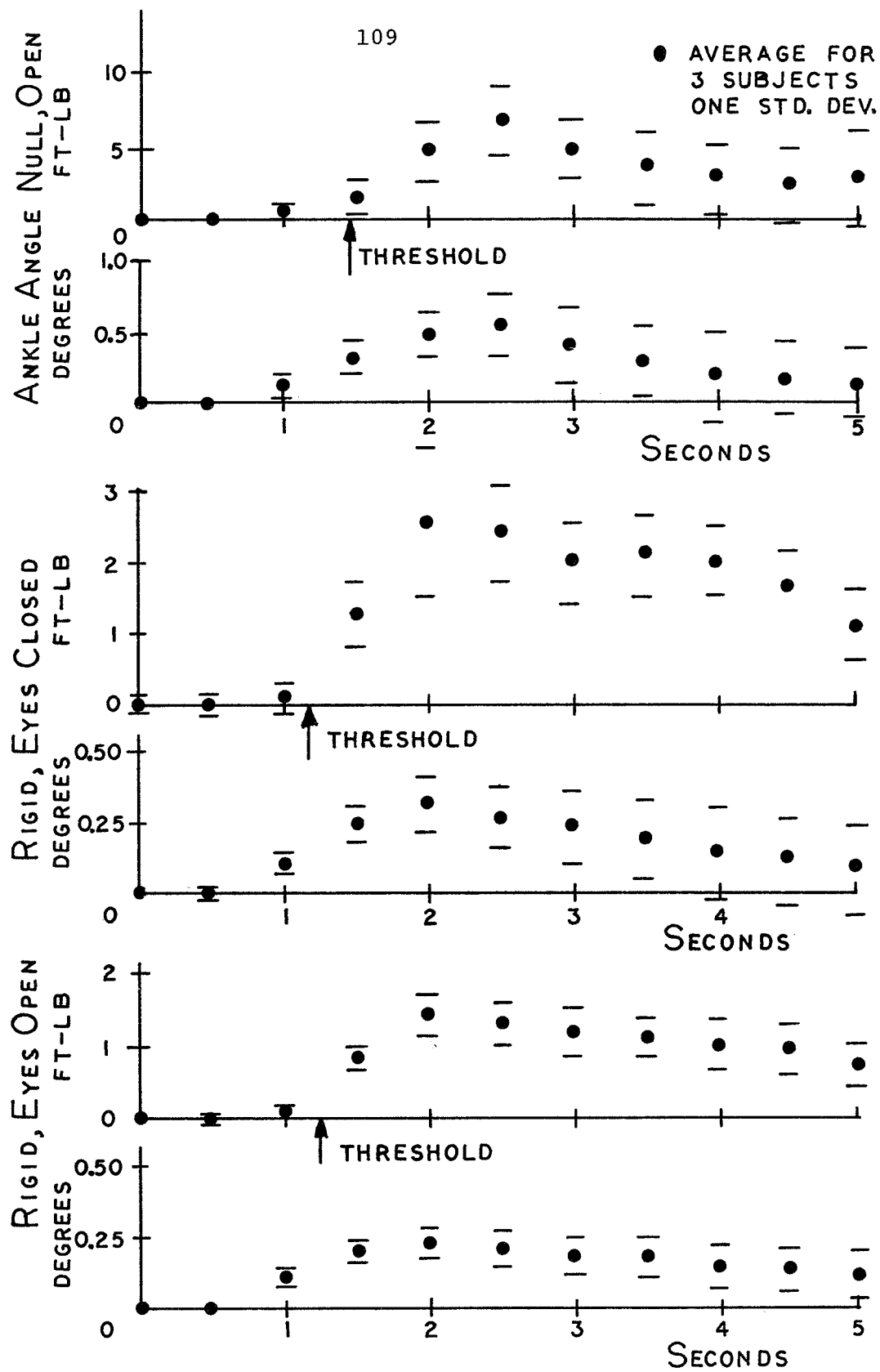


FIGURE 5.2 AVERAGE BODY ANGLE AND ANKLE TORQUE RESPONSE SEQUENCES DURING THREE CONTROL CONDITIONS

body again diverges, is improved with visual feedback. As indicated by average divergence rate, body angle error with eyes closed is  $0.05^\circ$ , and with eyes open  $0.025^\circ$ .

Average threshold values for the vestibular response during divergences are slightly smaller when eyes are open,  $0.29^\circ$ , than when eyes are closed,  $0.36^\circ$ . In both cases, eyes open and eyes closed, variations among the three subjects are statistically insignificant,  $p > 0.10$ . Visual cues, however, do not appear to directly effect the vestibular response threshold. The body angle threshold for vestibular response is dependent on the divergence rate of the body, which is more rapid when eyes are closed. This fully accounts for the difference between eyes open and eyes closed response thresholds. (See Figure 4.7.)

Visual cues do not appear to participate continuously in the regulation of posture. Referring to data above, visual resolution of body angle is about  $0.025^\circ$ . Noting the average body divergence characteristic in Figure 5.2, visual threshold should be reached about 0.75 seconds before the postural response is detected. Including the transmission time delay of 0.40 seconds, a visually initiated posture response would be observed at significantly lower threshold. We must, therefore, conclude that visual feedback is not active during the initial sway divergence, that it is activated only after vestibular detection of body sway.

### 5.2.3 Exteroceptive/Reflex Control

Basic changes in control are evident when exteroceptive cues and the reflex feedback loop are combined with vestibular regulation of posture. The following paragraphs explain these changes.

When reflex feedback control is included, the percentage of time during which subjects show static stability (i.e., when changes in reaction torque and body orientation cannot be detected) increases from an average of 20% to 40%. This increase is the result of "stiction" in the reflex loop, shown in section 3.1.2.

The threshold for detection of body sway decreases significantly when exteroceptive cues are added, (case 2), dropping from  $0.36^\circ$  to  $0.13^\circ$ . Variations in the exteroceptive threshold value among subjects is statistically insignificant,  $p > 0.10$ . Amplitude of the transient response is reduced in proportion to the nearly three-fold decrease in detection threshold.

Natural frequency of the transient response increases when the reflex feedback loop is added. Natural frequency with reflex stabilization is 0.35 Hz, significantly higher than that with only vestibular feedback control, 0.20 Hz.

Addition of visual cues, (case 3), shows slightly improved damping characteristics during the slow phase correction. Threshold for detection of sway remains virtually unchanged:

Damping ratio with visual cues	≈	0.5
Damping ratio without visual cues	≈	0.3
Threshold with visual cues	=	0.11 <sup>o</sup>
Threshold without visual cues	=	0.13 <sup>o</sup>

#### 5.2.4 Frequency Analysis of Control

Spectral analysis of postural responses provides an added means for observing the function of each mode of feedback control. Analysis is performed digitally. The program, Fourier, is described in Appendix C.

Coefficients are computed for six minute runs; three runs are made for each test condition with each subject.

Test conditions include:

1. eyes open; exteroceptive and reflex control removed  
(platform rotated to maintain ankle angle at zero)
2. eyes open; all other cues available (rigid platform)
3. eyes closed; all other cues available (rigid platform).

Comparing coefficients in cases 1 and 2 above, removal of exteroceptive cues and reflex control increases the amplitude of body sway motions at higher frequencies, Figure 5.3. Conversely, removal of visual cues, comparing cases 2 and 3, causes increases in body sway motion only at the lowest frequencies, Figure 5.4. (Complete spectra for each subject are included in Appendix E.)

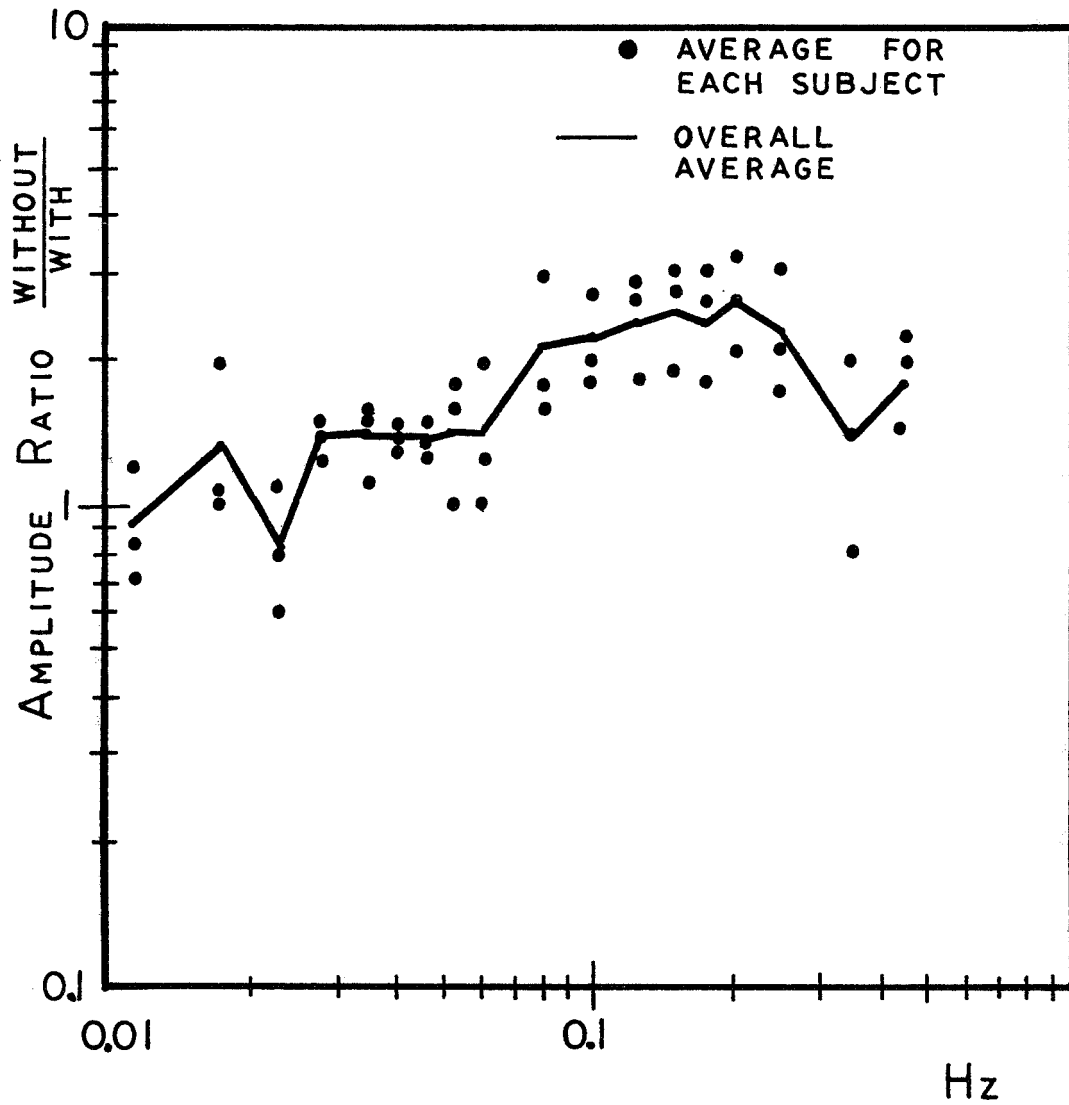


FIGURE 5.3 AMPLITUDE RATIO COMPARING FOURIER COEFFICIENTS OF BODY SWAY MOTION WITH AND WITHOUT REFLEX/EXTEROCEPTIVE CONTROL

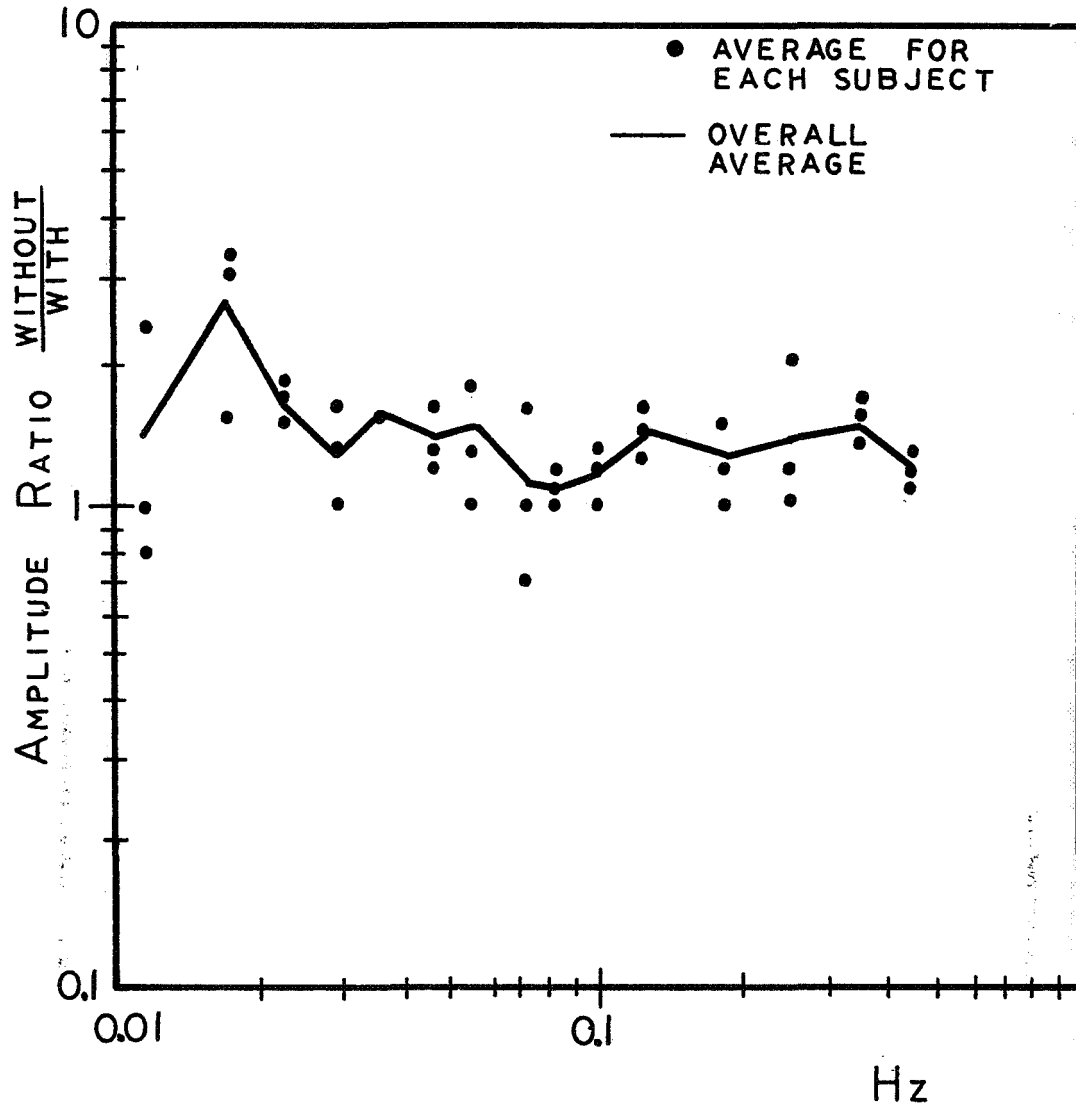


FIGURE 5.4 AMPLITUDE RATIO COMPARING FOURIER COEFFICIENTS OF BODY SWAY MOTION WITH AND WITHOUT VISUAL CUES

### 5.3 Model for Visual and Exteroceptive Control of Body Sway

#### 5.3.1 Reflex/Exteroceptive Control

The model configuration closely follows the basic strategy for reflex gain control developed in Chapter 3. More quantitative descriptions are included for exteroceptive and utricle otolith modulation of reflex feedback gain. The model is shown in Figure 5.5.

The exteroceptive sense is modeled as a low threshold sway detector with habituation. Otolith cues provide slow phase correction due to habituation of exteroceptive cues. Because quiet standing with reflex and exteroceptive cues is inherently very stable, little effort is noted when visual cues are added.

The model is simulated; the program is shown in Appendix D. Figure 5.6 compares responses predicted by the model with experimental observations.

#### 5.2.5 Vestibular and Visual Control

A visual feedback loop is added to the vestibular control model presented in Section 4.5. The visual sense is modeled as a linear feedback controller with prediction (rate compensation) and transmission delay of 0.40 seconds.

The model assumes that visual feedback participates in posture control only intermittently. Visual control is suppressed during stable periods and activated only after vestibular detection of divergence. The vestibular and visual control model is shown in Figure 5.7.

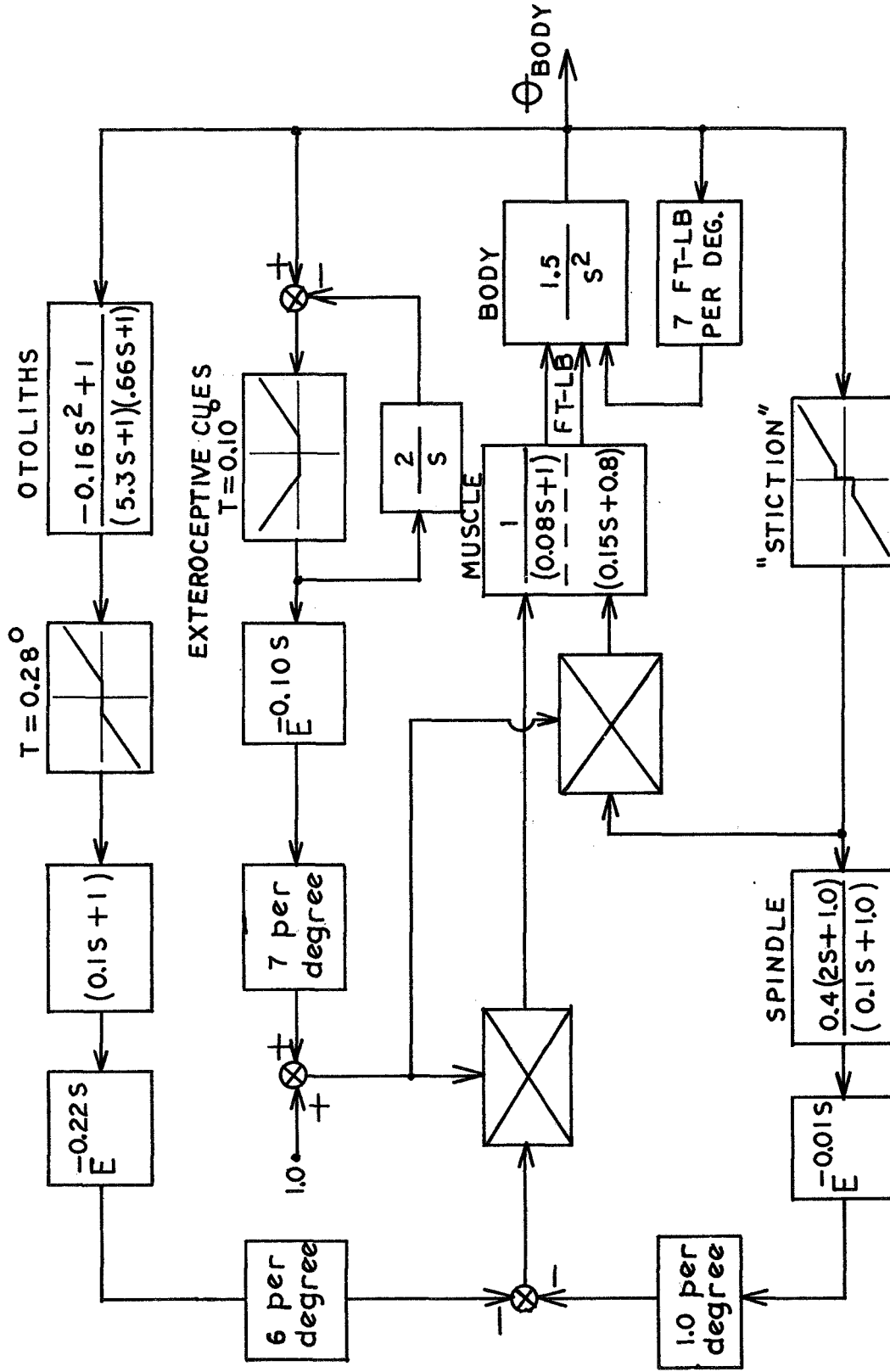


FIGURE 5.5 REVISED MODEL FOR REFLEX CONTROL OF POSTURE INCLUDING THE EXTEROCEPTIVE AND UTRICLE OTOLITH FEEDBACK LOOPS

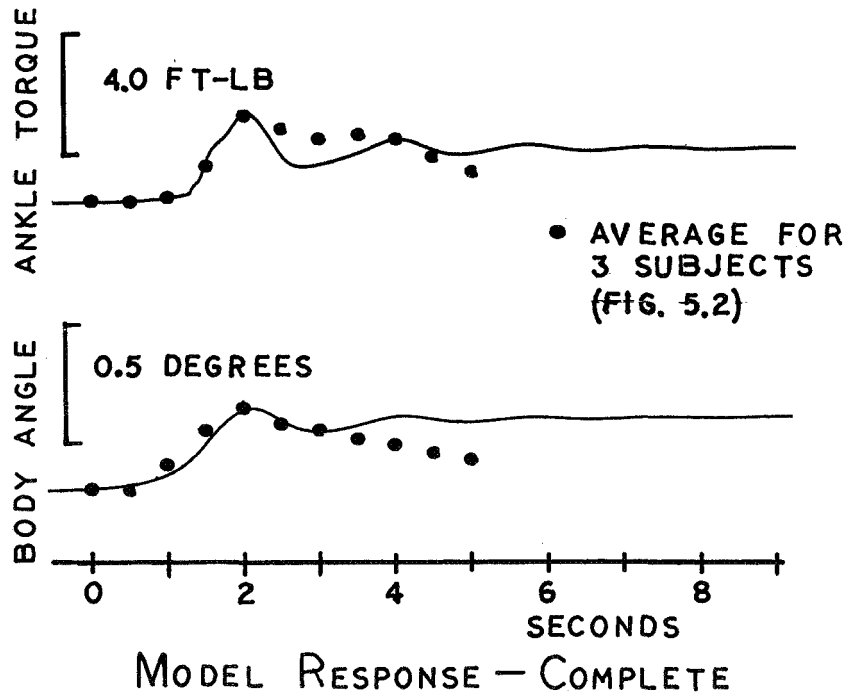
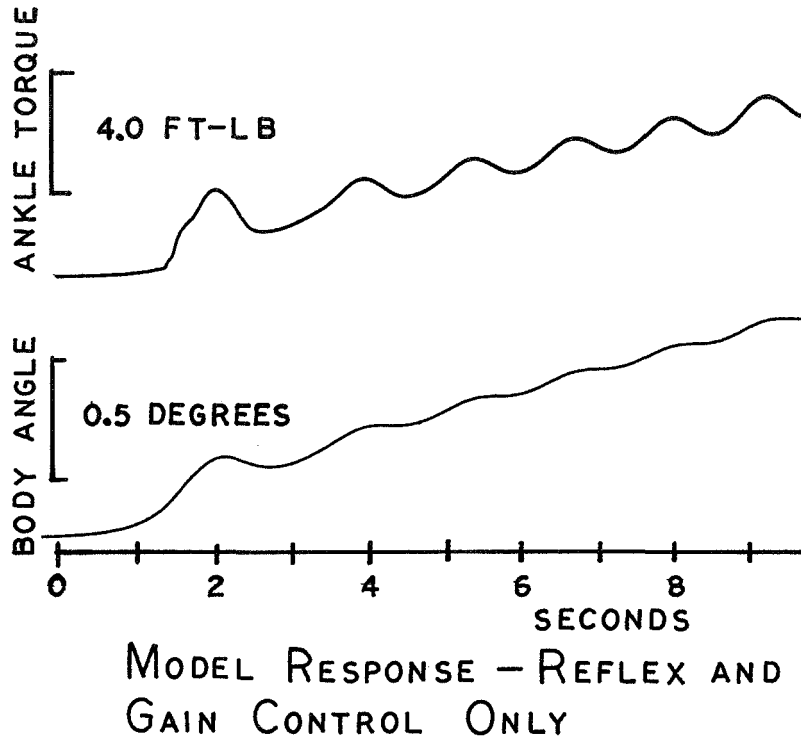


FIGURE 5.6 CHARACTERISTICS OF THE REFLEX/EXTEROCEPTIVE CONTROL MODEL COMPARED WITH EXPERIMENTAL DATA

Model responses are determined analytically. Figure 5.8 compares responses predicted by the model with experimental observation. Note that the linear model for visual control of the slow phase transient does not accurately predict amplitude of the oscillation. A higher gain in the visual feedback loop necessary to reduce amplitude of the slow phase oscillation also causes a considerable reduction in the damping of the response. Hence, it is likely that visual compensation is non-linear; its feedback gain is very large initially and decreases rapidly, resulting in the observed damping characteristics.

### 5.3 Conclusions

The basic strategy of separating dynamic and static feedback control functions applies to the exteroceptive and visual senses. Exteroceptive cues provide rapid, low threshold detection of body sway divergence. Visual cues effect well damped, high resolution correction of the slow phase drift.

Comparing properties of the vestibular systems with those of visual and exteroceptive senses, vestibular senses appear to be less accurate in all phases of control. Minimum canal detection threshold is about  $0.29^\circ$  compared to  $0.11^\circ$  with exteroceptive cues. Final resolution of utricle otolith slow phase correction,  $0.05^\circ$ , is less accurate than that using visual feedback,  $0.025^\circ$ .

Taken at face value, the above observations indicate that visual and exteroceptive feedback regulation is in every

LOGIC FOR INITIAL CLOSING

- 1  $\ddot{\theta}_B \neq 0$
- 0  $\ddot{\theta}_B = 0$

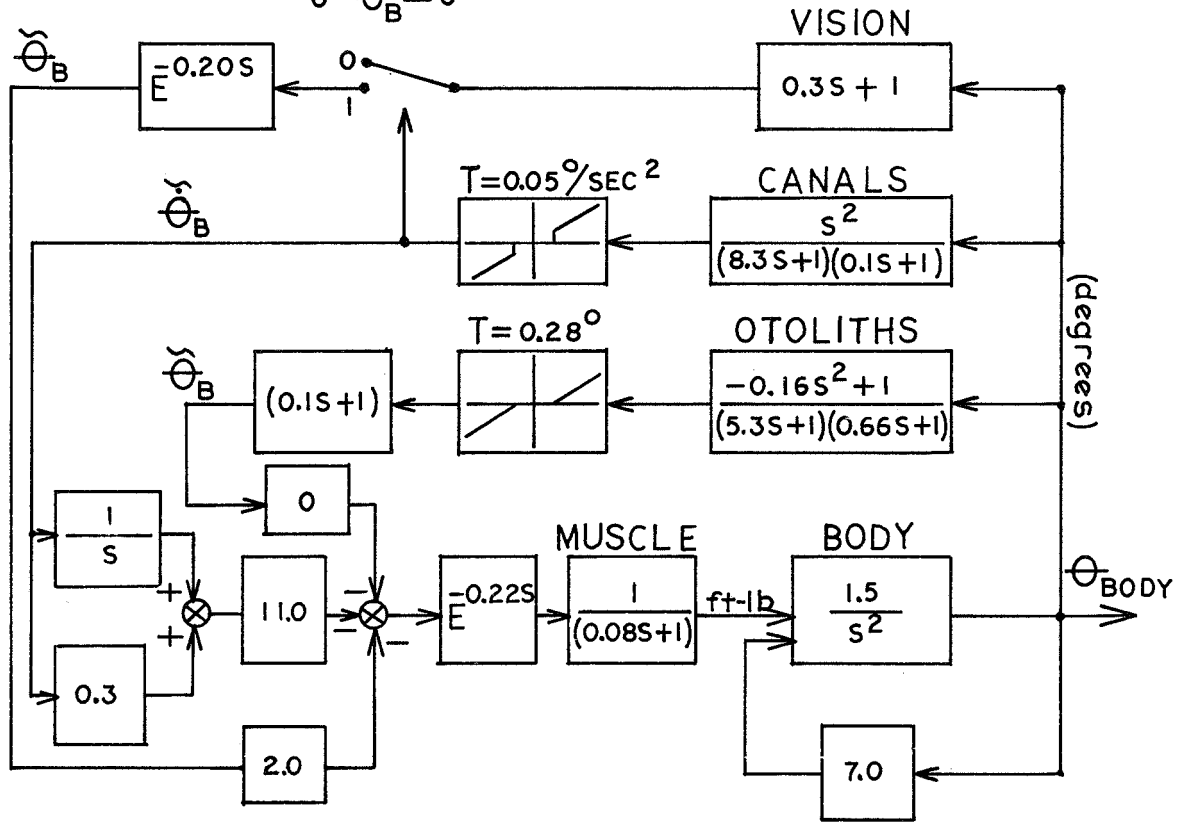


FIGURE 5.7 A MODEL FOR VESTIBULAR AND VISUAL CONTROL OF POSTURE

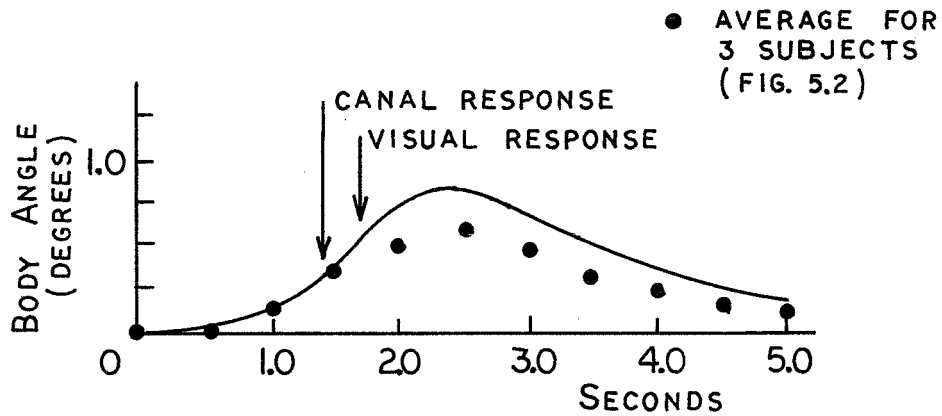


FIGURE 5.8 VESTIBULAR/VISUAL CONTROL MODEL CHARACTERISTICS COMPARED WITH EXPERIMENTAL DATA

respect superior to that using vestibular cues. Such an assumption, however, is incorrect. Exteroceptive-visual control of posture in normal subjects acts in conjunction with vestibular cues; it does not replace them. While results clearly show that threshold sensitivities of the exteroceptive and visual senses are superior, increased sensitivity may not be directly correlated with these sensors' ability to effect more accurate postural responses. In other words, threshold sensitivity is only one part of the total response characteristics of a sensor. Of equal importance in control of posture are the following:

1. continuous output characteristics of the sensor
2. the neural interface between the sensor and the postural response effectors.

Vestibular modulation of the visual posture control loop effectively allows the visual system to perform many functions in addition to regulation of posture by summoning visual control only when it is most needed. Hence, vestibular sensors are important even when full visual cues are available.

A description of posture control without vestibular cues in Chapter 6 enables further development of the description of visual and exteroceptive sensors.

## CHAPTER 6

POSTURE CONTROL WITHOUT VESTIBULAR SENSES

Posture regulation of a subject with complete loss of vestibular function is observed. During normal quiet standing, eyes open, performance is nearly normal. The combination of reflex/exteroceptive high frequency and visual low frequency stabilization is adequate for posture control in these circumstances.

With eyes closed, the subject is able to remain stable with considerable conscious effort. Tests show that eyes closed stability is achieved by a large increase in reflex loop gain, resulting in "rigid" stability.

6.1 The Subject

The subject, age twenty years, has complete loss of vestibular and auditory function due to bilateral transection of the eighth nerve. The subject's motor-sensory functions in the lower limbs are normal. Vestibular loss occurred about two years prior to the author's tests. Since loss of vestibular function, the subject has remained active and

has compensated for the sensory deficiency to the extent possible. Walking and standing on stable surfaces appears normal. Complex posture coordination, however, is clearly affected by the vestibular loss.

## 6.2 The Tests

The subject was observed standing quietly with eyes open and eyes closed. The following test was performed:

1. reflex response gains; eyes open and eyes closed  
(Section 3.1.2)
2. induced sway threshold tests; eyes open only  
(Section 4.3)
3. continuous recording of postural response and body angle motion (Section 5.2.1)
4. frequency spectra of body angle motions; eyes open and eyes closed (Section 5.2.4)

Test procedures are identical to these described in previous chapters. In all cases, tests are abbreviated versions of the original experiments.

## 6.3 Results

### 6.3.1 Reflex Response Gains

Recalling the conclusions in Chapter 3, the average gain of the stretch reflex response induced by small rotations of the ankle joint is shown to be about one-third that necessary for postural stability. During quiet standing with eyes open, the vestibular defective subject demonstrates

reflex responses at gains somewhat larger than those of normal subjects, Figure 6.1. The level of gain, however, is still well below that necessary for postural stability. The subject is most likely using the same strategy for control as normal subjects.

Average reflex gain of the vestibular defective subject increases markedly when eyes are closed, Figure 6.2. The average reflex gain for extension, 12.35 ft'lb per degree, is large enough to achieve "rigid" postural stability, while average gain for flexion increases by only a factor of two.

A likely explanation for the unsymmetrical increase in reflex gains is the following:

All subjects tend to lean forward slightly when their eyes are closed. The vestibular defective subject leans forward even more than the normal subject when eyes are closed, raising the operating level of the extensor muscles and allocating almost complete control function to these muscles.

### 6.3.2 Threshold for Detection of Induced Sway

This experiment tests the ability of the subject to detect sway divergence of reflex control and exteroceptive cues. Body sway is induced using backward and forward deflections of the platform at constant velocity. As sway is induced, the platform is rotated to track the rotation of the body, thus eliminating reflex and exteroceptive detection of sway via deflection of the ankle joints. The

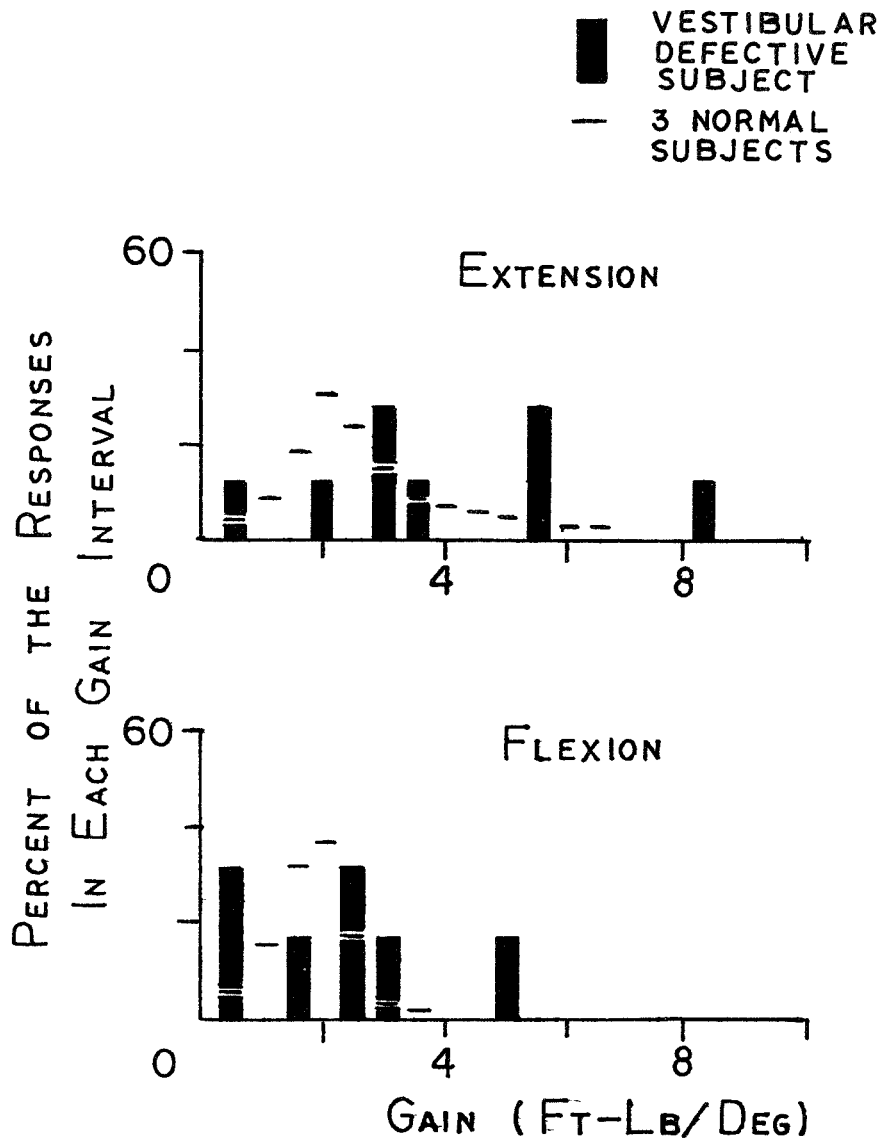


FIGURE 6.1 DISTRIBUTION OF REFLEX GAINS FOR 1/4 DEGREE STEPS, VESTIBULAR DEFECTIVE SUBJECT STANDING WITH EYES OPEN

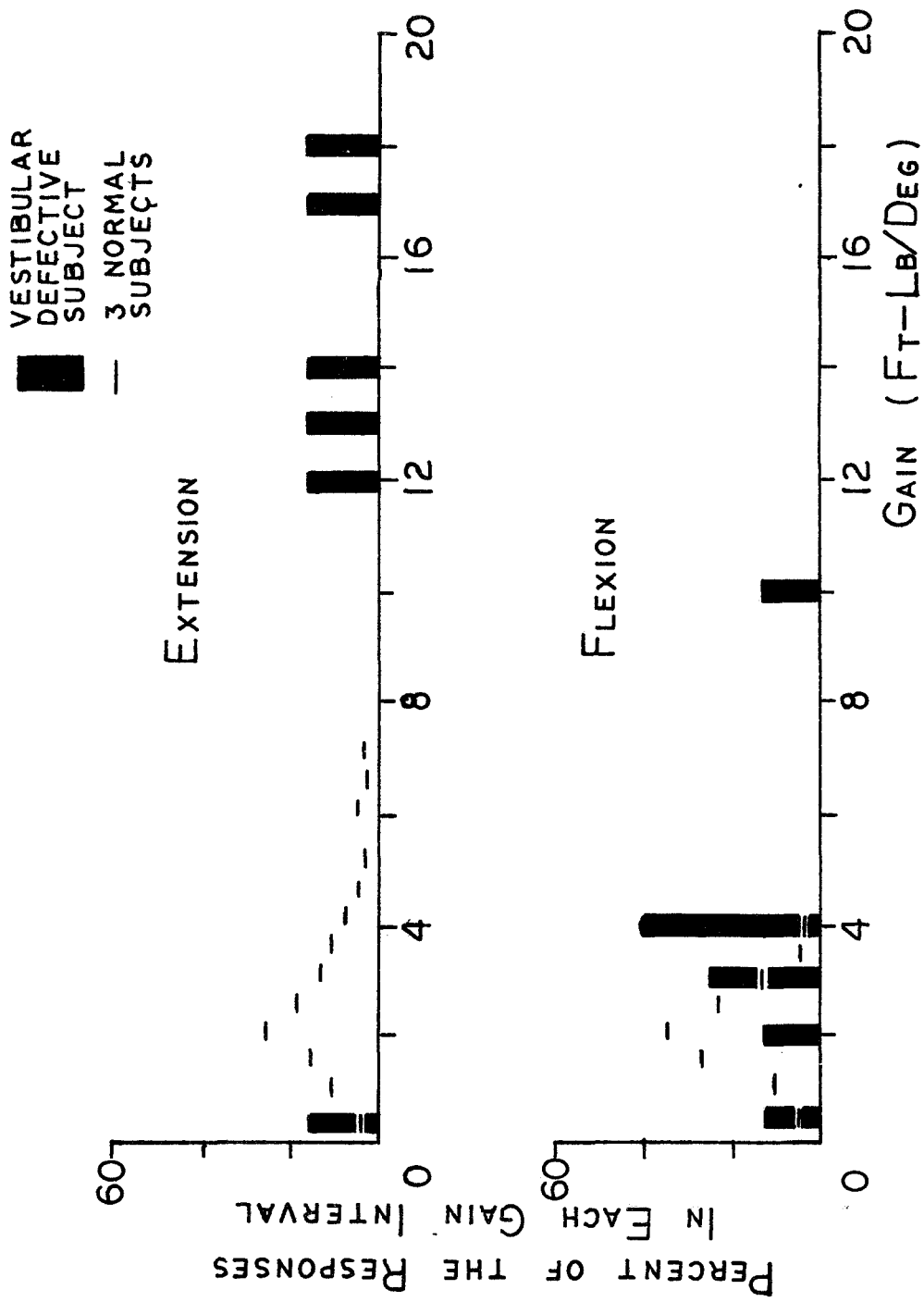


FIGURE 6.2 DISTRIBUTION OF REFLEX GAINS FOR 1/4 DEGREE STEPS, VESTIBULAR DEFECTIVE SUBJECT STANDING WITH EYES CLOSED

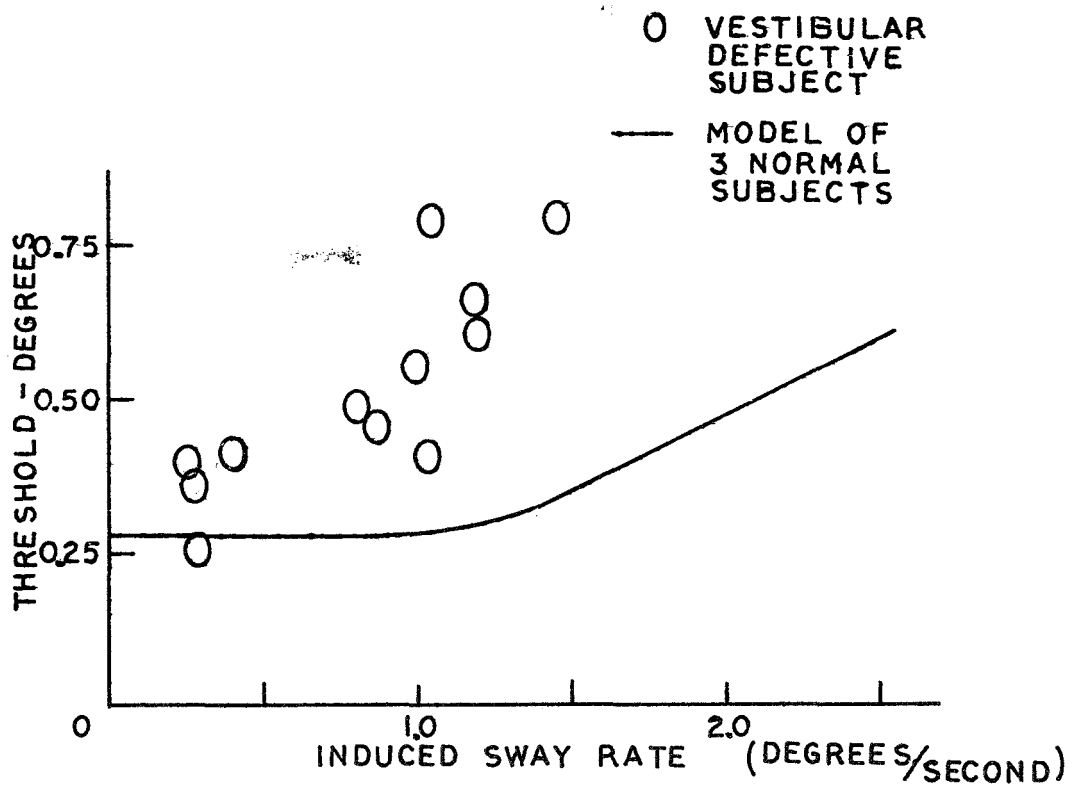
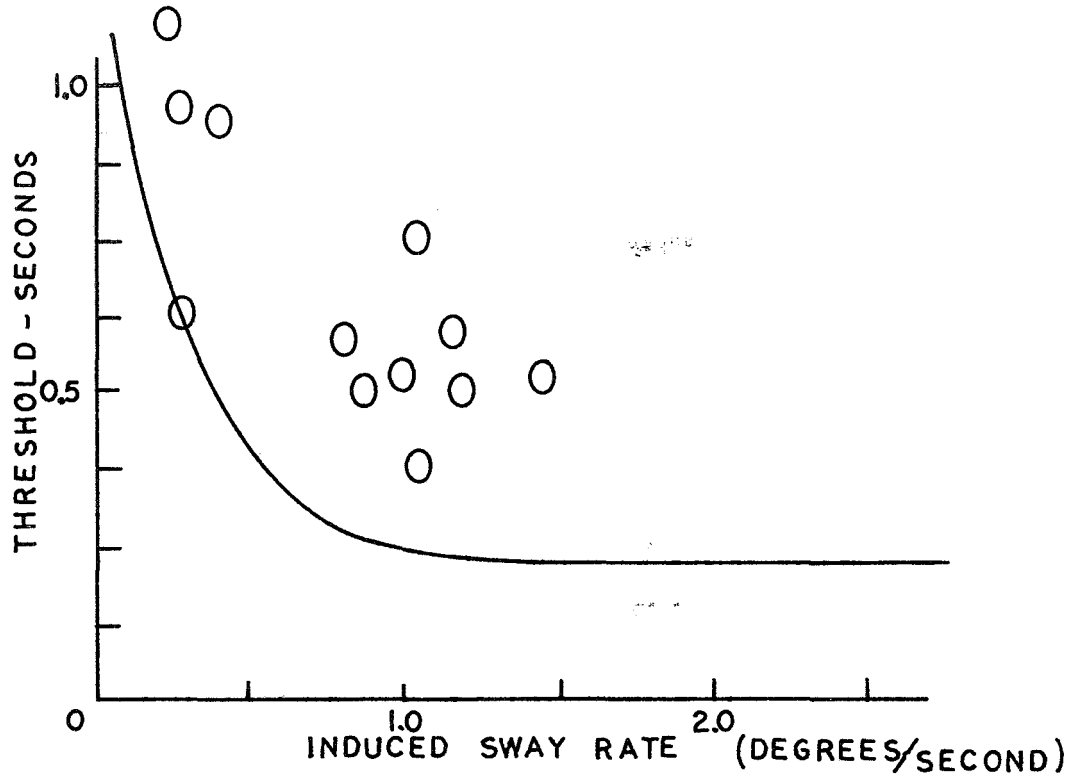


FIGURE 6.3 RESPONSE THRESHOLD TO INDUCED SWAY MOTION OF THE VESTIBULAR DEFECTIVE SUBJECT

validity of this technique is demonstrated in section 4.3.

The observed response sequence is similar to that seen in normal subjects: body angle begins to increase without a corresponding increase in ankle torque; motion is detected and torque increases rapidly; stability is re-established. Results in terms of response time and body angle shown in Figure 6.3, clearly demonstrate that threshold for detection of body motion is increased when vestibular cues are absent. Minimum delay time is about 0.45 seconds. The minimum body angle subtended before motion is detected is about 0.35 degrees. Note that the angle threshold increases continuously as the rate of induced sway increases, while normal subjects with the aid of vestibular cues show a constant threshold of 0.29 degrees for induced rates up to 0.80 degrees per second.

### 6.3.3 Continuous Postural Response Characteristics

Continuous records of postural response during eyes open and eyes closed control are shown in Figure 6.4. The intervals chosen generally characterize the types of responses seen through out each observation period of .4 minutes.

Comparable response characteristics for normal subjects are analysed in Section 5.2. These results show that "stiction: forces provide for complete static stability. During frequent transient disturbances, increases in reflex gain initiated by the higher centers maintain stability.

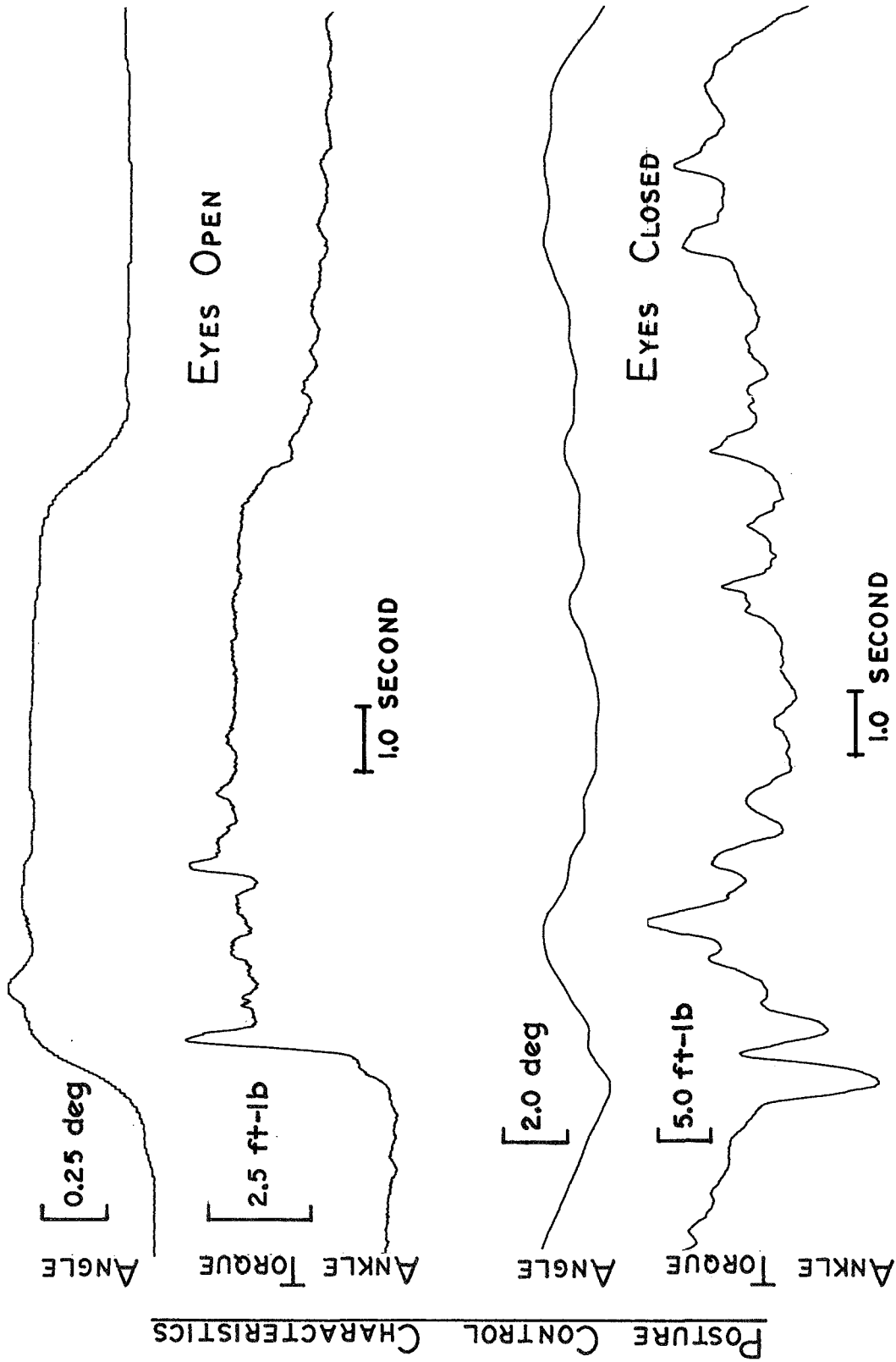


FIGURE 6.4 TYPICAL POSTURAL RESPONSES OF THE VESTIBULAR DEFECTIVE SUBJECT, STANDING ON A RIGID, FLAT SURFACE

This simple control strategy is seen in both eyes open or eyes closed test cases.

With eyes open, control strategy of the vestibular defective subject is the same as that observed for normal subjects. Records show periods of "stiction" stability and frequent diverging transients. Threshold for detection of the divergence transients is about the same as that observed for normal subjects, 0.10 degrees. Corrections of the transient disturbance, however are less consistent. Resulting divergence body angles are larger, 0.5 degrees versus 0.25 degrees for normals, and corrections are often underdamped.

When eyes are closed, the entire strategy of control changes significantly. No periods of "stiction" stability are present, rather small, higher frequency oscillations (about 3/4 to 1 Hz) are present almost continuously during quieter periods. During these quiet periods, body angle drifts continuously at rates ranging from 0.2 to 1.0 degrees per second. A rough estimate of the threshold for detection of this slow phase drift is about 2 to 4 degrees.

When slow phase drift is detected, larger transient responses are initiated. Characteristics of these responses are very erratic. Many of them are very poorly damped, showing many large oscillations at frequencies above 1 Hz.

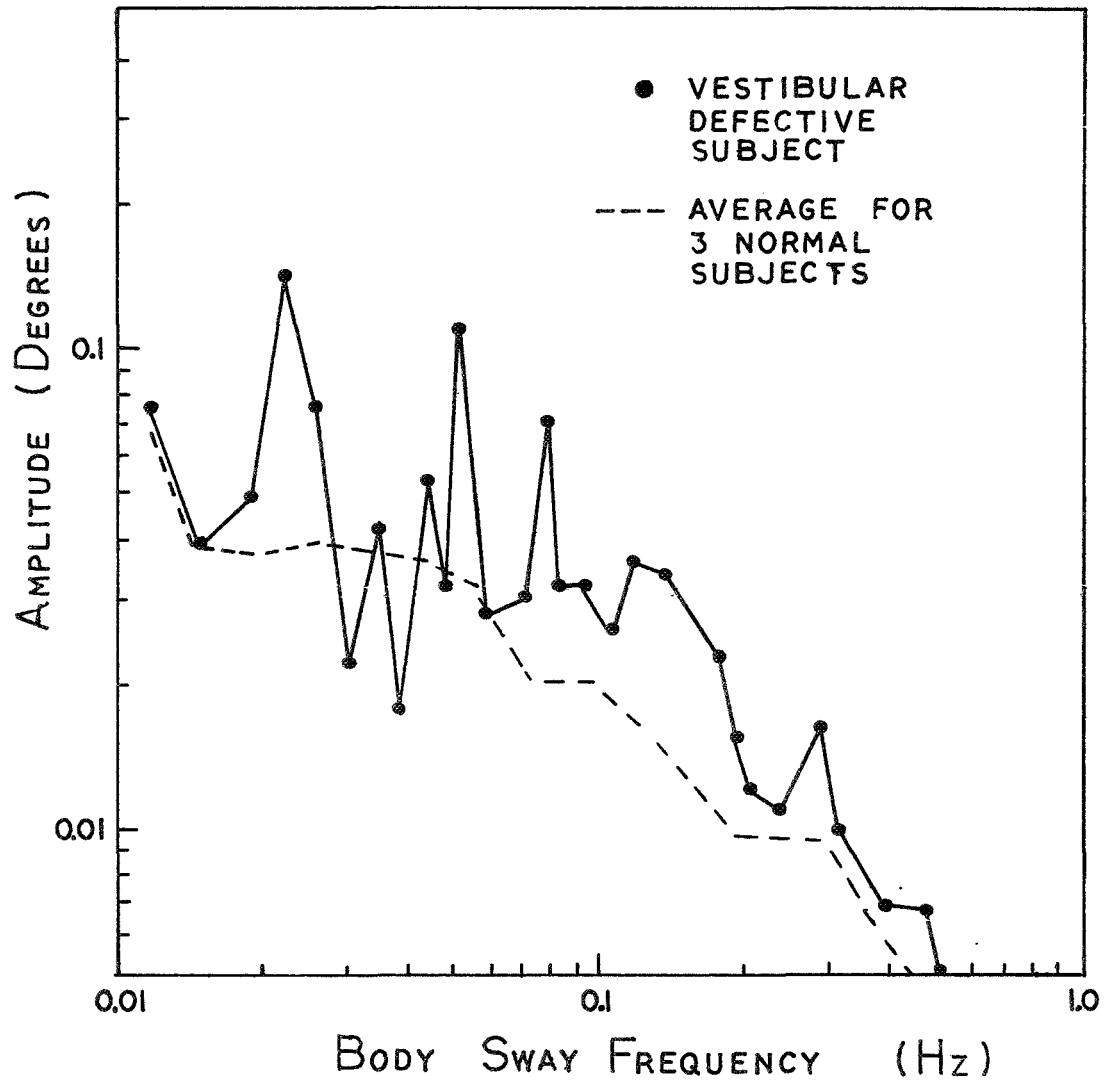


FIGURE 6.5 FOURIER COEFFICIENTS OF BODY SWAY MOTION FOR THE VESTIBULAR DEFECTIVE SUBJECT STANDING ON A RIGID, FLAT SURFACE WITH EYES OPEN

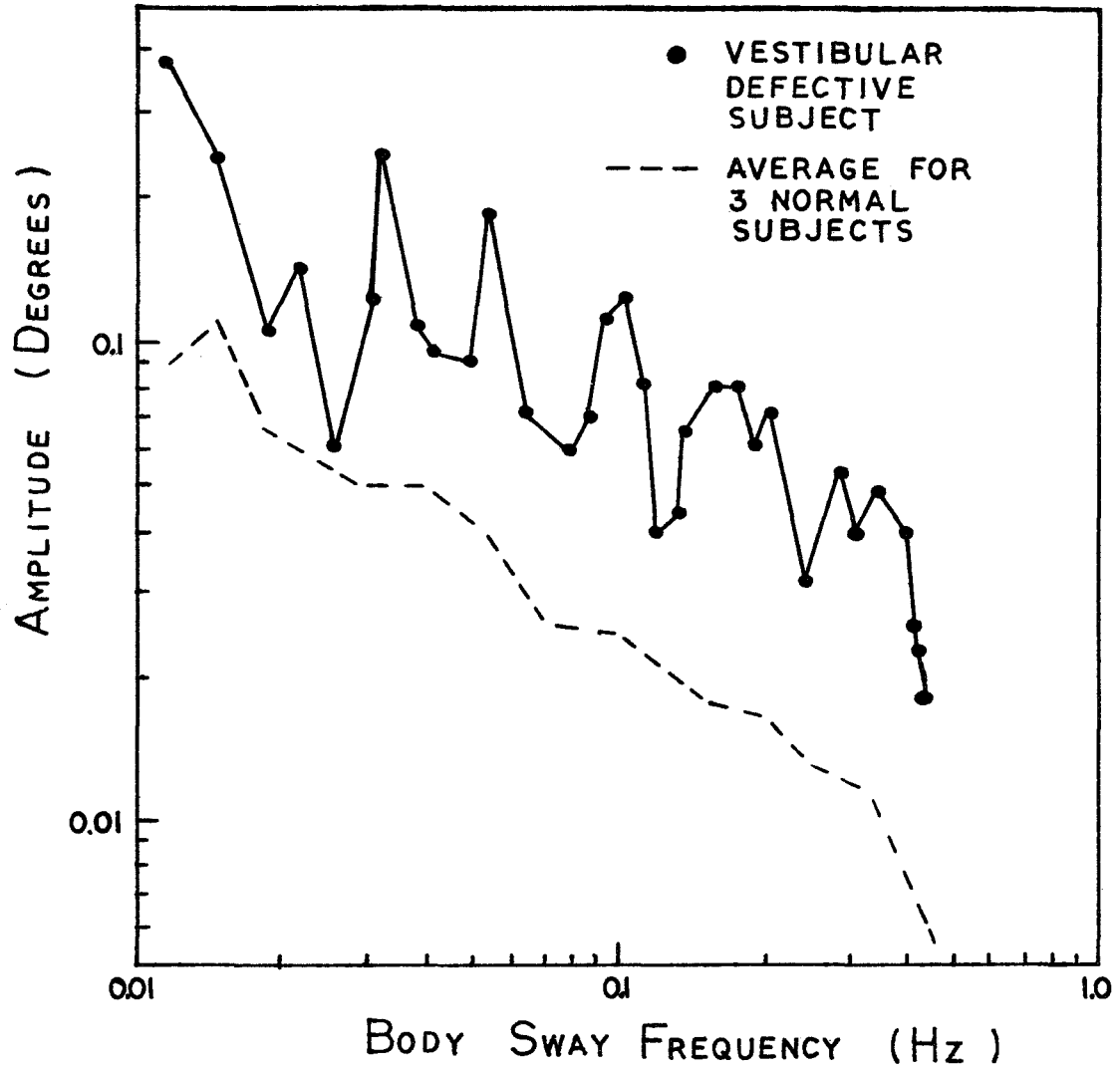


FIGURE 6.6 FOURIER COEFFICIENTS OF BODY SWAY MOTION FOR THE VESTIBULAR DEFECTIVE SUBJECT STANDING ON A RIGID, FLAT SURFACE WITH EYES CLOSED

#### 6.3.4 Fourier Coefficients

Fourier coefficients for body angle with eyes open or eyes closed control are compared to those of normal subjects under the same test conditions, Figures 6.5 and 6.6. Posture control with eyes open shows characteristics very nearly the same as those for normal subjects. Some increase in low frequency sway amplitude is seen.

When eyes are closed, body sway amplitude at all frequencies increases. Largest increases are noted at frequencies above 0.1 cycles per second.

#### 6.4 Conclusions

A vestibular defective subject is able to regulate posture during a quiet standing, eyes open task using the same control strategy as normal subjects. A radical shift in strategy, however, is necessary to maintain stability when the vestibular defective subject closes his eyes. These two statements are consistent with the reflex/exteroceptive control model described in Section 5.3. The observations substantiate two major characteristics of exteroceptive/reflex model:

1. Habituation of the exteroceptive gain control mechanism results in poor static stability of the exteroceptive/reflex control loop.
2. Gain of the reflex loop may be increased to achieve static "rigid" stability.

Because the primary mode of control has a slow drift instability, an additional sensory feedback mode, either vision or utricle otolith, is necessary to correct this slow drift. Hence, the vestibular defective subject with eyes open is able to maintain posture in a normal manner.

When the vestibular defective subject closes his eyes, both mechanisms for slow drift correction are lost. The large increase in average reflex gain may be seen as an attempt to minimize this drift by maintaining reflex gains at very high levels. The continued presence of drift likely results because the subject is not able to maintain reflex gains continuously above the level necessary for rigid stability. Habituation likely lowers reflex gain during quieter periods. Joint receptors most likely provide the very crude correction of the reflex/exteroceptive control loop drift.

A model for "rigid" reflex control of posture in the absence of both visual and otolith cues is proposed as follows. The basic configuration is the same as before; exteroceptive feedback modulates the reflex loop gain. Here, however, the background reflex gain setting is considerably higher, though not quite large enough for static stability. Habituation of the exteroceptive gain control loop results in the slow drift. Perhaps high threshold joint receptor or non-adapting pressure receptor feedback loops correct slow drift.

After observing the subject for several hours, a further qualitative observation can be made:

During simple postural tasks, walking, climbing stairs, etc., control without vestibular cues is very nearly as accurate as when they are included. The vestibular defective subject, however, must maintain a continuous visual awareness of body orientation, while in normal subjects the vestibular system continuously monitors postural orientation. Performance of the vestibular defective subject, dependent on the level of visual attention, is noticeably more erratic. While stability is generally good, the subject occasionally became unsteady for no apparent reason except that visual attention was inadvertently relaxed. These observations further support the proposal made in Chapter 5.

Vestibular cues, acting as a continuous monitor of posture orientation, free the visual system from a continuous monitoring function. Instead, vestibular cues alert the visual senses for postural control only when necessary during transient disturbances.

## CHAPTER 7

CONCLUSIONS

The goal of this thesis is to define the function of the feedback sensors in controlling posture and to model the neural interfaces between these sensors and the mechanisms that initiate motor responses. A general model is first developed from information found in a review of the motion sense models, muscle models and current sensory-motor neurophysiology. Using a specifically designed two-degree of freedom platform, observations from a series of experiments form the basis for specific models for the feedback sensors, the response effectors, and sensory-motor neural processing.

The posture control model can be subdivided into two basic parts: regulation with stretch reflex position feedback (standing on a rigid surface), and regulation relying on higher center feedback sensors (standing on a surface which rotates to track body angle motions, nulling ankle angle continuously.)

Posture control strategy in these two extreme cases is fundamentally different. Evidence is presented, however,

which suggests that for a large class of conditions between these extremes of a perfectly rigid flat surface and a surface with special compliant properties, a combination of these two control strategies can be expected.

### 7.1 Posture Control on a Rigid, Flat Surface

During quiet standing on a rigid, flat surface, the ankle stretch reflex gains are about one-third that necessary for posture stability. Small "stiction" forces acting between fibers within both intra- and extra-fusal muscle, however, supplement this reflex gain, and together they provide a gain adequate for complete stability for very small ankle deflections. Quiet standing shows periods of "stiction" stability punctuated by frequent transients during which the subject "breaks out" of stability and begins to diverge. Kinesthetic cues, changes in pressure distribution on the feet first detect this divergence, triggering a multiplicative increase in reflex loop gain proportional to disturbance amplitude. Because deep pressure sensation habituates, an additional sense, either visual or utricle otolith information is necessary to provide drift stabilization.

Average reflex gain is found to be a good measure of participation of the reflex mode of posture regulation. When small amplitude, low frequency platform rotational motions are introduced, the reliability of this mode of control is reduced. A corresponding decrease in reflex gain is seen. When the reflex feedback loop is removed

by maintaining ankle angle at zero, mean reflex gain drops to nearly zero.

## 7.2 Posture Control with Vestibular and Visual Senses

When reflex/exteroceptive feedback is removed, the subject must rely completely on higher center motion sensors, the vestibular and visual systems. With eyes closed, vestibular cues are sufficient to provide postural stability. In this case, the utricle otoliths and the semicircular canals operate as frequency selective feedback sensors. Canals, the higher frequency motion sensors, detect body divergence and initiate postural responses. Canal feedback control, however, is unstable at very low frequencies. The utricle otolith is a static and very low frequency sensor, indicating average body angle with respect to the gravity vector. An outer otolith feedback loop stabilizes the low frequency drift of the canals.

The addition of visual feedback during vestibular control of posture produces a significant improvement in accuracy of the slow phase correction of body angle. Vision, however, does not affect the threshold for detection of body angle divergence. Posture control experiments substantiate the fact that vision is primarily a static or very low frequency feedback sensor.

## 7.3 Posture Control without Vestibular Senses

Posture control without vestibular function is nearly normal when a defective subject stands on a rigid surface with eyes open. Detection of body divergence, exteroceptive

cues, is normal. Reflex gains are somewhat higher than normal. It may be concluded that exteroceptive detection of divergence and visual correction of slow drift are sufficient.

When eyes are closed, a radical change in control strategy is evident. Since neither visual nor utricle otolith static senses are available, reflex gain is increased about six-fold to enable "rigid" stability.

#### 7.4 An Overall Summary

Posture control is seen as a multiloop system in which a number of specialized feedback sensors contribute to the generation of commands. Proprioceptive sensors and neural processing at the lowest levels enable crude but fast acting responses based on information from body centered frames.

"Inertial" sensors and higher center processing provide more accurate, adaptable control but with longer processing delays. Hence, posture control is a highly non-stationary process in which responses to transient disturbances are initiated at the lowest levels. Allocation of control then "radiates" upwards to the higher centers where successive corrections, based on more complete information, fine tune the initial responses. Figure 7.1 reviews the basic features of the posture control system. Table 7.2 summarizes the properties of the posture control sensors.

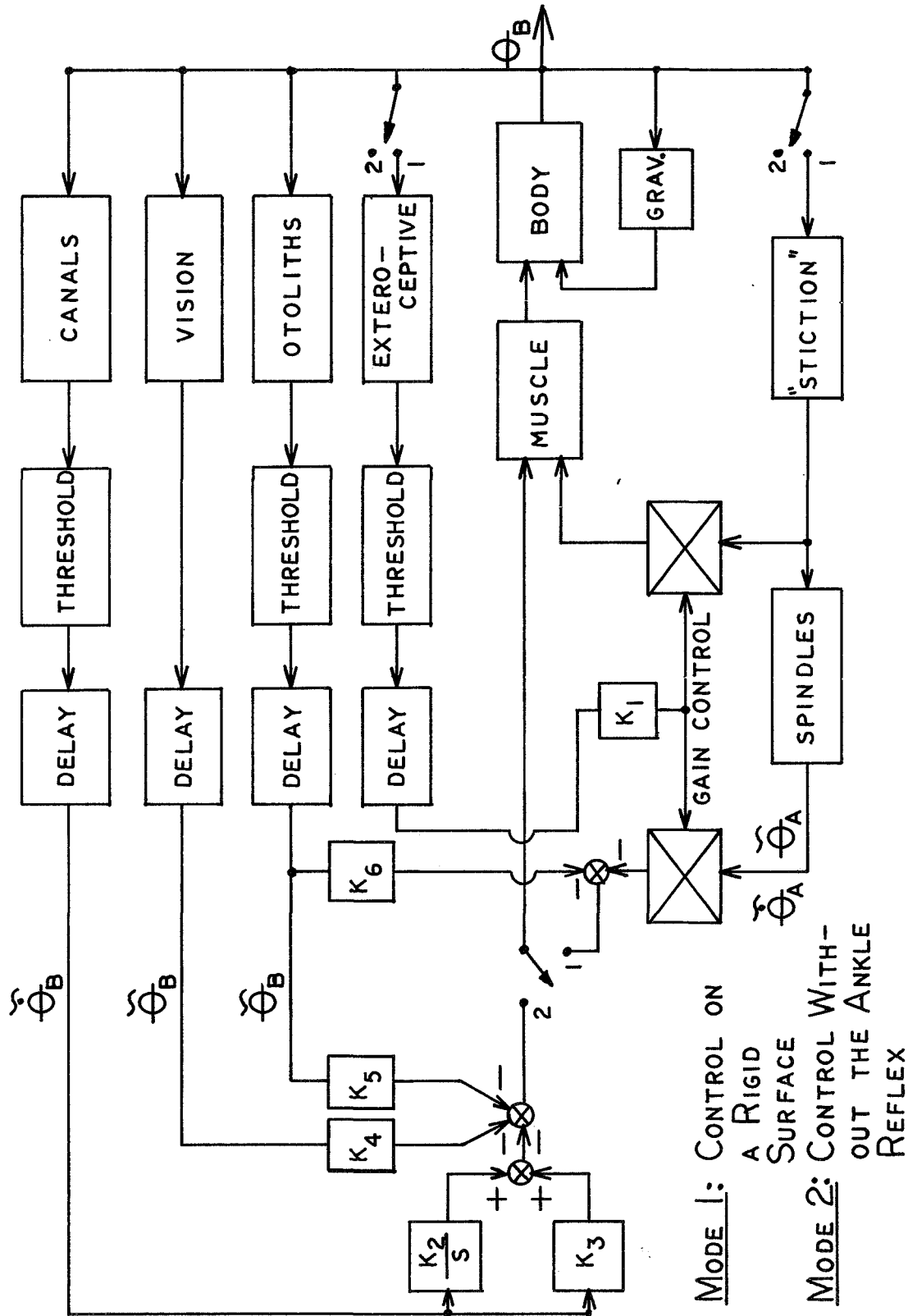


FIGURE 7.1 THE BASIC FEATURES OF THE POSTURAL CONTROL SYSTEM

	MUSCLE RESPONSE REFLEX RESPONSE	EXTERO-CEPTIVE	SEMICIRCULAR CANALS	VISION	UTRICLE OTOLITHS
INPUT	ANKLE DEFLECTION	ANKLE DEFLECTION AND PRESSURE ON THE FEET	ANGULAR ACCELERATION OF THE BODY	BODY MOTION	BODY ANGLE AND ANGULAR ACCELERATION OF THE BODY
OUTPUT	PROPORTIONAL TO $\theta_A$ AND $\dot{\theta}_A$	APPROXIMATELY PROPORTIONAL TO ANKLE DEFLECTION	BODY ANGULAR RATE	BODY ANGLE AND ANGULAR RATE	BODY ANGLE
DYNAMIC CHARACTERISTICS	$(0.15S+0.80)$ $\frac{0.4(2S+1)}{(0.1S+1)}$ "STICKTION"	$\frac{1}{(1+2/S)}$	$\frac{S^2}{(8.3S+1)(0.1S+1)}$	$\approx 1$	$\frac{-0.16S^2+1}{(5.3S+1)(0.66S+1)}$
THRESHOLD	$\approx 0$	$0.10^0$ BODY ANGLE	$0.05^0/\text{SEC}^2$	$\approx 0$	$0.29^0$ BODY ANGLE
TIME DELAY	$\approx 10$ MSEC.	$\approx 100$ MSEC	225 MSEC.	425 MSEC.	225 MSEC.
FUNCTION IN POSTURE CONTROL	RESISTS CHANGES OF THE ANKLE ANGLE (POSITION CONTROL LOOP)	CONTROLS THE REFLEX GAIN DURING TRANSIENT DISTURANCES	DETECTS SWAY DIVERGENCE AND INITIATES ANKLE TORQUE COMMANDS	CORRECTS SLOW DRIFT OF BODY ANGLE	CORRECTS SLOW DRIFT OF BODY ANGLE
	PHASIC CONTROL (MODE 1)	PHASIC CONTROL (MODE 1)	PHASIC CONTROL (MODE 2)	STATIC CONTROL (MODE 1 OR 2)	STATIC CONTROL (MODE 1 OR 2)

FIGURE 7.2 PROPERTIES OF THE POSTURE CONTROL SENSORS

## 7.5 Some Suggestions for Further Work

Expansion of the research presented in the thesis may proceed along two fronts: a deeper probe into the mechanisms of posture control outlined here, or accepting the basic form of the model, the application of the model to clinical research problems.

### 7.5.1 Multiplicative Increase in Reflex Gain During Transient Disturbances

A multiplicative increase in reflex gain during transient disturbances may be observed by introducing ankle angle step disturbances, not at random intervals but at various intervals after detection of a transient body angle disturbance. Questions to be answered include:

1. Does the reflex gain increase for a transient in a given direction apply only to deflections in that direction, or does the gain increase cover both extension and flexion disturbances?
2. Is the time history of the reflex response the same or different during a transient increase in reflex gain?

Answers to both questions would provide valuable insight into the physiological mechanisms for regulating reflex responses.

### 7.5.2 Clinical Diagnosis of Posture-Related Sensory Defects

This thesis research has shown the frequency selective nature of higher center sensory feedback modes, specifically

of the frequency differentiation for semicircular canal and utricle otolith functions. The two-degree of freedom experimental platform developed is able to remove reflex and exteroceptive cues, thus allowing observation of vestibular feedback control. Combining these results, a simple method for diagnosing utricle otolith or semicircular canal deficiencies is possible. This could be done in the following way.

Ask the subject to stand quietly on the platform with eyes closed. A simple reflex response test should give an immediate indication of utricle otolith function. Although the subject's performance may appear normal upon simple visual inspection, he will show an increase in reflex gain to compensate for deficiency in otolith sense of vertical.

If utricle function is normal, semicircular canal function may be tested by rotating the platform such that the reflex and exteroceptive cues are removed. Without canal function, the subject would be unstable during this procedure. A rough estimate of the degree of canal deficiency may be provided by slowly reducing the effects of reflex/exteroceptive feedback and observing the point at which instability is reached.

## APPENDIX A

BODY DYNAMICS

For motions about the ankle joint, the dynamic characteristics of the body may be compared to those of an inverted pendulum. Because of this inherently unstable configuration, forward-backward rotational motions of the body about the ankle joints represent a critical mode in the control of posture. Relative motion between upper body segments during quiet standing is of considerably less consequence and is assumed to be zero in the body dynamic model, Figure A.1.

Parameter values for body physical characteristics are taken from Dempster (23). Effects of variations in these characteristics among the three subjects are considered and found to have insignificant effects on performance characteristics of the posture control model.

The body dynamic equation is:

$$\ddot{\theta}_B = \frac{m_B g h_{cg}}{I_A} \theta_B + \frac{T_A}{I_A}$$

where  $I_A$  is the moment of inertia of the body about the ankle joint;

$m_B$  is the mass of the body;

$h_{cg}$  is the height of the center of mass

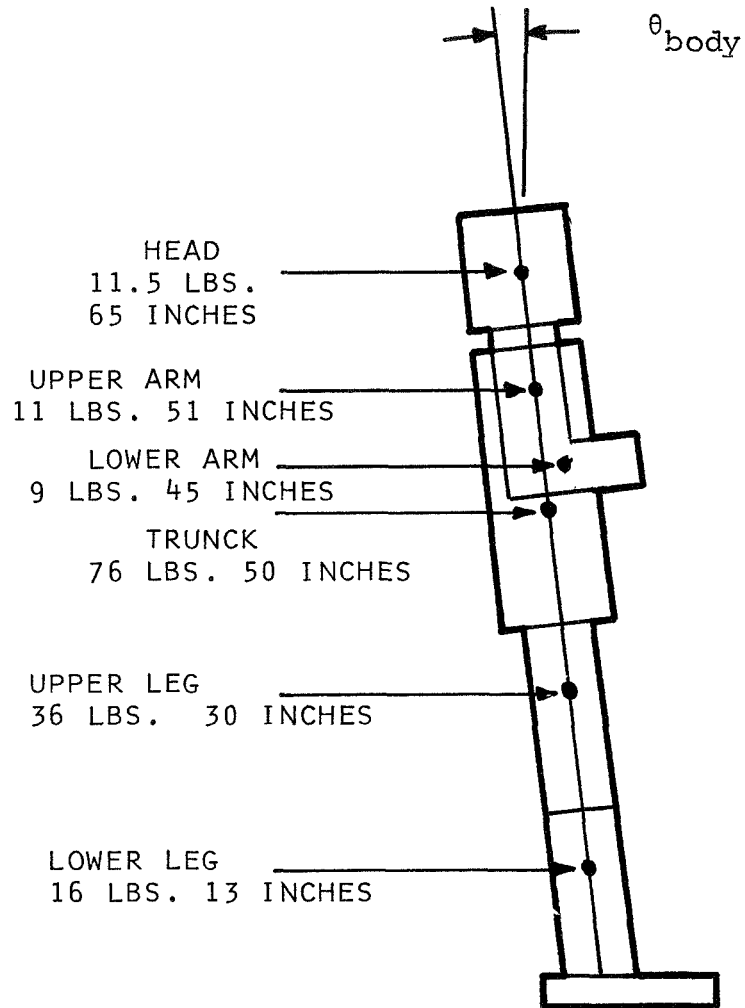


FIGURE A.1 PHYSICAL CHARACTERISTICS OF THE BODY

$T_A$  is the net reaction torque effected by posture muscle at the ankle joint;

$\theta_B$  is the body angle in the forward-backward plane.

The following are average values for these parameters:

$$\begin{aligned} I_A &= 750 \text{ lb-in-sec}^2 \\ m_B &= 166.5 \text{ lb} & \omega_B^2 &= 8.6/\text{sec}^2 \\ h_{cg} &= 38.7 \text{ in} & \omega_B &= 2.94/\text{sec} \\ & & & \approx 3.0/\text{sec} \end{aligned}$$

Size data for the three subjects are given:

	G.L.	D.R.	K.G.N.
Height	6'0"	5'9"	5'5"
Weight	155#	150#	125#

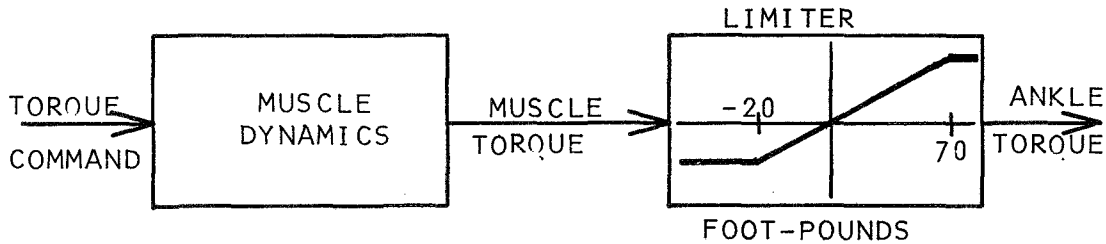
Combining these data with Dempster's average body configuration, the following estimates for each subject are made:

	G.L.	D.R.	K.G.N.
$I_A \approx$	720 lb-in-sec <sup>2</sup>	640 lb-in-sec <sup>2</sup>	490 lb-in-sec <sup>2</sup>
$m_B =$	155 lbs	150 lbs	125 lbs
$h_{cg} =$	40.1 in	38.1 in	35.9 in
$\omega_B^2 \approx$	8.7/sec <sup>2</sup>	8.9/sec <sup>2</sup>	9.1/sec <sup>2</sup>

The ankle response gain just necessary to stabilize the body to gravitational torque is  $\frac{T_A}{\theta} = m_B g h_{cg}$ . The average for the three subjects tested is  $\approx 7.5$  ft-lb/degree.

A word about the generation of stabilizing ankle torques during quiet standing is in order. The foot is a limited supporting surface; thus, there is a maximum torque after which the foot will not remain flat on the supporting surface. For positive torques (activation of the extensor muscles) the maximum torque is about 70 ft-lb. Since little foot length

extends behind the ankle as support, maximum negative torque is much smaller, about 20 ft-lb. The following torque response limiter is therefore defined:



The above relation essentially defines the limits of simple, feet-together posture control.

When conditions require greater net torques, stepping and more complex body motions are required. Therefore, experiments in this thesis consider only control of quiet standing, during which these torque response limits need not be exceeded.

## APPENDIX B

THE TWO-DEGREE OF FREEDOM EXPERIMENTAL PLATFORM

The platform provides the base on which the subject stands during experiments. It enables the experimenter to influence the control strategy of the subject and permits him to probe the states of the postural control system with small transient disturbances.

The platform performs two basic functions:

1. It measures ankle reaction torques and the body lean angle.
2. It introduces rotational and backwards and forward translational inputs to the ankle joints.

Figure B.1 shows the complete system with a subject in position.

B.1 Measurement of Postural Responses

## B.1.1 Ankle Torque Measurement

The plate on which the subject stands is supported at each of its four corners by a miniature variable resistance force transducer, (Clark Electronics, Micro-ducer No. CS-5-100L). Resistance bridges measure differential loading between front and back sensors on each side of the force plate. Differential

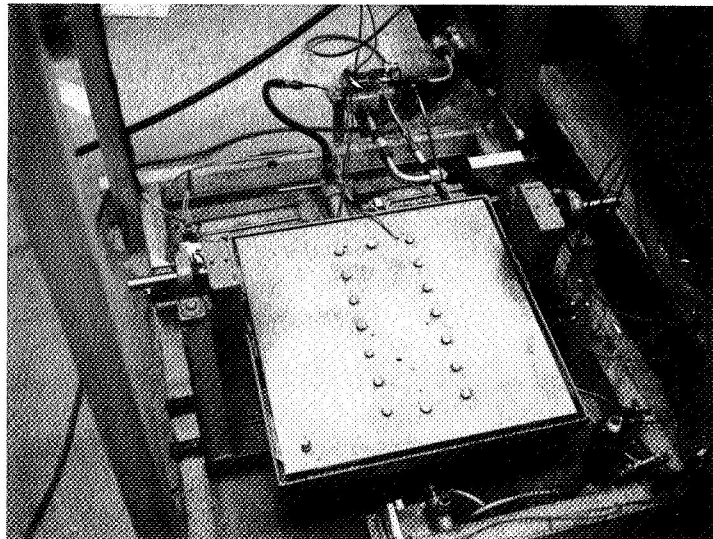
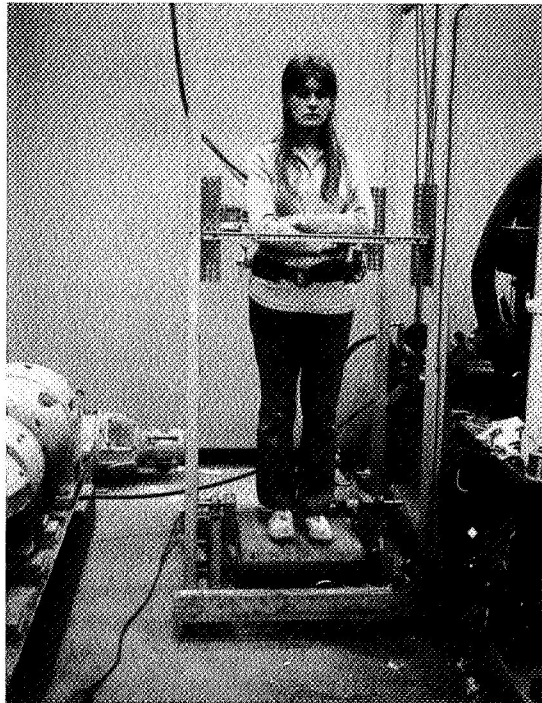


FIGURE B.1 THE EXPERIMENTAL PLATFORM

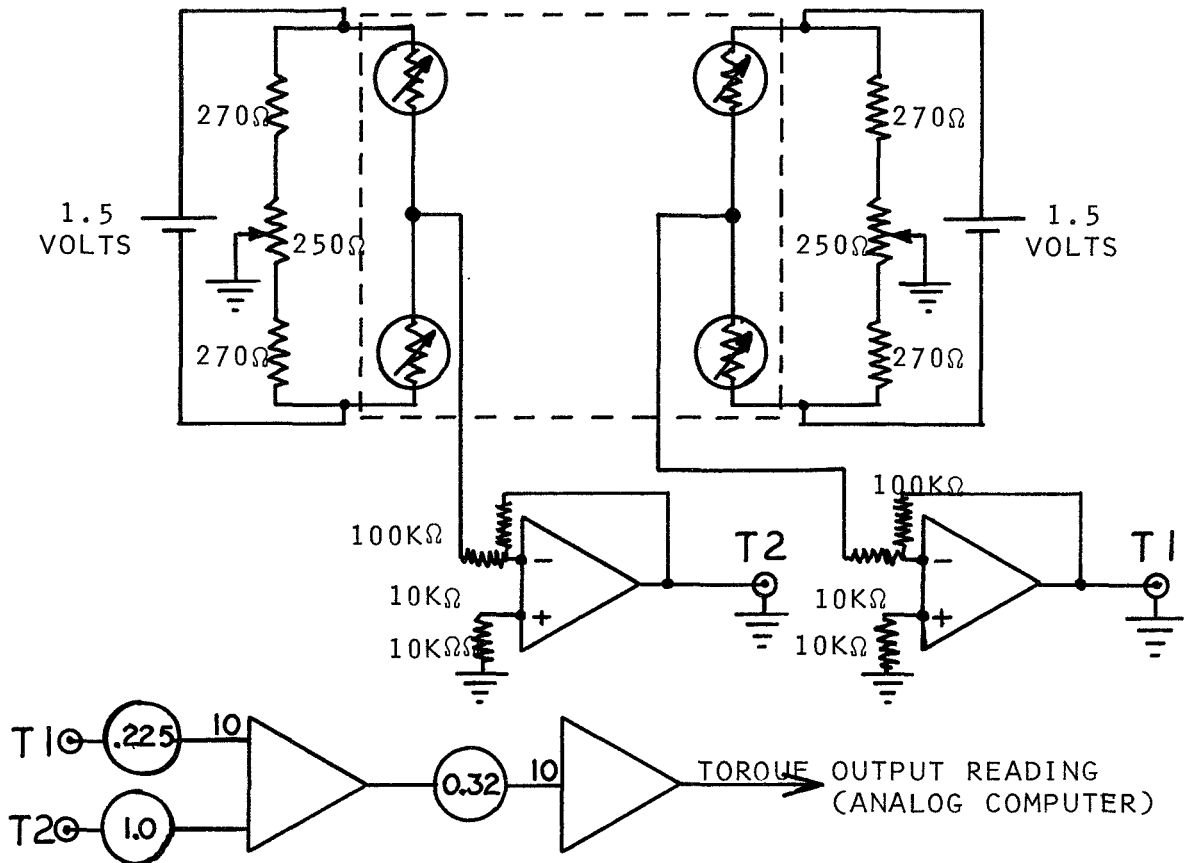


FIGURE B.2 READING TORQUE ON THE PLATFORM BASE

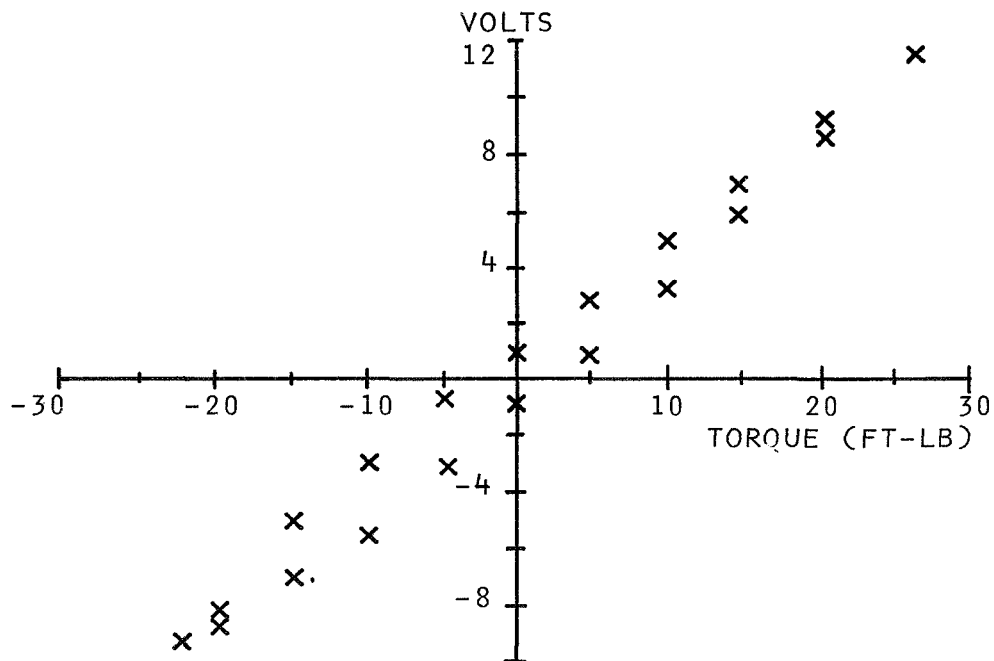


FIGURE B.3 CHARACTERISTICS OF THE TORQUE MEASUREMENT

load readings are amplified and summed, forming the net reaction torque reading. Figure B.2 shows the configuration.

Each force transducer is calibrated separately and resistance ranges are matched for each of the differential force bridges. Passive resistors in each bridge are set to balance the bridge at the nominal load of 70 pounds on each differential pair (one half the weight of an average subject).

The complete force plate is calibrated using large weights simulating the nominal load of 140 pounds.

Figure B.3 shows the static output characteristics of the force plate transducers as a function of net reaction torque. Linearity is within  $\pm 2.5\%$  at full scale. Hysteresis errors during a given cycle are within  $\pm 5\%$  of the maximum amplitude of the cycle.

The rated frequency response of each sensor is above 1000 hz, far better than necessary to measure postural responses.

#### B.1.2 Body Angle Measurement

Body angle is measured by the simple, 2-potentiometer and cable system, shown in Figure B.4. Two potentiometers, one on each hip, remove effects of vertical axis rotations. Sensitivity of the system is  $\pm 0.01$  degrees.

### B.2 Platform Motion Effectors

The force plate is maintained on a member which is able to rotate about an axis colinear to that of the ankle joint. A hydraulic ram and servo valve control the angle of the force plate member.

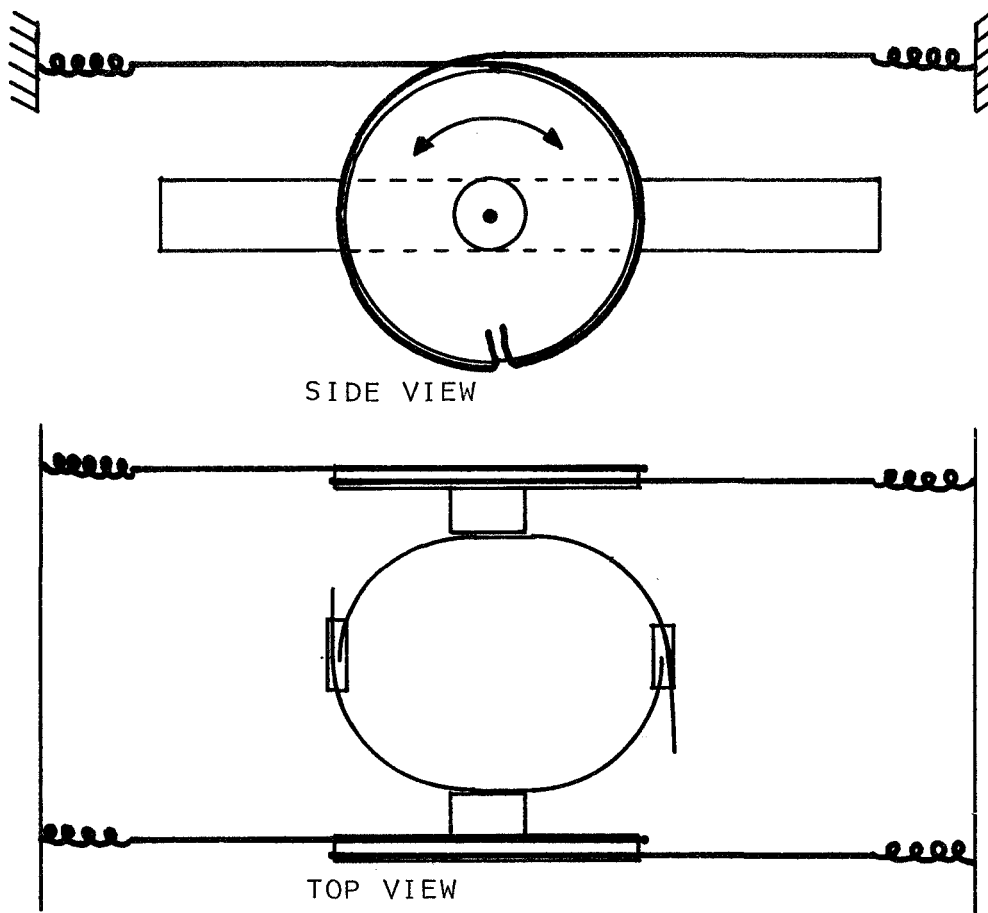


FIGURE B.4 READING BODY ANGLE WITH RESPECT TO VERTICAL

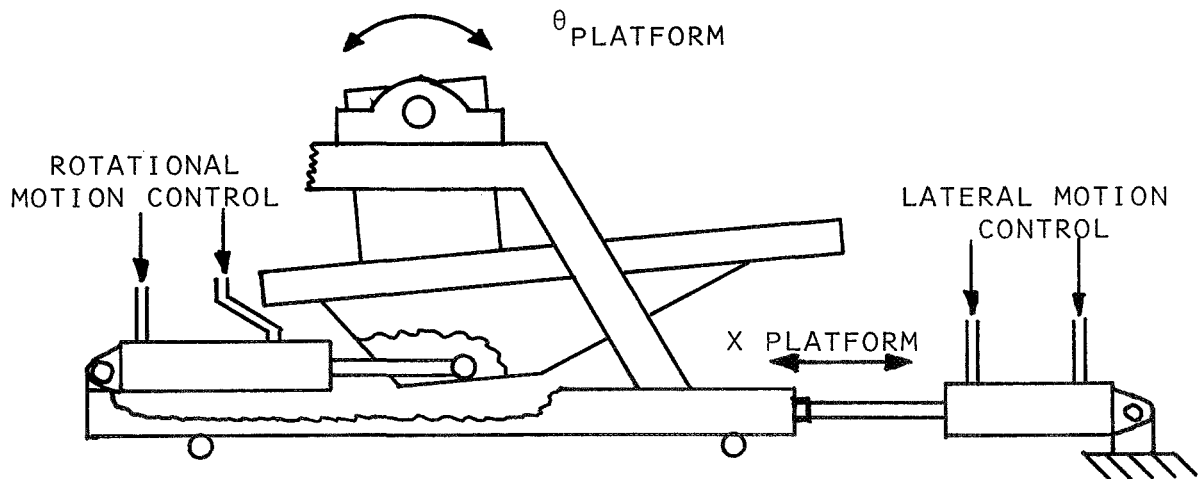


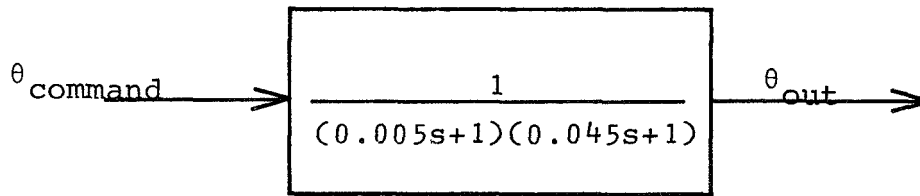
FIGURE B.5 THE TWO DEGREES OF PLATFORM MOTION

The entire supporting base rides on two roller bearings, allowing forward and backward motion of the platform. This motion is controlled by a second hydraulic ram and valve system. The system is shown schematically in Figure B.5.

The rotational servo loop consists of the following components:

1. proportional servo valve; Moog Model M-7770 @2700 psi; excitation push-pull.
2. 2-way hydraulic ram; 1 1/4 bore, 8" stroke.
3. rack and pinion potentiometer position feedback.

Flow rates within the control valve limit the performance of the system. The following transfer function describes closed loop platform rotational motion for amplitudes below  $\pm 2^\circ$ :



Frequency response is well above that required during experiments. The step response time, about 50 milliseconds, is adequate to observe a well defined reflex response.

The lateral position control loop operates open loop. Deflection velocity is controlled by a needle valve and monitored with rack and pinion potentiometer position feedback. Total deflection is fixed with adjustable restraining rings

mounted on the hydraulic ram. An on-off relay valve controls activation of the lateral deflection loop.

Components are as follows:

1. relay valve, 2-way
2. double acting hydraulic cylinder, 7/8" bore, 4" stroke, adjustable with inserts from 1/2" to 4"
3. rack and pinion actuated potentiometer for monitoring of lateral position.

Figure B.6 shows operation of the hydraulic motion control system.

Maximum deflection velocity is greater than 5 inches per second. Response (not including response time delay of the relay valve) is approximately first order with a response time of 10 milliseconds.

## APPENDIX C

DIGITAL COMPUTER PROGRAMSC.1 The Computer Facility

Digital computation is performed by a PDP-8 computer, built by Digital Equipment Corporation. Features of the machine include:

1. Single address
2. 12-bit 2" complement arithmetic
3. Cycle time of 1.5 microseconds - add time of 2 microseconds
4. Extended arithmetic element permitting multiplication (less than 21 microseconds) and division (less than 36.5 microseconds)
5. 4096 word memory
6. Two Dectape (magnetic tape) drives which read/write from tape to core in blocks of 128 words.

Programs are written in "PAL" machine language developed for the PDP-8.

Hybrid facilities include:

1. Seven analog to digital channels
2. Eight digital to analog channel

Operation of these converters is controlled by commands from

the digital computer.

3. Twelve control lines

4. Twelve sense lines

Control lines, enable the digital to give two-level commands to the analog computer. Similarly, sense lines enable the digital computer to read two-level logic signals initiated by the analog computer.

5. Program Interrupt

This input allows interruption of the digital program by the analog computer. Interrupt is used in programs presented here to control the sampling rate during the digital collection of data.

## C.2 Digital Operating Programs

Three digital programs are used. The first, Test, is a general purpose program which operates the experiments, collects the data, and stores it on digital tape. Fourier is a fast Fourier transform program. Model performs non-linear functions required during simulation of the posture control models. A description of each program follows.

### Test

Test performs the following functions:

1. Reads into core two channels of data, biasing each so that the initial sample of each is zero.
2. Introduces a digital to analog command (for initiation of rotational steps or lateral displacements of the platform) after a delay of 16 samples.

3. Writes data onto digital tape after each trial.
4. Allows sequential examination of data stored on digital tape.

Each trial reading is initiated by an analog command. The sampling rate during each trial is controlled by an analog clock.

### Fourier

The fast Fourier transform program performs the following functions:

1. Reads data from digital tape into core memory.
2. Performs the fast Fourier transform.
3. Prints frequency coefficients.

A complete description of the digital transform technique is given by Van Houtte (104).

### C.3 Model

Model converts six analog inputs to digital, performs nonlinear operations on these signals, and reconverts the transferred signal back into analog form. Model simulates the following nonlinear functions:

1. Three time delays
2. Two thresholds
3. One "stiction" model used to simulate muscle response characteristics to small deflections.

APPENDIX D

ANALOG COMPUTER PROGRAMS

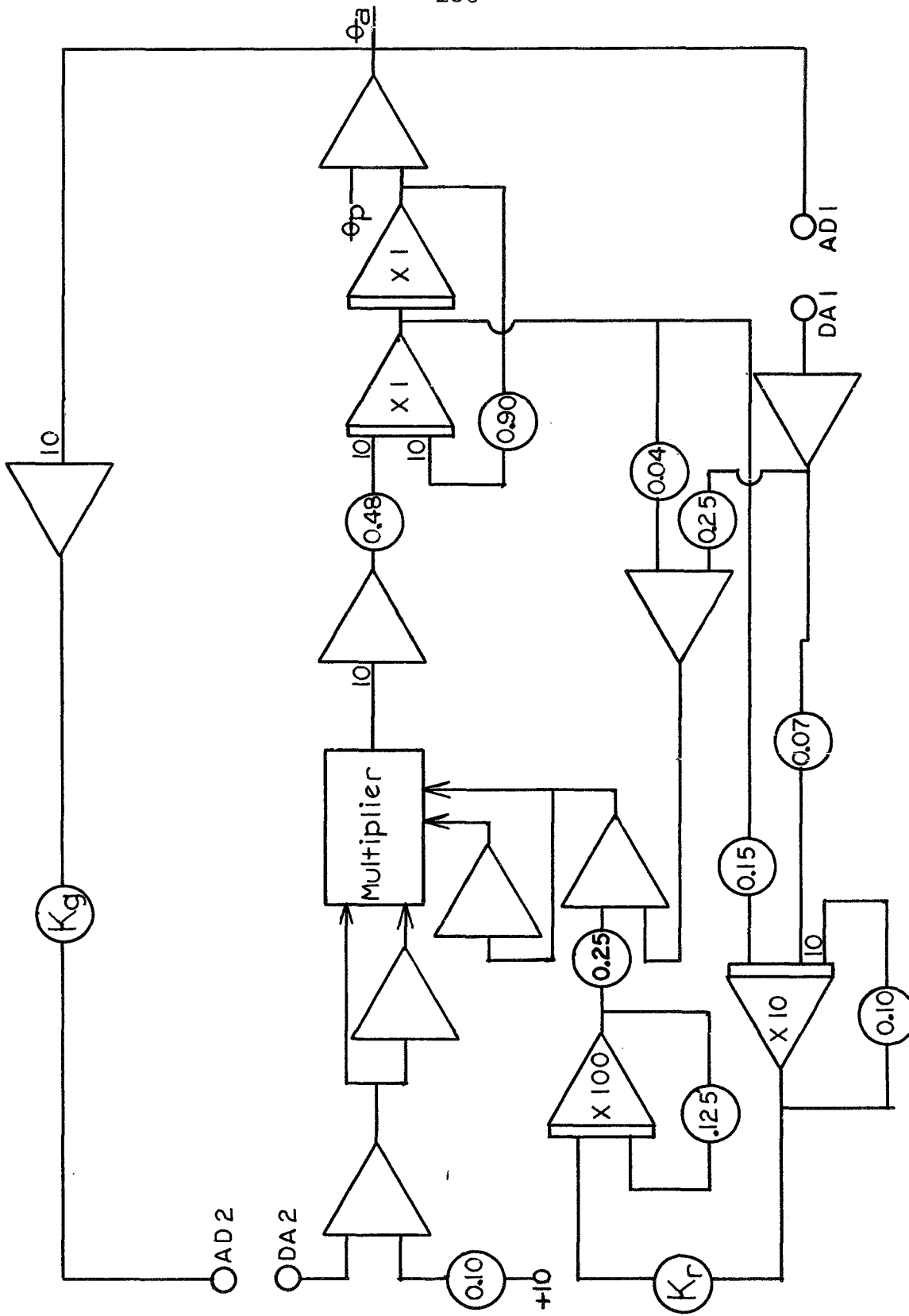


FIGURE D.1 ANALOG PATCH FOR SIMULATION OF THE REFLEX GAIN CONTROL

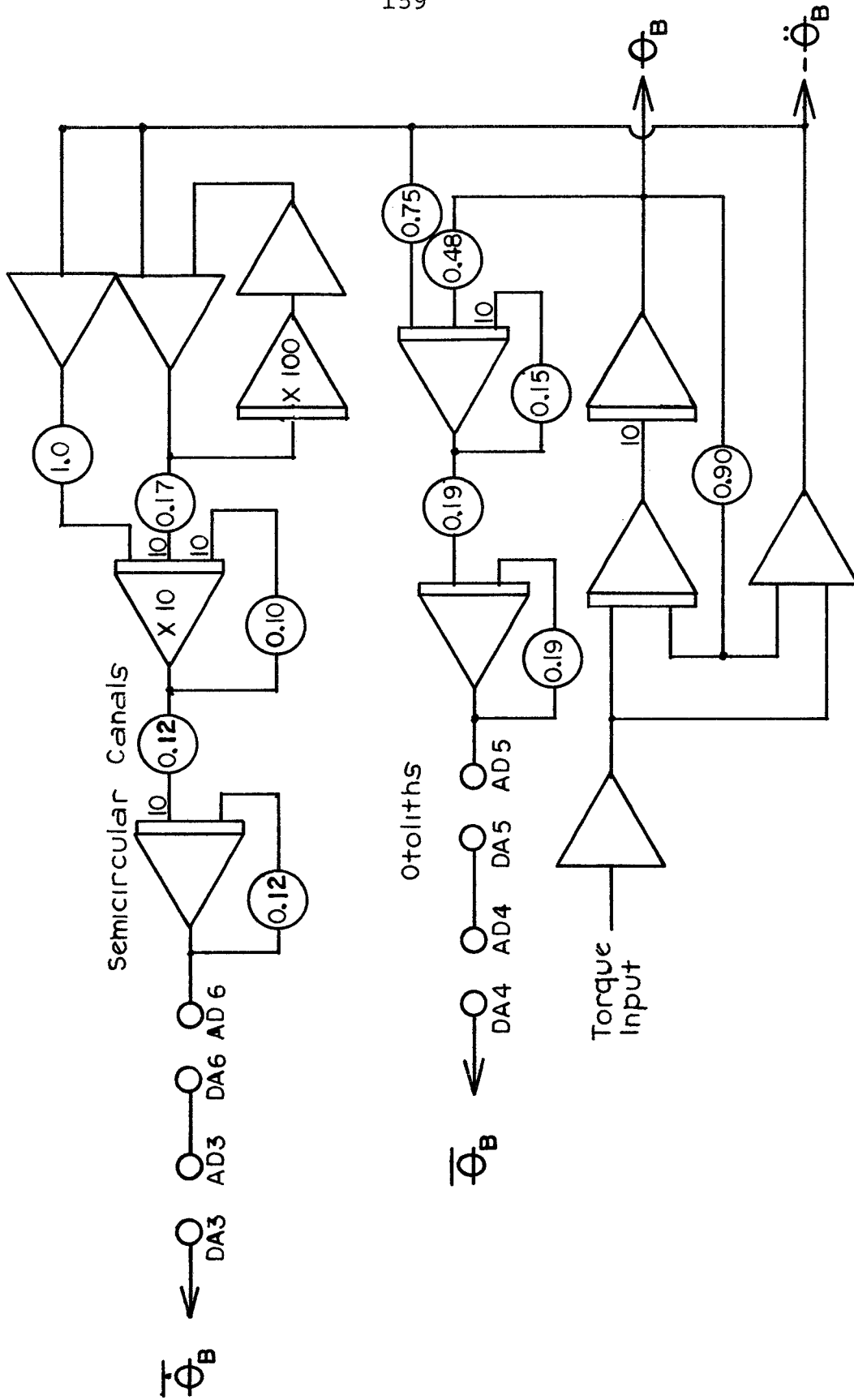


FIGURE D.2 ANALOG PATCH FOR SIMULATION OF THE VESTIBULAR SENSOR DYNAMIC CHARACTERISTICS



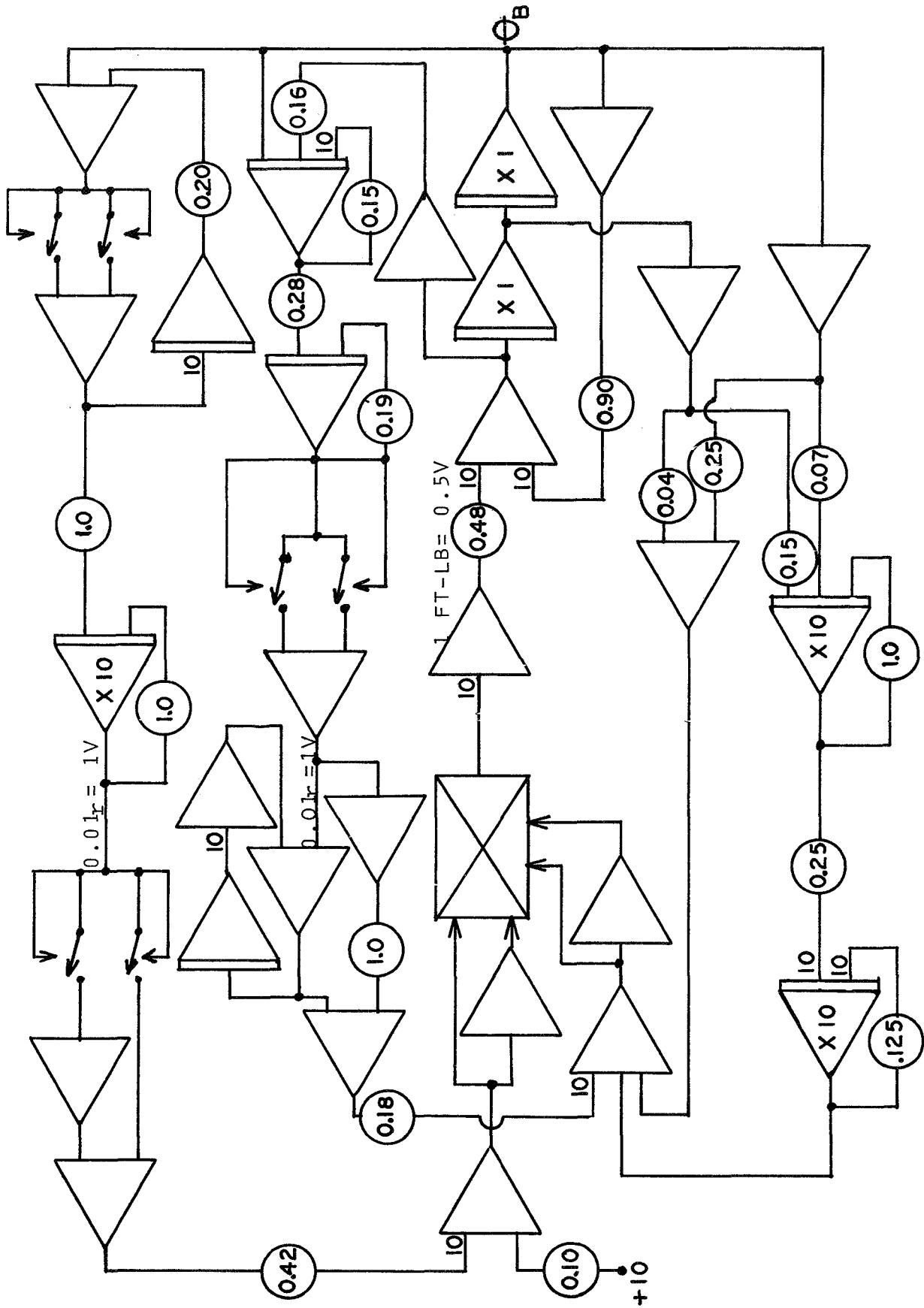


FIGURE D.4 ANALOG PATCH FOR SIMULATION OF REFLEX/EXTEROCEPTIVE CONTROL OF POSTURE

APPENDIX E

EXPERIMENTAL DATA

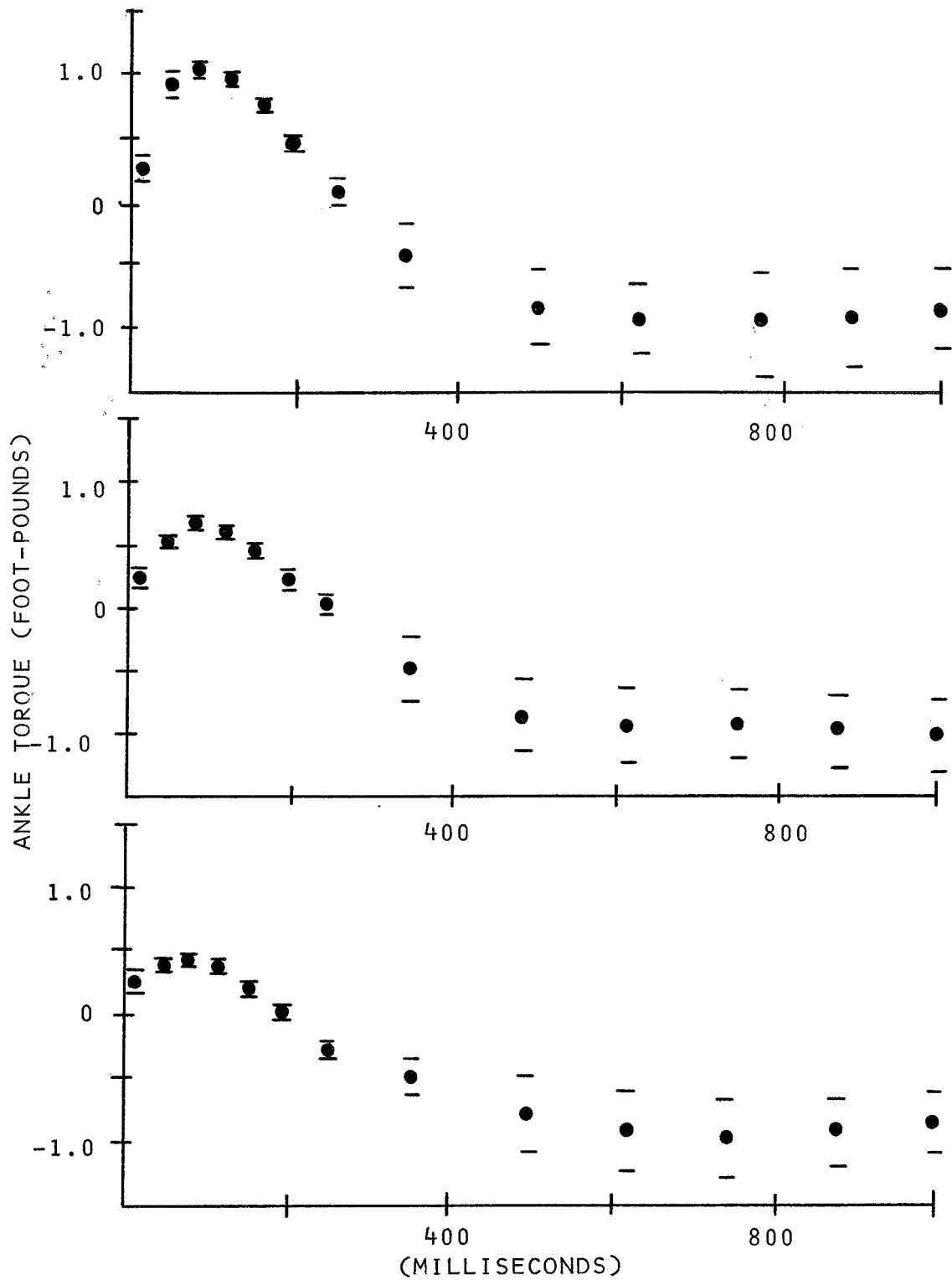


FIGURE E.1 AVERAGE RESPONSES TO  $1/4^\circ$  STEPS EXTENDING THE ANKLE JOINT, SUBJECT D. R.

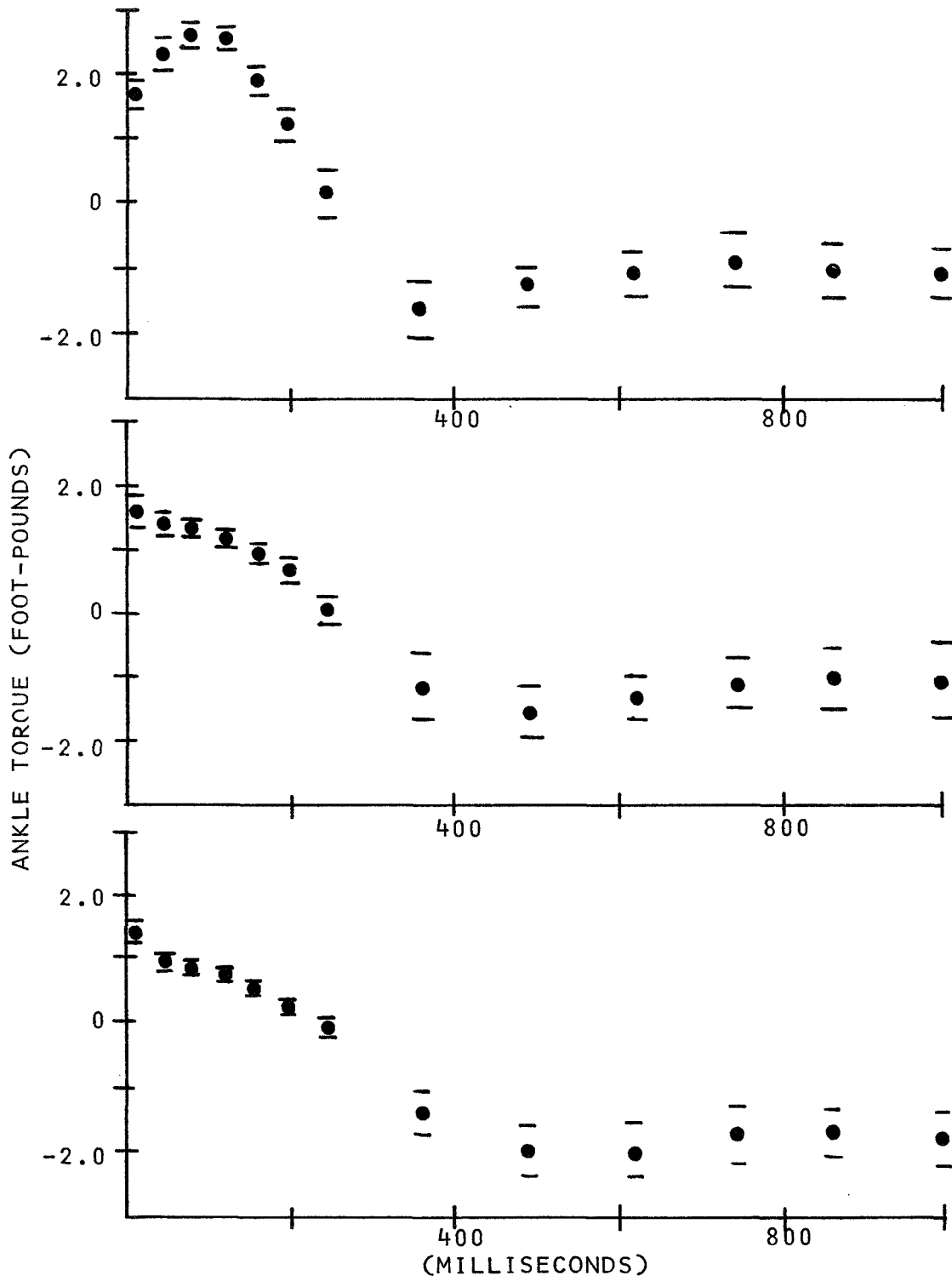


FIGURE E.2 AVERAGE RESPONSES TO  $1/2^\circ$  STEPS EXTENDING THE ANKLE JOINT, SUBJECT D. R.

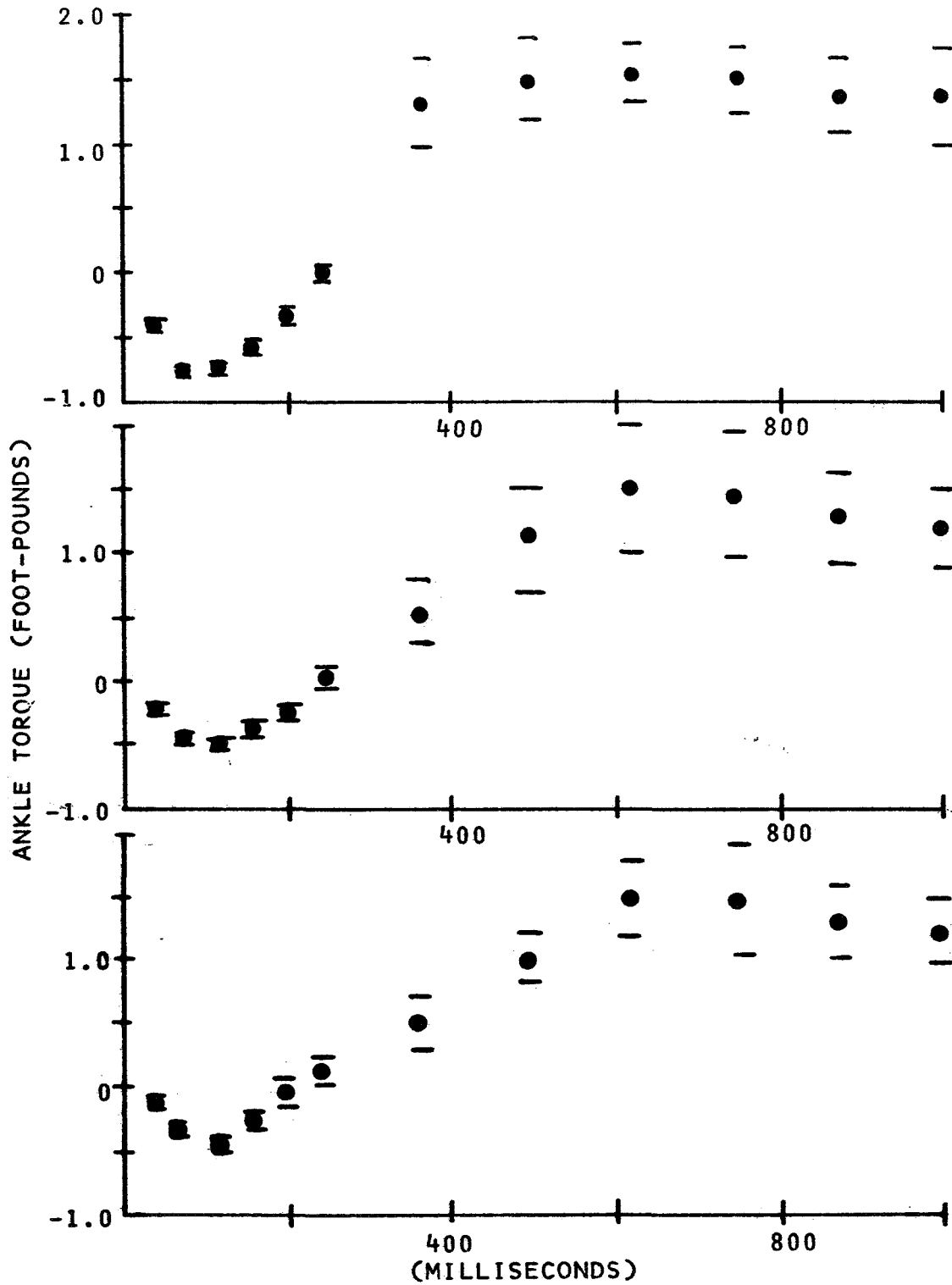


FIGURE E.3 AVERAGE RESPONSES TO  $1/4^\circ$  STEPS FLEXING THE ANKLE JOINT, SUBJECT D. R.

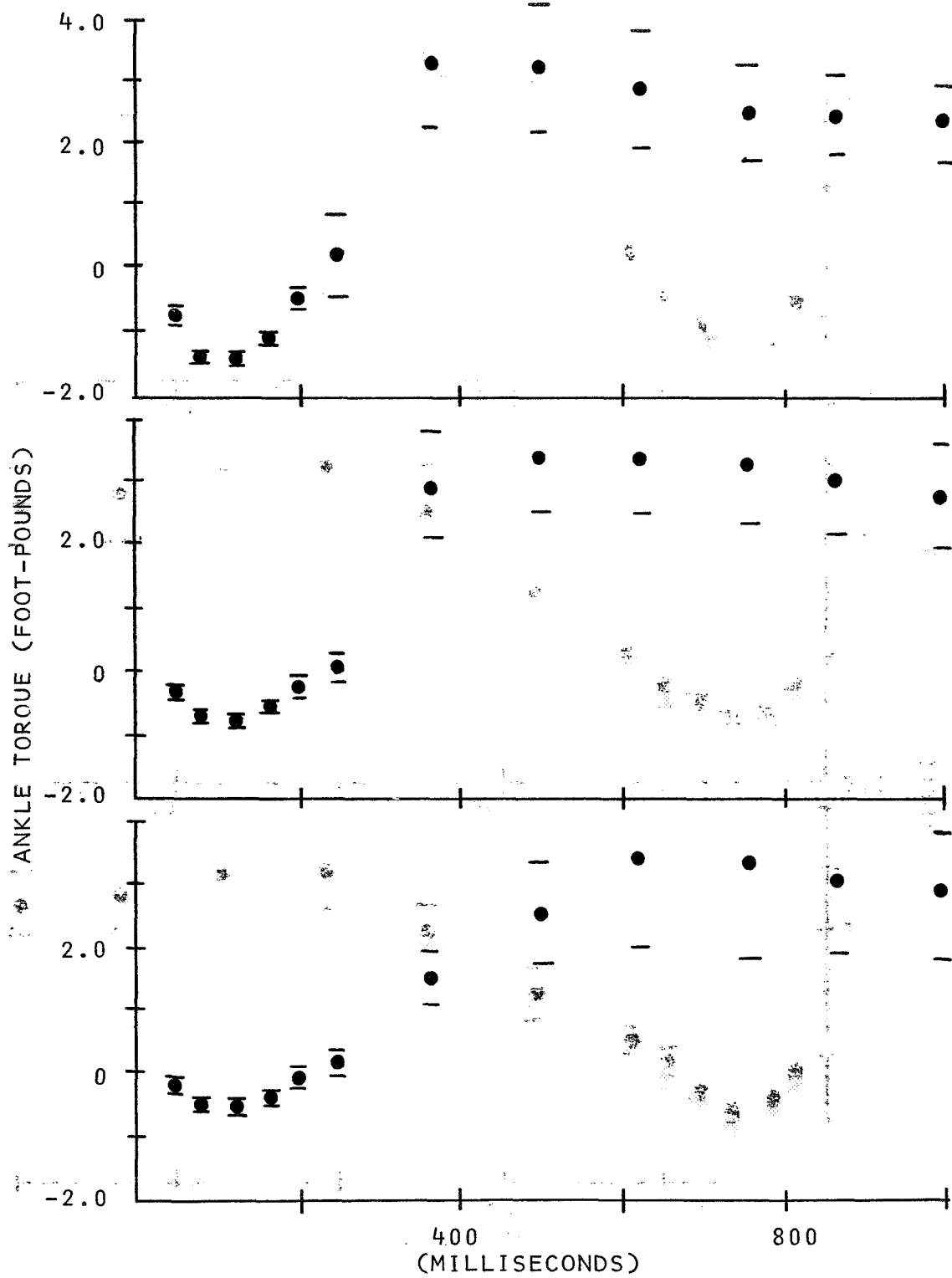


FIGURE E.4 AVERAGE RESPONSES TO  $1/2^\circ$  STEPS FLEXING THE ANKLE JOINT, SUBJECT D. R.

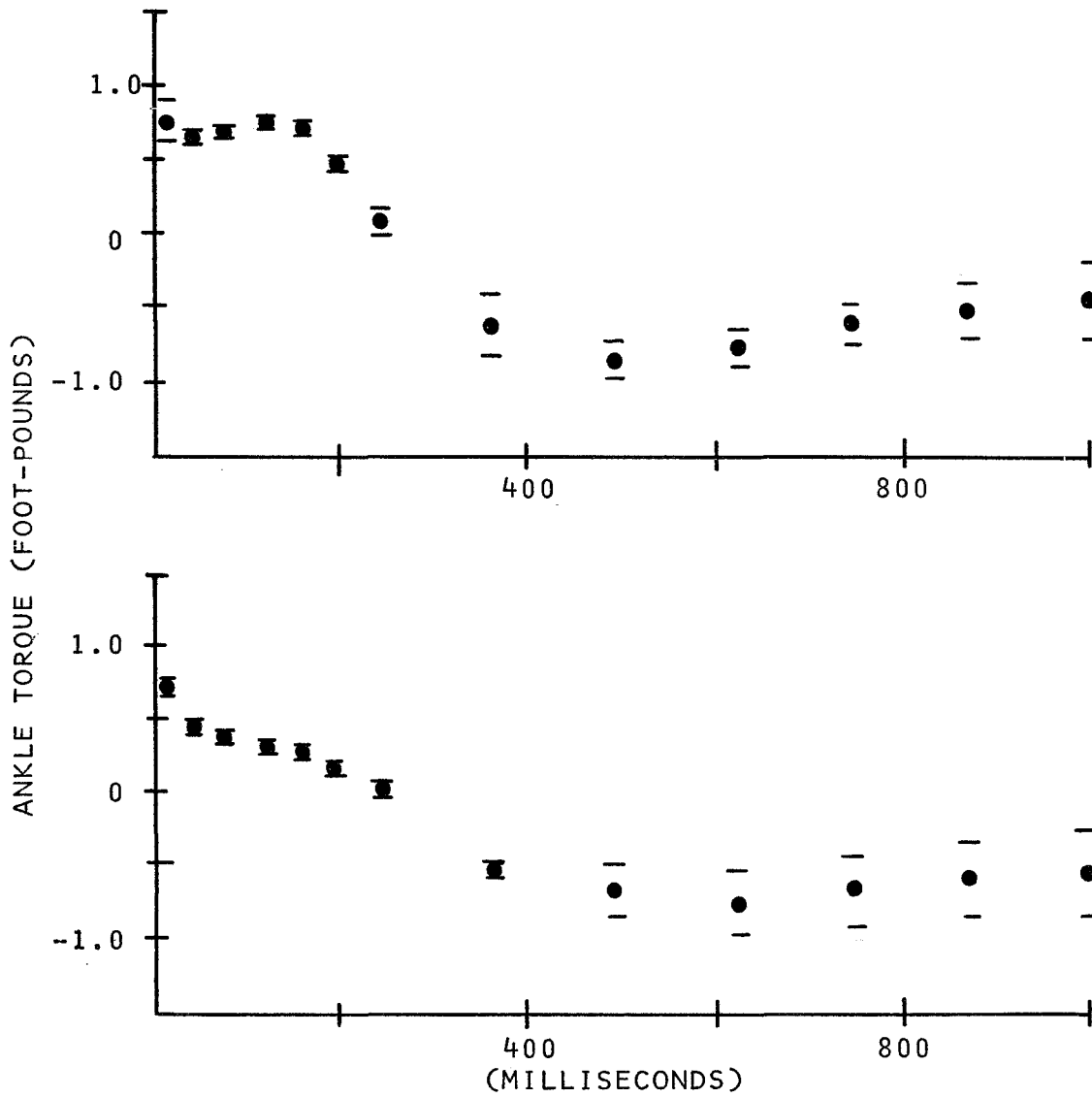


FIGURE E.5 AVERAGE RESPONSES TO  $1/4^\circ$  STEPS EXTENDING THE ANKLE JOINT, SUBJECT K. G. N.

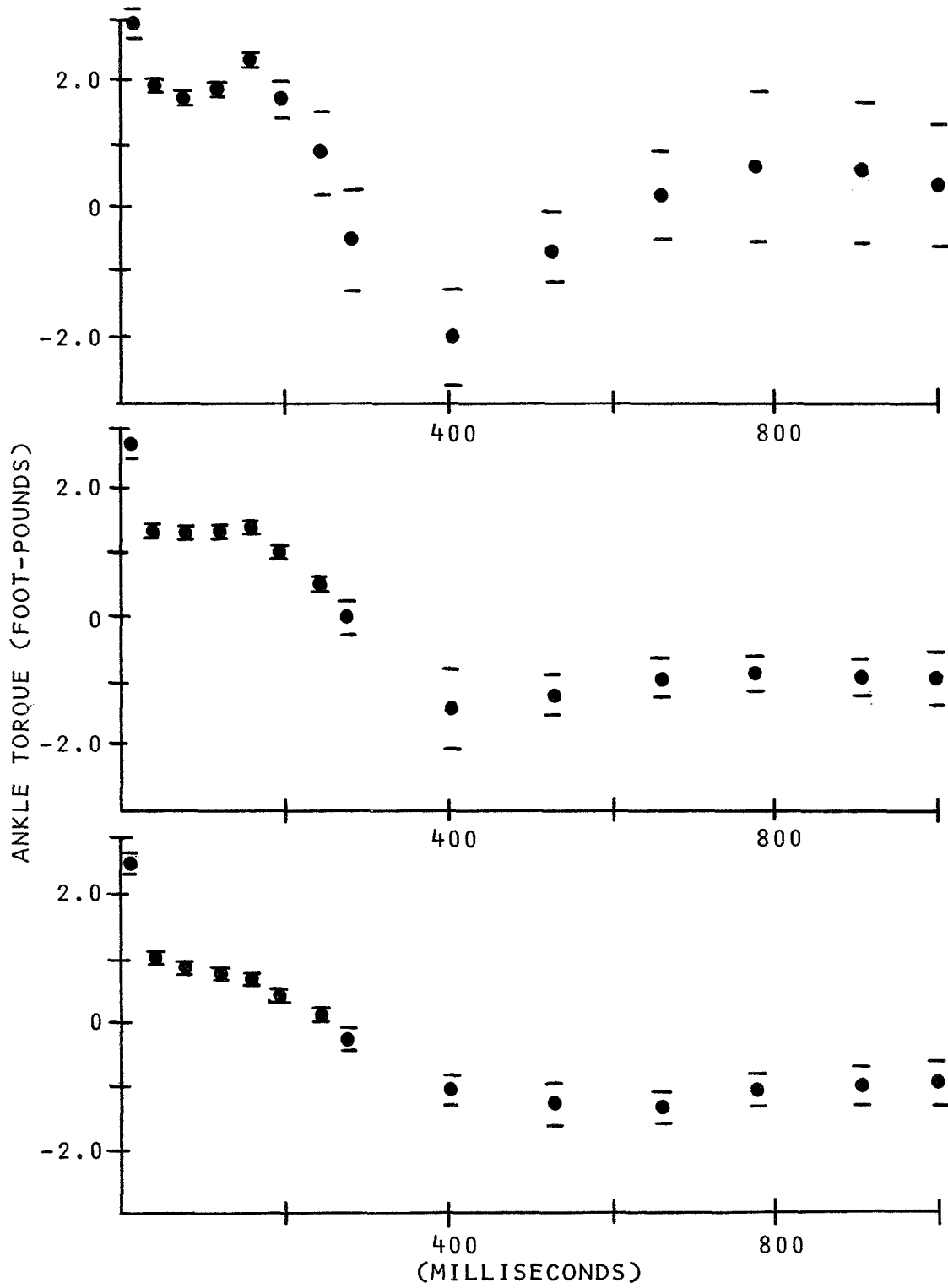


FIGURE E.6 AVERAGE RESPONSES TO  $1/2^\circ$  STEPS EXTENDING THE ANKLE JOINT, SUBJECT K. G. N.

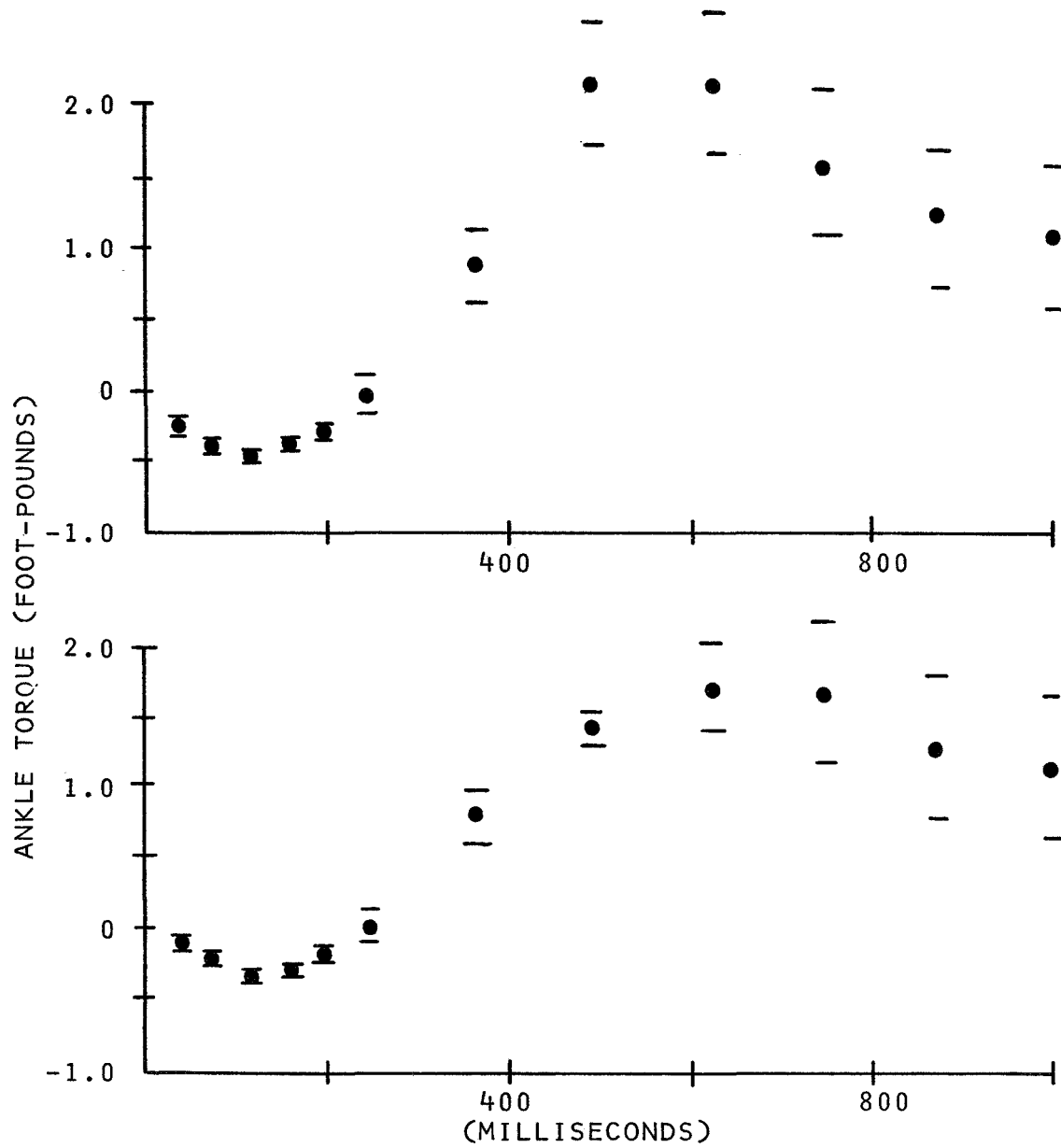


FIGURE E.7 AVERAGE RESPONSES TO  $1/4^\circ$  STEPS FLEXING THE ANKLE JOINT, SUBJECT K. G. N.

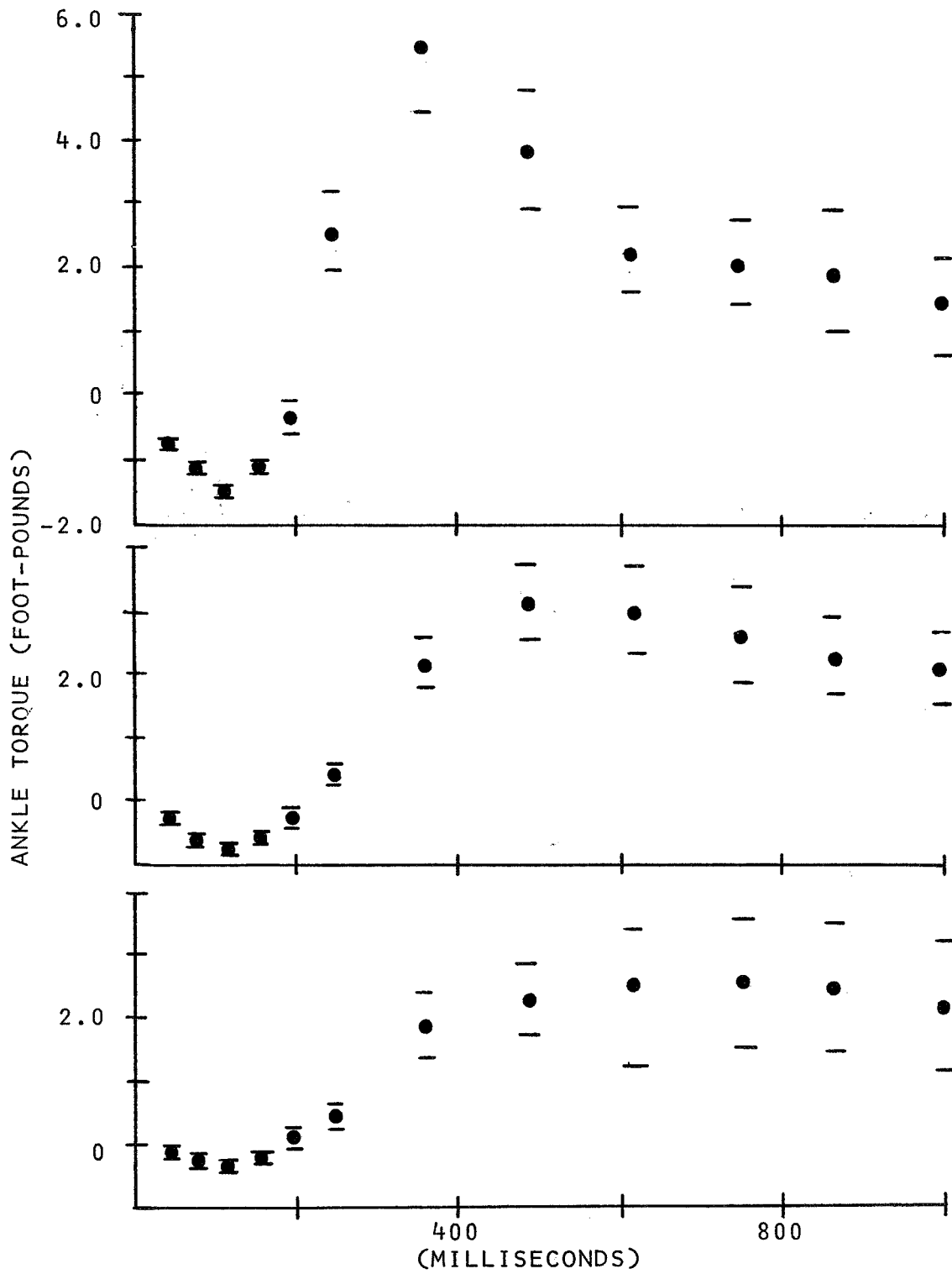


FIGURE E.8 AVERAGE RESPONSES TO  $1/2^\circ$  STEPS FLEXING THE ANKLE JOINT, SUBJECT K. G. N.

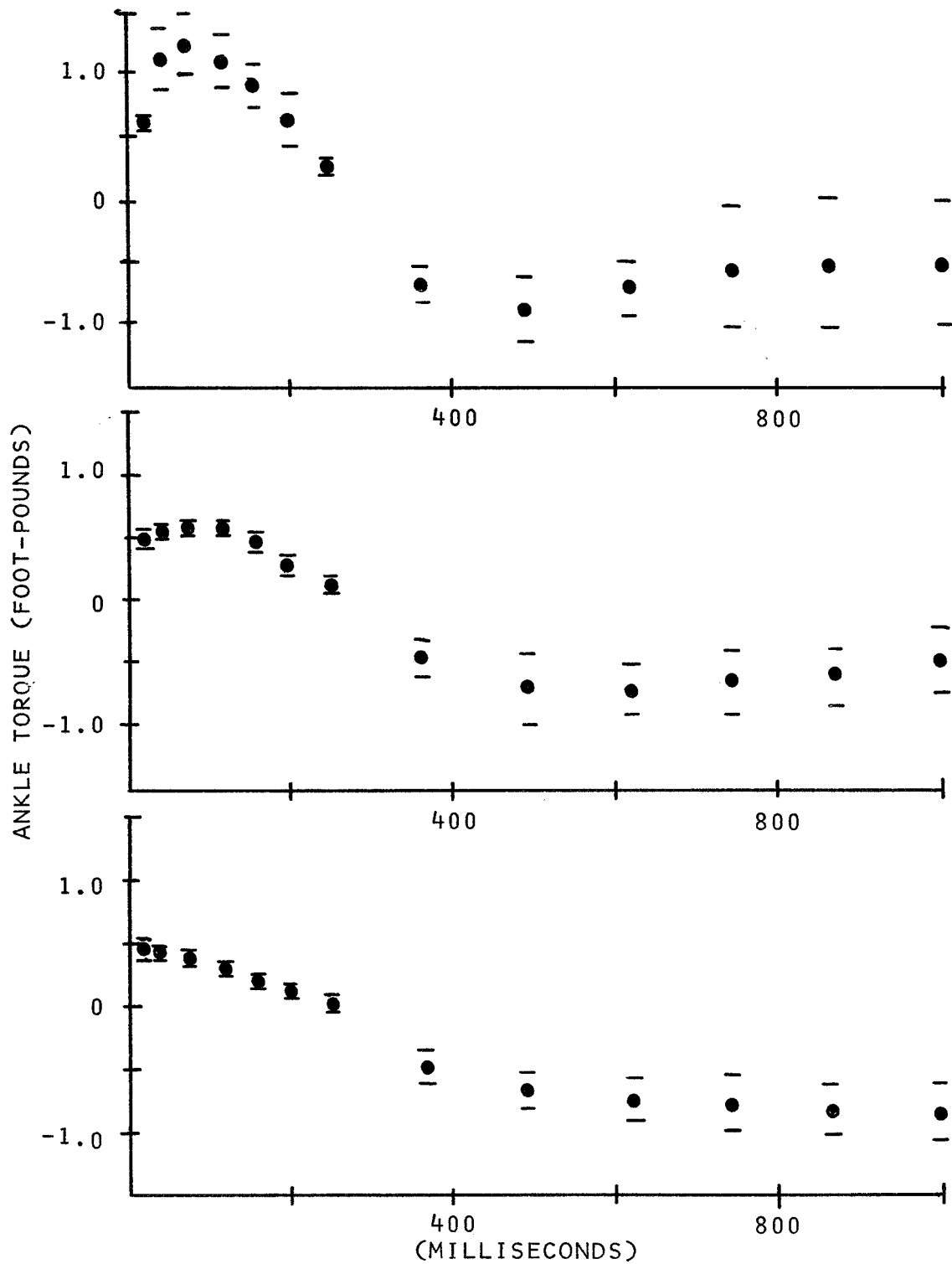


FIGURE E.9 AVERAGE RESPONSES TO  $1/4^\circ$  STEPS EXTENDING THE ANKLE JOINT, SUBJECT G. L.

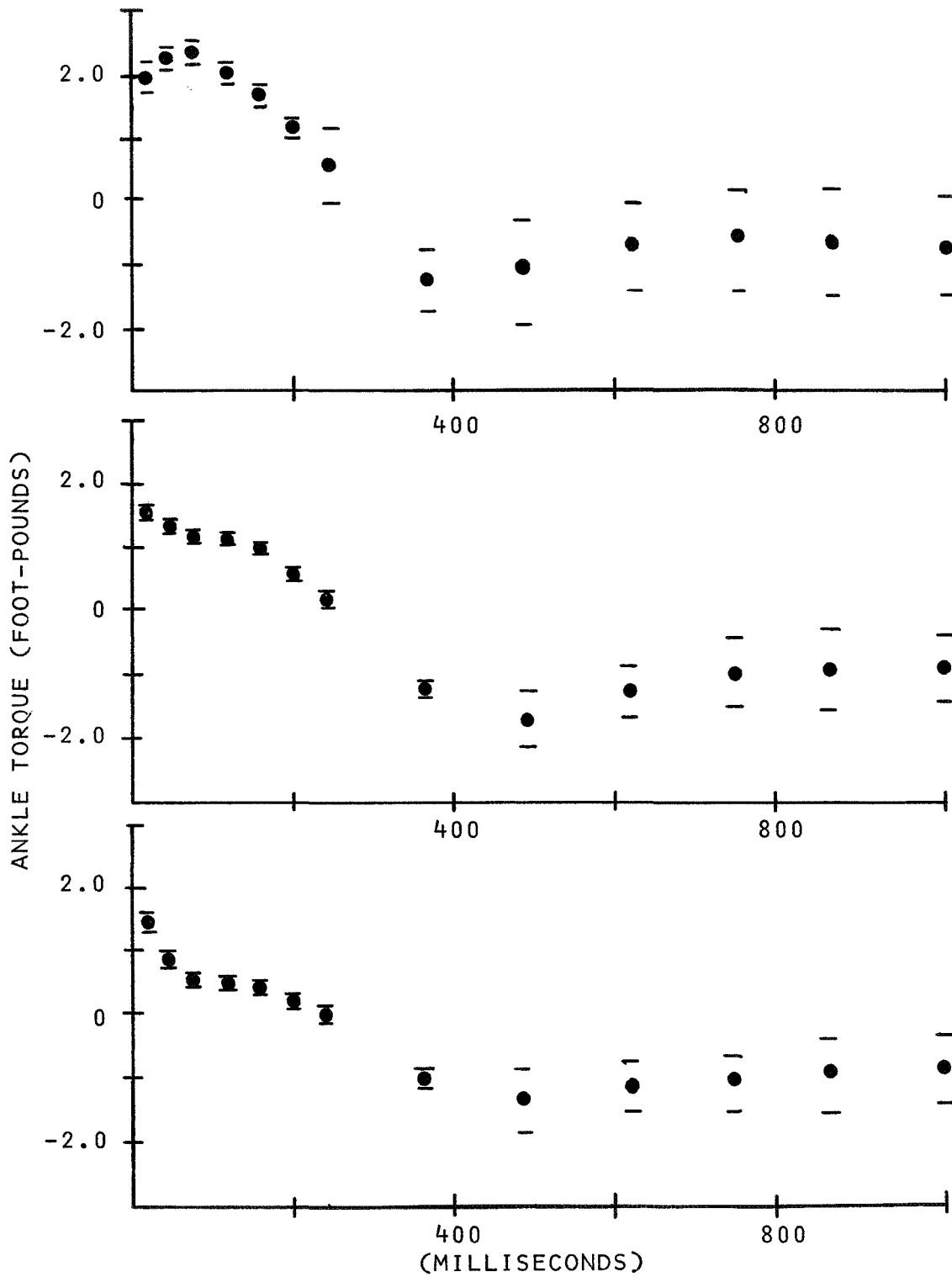


FIGURE E.10 AVERAGE RESPONSES TO  $1/2^\circ$  STEPS EXTENDING THE ANKLE JOINT, SUBJECT G. L.

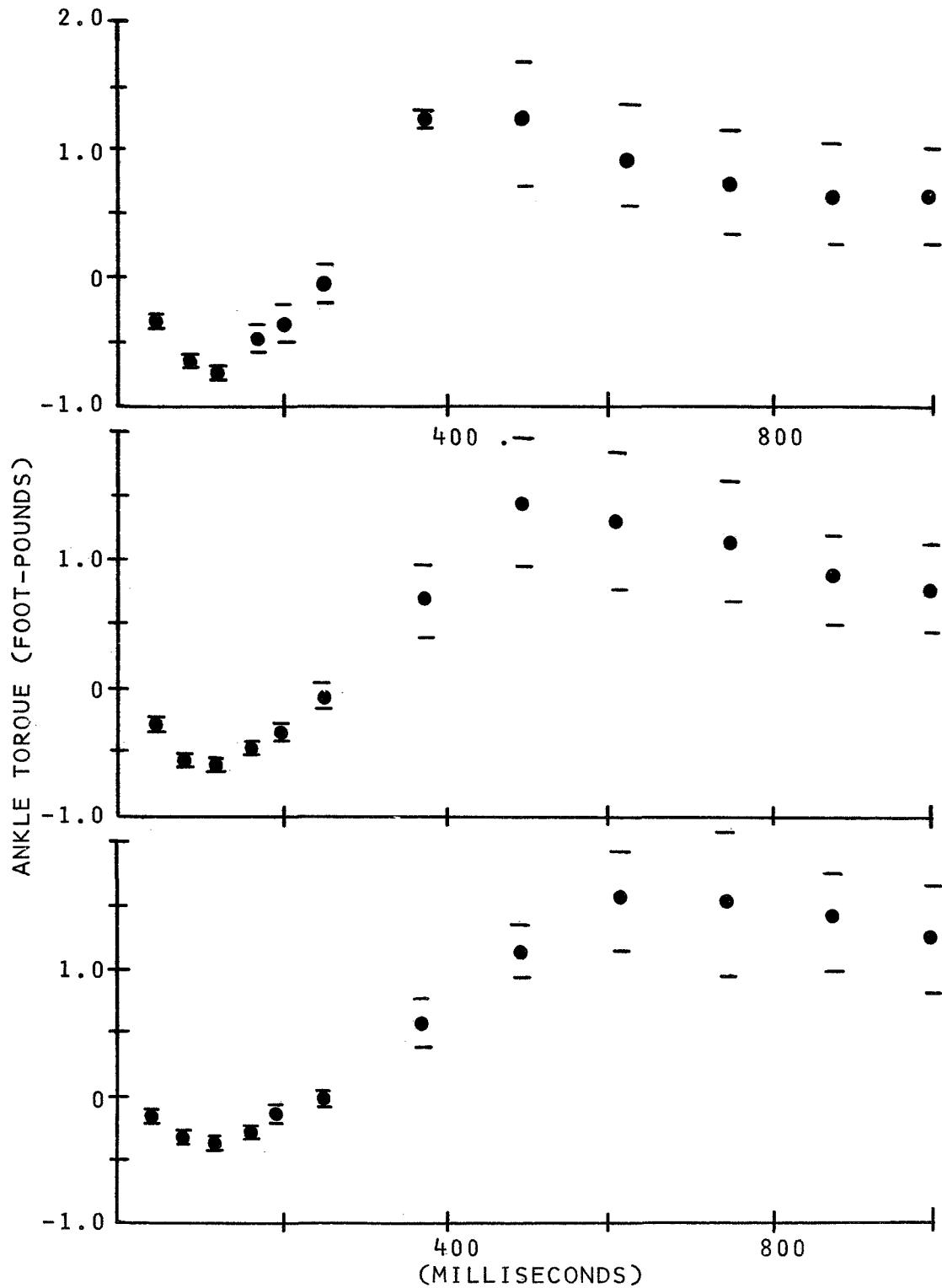


FIGURE E.11 AVERAGE RESPONSES TO  $1/4^\circ$  STEPS FLEXING THE ANKLE JOINT, SUBJECT G. L.

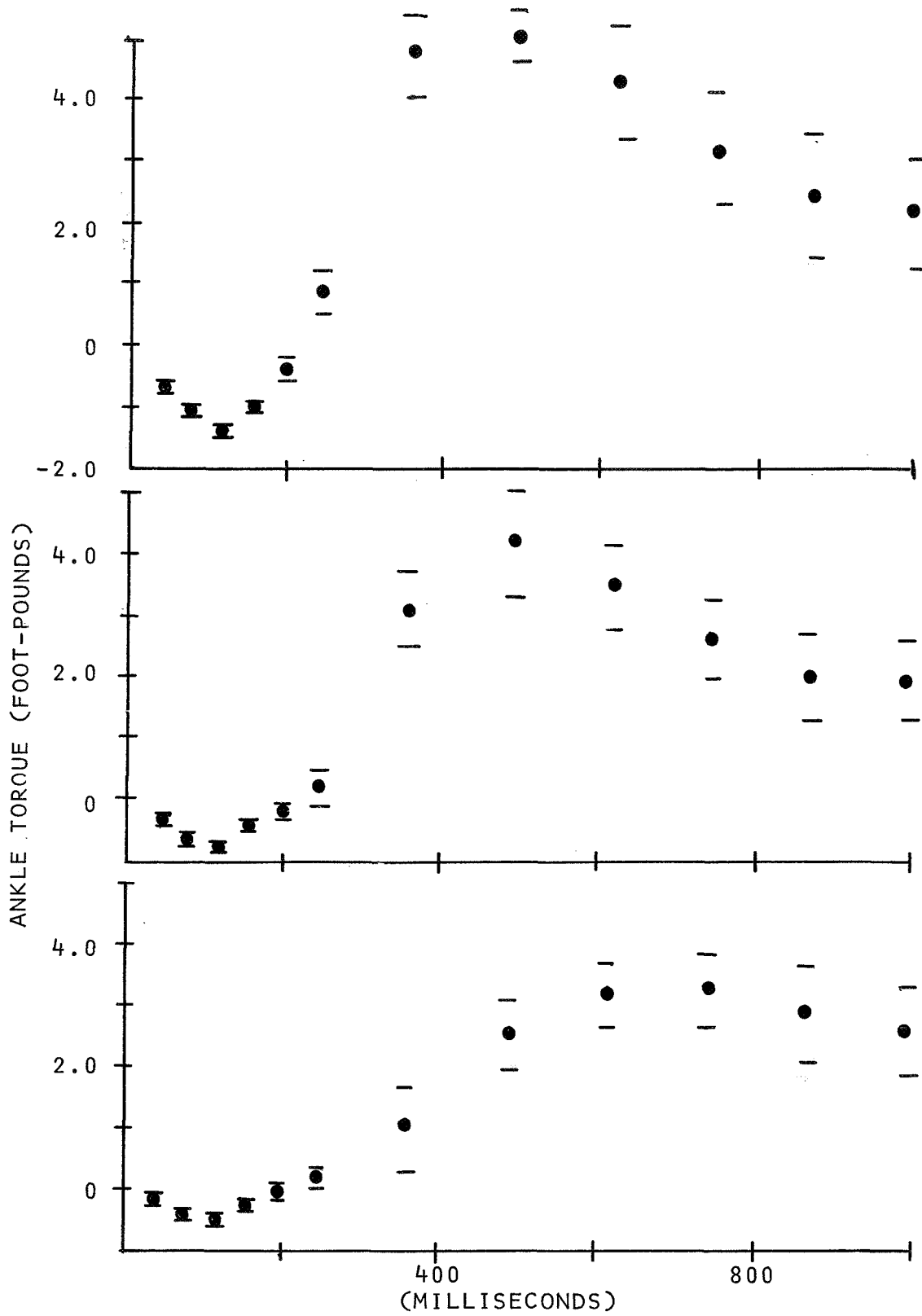


FIGURE E.12 AVERAGE RESPONSES TO 1/2° STEPS. FLEXING THE ANKLE JOINT, SUBJECT G. L.

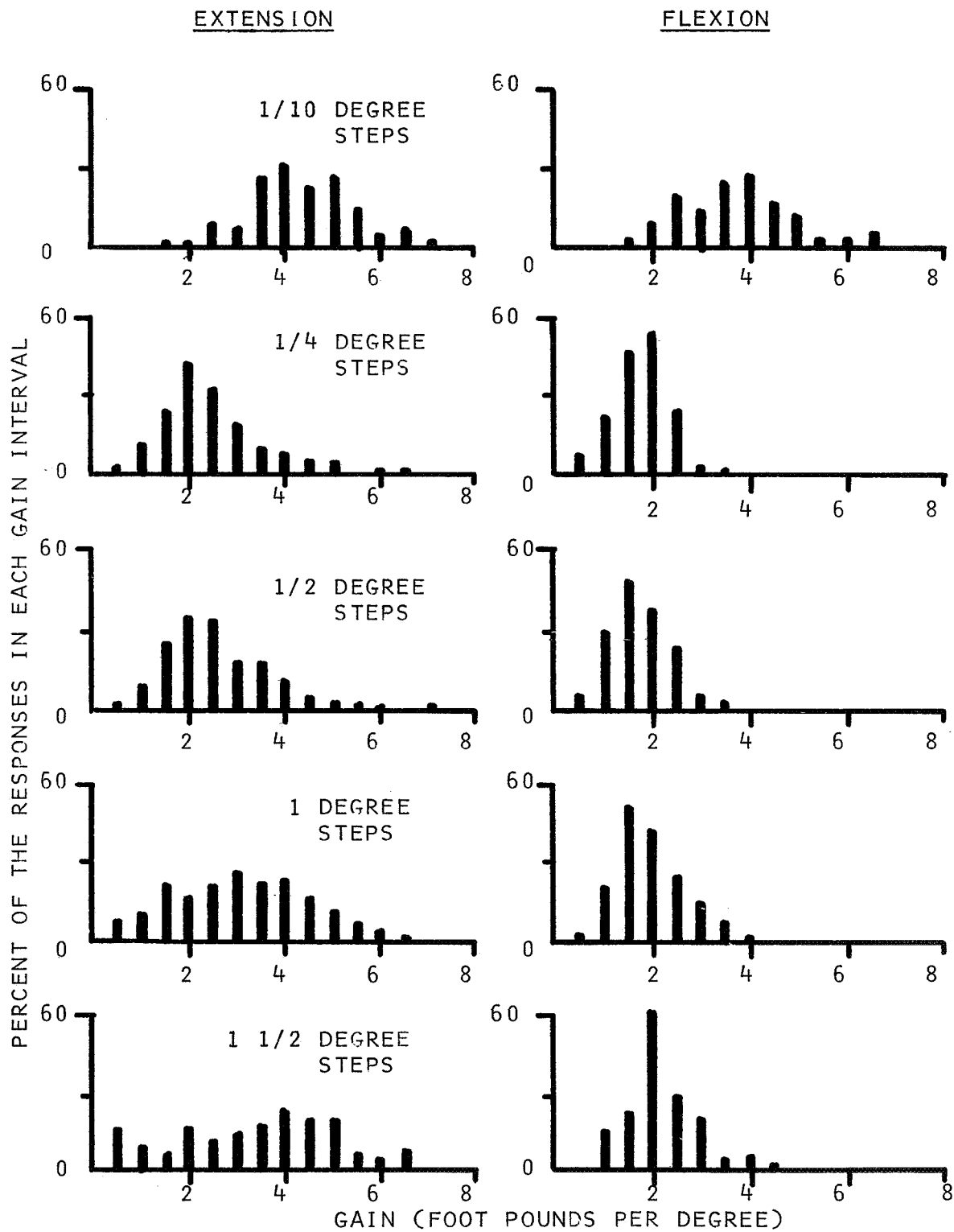


FIGURE E.13 DISTRIBUTION OF REFLEX RESPONSE GAINS FOR FIVE STEP SIZES

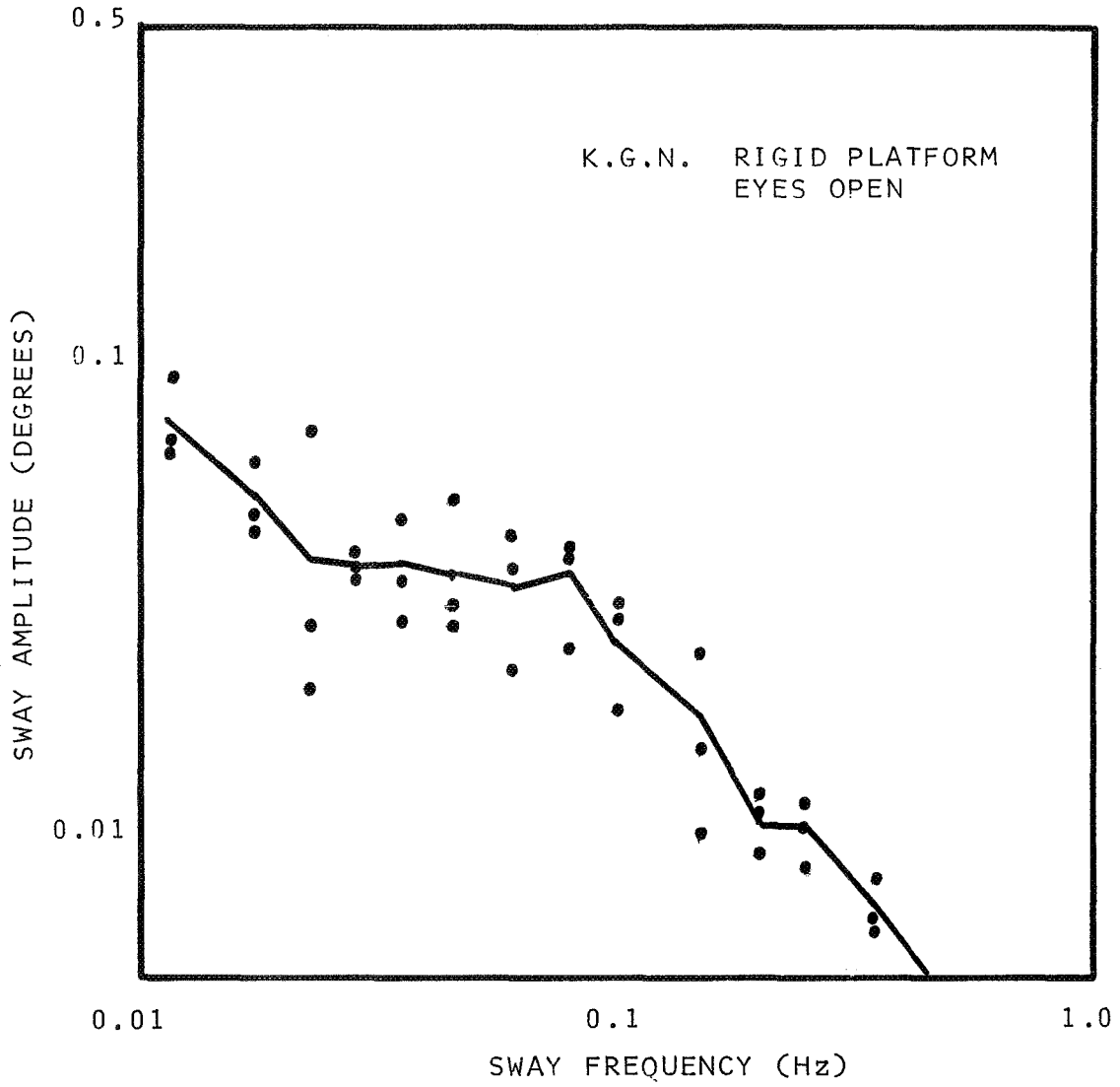
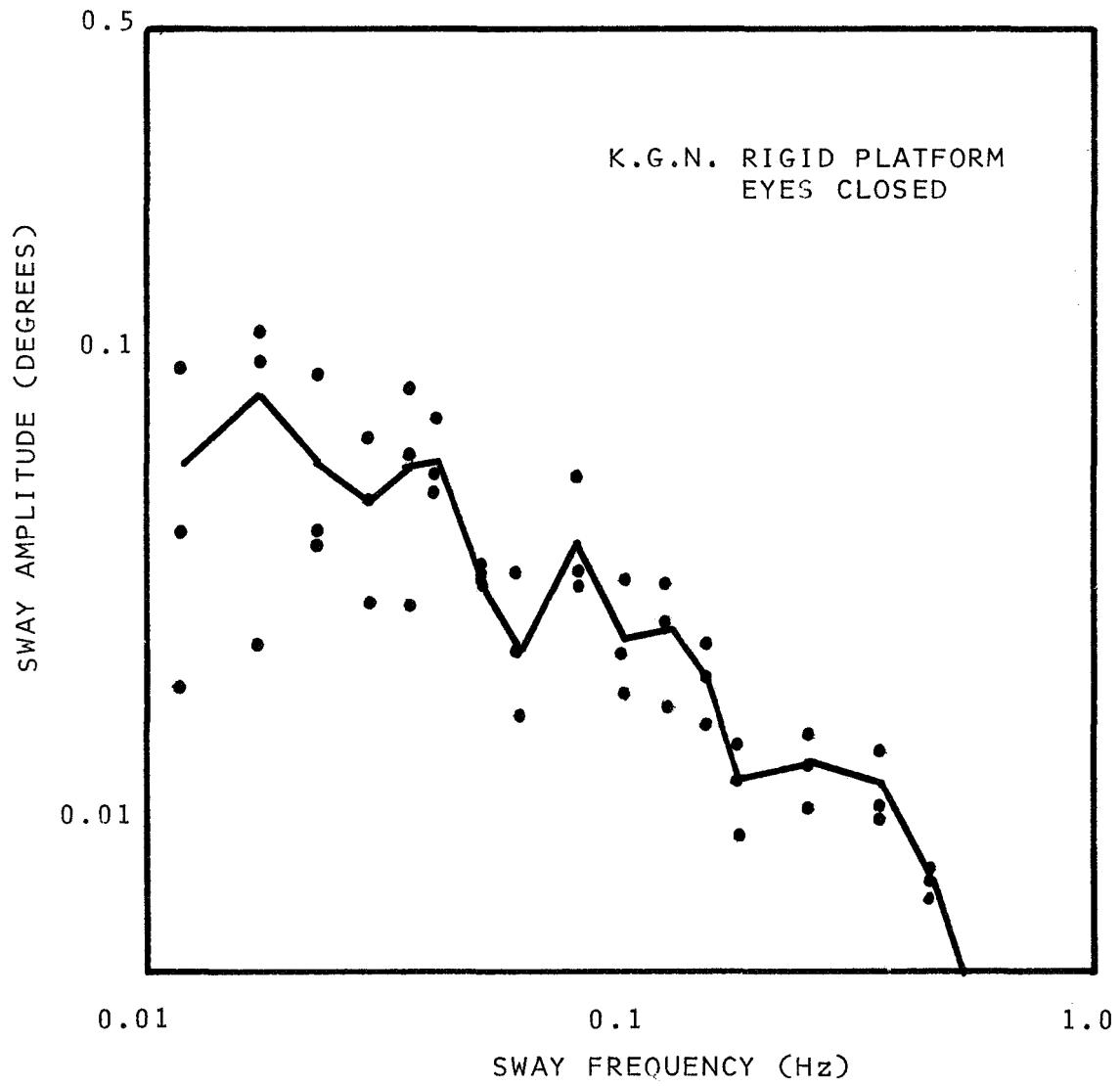


FIGURE E.14 FOURIER COEFFICIENTS FOR BODY SWAY MOTION



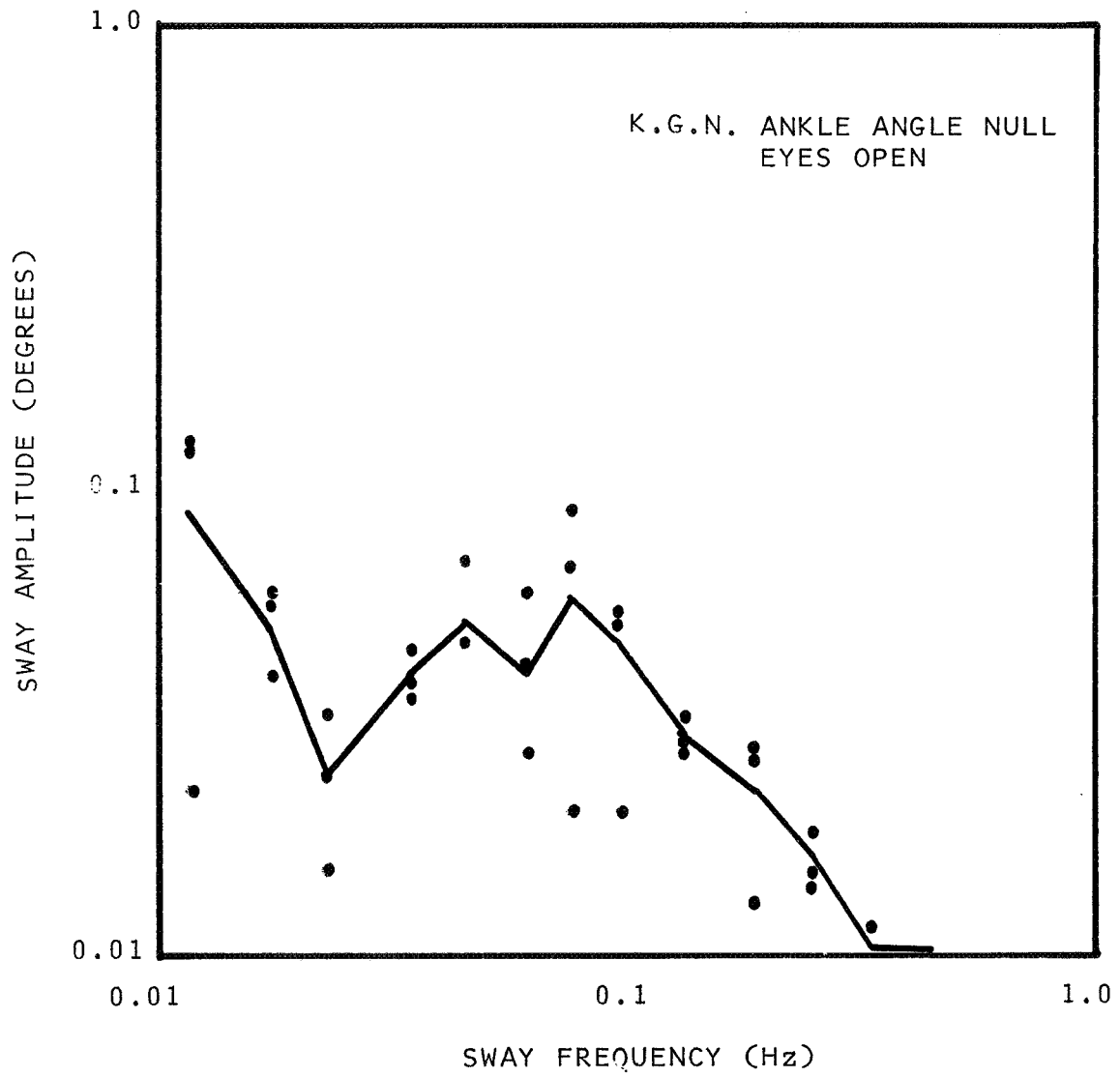


FIGURE E.16 FOURIER COEFFICIENTS FOR BODY SWAY MOTION

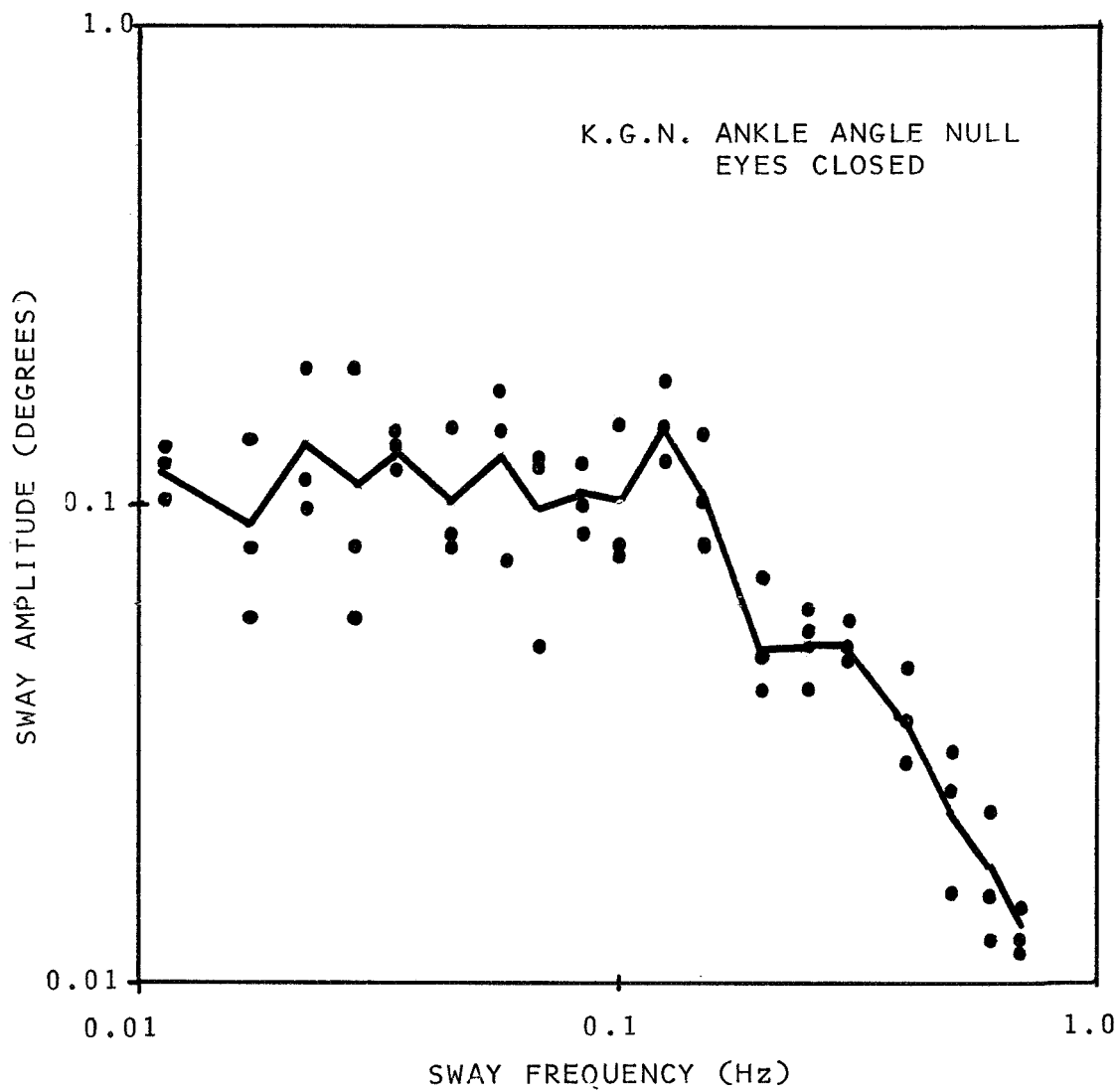


FIGURE E.17 FOURIER COEFFICIENTS FOR BODY SWAY MOTION

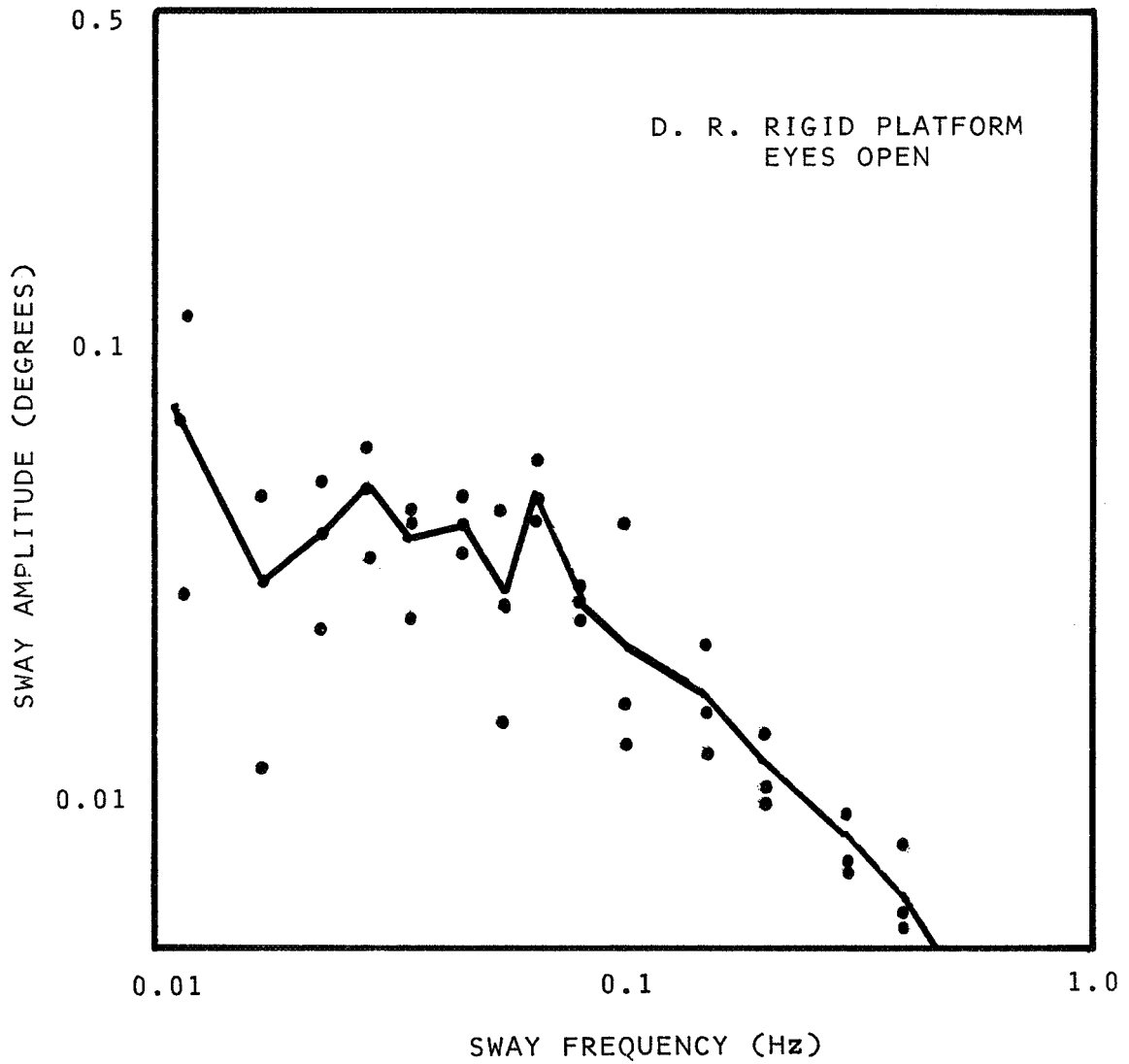


FIGURE E.18 FOURIER COEFFICIENTS FOR BODY SWAY MOTION

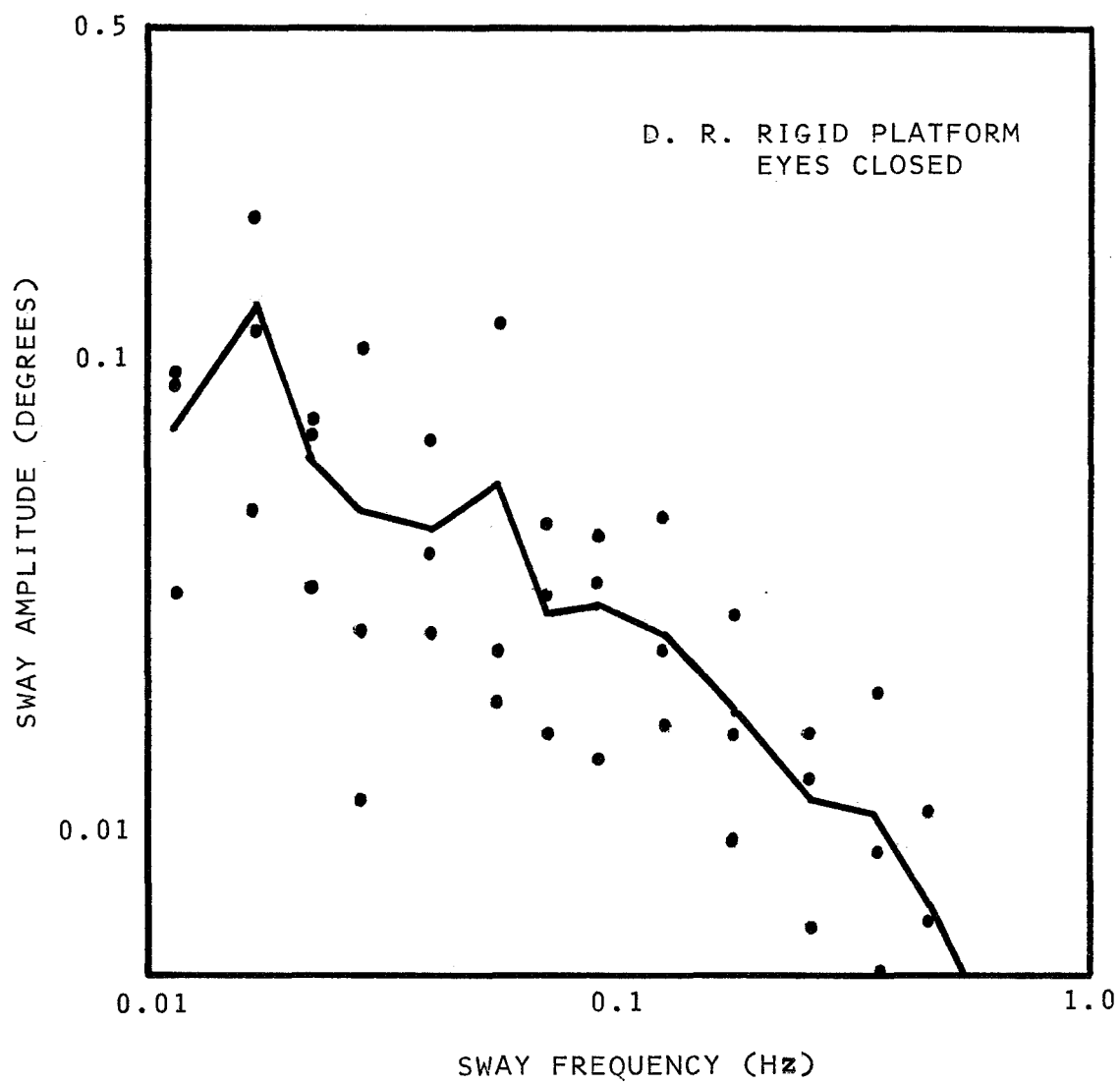


FIGURE E.19 FOURIER COEFFICIENTS FOR BODY SWAY MOTION

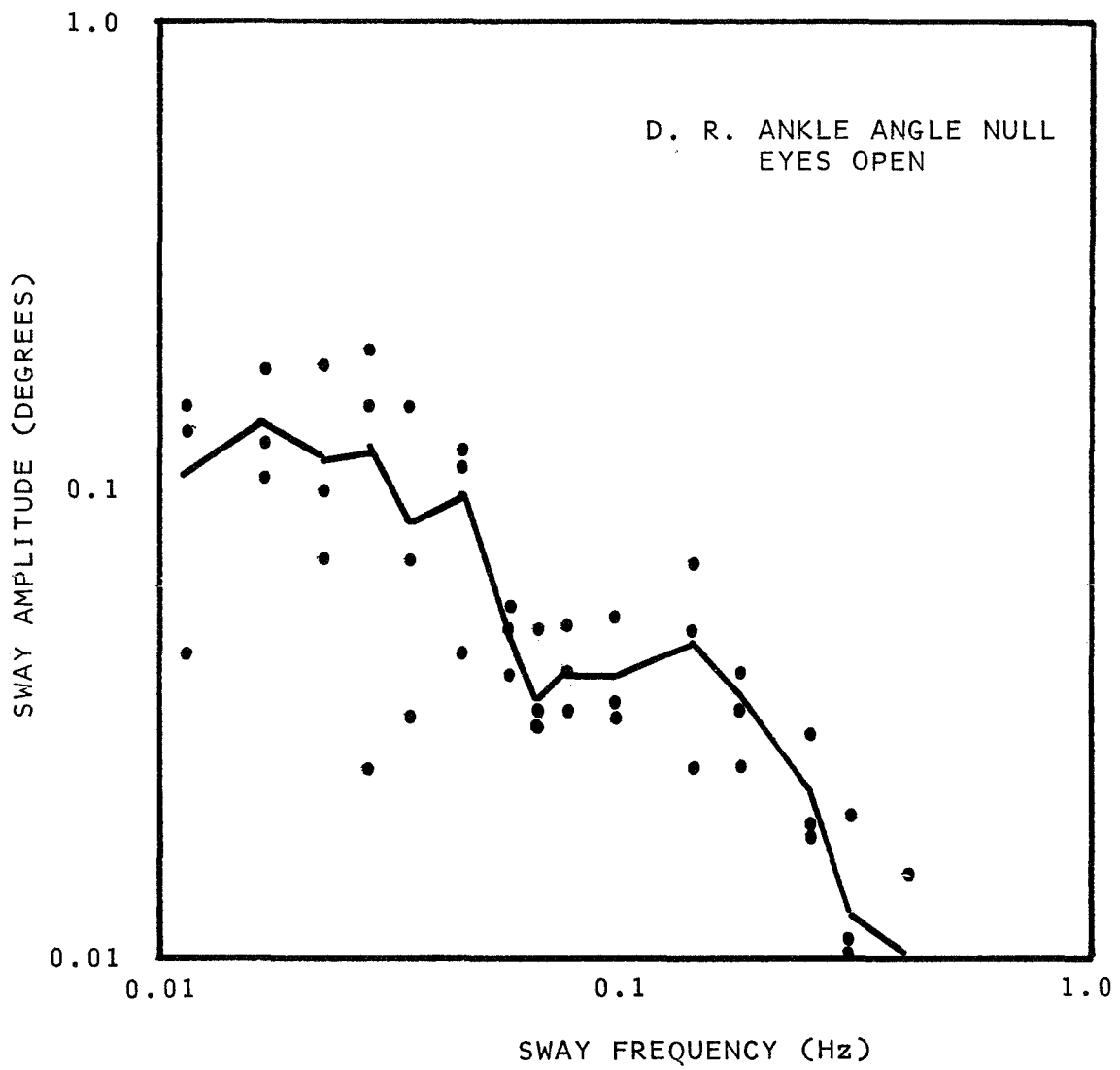


FIGURE E.20 FOURIER COEFFICIENTS FOR BODY SWAY MOTION

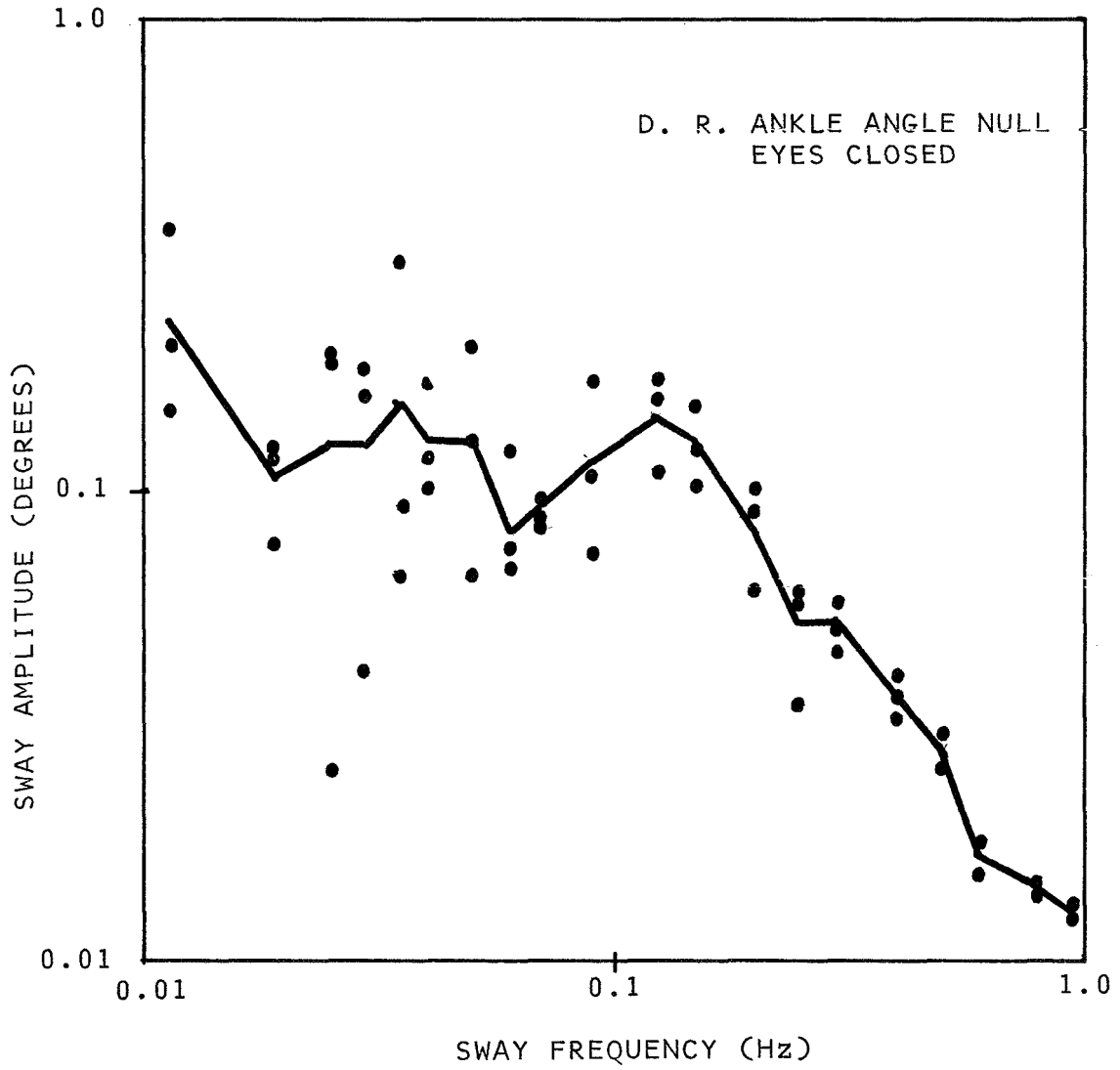


FIGURE E.21 FOURIER COEFFICIENTS FOR BODY SWAY MOTION

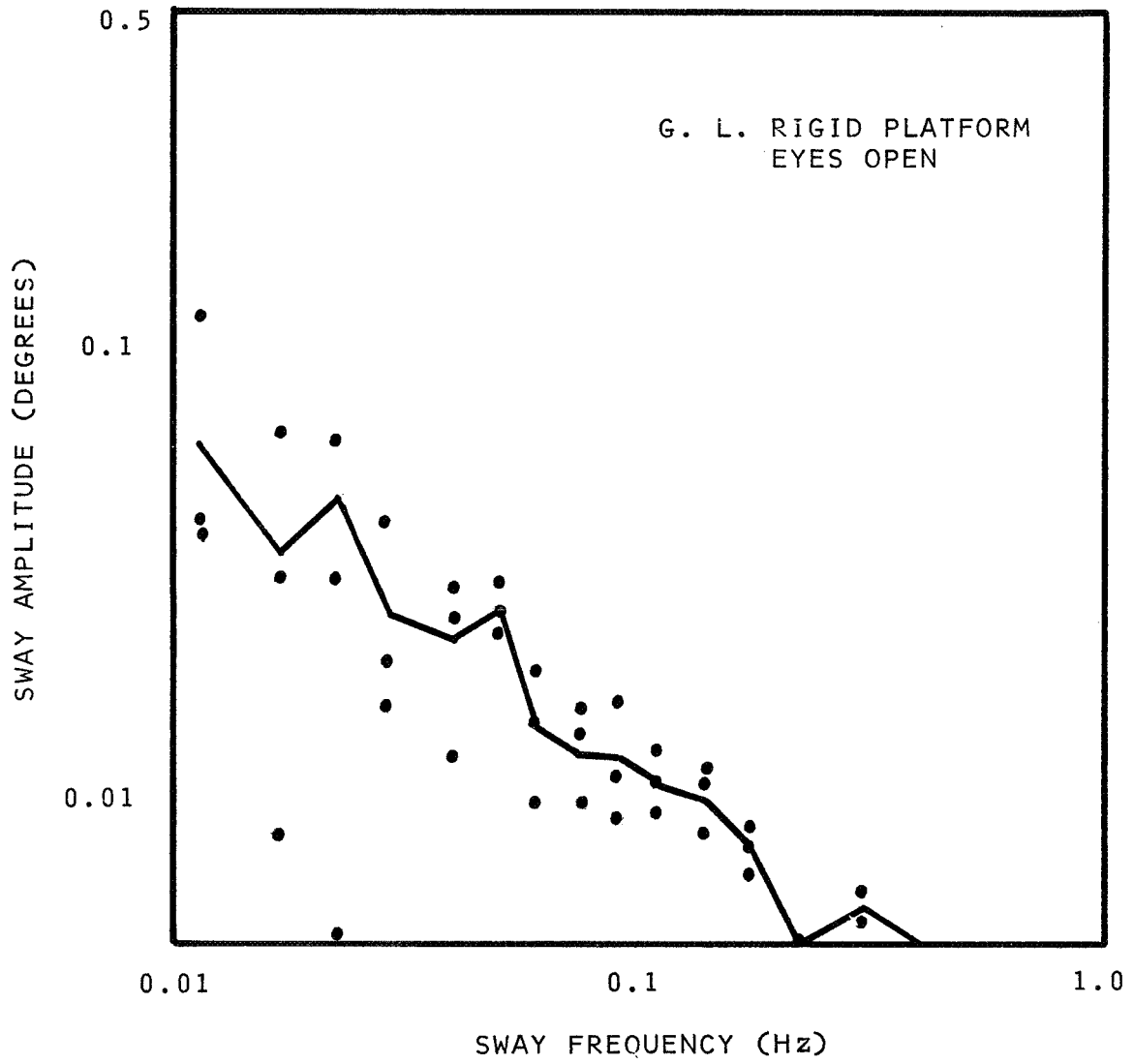


FIGURE E.22 FOURIER COEFFICIENTS FOR BODY SWAY MOTION

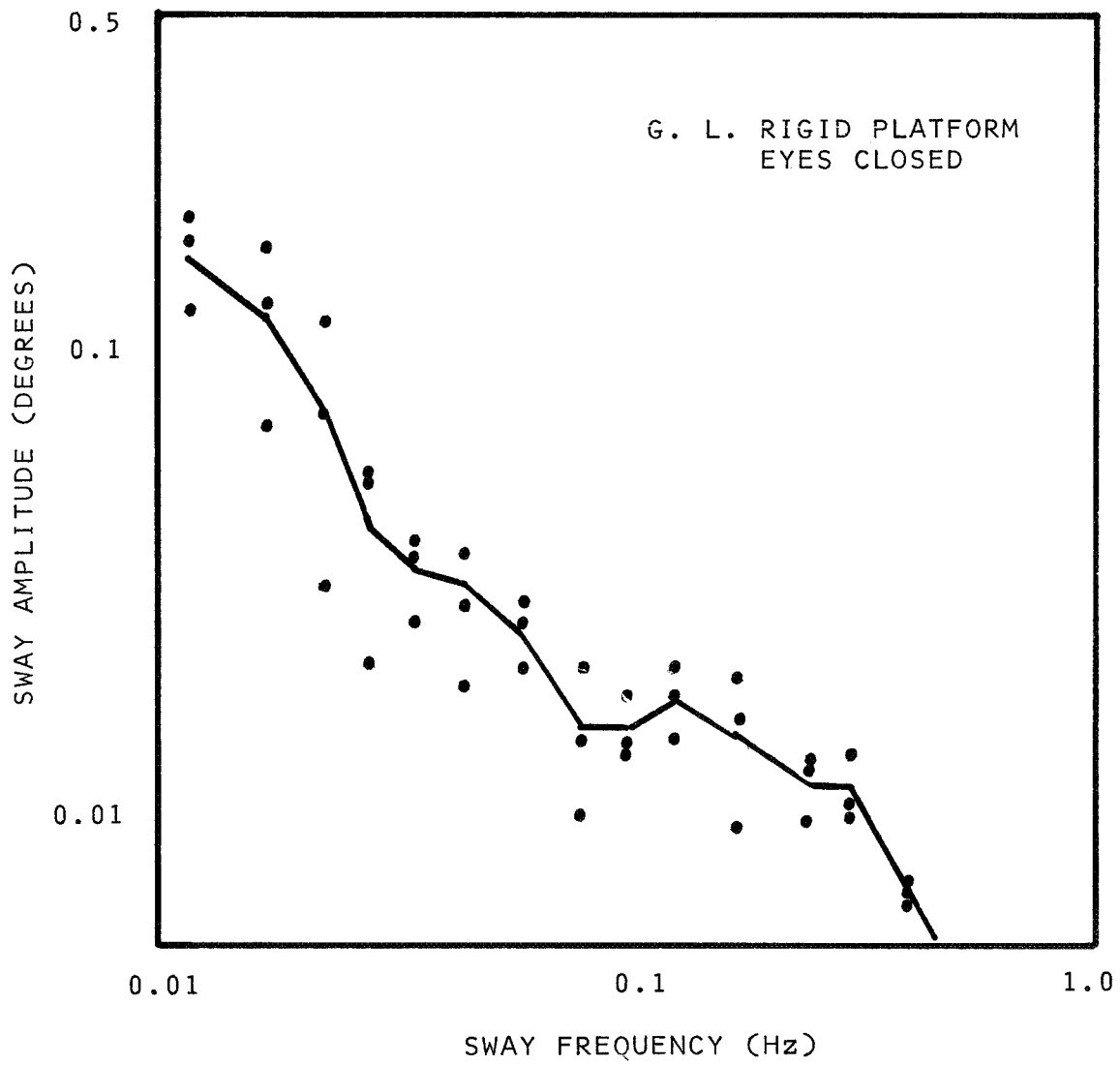


FIGURE E.23 FOURIER COEFFICIENTS FOR BODY SWAY MOTION

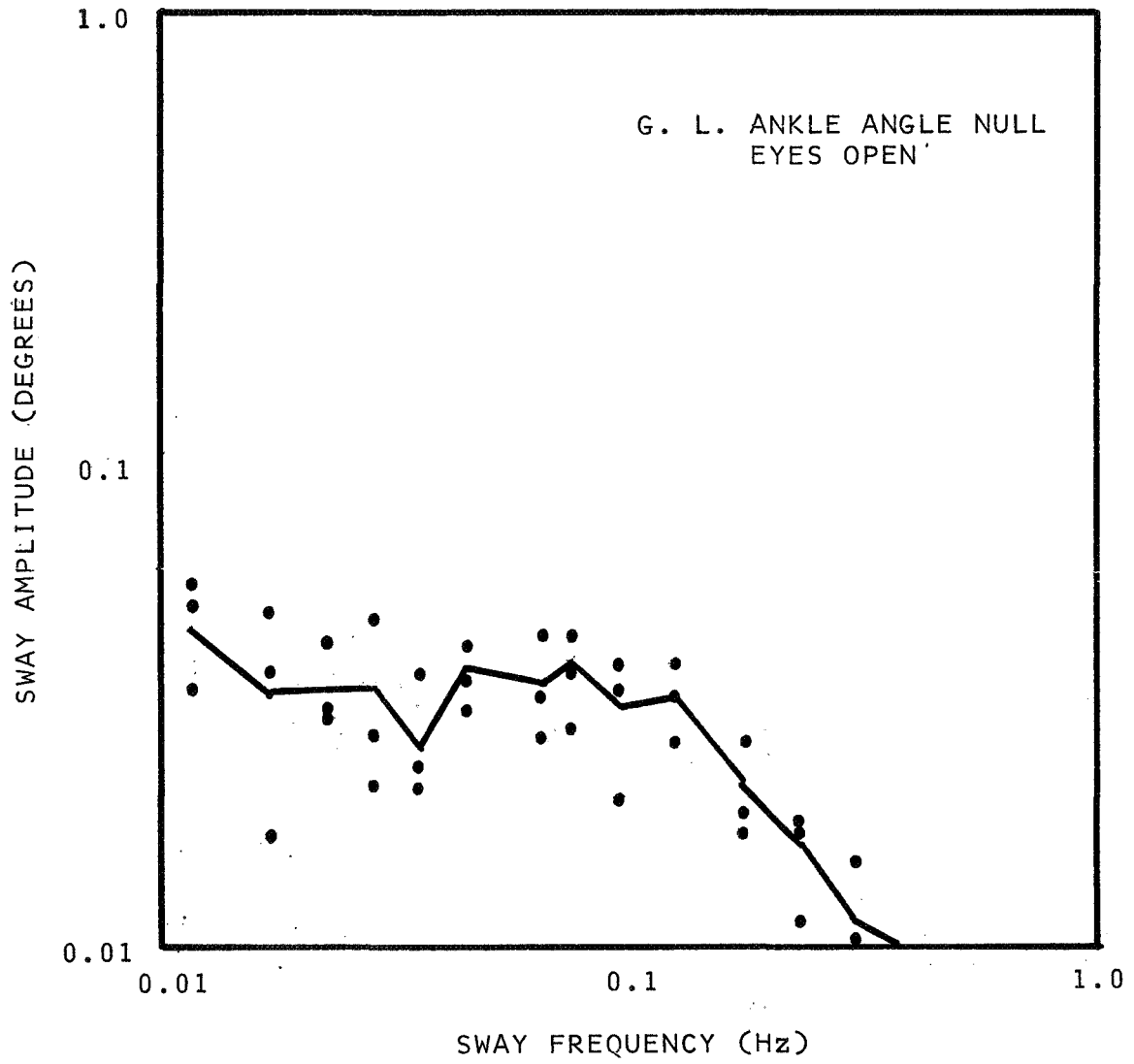


FIGURE E.24 FOURIER COEFFICIENTS FOR BODY SWAY MOTION

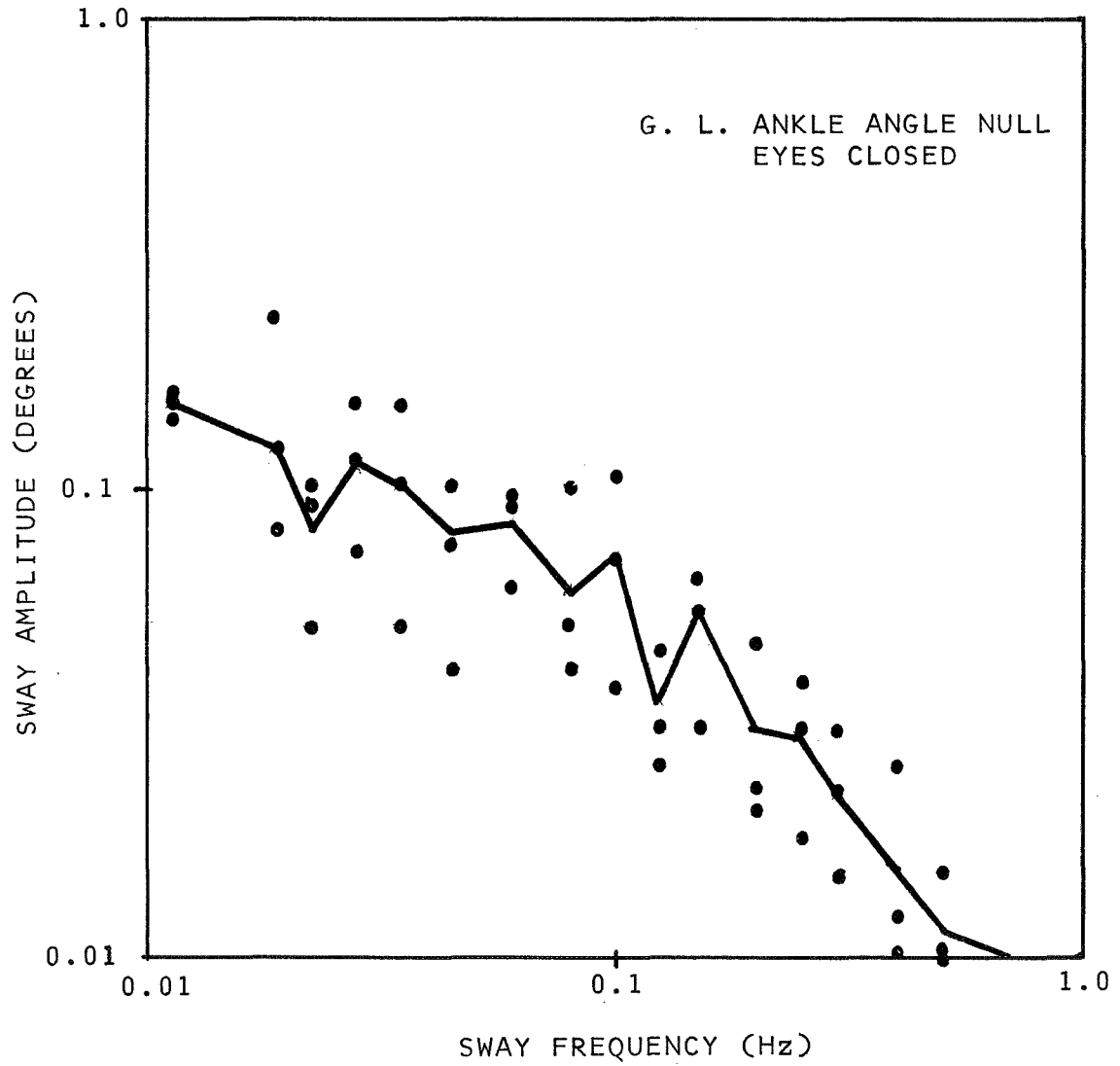


FIGURE E.25 FOURIER COEFFICIENTS FOR BODY SWAY MOTION

REFERENCES

1. Agarwal, G., Berman B., Hogins, M., Lohnberg, P., and Stark, L., "Effects of External Loading on Human Motor Reflexes," Fourth Annual NASA-University Conference on Manual Control, NASA SP-192, 1968.
2. Agarwal, G., Gottlieb, G. and Stark, L., "Models of Muscle Proprioceptive Receptors," Fourth Annual NASA-University Conference on Manual Control, NASA SP-192, 1968.
3. ed. Andrew, B. L., "Control and Innervation of Skeletal Muscles," 1966.
4. Appelberg, B., Bessou, P., and Laporte, Y., "Effects of Dynamic and Static Fusimotor Fibres on the Responses of Primary and Secondary Endings Belonging to the Same Spindle," J. Neurophysiology, No. 27, 1965, p. 63.
5. Apter, Julia, T., Groessley, William W., "Mathematical Development and Solution of a Physical Mode for Muscular Contractible Elements," Fifth Annual NASA-University Conference on Manual Control, 1969.
6. Begbie, G. H., "Some Problems of Postural Sway," CIBA Foundation Symposium on Myotatic, Kinesthetic and Vestibular Mechanisms, 1967, 80-104.
7. Bell, C. C., and Dow, R. S., "Cerebellar Circuitry," Neurosciences Research Symposium Summaries, MIT Press, Cambridge, Mass., 1967.
8. Bosemark, B., "Some Aspects on the Crossed Extensor Reflex in Relation to Motoneurons Supplying Fast and Slow Contracting Muscles," Nobel Symposium, 1965.
9. Bourossa, C. M., and Swett, J. E., "Sensory Discrimination Thresholds with Cutaneous Nerve Volleys in the Cat," J. Neurophysiology, No. 30, 1967, 515-528.
10. Bowsher, D., Introduction to Neuroanatomy, Blackwell Scientific Publishers, 1961.
11. Boyd, I. A. and Roberts, T. D. M., "Proprioceptive Discharges from Stretch Receptors in the Knee Joint of the Cat," J. Physiology, Vol. 122, 1953, 38.
12. Boyd, I. A., Eyzaguirre, C., Matthews, P. B. and Rushworth, G., "The Role of the Gamma System in Movement and Posture," New York Assoc. for the Aid of Crippled Children, 1964.

14. Brown, M. C., Goodwin, G. M. and Matthews, P. B. C., "After Effects of Fusimotor Stimulation on the Response of Muscle Spindle Primary Afferent Endings," *J. Physiology*, Vol. 205, 1969, 677-94.
15. Buller, A. J. and Lewis, D. M., "The Rate of Tension Development in Isometric Tetanic Contractions of Mammalian Fast and Slow Skeletal Muscle," *J. Physiol.*, Vol. 176, 1965, 337.
16. Clark, Brant, "Factors Influencing the Perception of Angular Acceleration in Man," Second Annual Status Report, NASA NGL-05-046-002, 1969.
17. Clark, Brant and Stewart, John D., "Effects of Angular Acceleration on Man: Thresholds of the Perception of Rotation and the Oculogyral Illusion," *Aerospace Medicine*, Vol. 40, 1969.
18. Clark, Robert N., *Introduction to Automatic Control Systems*, John Wiley and Sons, Inc., N.Y., 1962.
19. Coggshall, John C., "Mathematical Models of Muscle," USCEE Report 303, 1968.
20. Cohen, L. A., "Analysis of Position Sense in Human Shoulder," *J. Neurophysiology*, No. 21, 1958.
21. Condic, David N., "Bio-Mechanical Analysis of the Forces at the Human Ankle Joint," Proc. 8th International Conf. on Medicine and Bio. Eng., 1969.
22. Davson, Hugh, *A Textbook of General Physiology*, Little Brown and Co., Boston, 1964.
23. Dempster, Wilfred Taylor, "Space Requirements of the Seated Operator," WADC Technical Report, July 1967, 55-159.
24. Denny-Brown, Derek, *The Cerebral Control of Movement*, Charles C. Thomas, Inc., Illinois, 1966.
25. Dewhurst, David J., "Neuromuscular Control System," *IEEE Trans. on Bio-Medical Engineering*, July 1967, 167.
26. Dinsdale, P. B., "Relative Effects of Roll and Yaw Motion Cues in Manual Control," S.M. Thesis, M.I.T., Dept. of Aeronautics and Astronautics, 1968.
27. Doty, Richard L., "Effects of Duration of Stimulus Presentation on the Angular Acceleration Threshold," *J. of Exp. Psychology*, Vol. 80, No. 2, 1961, 317-21.

28. Eccles, J. C., "Functional Organization of the Cerebellum in Relation to its Role in Motion Control," Nobel Symposium, Muscular Afference and Motor Control, John Wiley and Sons, Inc., 1966.
29. Eccles, J. C., "Presynaptic Inhibition in the Spinal Cord," Physiology of Spinal Neurons, Elsevier Pub. Co., Amsterdam, 1964.
30. Eccles, J. C., Ito, Masao, Szentagothai, Janos, The Cerebellum as a Neuronal Machine, Springer-Verlag, Inc., 1967.
31. Eccles, R. M. and Lundberg, A., "Supraspinal Control of Interneurons Mediating Spinal Reflexes," J. Physiol., Vol. 147, 1959.
32. Eccles, J. C. and Schade, J. P., editors, "The Motor Pools of the Spinal Cord," Progress in Brain Research, Vol. 11, Elsevier Pub. Co., N.Y., 1964, 93-119.
33. Eldred, E., Granit, R. and Merton, P. A., "Supraspinal Control of the Muscle Spindle and its Significance," J. Physiol., Vol. 122, 1953, 498.
34. Erulkar, S. D., Sprague, J. M., Whitsel, B. L., Dogai, S., and Janetta, P. J., "Organization of the Vestibular Projections to the Spinal Cord of the Cat," J. Neurophysiol., Vol. 29, 1966.
35. Fearing, F. S., "The Factors Influencing Static Equilibrium I," J. Comparative Psychol., Vol. 4, 1924.
36. ed. Field, John, Handbook of Physiology, Vol. I, Section 1, American Physiological Society, 1965, 409-415.
37. Freund, John E., Mathematical Statistics, Prentice-Hall, Inc., Englewood Cliffs, New Jersey, 1962.
38. Gardner, E., "Spinal Cord and Brain Stem Pathways for Afferents from Joints," Myotactic Kinesthetic and Vestibular Mechanisms, CIBA Foundation Symposium, Little Brown and Co., Boston, 1967, 56-76.
39. Gernandt, B. E., Magdolna, I., and Livingston, R. B., "Vestibular Influences on Spinal Mechanisms," Experimental Neurology, Vol. 1, 1959.

40. Gibson, John E., Nonlinear Automatic Control, McGraw-Hill Book Co., New York, 1963.
41. Glaser, G. H. and Higgens, D. C., "Motor Stability, Stretch Responses and the Cerebellum," Nobel Symposium, Muscular Afference and Motor Control, John Wiley and Sons, Inc., 1966.
42. Gottlieb, G. L. and Agarwal, G. C., "Muscle Spindle Models: Multiple Input-Multiple Output Simulations," Fifth Annual NASA-University Conference on Manual Control, 1969.
43. Granit, Ragnar, "Neuromuscular Interaction in Postural Tone of the Cat's Isometric Soleus Muscle," J. Physiol., Vol. 143, 1958.
44. Granit, R., Holmgren, B. and Merton, P. A., "The Two Routes for Excitation of Muscle and Their Subsistence to the Cerebellum," J. Physiol., Vol. 130, 1955.
45. Granit, R., Pomperiano, O. and Waltman, B., "Fast Spinal Control of Mammalian Muscle Spindles," J. Physiol., Vol. 147, 1959.
46. Groen, J. J. and Jongkees, L. B. W., "The Threshold of Angular Acceleration Perception," J. Physiol., Vol. 107, 1948.
47. ed. Guyton, A. C., Textbook of Medical Physiology, W. B. Saunders. Co., Philadelphia, 1962.
48. Hammond, P. H., "An Experimental Study of Servo Action in Human Muscular Control," Proceedings of the Third International Conference on Medical Electronics, 1960.
49. Hellebrandt, F. A. and Fries, E. C., "Consistency of Oscillographic Stance Patterns," Physiotherapy Rev., Vol. 22, 1942.
50. Hellebrandt, F. A. and Fries, E. C., "Eccentricity of Near Vertical Projection of Center of Gravity During Standing," Physiotherapy Rev., Vol. 22, 1942.
51. Higgens, D. C., Partridge, L. D. and Glaser, G. H., "A Transient Cerebellar Influence on Stretch Responses," J. Neurophys., Vol. 25, 1962.

52. Hilding, A. C., "Studies on the Otic Labyrinth: III. On the Threshold of Minimum Perceptible Angular Acceleration," *Ann. Otol. Rhin. and Laryng.*, Vol. 62, No. 5, 1953.
53. Hill, A. V., "The Heat of Shortening and the Dynamic Constants of Muscle," *Proceedings of the Royal Society of Britain*, Vol. 126, 1938.
54. Hill, D. K., "Tension Due to Interaction Between the Sliding Filaments in Resting Striated Muscle. The Effect of Stimulation," *J. Physiol.*, Vol. 199, 1968.
55. Houk, J. C., "Mathematical Model of the Stretch Reflex in Humans," S. M. Thesis, M. I. T., 1963.
56. Houk, J. C., "A Viscoelastic Interaction Which Produces One Component of Adaptation in Responses of Golgi Tendon Organs," *J. Neurophysiology*, Vol. 30, 1967.
57. Houk, J. C., Cornew, R. W.. and Stark, L., "A Model of Adaptation in Amphibian Spindle Receptors," *J. Theoretical Biol.*, Vol. 12, 1966.
58. Houk, J. C. and Henneman, E., "Feedback Control of Skeletal Muscles," Medical Physiology, 12th Edition, ed. V. B. Mountcastle, Mosby Press, St. Louis, 1967.
59. Houk, J. C. and Henneman, E., "Responses of Golgi Tendon Organs to Active Contractions of the Soleus Muscle of the Cat," *J. Neurophysiology*, Vol. 30, 1967.
60. Houk, J. C. and Simon, W., "Responses of Golgi Tendon Organs to Forces Applied to Muscle Tendon," *J. Neurophysiology*, Vol. 30, 1967.
61. Houk, J. C. and Stark, L., "An Analytical Model of a Muscle Spindle Receptor for Simulation of Motor Coordination," QPR 66, Res. Lab. of Elec., M.I.T., 1962.
62. House, E. L. and Pansky, B., A Functional Approach to Neuroanatomy, McGraw-Hill Book Co., New York, 1960.
63. Jansen, J. K. S., "On Fusimotor Reflex Activity," Nobel Symposium, Muscular Afference and Motor Control, John Wiley and Sons, Inc., 1966.

64. Jansen, J. K. S. and Matthews, P. B. C., "The Central Control of the Dynamic Response of Muscle Spindle Receptors," *J. Physiol.*, Vol. 161, 1962.
65. Jansen, J. K. S. and Rudjord, T., "On the Silent Period and Golgi Tendon Organs of the Soleus Muscle of the Cat," *Acta. Physiol. Scand.*, Vol. 62, 1964.
66. Jewell, B. R. and Wilke, D. R., "An Analysis of the Mechanical Components in Frog's Striated Muscle," *J. Physiol.*, Vol. 143, 1958.
67. Johnson, A. R., "The Servo-Analysis of Postural Reflexes," Ph.D. Thesis, M.I.T., 1960.
68. Joyce, G. C. and Rack, P. M. H., "Isotonic Lengthening and Shortening Movements of Cat Soleus Muscle," *J. Physiol.*, Vol. 204, 1969.
69. Joyce, G. C., Rack, P. M. H. and Westbury, D. R., "The Mechanical Properties of Cat Soleus Muscle During Controlled Lengthening and Shortening Movements," *J. Physiol.*, Vol. 204, 1969.
70. Katz, Bernard, Nerve, Muscle and Synapse, McGraw-Hill Book Co., New York, 1966.
71. Kim, J. H. and Partridge, L. D., "Observations on Types of Response to Combinations of Neck, Vestibular, and Muscle Stretch Signals," *J. Neurophysiology*, Vol. 32, 1969.
72. Lippold, O., Nicholla, J., and Redfearn, J., "Electrical and Mechanical Factors in the Adaptation of a Mammalian Muscle Spindle," *J. Physiol.*, Vol. 153, 1960.
73. Livingston, R. B., "Central Control of Receptors and Sensory Transmission Systems," Handbook of Physiology, Vol. I, American Physiol. Society, 1959, 759-86.
74. Lundberg, A., "Integration in the Reflex Pathway," Nobel Symposium, Muscular Afference and Motor Control, John Wiley and Sons, Inc., 1966.
75. McPhedran, A., Wuerker, R. and Henneman, E., "Properties of Motor Units in a Homogeneous Red (Soleus) Muscle of the Cat," *J. Neurophysiology*, Vol. 28, 1965.

76. McRuer, D. T., Magdaleno, R. E., and Moor, G. P., "A Neuromuscular Activation Systems Model," Thrid Annual NASA-University Conference on Manual Control, 1967.
77. Magdaleno, R. E. and McRuer, D. T., "A Closed Loop Neuromuscular System Explanation of Force Disturbance Regulation and Tremor Data," Fourth Annual NASA-University Conference on Manual Control, 1968.
78. Marshall, C. and Lazier, E. L., An Introduction to Human Anatomy, W. B. Saunders Co., Philadelphia, 1963, 55-68, 97-116.
79. Martin, P., "The Role of the Vestibular System in the Control of Posture and Movement in Man," CIBA Symposium on Myotatic, Kinesthetic and Vestibular Mechanisms, 1967.
80. Matthews, P. B. C., "Evidence that the Secondary as Well as the Primary Endings of the Muscle Spindles May be Responsible for the Tonic Stretch Reflex of the Decerebrate Cat," J. Physiol., Vol. 204, 1969.
81. Matthews, P. B. C., "Muscle Spindles and Their Motor Control," Physiol. Rev., Vol. 44, 1964.
82. Mayne, R., "Some Engineering Aspects of the Mechanism of Body Control," Electrical Engineering, Vol. 70, 1951.
83. Meiry, J. L., "The Vestibular System and Human Dynamic Space Orientation," NASA-CR-628, 1966.
84. Merton, P.A., "The Silent Period in a Muscle of the Human Hand," J. Physiol., Vol. 114, 1951.
85. Miles, W. R., "Static Equilibrium as a Useful Test of Motor Control," J. of Industrial Hyg., Vol. 3, 1921.
86. Okabe, Y., Rhodes, H. E., Stark, L., and Willis, P. A., "Simultaneous Hand and Eye Tracking Movements," QPR 66, Res. Lab. of Elec., M.I.T., 1962.
87. Partridge, L. D. and Kim, J. H., "Dynamic Characteristics of Response in a Vestibular Reflex," J. Neurophysiology, Vol. 32, 1969.
88. Patton, H. D. and Amassian, V. E., "The Pyramidal Tract: Its Excitation and Function," Handbook of Physiology, Vol. III, American Physiol. Society, 1960, 837-61.

89. Ritchie, J. M. and Wilke, D. R., "The Dynamics of Muscular Contraction," *J. Physiol.*, Vol. 143, 1958.
90. Roberts, T. D. M., Neurophysiology of Postural Mechanisms, Plenum Press, Butterworths, England, 1967, 90-120, 81-89, 120-175.
91. Roberts, W. J., McKean, T. A., Rosenthal, N. P. and Terzvolov, C. A., "Loop Gain of the Stretch Reflex," Conference on System Analysis in Neurophysiology, University of Minnesota, 1969.
92. Saasaki, K. and Tanaka, T., "Phasic and Tonic Innervation of Spinal Alpha Motoneurons from Upper Brain Centers," *Jap. J. Physiol.*, Vol. 14, 1964.
93. Schone, H., "On the Role of Gravity in Human Spatial Orientation," *Aerospace Medicine*, Vol. 35, 1964.
94. Shapovalov, A. I., "Excitation and Inhibition of Spinal Neurons During Stimulation," Nobel Symposium, Muscular Afference and Motor Control, John Wiley and Sons, Inc., 1966.
95. Shimazv, H., Hongo, T. and Kubota, K., "Nature of Central Regulation of Muscle Spindle Activity," Symposium on Muscle Receptors, U. of Hong Kong, 1962.
96. Shirley, R. S., "Motion Cues in Man-Vehicle Control," Sc.D. Thesis, M.I.T., 1968.
97. Skogland, J. E., "A Quantitative Study of Normal and Pathological States in Human Subjects," *Medical Records*, Vol. 155, 1942.
98. Stark, L., Neurological Feedback Control Systems, Plenum Press, New York, 1966.
99. Stevens, S. S., ed., Handbook of Experimental Psychology, John Wiley and Sons, Inc., New York, 1951.
100. Swett, J. E. and Bourassa, C. M., "A Comparison of Sensory Discrimination Thresholds with Muscle (Spindle) and Cutaneous Nerve Volleys in the Cat," *J. Neurophysiology*, Vol. 30, 1967.
101. Swett, J. E. and Bourassa, C. M., "Short Latency Activation of Pyramidal Tract Cells by Group I (Spindle) Afferent Volleys in the Cat," *J. Physiol.*, Vol. 189, 1967.

102. Terzuolo, C. A. and Llimas, R., "Distribution of Synaptic Inputs in the Spinal Motoneuron and Its Functional Significance," Nobel Symposium, Muscular Afference and Motor Control, John Wiley and Sons, Inc., 1966.
103. Travis, R. C., "An Experimental Analysis of Dynamic and Static Equilibrium," Jour. of Exp, Psychol., Vol. 35, 1945.
104. Van Houtte, N. A. J., "Display Instrumentation for V/STOL Aircraft in Landing," Vol. III, Sc.D. Thesis, M.I.T., 1970.
105. Viernstein, L. J., "Dynamic Properties of First Order Afferents Responsive to Joint Rotation," Eighth ICMBE, Chicago, 1969.
106. Webb, Paul, Bioastronautics Data Handbook, NASA SP-3006, 1964.
107. Wilke, D. R., "The Relation Between Force and Velocity in Human Muscle," J. Physiol., Vol. 110, 1950.
108. Wilke, D. R., "The Mechanical Properties of Muscle," British Medical Bulletin, Vol. 12.
109. Wuerker, R. B., McPhedran, A. M. and Henneman, E., "Properties of Motor Units in a Heterogeneous Pale Muscle (Gastrocnemius) of the Cat," J. Neurophysiology, Vol. 28, 1965.
110. Yelelyanov, M. D., Kuznetsov, A. G., Yuganov, E. M. and Gurjian, A. A., "Problems Concerning the Interplay of Physiological Sensing Mechanisms (Analysers) During Space Flight," Man in Space I, USSR Academy of Sciences, Moscow, 1967.
111. Young, L. R., "The Current Status of Vestibular System Models," Automatica, Vol. 5, 369-383, 1969.
112. Young, L. R. and Meiry, J. L., "A Revised Dynamic Otolith Model," Aerospace Medicine, Vol. 39, 1968.
113. Young, L. R. and Stark, L., "Biological Control Systems: A Critical Review and Evaluation," NASA CR-190, 1965.

114. Yung, R. and Hassler, R., "The Extrapyramidal Motor System," Handbook of Physiology, Vol. III, American Physiological Society, 1960.
115. Zajac, Felix, "The Mathematical Formulation of the Kinematic Properties of Muscle Derived from an Experimental Investigation," Ph.D. Thesis, Stanford University, 1968.

BIOGRAPHICAL SKETCH

Lewis Michael Nashner was born on October 9, 1943, in Pine Bluff, Arkansas. He entered the Massachusetts Institute of Technology in 1961. He was awarded the James Means Memorial Prize in his senior year and graduated with a S.B. in Aeronautics and Astronautics in June 1965.

From 1965 to 1966 he was a NASA Fellowship student. At this time he worked toward his S.M. in Aeronautics and Astronautics, which he was awarded in January 1967.

From 1967 to 1970 he has been a Research Assistant in the Man-Vehicle Laboratory where he carried out the research which generated this thesis.

Mr. Nashner is a member of Sigma Xi and the International Society of Posturography.